AN INTRODUCTION TO APPLIED OPTICS

BY

L. C. MARTIN
D.Sc., A.R.C.S., D.I.C.
ASSISTANT PROFESSOR IN THE TECHNICAL OPTICS DEPARTMENT,
IMPERIAL COLLEGE OF SCIENCE AND TECHNOLOGY, LONDON

VOLUME I

GENERAL AND PHYSIOLOGICAL

LONDON
SIR ISAAC PITMAN & SONS, LTD.
PARKER STREET, KINGSWAY, W.C.2
BATH, MELBOURNE, TORONTO, NEW YORK
1930

PREFACE

THE enormous range of the modern study of Physics makes it clear that the main justification for the study of optics is the possibility of arriving at an understanding of the principles of real instruments. Of the books available in English, however, there are few which occupy a position intermediate between advanced mathematical treatises on the one hand, and very superficial discussions on the other. Textbooks on " Light " rarely get to grips with any serious problems in connection with optical instruments.

The teacher of Light must perforce revise his syllabus! While he may curtail the time devoted to non-essential parts of "geometrical optics," he will do well to bring the instruction as far as may be into vitally close relations with instruments, such as spectacles, telescopes, and microscopes. The present work will be well justified if it helps along such lines, not as a " cram " book, but one which may provide guidance for the teachers and students who are interested in the modern aspects of the subject.

While Professor Conrady's recent treatise on *Applied Optics and Optical Design* will fill the need for a textbook for those interested in the designing and computing of optical systems, the present book will deal with more general aspects of the subject, and will not go into the methods of design. Unless the hundred-year efforts automatically to produce non-spherical surfaces should bear unexpected fruit it is unlikely that the present attainments of optical science will ever be greatly surpassed. Many modern systems function efficiently up to the limits which are imposed by the nature of light, and the main possible designs of systems involving spherical surfaces have become fairly well known. While there can be little to add to the results of theory, the presentation of the latter can doubtless be improved.

It has been the recent fashion to criticize the " optics " developed by Gauss and Abbe on the score of unreality. Gullstrand and others have sought to introduce " real optics," again beginning with rays, but relieved from the restrictions of the usual treatments; they make an early attack on the case of the astigmatic refraction of a pencil of rays obliquely incident on a curved refracting surface. This appears to the writer as being no nearer " real optics " than before. The only contact with reality in applied optics is a thorough discussion of interference and diffraction phenomena in the optical image.

While there can be no doubt that the powerful method associated with the characteristic function afford the most direct approach to the essential problems for those having the necessary mathematical attainments, it is impossible and inadvisable to begin along such lines. For the majority, I believe, the main steps will be the " rectilinear propagation," Huygen's principle, and Young's principle of superposition. Fermat's principle can be invoked to obtain some of the more important properties of instruments.

The fact that we employ the " rectilinear propagation " and all the conceptions of ray paths to approach the paraxial theory of thin and thick lenses, will have no terrors for the beginner if we put the methods of exact ray tracing into his hands at an early stage.

I have introduced the " wave curvature " method of dealing with simple optical problems into the Appendix of this book, and a short discussion on these lines will also appear in Vol. II. It is undoubtedly very useful and instructive to make the suggestion to the student and let him devise his own methods of arriving at the familiar formulae. The wave-curvature method is, unfortunately, no nearer " reality " than the ray; it tells us nothing directly as to what actually happens in the region of the focus. We can only get at that via " optical paths," " Huygens' principle," and the " principle of superposition." It is, however, very instructive to obtain the elementary thin lens formulae by conceptions of optical path, and the oblique astigmation of a tilted thin lens can be discussed most instructively on such lines.

The vexed questions of optical sign conventions is not an easy one to decide. A committee formed by the Physical Society of London is debating the subject at the present time. For the great majority of optical problems the simple and convenient conventions adopted for optical computing are available. Where a reversal of the direction of the light occurs, in reflection problems, the simplest plan is to change the sign of the refractive index. The numerical " power " of lenses or surfaces is then independent of the direction of the light, and agrees with the convention of ophthalmic optics, when the correct Gaussian equations are employed.

Volume I contains sufficient material to introduce the reader to the theory of spectacles. While space forbids the thorough discussion of the large general subject of lenses, it appeared to the writer that a concise account of spectacle theory would appeal to many whose attainments permit them to proceed more quickly than the usual elementary textbook on " refraction."

The author is indebted to many friends for kind criticism and advice, especially to Prof. A. O. Rankine, O.B.E., D.Sc., Head of

the Technical Optics Dept., Mr. Rudolph Kingslake, M.Sc., of the University of Rochester, U.S.A., and Mr. H. H. Emsley, B.Sc., of the Northampton Polytechnic Institute. Mr. Emsley's long experience and detailed knowledge of ophthalmic optics have made his suggestions of the greatest value. Much of the book, and especially Chapter IV, has been directly inspired by the pioneer work of Professor Conrady, whose successful efforts to base the methods of optical designing on the sure foundation of the wave-nature of light have totally changed the emphasis in modern optical theory. The author is further indebted to Thos. Murby & Co., Ltd., the School of Optics, Ltd., and Carl Zeiss (London), Ltd., for kind permission to copy diagrams.

L. C. MARTIN.

IMPERIAL COLLEGE OF SCIENCE
AND TECHNOLOGY,
1930.

CONTENTS

AN INTRODUCTION TO
APPLIED OPTICS

CHAPTER I

ELEMENTARY THEORY

The Rectilinear Propagation of Light. The historical approach to a subject has a twofold value. Not only can we obtain a review of its development, but we trace in the writings of the early thinkers the conquest of our own initial difficulties; we understand the way in which the more obvious facts of experience begin to guide the process of thought. Even in a discussion of applied optics this method is of value.

" Optics " was the Greek science of *vision*; the word is given a wider meaning to-day, since it includes the study of optical instruments, or the means whereby vision is aided or supplemented. The most superficial observation indicates the eye as the organ of vision, but many philosophers, from Epicurus (342–270 B.C.) to Damianus (fifth century), conceived that the eye emanates something which affects the objects thus rendered visible. This view had appeared inadequate to Plato (429–347 B.C.) and his followers, who recognized that the presence of a self-luminous body plays a great part in the visual process, and who argued therefore that rays from a source of light like the sun unite with rays from the eye to meet rays emanating from the object seen.

Plato's sometime pupil, Aristotle (384–322 B.C.), who had a greater regard for the observation of phenomena than many of his predecessors or successors, doubted the emission of rays from the eye as a factor in vision. In considering the relation between the object and the eye he argued that the activity of some intervening medium, which he termed the *pellucid*, was necessary; a theory of the greatest interest which was not, however, developed for two thousand years afterwards, and was generally not accepted by the contemporary Platonists. These latter, following the Pythagoreans, considered the " radiations " to consist of a stream of particles moving in straight lines, a natural way of explaining the early observed fact of the " rectilinear propagation of light."

The sizes and shapes of shadows, the familiar sight of a " shaft of

sunlight " descending from a distant gap in the clouds, are a sufficient guide to the establishment of this very fundamental idea, that light in such a medium as air travels in straight lines. Even Damianus, who would not have regarded these observations as directly concerned with that " light " which is the means of vision, must have known, for example, that if three screens are placed between an eye and a small object, the latter only becomes visible if the screens are pierced by holes through which a straight line can pass from the object to some point of the pupil of the eye; hence, he asserts the fact that " light " moves in straight lines which are the tracks of " rays."

Euclid (300 B.C.) spoke of the emanation of rays of light radiating out in straight lines from the eye as centre; it is not clear whether we are to regard this as consenting to the theory of emission from the eye, but in any case Euclid really laid the first foundations of " perspective " with the idea of the " centre of perspective " from which the actual directions of objects in space are determined by the directions in which they are seen from this centre. The apparent size of an object may be estimated, partly by the rotation of the eye in passing from one extreme of the object to the other, partly by the apparent size of the retinal image. Thus, in any case the estimate depends upon the angular subtense of the object at the eye.

Perspective. Much later, Leonardo da Vinci (A.D. 1492–1519) first actually formulated the rule of perspective, indicating that a true picture of an object could be made by holding a transparent plate between object and eye, and marking on the plate the projection of the object (Fig. 1A). Supreme artist and scientist, Leonardo wrote down only a part of his scientific discoveries, but it is practically certain that he knew of the principle of the " camera obscura " described a few years later (1558) by Giambattista della Porta in his *Magia naturalis* . . .

In the demonstration of the " camera " a room is provided with a dark shutter for the window, which is pierced by a small hole. On the white wall opposite the opening, an inverted image of exterior objects now appears in its natural colours. If a white screen is moved between the aperture and the wall (keeping it parallel to the wall) it will receive an image of an exterior object, the size of the image being proportional to the distance of the screen from the hole. Such a simple experiment provided a direct disproof of the theory that " light " emanates from the eye. In a later section the " definition " or sharpness of detail in the image will receive consideration.

There are a few simple geometrical ideas of some importance in

applied optics which arise directly owing to the effects of our experience in connection with the rectilinear propagation of light and the accompanying laws of perspective. In Fig. 1A, h and h' are the vertical dimensions of the object AB and the projection A′B′; imagine this projection drawn on glass.

When AB and A′B′ are both perpendicular to the line BB′O, a natural measure of the visual angle under which the object appears

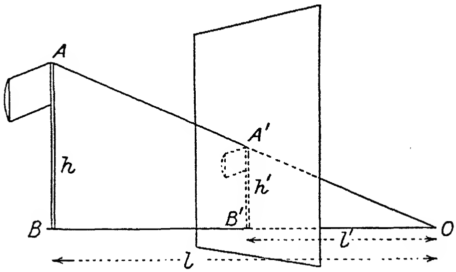

FIG. 1A

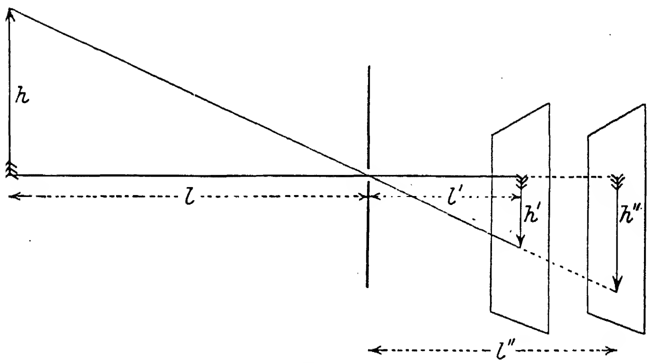

FIG. 1B

from the perspective centre is the tangent of the angle, i.e. $\frac{h}{l}$; clearly the projection as actually drawn on the glass subtends the same angle when held as shown in the figure, so that

$$\frac{h'}{l'} = \frac{h}{l}$$

but the picture when drawn can be made to subtend a greater or less angle at the perspective centre by varying the distance or inclination of the plate relatively to the eye.

Similarly, in the camera obscura, when we deal for simplicity

with the projection of images on screens parallel to the object, of which the perpendicular distances from the "pinhole" are l', l'', while the respective sizes of the images are h', h''

$$\frac{h}{l} = \frac{h'}{l'} = \frac{h''}{l''}.$$

Whatever the position or inclination of the image planes, we may (if we please) reproduce the pictures by drawing, or by receiving them on photographic plates, and these reproductions *when put back into the original image positions* will subtend the same angle at the "pinhole" as the original object; or again, by altering the distance or inclination of the picture, it can be viewed under varying angular subtenses. Of course the picture can be turned "right way up," while still retaining the correct visual angles. There are

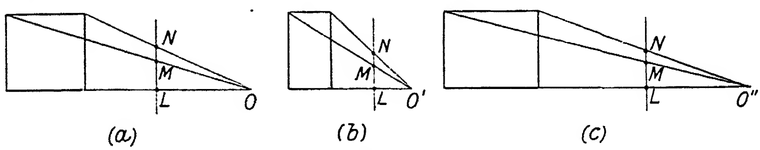

FIG. 2

special reasons for viewing such a reproduction, or any picture made truly in the laws of perspective projection, under the proper visual angle.

Distortion through False Perspective. Fig. 2A illustrates the production of a projection LMN of a square framework viewed (edge-on) from O; in Fig. 2B the reproduction is shown as viewed from a point O′ too close to L; O′ thus acts as a perspective centre. The lines O′L, O′M, O′N now determine the directions in which the corners of the framework are seen, but their distances are indeterminate unless our experience of the original object furnishes a rough guide. If we knew the framework were rectangular, so that the front and back parts must appear of equal height (allowing mentally for the requisite distance interval), the shortness of the distance O′L in relation to OL will produce an apparent foreshortening of the image; conversely, the case shown in Fig. 2C exhibits the apparent lengthening due to a view-point at too great a distance.

Such distortion of the apparent space relations in the image as interpreted through the projections often arises in the viewing of photographs, especially of buildings, galleries, and the like, where experience makes us see what the relative proportions of the original object must have been. We shall return to this subject when dealing

with photographic optics, but students should select a suitable photograph and study the apparent space distortion produced by viewing the picture at different distances. Similar space distortion effects are often encountered in the images presented by various optical instruments; we shall deal with these in later sections.

The conception of the "ray" of light proved a fruitful principle in the development of optics; the properties of shadows found a ready explanation, and the development of photometry (the measurement of quantities of light) was begun on right lines, but it must be remembered that while this idea is a most useful servant, it must in the end be subordinated to the more exact physical conceptions of the wave nature of light and its properties of periodicity.

The Law of Reflection. The Greeks were aware of the equality of the angles of incidence and reflection when rays of light are reflected

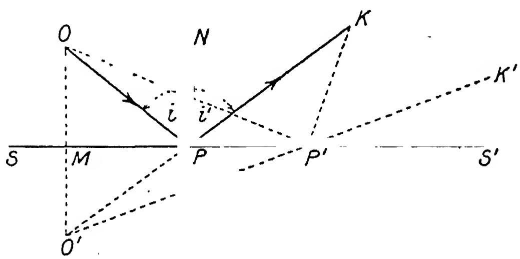

FIG. 3

from the surface of a mirror, but the complete statement of the law of reflection was first given by the Arab *Alhazen* (A.D. 1100), who added that the incident and reflected rays both lie in one plane perpendicular to the mirror surface at the point of reflection. However, *Hero* of Alexandria (2nd century A.D.) had discovered a useful property of the ray path which is a finger-post pointing to a most important and general principle. In Fig. 3, SS′ is the trace of a plane reflecting surface perpendicular to the plane of the diagram. A ray starts from the point O, is reflected at P, and passes through the point K. The normal to the surface at P is PN, and the rays OP, PK make equal angles i and i' with it; they both lie in the plane perpendicular to the surface, i.e. the plane of the diagram.

It is then easily seen that the path OPK taken by the deflected ray is the shortest possible for the reflected light. Dropping a perpendicular OM on SS′ and producing to O′, so that OM is equal to MO′, we can then draw the line O′P which is equal to OP, and, moreover, the line O′PK is evidently straight.

Any other route from O to K involving one point in the surface, OP′ + P′K, for example, is now seen to be longer than OPK, for

$$OP' + P'K = O'P' + P'K$$

and, since two sides of a triangle are greater than the third, it is clear that the route involving equal angles of incidence and reflection is the shortest of all.

A ray OP′ reflected at P′ will evidently be reflected in the direction P′K′, i.e. in continuation of the line O′P′, if it is to satisfy the law of reflection. Hence, all the rays such as OP, which before reflection diverge from the point O, appear after reflection to be diverging from a point O′ which we term the *image* of the object point O.

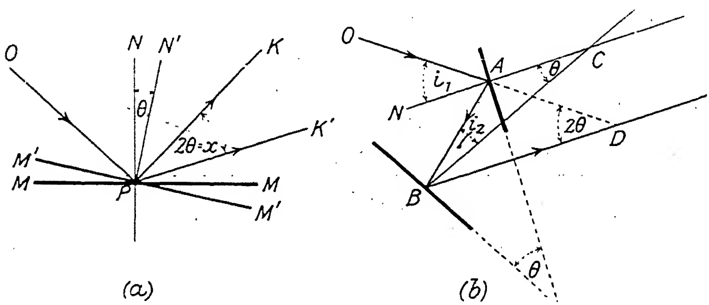

FIG. 4

It is a *virtual image* because the rays do not actually intersect in the image; however, if the surface is perfectly plane, the image looks perfect also; every ray from O in any colour will, after reflection, appear to diverge from the same image point O′. The image is free from *aberration*.

Corollaries of the Law of Reflection. There are two simple corollaries of the law of reflection which it is worth while to recall at the present stage. The first shows that if the mirror is rotated about an axis perpendicular to the plane of incidence the deflection of the reflected ray is double that of the mirror. In Fig. 4A, PN, PN′ show the two positions of the normal to the mirror which rotates about P. PK, PK′ are the two positions of the reflected ray.

Then $$O\hat{P}N = N\hat{P}K$$

and $$O\hat{P}N' = N'\hat{P}K'.$$

From the second equation

$$\widehat{OPN} + \theta = \widehat{NPK} - \theta + x,$$

whence

$$x = 2\theta.$$

The second concerns the case when a ray is reflected in turn from two mirrors, the normal of the second lying in the plane of incidence of the first reflection; the three parts of the ray path then all lie in one plane.

In Fig. 4B, the ray is shown reflected at A and B, the angles of incidence at these points being i_1 and i_2 respectively; the normals intersect at C, including the angle θ. If the incident ray is produced it meets the final path BD in the point D; the angle $\widehat{ADB}$ is thus the *deflection* of the ray. Since NA is the normal at A,

$$\widehat{NAB} = i_1 = i_2 + \theta \text{ (from the triang'e BAC)} \quad . \quad . \quad (a)$$

also

$$\widehat{OAB} = 2i_1 = \widehat{ABD} + \widehat{ADB} \text{ (from the triangle ABD)},$$

$$= 2i_2 + \widehat{ADB}$$

but

$$2i_1 = 2i_2 + 2\theta \text{ (from } (a) \text{ above)}.$$

Therefore $\widehat{ADB}$, the angle of deflection, is twice the angle between the mirrors. Hence, for example, if θ is 45°, the ray will be deflected through 90°, quite independently of the particular values of i_1 and i_2; if θ is 90° the ray will be returned in an opposite direction but parallel to its own path.

The Law of Refraction. The qualitative effects of refraction were known to the Greeks, and quantitative measurements of angles of incidence and refraction at a water surface were made by Ptolemy (A.D. 100). He found that for small angles the ratio of the angle of refraction to that of incidence was approximately constant, and considered this constancy to be the *law* of refraction, even although his own observations show that it is not fulfilled for large angles.

Alhazen pointed out that the incident and refracted rays lie in one plane with the normal to the surface at the point of refraction, but neither he nor later workers such as Kepler succeeded in formulating the true quantitative relation; Kepler sought, in fact, for some relation between the *deflection* and the angle of incidence. It was left for Willebrord Snell (1591–1626) to find the first exact form of the law; this he put in a useful geometrical relation which still has its value in graphical methods of ray-tracing used in the design of optical systems. In Fig. 5A, OD shows a plane refracting surface

(say of water), and C is an object beneath it; CD is a normal to the surface. A ray from C refracted at O will travel in the direction OA, so that the object will be seen apparently to lie at some point on this line produced backwards. This gives an experimental means of locating the point B where AO (produced) meets CD. Snell found that for a given pair of media such as air and water, the ratio OC : OB is constant. If the angles of incidence and refraction

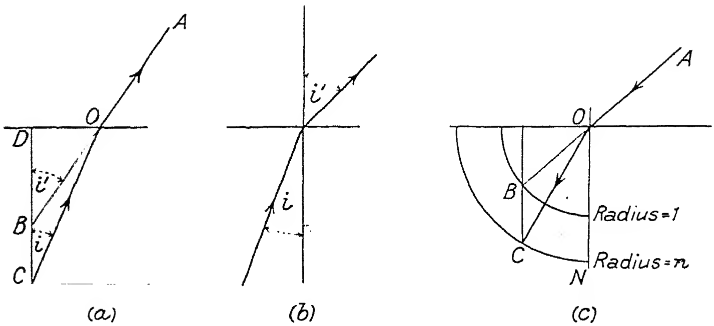

FIG. 5

between the ray and the normal are i and i' respectively (Fig. 5B), then clearly

$$\frac{OC}{OB} = \frac{\dfrac{OD}{OB}}{\dfrac{OD}{OC}} = \frac{\sin i'}{\sin i} = \text{constant}$$

The statement of the law involving the constant ratio of the sines of the angles, a convenient mathematical form, was first given by Descartes (A.D. 1637).

Graphical Ray-tracing. The following are practical examples of the use of a graphical method of ray-tracing based on Snell's construction. Fig. 5C shows a simple method of finding the path of a ray AO after refraction at a surface separating two different homogeneous media. If the law of refraction is given in the form

$$\sin i = n \sin i'$$

then n is called the refractive index of the medium (containing the refracted ray) with respect to the first medium. Take O as centre, and draw two circles with radii of "unity" and "n" respectively, using any convenient units. For example, the radii in a case of refraction from air into water might be 1 in. and 1·333 in., as n for water = 1·333. Produce AO to meet the unit circle in B; then draw

through B a line BC parallel to the normal ON at the point of refraction. The line BC cuts the second circle in C; then OC is the path of the refracted ray.

This method of ray tracing is often used by optical designers in company with an exact trigonometrical trace; the graphical control is a useful check when forming a new design, and helps to avoid subtle but dangerous errors in numerical work, such as giving too small a thickness to a lens; see below.

The important fact that a ray when reversed retraces the forward path was known to Alhazen; it is easily inferred that a ray traversing

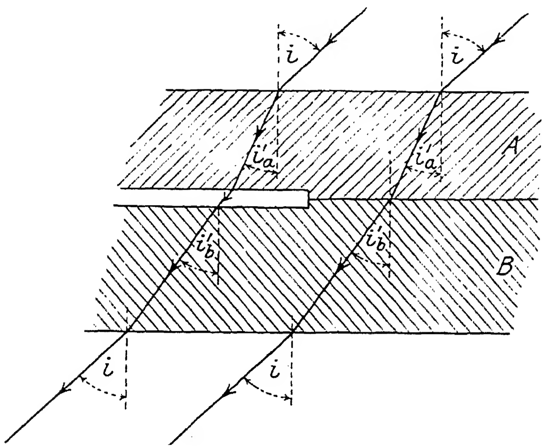

FIG. 6

a plane parallel slab of one medium, which is immersed in another medium, emerges in a direction parallel to the original path. This will also be the case after traversing *two* plane parallel slabs A and B, of different material as in Fig. 6. Under these circumstances, the initial angle of incidence on A is equal to the final angle of emergence from B. If the law of refraction from " air " to slab A is

$$\sin i = n_a \sin i'_a$$

and that from air to slab B is

$$\sin i = n_b \sin i'_b$$

these, and the principle of reversibility, make it clear that refraction from block A to block B fulfils the equation

$$n_a \sin i'_a = n_b \sin i'_b$$

In accordance with the usual practice of designating the quantities

of the image space by a dash, the generalized law of refraction can be written

$$n \sin i = n' \sin i'$$

where n and n' are the "refractive indices" of the media of incidence and refraction respectively, with respect to air.

Imagining that the two slabs are situated in a vacuum, while slab A is of air, the law of refraction shows that the apparent refractive index of medium B with respect to air would be $\frac{n_{bv}}{n_{av}}$, where n_{bv} and n_{av} are *absolute* refractive indices measured with respect to a vacuum. The refractive index of air under ordinary

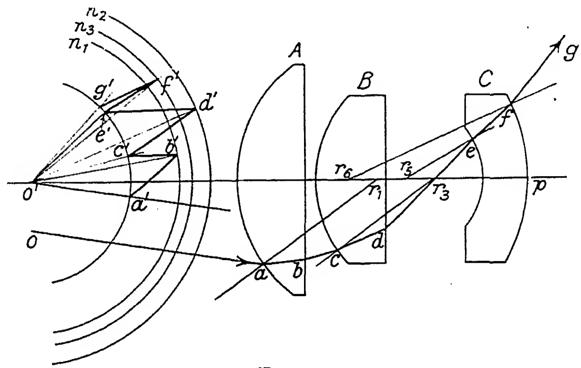

FIG. 7

conditions is about 1·00029, so that if the actual physical measurement is made in air the result must be corrected by multiplying by the proper factor, taking account of temperature pressure, etc., if the absolute refractive index is required. Ordinary "refractive indices" such as are given in glass lists and tables are usually as measured with respect to air at normal temperature and pressure.

Fig. 7 shows all the construction required in tracing an incident ray through the three lenses A, B, and C; the centres of the curved surfaces are shown in the drawing, which is of course drawn accurately to scale. This system of the application of Snell's construction is due to Dowell, and is taken from a paper contributed to the Optical Convention in 1926.

The laws of refraction for the three lenses are of the form

$$\sin i = n_a \sin i' \quad \text{(air to glass)}$$

and

$$\sin i' = \frac{1}{n_a} \sin i \quad \text{(glass to air)}$$

A suitable point o' is taken, and circles are drawn with radii of unity, and n_1, n_2, n_3, for the three lenses A, B, and C, as shown.

The line oa is the incident ray, and ar_1 gives the normal at the point of incidence. Draw $o'a'$ parallel to oa, intersecting the unit circle in a'; then draw $a'b'$ parallel to the normal ar_1, cutting the n_1 circle in b'; $o'b'$ represents the direction of the refracted ray ab which can itself conveniently be drawn by the aid of a parallel ruler.

When tracking a glass to air refraction, the n circle and the unit circle can be considered as having radii proportional to 1 and $\frac{1}{n}$ respectively, so the procedure in tracking the ray will be understood; $b'c'$ is drawn parallel to the normal at b; $o'c'$ then represents the *direction* of the ray from b to c.

Total Reflection and the Critical Angle. The law of refraction

$$n \sin i = n' \sin i'$$

whence

$$\sin i' = \frac{n}{n'} \sin i,$$

applied to a passage from a rarer to a denser medium, so that $\frac{n}{n'}$ is less than unity, shows that i' has a real value for all possible values of i from 0° to 90°. If we consider the reversed ray direction for which the same law is valid, the relation

$$\sin i = \left(\frac{n'}{n}\right) \sin i'$$

in which $\frac{n'}{n}$ is greater than unity, shows that i can only have a real value provided that the right-hand side of the last equation is not greater than unity. If such were the case, the equation would cease to be valid, the refracted ray would no longer be found in the rarer medium. Experience shows that a certain proportion of the light energy, about 5 per cent in the case of a " glass to air " transmission, is reflected at the surface when the incidence is normal. As the angle of incidence increases the proportion of energy reflected rises, slowly at first, but more quickly later, until the angle of the refracted ray in the rarer medium would be 90°, which occurs at the so-called " critical angle " of incidence in the denser medium, when

$$(\sin i')\,\frac{n'}{n} = 1, \text{ or } \sin i' = \frac{n}{n'}$$

There is then a comparatively sudden increase in the intensity of the reflected light; *total reflection* occurs and persists for all greater

angles of incidence. This matter will be considered more closely in the discussion of polarization.

The phenomena of the critical angle are of great importance in practical methods of measuring refractive index.

Dispersion. The effects of colour associated with the refraction of light were the subject of much discussion from the earliest times. A German monk, Theodoricus de Saxonia (about A.D. 1305), showed that the rainbow was formed by the refraction and internal reflection of sunlight in spherical raindrops, and the discussion was amplified later by Descartes (A.D. 1637). The general idea up to the time of Newton was that "colour" was a modification of light varying with the degree of refraction. About 1666 Newton began the series of experiments which showed that sunlight subjected to two refractions in passing through a prism gave rise to "rays" of differing colour which, if re-united by suitable optical means, would again produce white light. Light of one colour, when isolated, was shown to possess a particular degree of refrangibility (relative degree of refraction) associated with the colour, and it was further shown that such more or less "homogeneous" light suffered no change of colour by reflection, refraction, or absorption. Newton also showed that the sine law of refraction was obeyed by each coloured light separately, but no precise fixing or determination of that variation of light associated with a change of colour was possible until the time of Fraunhofer, who described the *dark* lines of the solar "spectrum."

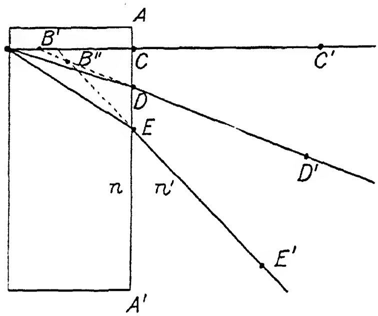

FIG. 8

The light from certain sources when dispersed by refraction through a prism is found to be resolved into a limited number of very homogeneous components, giving corresponding sharp bright lines in the spectrum. It is possible to measure a *precise* refractive index for the prism, corresponding to each line, and consequently we can first discuss the action of optical systems in homogeneous light on the basis of a *precise* law of refraction. The question of the dispersion of light, the properties of materials in this respect, and the production of a "spectrum" will receive fuller discussion in a later section.

Image Formation by Refraction. It is instructive to consider the

refraction of rays at a plane surface by tracing them geometrically (or practically with the aid of the familiar "pin method," using a slab of glass with polished parallel sides), as shown in Fig. 8. Light is imagined to be derived from an object point B, and the three rays, of which the first is normal to a refracting surface AA′, are found to have the paths CC′, DD′, and EE′ after refraction. An eye looking in the direction D′D sees the image somewhere along that line; if D′D and C′C are sufficiently close to enter the pupil of the eye together, the accommodation may be adjusted so as to bring these rays to a common focus on the retina; we then regard these two rays as if they were derived from a point B′ situated at the crossing point of C′C and D′D produced. This is the "image" of the object B. The object B lies in the medium of the object space, of refractive index n; the image B′ is considered to lie in the "image space" of refractive index n', for the imaginary part of a ray, such as B′D, derived from that image is not refracted at the position of the surface in actual space; the image is a *virtual* image like the one formed of a real object by a plane mirror. If $n' = 1$, then n is the refractive index of the medium containing B. Snell's law then gives the equation

$$\mathrm{BD} = n\mathrm{B'D}$$

and if C and D are close together we may write with near approximation,

$$\mathrm{BC} = n\mathrm{B'C}^*$$

Aberration from Refraction at a Plane Surface. Referring to Fig. 9, let B, as before, be an object point situated in a medium of refractive index n with a plane boundary perpendicular to the diagram and represented by its trace DK. We can again trace the course of a refracted ray emerging into a medium of refractive index unity.

In order to understand the directions taken up by these refracted rays, consider the ray BD refracted into the direction DP. BC is the normal to the surface; produce it to G where CG = BC, and lay a circle through the points B, D, and G. Now produce PD backwards to meet this circle in F. It is easy to show that the point F will lie on an ellipse with its focus at B and having a semi-major axis of length $n \cdot \mathrm{BC}$.

* If it is desired to measure the refractive index of some medium with a plane surface, a useful approximate method is to measure, first, the real depth, second, the apparent depth of some object situated a short distance (1 or 2 centimetres) below the surface. These measurements are conveniently made with a microscope carrying a 2-in. or 3-in. objective and possessing a scale to register the displacement of the microscope parallel to its axis. The surface may be located by focussing some fine dust upon it.

$$\text{Then refractive index} = \frac{\mathrm{BC}}{\mathrm{B'C}} = \frac{\text{real depth of B}}{\text{apparent depth}}$$

The angles of incidence and refraction are i and i' respectively, and consideration of the diagram will soon show that

$$\widehat{BFE} = \widehat{EFG} = i, \text{ while } \widehat{BEF} = \widehat{DEG} = i'$$

Hence $$\frac{BE}{BF} = \frac{\sin i}{\sin i'}, \text{ (from the triangle BEF)}$$

and $$\frac{EG}{FG} = \frac{\sin i}{\sin i'}, \text{ (from the triangle EFG)}$$

Whence $$\frac{BE + EG}{BF + FG} = \frac{\sin i}{\sin i'}, = \frac{1}{n}, \text{ or } BF + FG = n(BG)$$

The equality of BF + FG is a well-known property of an ellipse. It will pass through the point H where CH = nCB; the foci are at B and G.

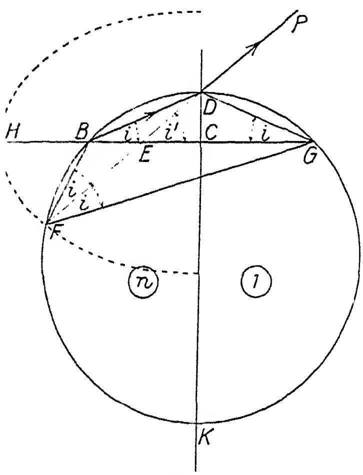

Fig. 9

It is easily proved that FD, the bisector of the angle between the lines from the foci to a point on the ellipse is normal to the curve at F. (Smith's *Conic Sections*, page 126.)

Hence, the directions of the refracted rays are all normals to the ellipse. The eccentricity of the ellipse is exaggerated in the figure to make its mode of departure from the circular form rather more evident.

It is instructive to construct the refracted ray for several successive positions of the point D (Fig. 9), when the intersection point of each pair of successive rays will be found to be different. Hence there is no single image point, as was found in the case of reflection at a plane surface; *the image is subject to aberration.* If we draw a great number of refracted rays they will be found to touch a curve which is called the *caustic*. Such a curve is shown in Fig. 10.

The caustic is the curve touched by all the refracted rays, and these are normals to the ellipse. (The ellipse is an orthomic curve to the rays). In geometrical language the caustic is the envelope of these normals, and is therefore the *evolute* of the ellipse.

The equation of the ellipse, taking HC as the axis of x, becomes

$$\frac{x^2}{n^2h^2} + \frac{y^2}{h^2(n^2 - 1)} = 1, \text{ where } h \text{ is the depth CB,}$$

and that of the evolute (the caustic) is

$$\left(\frac{n}{h}x\right)^{\frac{2}{3}} + \left\{\frac{\sqrt{(n^2-1)}}{h}y\right\}^{\frac{2}{3}} = 1.$$

Note that the caustic meets the line $y = 0$ in the point $x = \frac{h}{n}$, and the line $x = o$ in the point $y = h(n^2 - 1)^{-\frac{1}{2}}$, which would cause the incident ray at this place to fall at the critical angle.

Spherical Surfaces and their Importance in Applied Optics. A convex spherical surface formed on a stable material will exactly fit into a concave spherical surface of the same radius formed in another piece, in *any* relative positions. In the process of grinding two such surfaces together it will be understood that any excrescence remaining on either surface will have to bear a great proportion of the pressure which may be exerted to hold the pieces in contact, and therefore will be subject to proportionately great wear if the surfaces are moved relatively to each other; such wear can be greatly increased by the use of a suitable grinding material or abrasive. Hence the production of spherical surfaces of great accuracy of form is possible by more or less automatic working, and is not altogether dependent on human skill. As the most inexperienced draughtsman can produce a nearly perfect circle with the aid of a pair of compasses if he is trained to take a few simple precautions in their use, so the lens grinder produces surfaces which do not depart from the spherical form by so much as the ten-thousandth part of a millimetre, although it is true that in the latter case a far higher degree of skill is called for in managing the relative movement of the grinding surfaces, since these only consist, usually, of *segments* of spheres. The final smoothness and polish is the ultimate result of the increasing accuracy of form in the microscopic sense; polish is the result of a smoothness in which local irregularities are small in proportion to the wave-length of light.

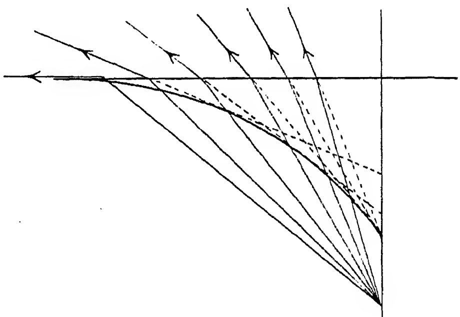

FIG. 10

In view of this comparative ease and certainty of production, the spherical surface is by far the most important of all forms of refracting surface. The majority of exact instruments are fitted with lenses having only spherical and plane surfaces. In some few cases accurate aspherical surfaces are employed in instruments, but

the largest use of non-spherical surfaces is in connection with the cylindrical and toric surfaces of spectacles in which the accuracy of figure is generally subject to a much greater tolerance, and, in fact, such surfaces usually show considerable errors when subjected to exact tests.

Trigonometrical Ray Tracing—Spherical Surfaces. The great majority of optical instruments are composed of lenses which are mounted co-axially, so that all the centres of curvature fall on the optical axis. Suitable choice of the components (i.e. proper selection of the refractive indices, radii of curvature, thicknesses, and separations) is required in order to obtain freedom from aberration in the final image.

In early days an approximation to the required construction was often arrived at by empirical trials, but when the alteration of radii

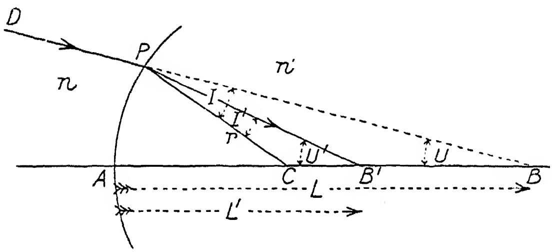

FIG. 11

was involved (requiring re-grinding and polishing), this was naturally an expensive and lengthy affair. By the beginning of the eighteenth century, however, astronomers like Flamsteed[2] tested their designs by the trigonometrical tracing of rays starting from some object point and passing through the system; in this way the union of the rays in the image point can be investigated and the defects of the system discovered. A design need not then be constructed in glass till it had been perfected by trials on paper. These trigonometrical trials are still of the greatest importance for all classes of optical instruments, including some types of spectacles, although methods have been developed whereby the approximate data for many types of optical systems may be calculated apart from empirical trials of any kind.

In the majority of cases the rays selected for tracing through a system of centred spherical surfaces lie in a plane containing the optical axis. In Fig. 11 the incident ray DP is defined by the point P (in which it intersects the trace of the spherical interface AP between media of refractive indices n and n') and the point B in

which it cuts the optical axis ACB passing through the centre of curvature C.

Similarly, the refracted ray will be determined by the point P and the point B′ in which it intersects the optical axis; since the incident ray lies in an axial plane, the refracted ray must also lie in the same plane, and therefore intersects the axis.

Distances measured to the right are counted positive; those to the left are negative. Similarly, those measured upwards perpendicular to the axis are positive and those measured downwards are negative.

The angles at which the ray directions meet the axis are counted positive if a clockwise turn will bring a line from the axis direction to the ray direction by the lesser angular movement. We adopt the following symbols for trigonometrical work—

AC $= r$ (the radius of curvature is positive when the centre lies to the right of the vertex, and negative when lying to the left of the vertex.)

$AB = L$	$PBA = U$	$CPB = I$
$AB' = L'$	$\widehat{PB'A} = U'$	$\widehat{CPB'} = I'$

The triangle PCB then gives $\quad \sin I = \dfrac{(L - r)}{r} \sin U \qquad$ (1) *m*

Also the law of refraction gives $\quad \sin I' = \dfrac{n}{n'} \sin I \qquad$ (2) *m*

It is also easily seen from the diagram that $PCA = U + I = U' + I'$ whence

$$U' = U + I - I' \quad . \quad . \quad . \quad . \qquad (3)\ m$$

The triangle PCB′ then gives

$$L' - r = \frac{r \sin I'}{\sin U'} \quad . \quad . \quad . \quad . \quad . \qquad (4)\ m$$

Lastly $\qquad L' = (L' - r) + r \qquad$ (5) *m*

These formulae are sufficient to calculate the final intersection distance of the refracted ray, and are of general utility.

Paraxial Rays. Imagine that the ray DP continues to pass through the point B when produced, but that the point P is brought so close to the axis that the inclination of the ray to the axis becomes very small; these conditions are characteristic of a "paraxial" ray. The angles U, U′, I, and I′ then become so small that their sines may be replaced by the angular values of the angles themselves.

Small type will be employed in formulae dealing with paraxial rays, so that we now have a new set of formulae corresponding to those above—

$$i = \frac{l-r}{r} u \quad . \quad . \quad . \quad . \quad . \quad (1)\ p$$

$$i' = \frac{i \,.\, n}{n'} \quad . \quad . \quad . \quad . \quad . \quad (2)\ p$$

$$u' = u + i - i' \quad . \quad . \quad . \quad . \quad (3)\ p$$

$$l' - r = \frac{r \,.\, i'}{u'} \quad . \quad . \quad . \quad . \quad . \quad (4)\ p$$

$$l' = (l' - r) + r \quad . \quad . \quad . \quad . \quad (5)\ p$$

In using the above paraxial formulae for calculation it will be noticed that the units in which the paraxial angles are measured have no significance in determining the final result. Hence it is possible to assume any numerical value for u in commencing a calculation. An example of the use of a logarithmic trace for two rays, of which one is a paraxial ray, will be given on page 19.

Suitable tables are those of Bremiker (five or six figures). Note that the numerical values of the angles are entered in the lower section as their logarithms are obtained during the course of the standard schedule. Hence, U′ and u' are found, which are needed to complete the calculation.

Note also that the initial log u in the paraxial work is taken as equal to log sin U in accordance with the freedom of choice of units mentioned above. In this way comparable figures are obtained in the paraxial and "marginal" schedules; in fact, the figures obtained when commencing a calculation with the same L and l in this way are the same (down to line 12) at first in both columns; but if it were desired to continue tracing the rays through another surface, say at a distance of + 1 cm., we should then have for the two rays

L (new surface) $= 28{\cdot}089 - 1{\cdot}0 = 27{\cdot}089$ $\quad$ $\mathrm{U} = 1^\circ\, 47'\, 22''$

l (,, ,,) $= 28{\cdot}701 - 1{\cdot}0 = 27{\cdot}701$ $\quad$ $u = 0{\cdot}03040$

and we would carry through the calculation just as before with these new data.

In some cases calculating machines are used rather than employing logarithm methods, but trigonometrical calculation should be used by beginners, as a record of each step in the calculation is thus obtained; in certain cases checks and additions are needed to the standard schedule above; the whole art of computing, even as far as it goes in the testing of optical systems by trigonometrical ray

tracing, is a large subject, while the analytical design of new systems is yet another. Professor Conrady's book on *Applied Optics and Optical Design* may be recommended to those who wish to go more deeply into these subjects.

DATA. $n = 1$ $\qquad$ $L = l = -25$ cm.
$n' = 1{\cdot}5207$ $\qquad$ $r = 5{\cdot}6$ cm.

Calculate l' and L' for $U = -2°$.

			Paraxial
L	− 25·0	l	− 25·0
subtract r	5·6		5·6
L − r	− 30·6		− 30·6
log sin U	8·54282 n *	log u	8·54282 n
add log (L − r)	1·48572 n		1·48572 n
Sum =	·02854		·02854
subtract log r	·74819		·74819
log sin I	9·28035	log i	9·28035
subtract log $\frac{n'}{n}$	·18204		·18204
log sin I′	9·09831	log i'	9·09831
add log r	·74819		·74819
Sum =	9·84650		9·84650
subtract log sin U′	8·49452	log u'	8·48287
log (L′ − r)	1·35198		1·36363
(L′ − r) =	22·489		23·101
add r	5·6		5·6
L′	28·089	l'	28·701
U	−2° 0′ 0″	u	− ·03490
add I	10 59 37	i	·19070
U + I	8 59 37	$u + i$	·15580
subtract I′	7 12 15	i'	·12540
U′	1 47 22	u'	·03040

* The n shows that the log is of a negative natural number. Also it is usual, in place of $\bar{2}$, to write 8 (i.e. 10 − 2), thus saving the use of a negative characteristic.

The graphical method explained in a previous paragraph is often useful when tracing rays through a system for the first time, as it keeps a clear picture of the progress of the rays before the computer and may help to avoid error. The rays should be traced graphically as the trigonometrical calculation proceeds.

The "Aplanatic"* Surfaces of a Sphere. There are one or two cases of special importance in connection with refraction at spherical surfaces which may now be considered. In Fig. 12 let P be a point on the circumference of a solid refracting sphere of radius r. The ray DP lies in the plane containing the radial line CB′B, and is

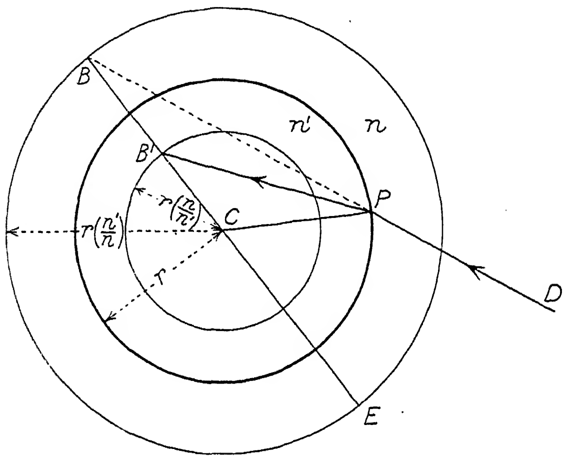

FIG. 12

directed towards the point B. The points B′ and B lie on the circumference of spheres struck with radii $\frac{rn}{n'}$ and $\frac{rn'}{n}$ respectively, where n' is the refractive index of the sphere, and n that of the medium surrounding it.

Then it may be shown that any ray DP directed towards the point B will be refracted so as to pass through B′; to this end it

* The full significance of the term "aplanatic" will only appear in a later section. From the above work, $\widehat{CBP} = \widehat{CPB'}$. Hence

$$\frac{\sin \widehat{CB'P}}{\sin \widehat{CBP}} = \frac{\sin \widehat{CB'P}}{\sin \widehat{CPB'}} = \frac{CP}{CB'} = \frac{n'}{n} \text{ (constant)}$$

This shows that the refraction fulfils the "sine condition"; it is free from both spherical aberration and coma. (See Chapter IV, page 112.)

by exact calculations, and it should be the aim always to understand how far the approximations actually depart from the truth.)

Particularly in the theory of ophthalmic lenses it has been usual to reserve the use of capital letters to denote the reciprocal of a length symbolized by the small letter. Thus, if r represents a radius of curvature, the symbol R may often be used to denote the curvature $\frac{1}{r}$. However, in order to save confusion as far as possible, the reciprocal quantities will be written in the cursive form, thus

$$\mathscr{R} = \frac{1}{r} = \text{curvature.}$$

$$\mathscr{L} = \frac{1}{l}, \text{ and so on.}$$

The computing equations above are given in the form used at the Imperial College, but it has been found that many elementary students have been accustomed to writing u and v for object and image distances in the manner used by Coddington. It is the general experience that it is more convenient to use the same letter for corresponding quantities in object and image spaces, distinguishing the latter by a " dash " (thus, l'), and we shall adhere to this usage adopted in the computing formulae, with the exception that the angles between ray and axis in the object and image space will be denoted by a and a'. The standard equations then become

$$\sin \mathrm{I} = \frac{(\mathrm{L} - r)}{r} \sin a \quad . \quad . \quad . \quad . \quad (1)$$

$$\sin \mathrm{I}' = \frac{n}{n'} \sin \mathrm{I} \quad . \quad . \quad . \quad . \quad (2)$$

$$a' = a + \mathrm{I} - \mathrm{I}' \quad . \quad . \quad . \quad . \quad (3)$$

$$\mathrm{L}' - r = \frac{r \sin \mathrm{I}'}{\sin a'} \quad . \quad . \quad . \quad . \quad . \quad (4)$$

$$\mathrm{L}' = (\mathrm{L}' - r) + r \quad . \quad . \quad . \quad . \quad (5)$$

in which the Roman capitals still stand for exact lengths.

Refraction of a Ray in the Axial Plane at a Spherical Surface. 1st *Approximation.* Formulae 1 and 4 of the section above give

$$\sin \mathrm{I} = \frac{\mathrm{L} - r}{r} \sin a$$

$$\sin \mathrm{I}' = \frac{\mathrm{L}' - r}{r} \sin a'$$

Dividing, we obtain

$$\frac{\sin \mathrm{I}}{\sin \mathrm{I}'} \quad \frac{n'}{n} = \frac{\mathrm{L} - r}{\mathrm{L}' - r} \cdot \frac{\sin a}{\sin a'}$$

whence (see Fig. 11)

$$\frac{n'}{n} \quad \frac{\mathrm{L} - r}{\mathrm{L}' - r} \cdot \frac{\mathrm{PB}'}{\mathrm{PB}}$$

When we restrict the rays concerned to the paraxial region so that AP is very small, then

$$PB = l, \text{ and } PB' = l', \text{ sufficiently nearly.}$$

Hence, in the paraxial form, the exact equation becomes reduced to,

$$\frac{n'}{n} = \frac{(l-r)l'}{(l'-r)l} \tag{6}$$

and thus
$$\frac{n'}{l'} - \frac{n}{l} = \frac{n'-n}{r} \tag{7}$$

It seems at first sight as if the calculation of l', given the other quantities, by means of this formula would be considerably shorter

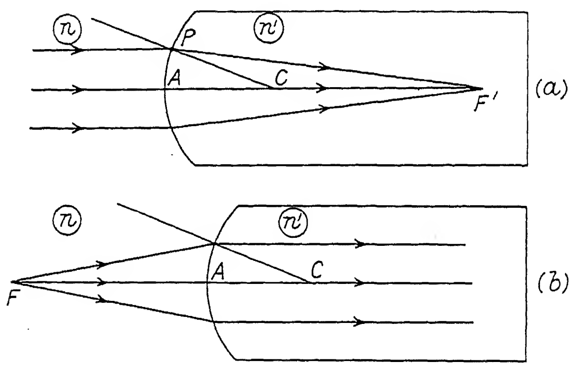

FIG. 15

than the logarithmic computation previously given; it is true that approximate results using tables of reciprocals can be obtained quickly, but if the calculation is to be performed to the same degree of accuracy as before the process will not be found to be shortened. The paraxial formula itself indicates that while AP (Fig. 11) is sufficiently small, any ray thus directed towards one point B at a distance l will be refracted towards a point B′ at a distance l' along the axis containing the centre C. The whole of the rays in a narrow cone with its apex at B will thus be refracted so as to form a fresh cone still narrow with its apex at B′. The formula holds also for rays diverging from one object point on the axis, and shows that they will after refraction pass through one image point or appear to diverge from it.

In the computing exercise, however, and in the preliminary discussion of "aplanatic" refraction, the exact paths of rays not

confined to the paraxial region were found, and further inquiry on these lines will show that the paraxial formula (exact for paraxial rays) generally gives a useful approximation also for the distances at which those rays cross the axis, which make appreciable angles with it, and so enable us quickly to calculate the results obtained with beams of larger apertures, such as are dealt with by optical instruments in practice. Further experience will teach the restrictions under which these approximations are of use.

The Focal Lengths of a Single Refracting Surface. Imagine an axial object point or source of light at an infinite distance away to the left from a spherical refracting surface. Such a source gives

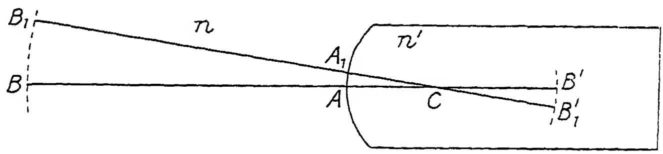

FIG. 16

rays which are parallel to the axis when reaching the refracting surface (Fig. 15A). If $l = -\infty$, equation (7) gives

$$l' = \frac{n'r}{(n'-n)} = f'$$

and this distance is called f', the *second focal length* of the refracting surface. On the other hand, if the rays are to be rendered parallel after refraction at the surface (Fig. 15B), $l' = +\infty$, and this requires $l = -\frac{nr}{(n'-n)} = f$. This distance is called f, the first focal length of the refracting surface. This notation distinguishes points relating to the image space by a " dash."

In cases where, as in Fig. 15, the incident light proceeding from left to right encounters a convex refracting surface of a medium of greater refractive index, the first focal point, F, is situated at a distance f, which will be numerically negative, from the surface, so that it lies to the left; the second focal point F′ at a distance f' (positive in this case) will lie to the right. Note especially that $\frac{f}{f'} = -\frac{n}{n'}$.

Students should draw the diagram showing the positions of the focal points for a case of a concave surface, and a selected pair of refractive indices. For the sake of clearness in the diagrams, rays are shown in Fig. 15 which are far outside the paraxial region.

Object of Finite Size. In Fig. 16 the points B and B′ represent an axial object and image respectively, the image being produced by refraction of a paraxial bundle of rays from B at the spherical surface shown with centre C and apex A. Let the line BCB′ rotate about the centre C, then the points B_1 and B_1', at the extremities of the line in a new position at a small angle with the first, must equally well represent object and image points, i.e. conjugate foci with respect to the same surface.

Therefore, while BB_1 and $B'B_1'$ are indefinitely small, they represent a small linear object and image, both perpendicular to BCB′. If the line BCB′ be taken as the optical axis, it is to be

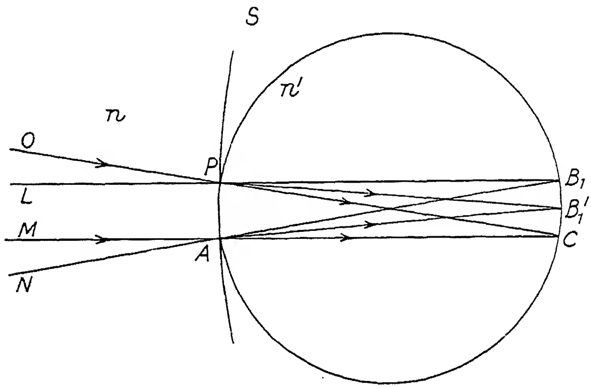

FIG. 17

noticed that rays are concerned in the " imaging " of B_1 which do not lie in a plane containing BCB′, as they may have all directions making small angles with $B_1 A_1 B_1'$.

The above reasoning applies satisfactorily only to objects and images which are not close to the centre of curvature of a surface. Therefore, in order to make the reasoning more general, it is necessary to show that a small linear object situated at the centre of curvature and perpendicular to the axis has also an image perpendicular to the axis.

In Fig. 17, C is the centre of curvature of the spherical refracting surface shown by its trace APS. The rays OPC and MAC are evidently radial, and suffer no change of direction at the surface. The rays NA and LP are, however, directed towards B_1, where B_1 is close to C, and lies on a circle laid through A, P, and C. We may consider CB_1 as a small virtual object perpendicular to the axis. The arc AP is also small, so that the discussion is confined to paraxial rays.

The angles $\widehat{OPL}$ and $\widehat{MAN}$ are clearly equal, and these are the angles of incidence of the rays LP and NA. Therefore the angles of refraction will be equal, and the refracted rays will be directed towards the point

B_1' on the arc of the same circle; also it is easily seen that $n'(CB_1')$ $= n(CB_1)$ very nearly. CB_1' is evidently to be regarded as the image.

The object and image in both instances are situated on spherical surfaces, and it will be shown in a later section that, in general, the curvature of the image surface corresponding to a plane object surface may be calculated from the properties of the optical system. Nevertheless, it is a useful conception that, bearing in mind the paraxial restrictions and dealing with small objects and images, we may conceive the planes of the object space in the neighbourhood of the axis to be represented by corresponding planes in the image space.

In corrected optical systems such as those of photographic lenses this correspondence may take on a much wider significance, and release itself from the restrictions of the paraxial region.

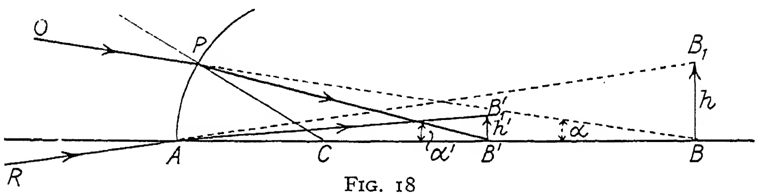

FIG. 18

Magnification. In Fig. 18, B' and B are the axial points of two "conjugate planes" in which an image of height h' and a virtual object of height h are found. As in previous cases, the perpendicular dimensions in the diagram are exaggerated for the sake of clarity.

The points B and B' are determined as in Fig. 11 by the axial crossing points of the incident and refracted rays, and we have

$$PB \sin \alpha = PB' \sin \alpha'$$

which under restriction to the paraxial limitations will give

$$l\alpha = l'\alpha'$$

with sufficiently close approximation.

The conjugate points B_1 and B_1' are determined, on the theory of conjugate planes, by the points in which these planes are intersected by the incident ray AB_1, and the refracted ray AB_1' respectively. The law of refraction gives—

$$\frac{nh}{AB_1} = \frac{n'h'}{AB_1'}$$

and again under the paraxial restriction this becomes, sufficiently nearly,

$$\frac{nh}{l} = \frac{n'h'}{l'} \quad . \quad . \quad . \quad . \quad . \quad (8)$$

Multiplying equation) by the second equation above we obtain the important relation

$$nh\alpha = n'h'\alpha' \qquad (9)$$

This relation, first used by R. Smith, has also been credited to Helmholtz and Lagrange. Huygens used it in a modified form. A form sometimes useful is

$$\frac{l'-r}{h'} \quad \frac{l-r}{h}$$

This is easily obtained by combining equation (8) with equation (6).

An Optical Invariant. The equation (9) is one of great importance. Imagining a system of centred co-axial refracting surfaces, the equation asserts that the product of the refractive index, the image height, and the angle of inclination of a ray intersecting the axis

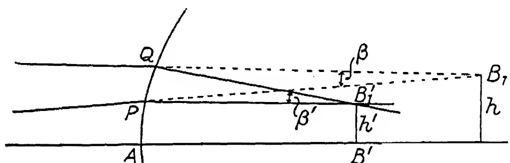

FIG. 19

in that image plane will be constant throughout the system. (The same ray is naturally to be considered always.) Thus for surfaces 1, 2, 3, etc.

$$n_1h_1\alpha_1 = n_2h_2\alpha_2 = n_3h_3\alpha_3$$

We now have all the material for building up a theory of the action of optical systems consisting of such a series of centred co-axial spherical refracting surfaces.

There is a rather wider meaning, however, which may be attached to the invariant formula (9), which is illustrated by Fig. 19. As usual, let APQ be the refracting surface and let P and Q be points on this surface through which rays are directed to the virtual object point B_1, making a small angle ($\widehat{QB_1P} = \beta$) with each other, which is small in the paraxial sense; both Q and P are supposed close to A, so that the discussion is again confined to paraxial rays. The refracted directions intersect in the image point at an angle β'.

Then under these restrictions

$$\beta l = \beta' l'$$

whence from equation (8)

$$nh\beta = n'h'\beta' \quad . \quad . \quad . \quad . \quad (10)$$

so that the invariant relation holds not only for angles α and α' made with the axis by a ray intersecting the axial points of object and image, but also for the angles β and β' between pairs of rays passing through conjugate points in the object and image spaces, that is, within the limitations set forth above.

The Thin Lens. The originators of the general theory of centred optical systems owed a great deal to the study of the properties of ordinary convex and concave thin lenses, which have been used for spectacles certainly since the thirteenth century. We shall study the properties of a single thin lens before going on to the general cases.

Consider a lens* of small aperture constructed of a medium of refractive index n to be bounded by two surfaces of radii r_1 and r_2 and to be situated in a medium of refractive index 1. Assuming an axial object point at a distance l from the vertex of the first surface, equation (7) gives for refraction at that surface

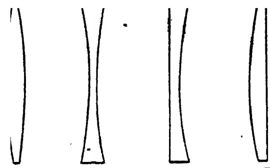

a b c d

FIG. 20

a = double convex.
b = double concave.
c = plano concave.
d = plano convex.

$$\frac{\quad}{l_1'} - \frac{\quad}{l_1} = \frac{n - 1}{r_1}$$

Note that "n" and "1" are written instead of n' and n in this equation. The "image" formed by refraction at the first surface now acts as the "object" for the second surface, and the general equation gives

$$\frac{1}{l_2'} \cdot \cdot \frac{n}{l_2} \qquad 1 - n$$

But if the lens be considered to be indefinitely thin, $l_1' = l_2$, and the two equations when added give

$$\frac{1}{l_2'} - \frac{1}{l_1} = (n - 1)\left(\frac{1}{r_1} - \frac{1}{r_2}\right)$$

For the present purpose the equation can be written simply

$$\frac{1}{l'} - \frac{1}{l} = (n - 1)\left(\frac{1}{r_1} - \frac{1}{r_2}\right) \quad . \quad . \quad . \quad (11)$$

where l' and l are axial distances of image and object measured "from the lens."

* Those who must consult a diagram for help may refer to Fig. 13, in which r_1 and r_2, as well as the distances of the axial conjugate points, are all positive; but the investigation is quite general for any type of thin lens. The lens of Fig. 13 obviously is not thin.

Fig. 20 represents various familiar forms of lenses. Evidently the lenses which are thicker at the axis than at the edge cannot be made indefinitely thin without reducing the diameter of the lens also indefinitely; therefore it is not surprising that the approximate theory is more generally accurate for those lenses which are thinnest in the middle. However, it is always useful for approximate calculation. Experience will teach the restrictions of use.

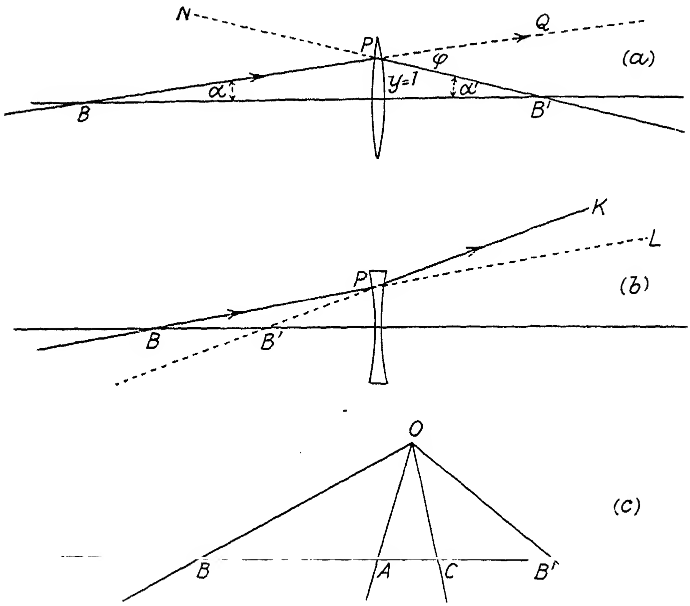

FIG. 21. GEOMETRICAL INTERPRETATION OF PARAXIAL FORMULAE

Taking an object at an infinite distance to the left (incident parallel light) we find, writing f' in place of l'

$$\frac{1}{f'} = (n-1)\left(\frac{1}{r_1}-\frac{1}{r_2}\right) = \frac{1}{l'}, -\frac{1}{l} \qquad (11a)$$

When l' is to be infinite, $l = -f'$. In this case l becomes f, then we have as in the case of a single refraction two "focal lengths" of opposite sign, but in this case equal numerically. Note that the refractive index of the object space is now identical with that of the final image space.

Geometrical Illustration of the "Thin Lens" Formula. Consider first the thin lens formula above, and refer to Fig. 21A, in which we represent a ray passing through the lens at unit distance from

the axis, and passing through the object and image points B and B′ at angles α and α' respectively with the axis. Then

$$\alpha = \frac{1}{l} \text{ and } \alpha' = \frac{1}{l'}$$

Note that α will be numerically negative in the diagram. But

$$\widehat{QPB'} = \phi = \widehat{PBB'} + \widehat{PB'B};$$

in this equation all the angles are treated as positive, so that

$$\phi = \alpha' + (-\alpha) = \frac{1}{l'} - \frac{1}{l} = \frac{1}{f'}$$

Thus, the equation implies that the numerical sum of the angles α and α' will be constant, and that the ray from the object point incident at unit height will suffer a constant deviation.

A wire bent thus into two straight pieces at an angle ($180° - \phi$) and pivoted at the junction at unit height from the axis could be swung into various positions; the crossing points of the axis with the wires will illustrate the relations of the conjugate points.

Imagining a clockwise rotation of the wires, BP will become parallel to the axis when B′ intersects the second principal focus F′; after a further rotation the object point is "virtual," and an additional wire added to the framework would be necessary if it were to be mechanically indicated. The addition is indicated by the dotted line PQ which would intersect the axis in the virtual object point. Similarly, imagining an anti-clockwise rotation, the point B′ travels outwards to an infinite distance when B coincides with the first principal focus, and the portion PB′ will no longer cross the axis; if, however, we add to the framework a portion PN (so that we now have simply two wires fixed at the angle ϕ) this fresh portion will serve to indicate the virtual image points which arise when the object is closer to the lens than the first principal focus.

It is very instructive to construct such a framework for a lens of, say, 4 in. focal length, taking y as 1 in., and to follow the various relative position of the object and image. PB and PB′ may be painted red; the other arms blue.

Fig. 21B represents the corresponding framework for a "diverging" lens, which is seen to bend the ray BP away from the axis into the direction PK. In this case the arms PB and PK of the framework may be coloured red, and PB′ and PL coloured blue.

Note that when PB is parallel to the axis the blue wire PB′ will mark the "second principal focus" which will be at a distance from the lens which is numerically negative; the sign of this second

principal focal length has often been taken as distinguishing between "positive" lenses (thicker in the middle, as in Fig. 21A) and negative lenses (thicker at the margin, as in Fig. 21B).

It is to be noted that a real wire framework of this kind does not quite correctly represent the paraxial formula, since the relative inclinations of the represented "rays" will be fairly large, but it will be useful for gaining first ideas.

Geometrical Interpretation of the Single Surface Formula. Formula (6) gave

$$\frac{(l-r)l'}{(l'-r)l} = \frac{n'}{n}$$

Applying this relation to the case of Fig. 16, where B and B′ represent conjugate points, A the apex of the refracting surface, and C the centre of curvature, we obtain (noting that l in Fig. 16 will be numerically negative while r is numerically positive, so that $(l-r)$ = CB (numerically negative)).

$$\frac{\mathrm{CB} \cdot \mathrm{AB}'}{\mathrm{CB}' \cdot \mathrm{AB}} = \frac{n'}{n}$$

In Fig. 21C set out B, A, C and B′ on a straight line and, taking any point O (for clearness it should be placed approximately as shown), join it to all these points and produce the lines beyond them. Imagine a perpendicular of length p dropped from O on the line BB′; we easily see that

$$\begin{aligned}
p \cdot \mathrm{CB} &= 2(\text{area of triangle OBC}) = \mathrm{OB} \cdot \mathrm{OC} \cdot \sin \widehat{\mathrm{COB}} \\
p \cdot \mathrm{AB}' &= \mathrm{OA} \cdot \mathrm{OB}' \sin \widehat{\mathrm{AOB}'} \\
p \cdot \mathrm{CB}' &= \mathrm{OC} \cdot \mathrm{OB}' \sin \widehat{\mathrm{COB}'} \\
p \cdot \mathrm{AB} &= \mathrm{OB} \cdot \mathrm{OA} \ \sin \widehat{\mathrm{AOB}}
\end{aligned}$$

$$\text{Hence, } \frac{\mathrm{CB} \cdot \mathrm{AB}'}{\mathrm{CB}' \cdot \mathrm{AB}} = \frac{\mathrm{OB} \cdot \mathrm{OC} \cdot \mathrm{OA} \cdot \mathrm{OB}' \cdot \sin \widehat{\mathrm{COB}} \cdot \sin \widehat{\mathrm{AOB}'}}{\mathrm{OC} \cdot \mathrm{OB}' \cdot \mathrm{OB} \cdot \mathrm{OA} \cdot \sin \widehat{\mathrm{COB}'} \cdot \sin \widehat{\mathrm{AOB}}} = \frac{\sin \widehat{\mathrm{COB}} \cdot \sin \widehat{\mathrm{AOB}'}}{\sin \widehat{\mathrm{COB}'} \cdot \sin \widehat{\mathrm{AOB}}}$$

If OB, OA, OC, OB′ represented a fixed framework of wires at definite angles, then the right-hand side of the above equation would be constant, and the condition of formula (6) would be fulfilled. In order to make the wires OB and OB′ mark the object and image points by their axial crossing point it will be sufficient to drive in

two pins at A and C, so that the fixed radius of curvature of the surface is taken into account. Then the framework will move over the pins and the wires OB and OB′ (or extensions which may be added to mark virtual points as above) will indicate the true positions of conjugate foci.

In geometry the ratio $\frac{\text{CB . AB}'}{\text{CB}' \text{. AB}}$, or $\frac{\text{CB}}{\text{AB}} : \frac{\text{CB}'}{\text{AB}'}$ is called the "cross ratio of the range CBAB′," and may be shown as above to be equal to the "cross ratio of the pencil" given by the ratio of the products of the sines given above. It is a case of so-called "collinear correspondence" between the object space and the image space, and was first worked out in the above form by Möbius.[1]

"Powers" of Lenses and Surfaces. The early classification of lenses (spectacle lenses) was in terms of "lens numbers." For an equi-convex lens of radii r

$$f' = \frac{r}{2(n-1)}$$

Since for the crown glass usually employed n was roughly 1·5, the focal length was nearly equal to the radius; the radius of the curve in inches gave the "lens number." On the Continent, amongst the units of length representing the English *inches* were the German *zolle* and the Parisian *pouce*, which were also used to give lens numbers, but owing to the disagreement in these units, there was considerable disagreement in lens specification; furthermore, the notation was inconvenient for short focus lenses.

In theoretical optics the conception of the "powers" of lenses and the "curvatures" of surfaces had proved very useful. Thus, the power of a lens is the reciprocal of the focal length; the curvature of a surface is the reciprocal of the radius of curvature. Writing $\mathscr{F}$ for "power" and $\mathscr{R}$ for curvature, the equation

$$\frac{1}{f'} = (n-1)\left(\frac{1}{r_1} - \frac{1}{r_2}\right)$$

becomes

$$\mathscr{F} = (n-1)(\mathscr{R}_1 - \mathscr{R}_2) \quad . \quad . \quad . \quad (11a)^*$$

and it is sometimes useful to write $\mathscr{R} = \mathscr{R}_1 - \mathscr{R}_2$, so that

$$\mathscr{F} = (n-1)\,\mathscr{R}$$

In dealing with spectacles, it is now usual to take the unit of length as 1 metre; the power of a spectacle lens is then the reciprocal of the focal length measured in metres, and the unit of power is then known as the "Diopter." This name for the unit of power

* See page 34, line 12, for an important note.

is ascribed to F. Monoyer of Strassburg, and was introduced in the seventies of last century. Nagel made a similar suggestion in 1868. In this system the "curvature" of a surface is the reciprocal of the radius in metres as first suggested by Herschel in 1827.

Lloyd has also introduced the term of "vergence." The "thin lens" formula,

$$\frac{1}{l'} - \frac{1}{l} = \frac{1}{f'}$$

may be re-written (under certain conditions, see Appendix, page 313).

$$\mathscr{L}' - \mathscr{L} = \mathscr{F} \qquad . \quad . \quad . \quad . \quad (11b)$$

where $\mathscr{L}'$ and $\mathscr{L}$ are the "vergencies" to image and object respectively. Note that in dealing with spectacles the focal power will invariably be $\frac{1}{f'}$, so that a "dash" to the $\mathscr{F}$ is unnecessary.

The equation

$$\frac{n'}{l'} - \frac{n}{l} = \frac{n' - n}{r_1}$$

can also be written in a simplified form in the notation of "reduced vergencies"; if

$$\bar{l} = \frac{l}{n} \text{ and } \bar{l}' = \frac{l'}{n'}$$

it then becomes

$$\frac{1}{\bar{l}'} - \frac{1}{\bar{l}} = \frac{n' - n}{r_1}$$

or, alternatively, if $\frac{n}{l} = \frac{1}{\bar{l}} = \bar{\mathscr{L}}$ and so on, the equation can then be written

$$\bar{\mathscr{L}}' - \bar{\mathscr{L}} = (n' - n)\,\mathscr{R}_1 = \mathscr{F}_1$$

where $\mathscr{F}_1$ is defined as the focal power of the surface.

In the case of a "thin lens," the equation becomes transformed thus—

$$\mathscr{L}' - \mathscr{L} = (n - 1)\left(\frac{1}{r_1} - \frac{1}{r_2}\right) = \frac{(n - 1)}{r_1} + \frac{(1 - n)}{r_2} = \mathscr{F}_1 + \mathscr{F}_2 = \mathscr{F}$$

Hence, the power of the lens is the sum of the powers of the two surfaces. It should be noted that the *power of a surface* is *not* in general the reciprocal of its focal length. Thus, in the general equation (7), when l is infinite

$$l' = f' = \frac{r_1 n'}{(n' - n)} \qquad \frac{n'}{\mathscr{F}_1}$$

It is often the case that expressions can be considerably simplified by introducing such symbols as are used above.

Calculation through a series of surfaces. When the "vergence" relations are used, the paraxial ray may be followed through a system of coaxial refracting surfaces as follows—

First surface: $\mathscr{L}_1' = \mathscr{L}_1 + \mathscr{F}_1$

For the second surface, at a distance d_1' from the first, we have—

$$l_2 = l_1' - d_1'$$

Dividing by the refractive index we obtain

$$\bar{l}_2 = \bar{l}_1' - \bar{d}_1'$$

or

$$\mathscr{L}_2 = \frac{1}{1 - \frac{\bar{d}_1'}{\bar{l}_1'}} \qquad \frac{\overline{\mathscr{L}}_1'}{1 - \bar{d}_1' \, \overline{\mathscr{L}}'_1}$$

Then $\overline{\mathscr{L}}_2' = \overline{\mathscr{L}}_2 + \mathscr{F}_2$, and so on.

Such a method may save time if the powers of the successive surfaces are given. A numerical example appears on page 149.

Owing to the reversibility of the path of a ray, such equations as the above can be used for tracing rays from left to right or from right to left; most simply if, *just for this purpose*, the "dash" denotes something measured in the medium lying to the right of a point or surface, and its absence denotes a corresponding value referred to the medium lying to the left. (See the Appendix to this book, on page 311.)

In the general equations the "dashed" and plain symbols refer to the object and image spaces respectively; the conditions under which they can be used for tracing the paths of rays from right to left without involving a change in the sign of the power of a lens or a surface are also examined in the appendix.

REFERENCE

[1] *Leipziger Berichte*, VII (1855), 8–32.

CHAPTER II

GENERAL THEORY OF OPTICAL SYSTEMS

THE simple laws which were known to relate the sizes and positions of objects and images in the simple cases of refraction of a paraxial bundle by a spherical surface, or by a thin lens, naturally led to attempts to extend these laws to more complex cases, such as a succession of spherical refracting surfaces with their centres on one axis.

The case of a centred system of thin lenses was discussed by Cotes, who investigated the relation between the angles made with the axis, by a ray in an axial plane, before and after refraction by the system. The treatment was given in R. Smith's *Compleat System of Opticks* (1738); the general case of a succession of refracting surfaces was also dealt with in this book, but not in a manner which has been found very convenient. Amongst other early workers in the field were Euler, and Lagrange, who derived general laws, but the greatest advance must be credited to Gauss.[1] His method was to apply the simple formulae to the case of successive refractions at a number of centred spherical surfaces separating media of different refractive indices; then by making certain substitutions he was able to express the final relation between the dimensions of the object and image spaces in a more general form, of a type which could always be obtained no matter what the number of refractions.

The work of Möbius (1855) indicated, however, that the "collinear" relationship found between the object and image spaces for a single refraction would entail as a direct consequence a geometrical relationship between the object and image spaces after any number of refractions, again of a type which would be independent of the construction of the optical system. Then in 1856 and 1858 Clerk Maxwell published a discussion of the properties of a "perfect" optical system in which the discussion of the "mechanism" of the image formation is not introduced, with the exception of the single provision that the image is formed by the union of rays which are straight lines in the object and image spaces.

The features of a "perfect" imagery in the sense imagined by Maxwell may be shortly stated as follows—

1. Every ray of a pencil passing through a single point of the object space must, after transmission, pass through a single point

of the image space. Failure to fulfil this condition may be termed *Astigmatism*.*

2. To every plane perpendicular to the axis in the object space there corresponds a plane also perpendicular to the axis in the image space. Failure to fulfil this condition may be termed *Curvature of the field*.

3. The image of any figure found in an image plane must be geometrically "similar" to the corresponding figure in the corresponding or "conjugate" object plane. Failure to fulfil this conditions may be known as *Distortion*.

From these premises Maxwell showed by means of simple geometrical considerations that if an instrument can be assumed to give perfect images of plane figures situated in two planes of the object space, perpendicular to the axis, the imagery will be perfect for all other pairs of conjugate planes.

A thorough collinear relation of this kind is, of course, free from restrictions as to angles of rays, sizes of object and image, and separations and radii of surfaces, but the results may only be applied to actual cases of image formation in so far as the system can be shown to fulfil the necessary conditions; thus, in the general case this theory only holds for the paraxial region, but its validity may be extended in special cases such as those of highly-corrected photographic lenses, which may be corrected for rays passing through the margins of the lenses and forming images at a comparatively large distance from the axis.

The method of discussion used by Abbe (1872), and developed independently of Maxwell, was to assume the existence of two pairs of conjugate planes for which the imagery is perfect in the Maxwellian sense. The two planes in the object space are parallel, and perpendicular to the axis of that space; likewise for the image space. The magnification for each pair of conjugate planes is assigned unique values, M_1 and M_2 (say); then it is shown that any other pair of conjugate planes must give perfect imagery and possess a unique value of the magnification.

Parallel rays in the object space are brought to a single focus in the second focal plane; rays from points in the first focal plane (in the object space) are rendered parallel in the image space. When the axial distances of conjugate planes are measured from these focal planes, specially simple relations are found to hold between such distances, and simple equations are also obtained for the magnification. The existence of a pair of planes for which the

* The term is here used in a more general sense than in the usual connotation, which will be explained in Chapter IV.

magnification is unity is evident from the possibility of choosing one, and only one, pair of conjugate planes to give any real value, positive or negative, of magnification.

The Abbe theory of general optical systems is available in English[2]; in the present book the main results will first be obtained in a more geometrical discussion.

The analytical relations between collinear or homographic spaces have been applied to the general theory of image formation by Czapski. The forms of the expressions giving the correlation of the two spaces lead at once to the equations of two planes of discontinuity which appear in the rôles of the focal planes. When these planes are chosen as reference planes, the equations giving the relations between co-ordinates of the object and image spaces can be put into specially simple forms. The general cases of image formation are comprised by the *obverse* and the *reverse* modes; the

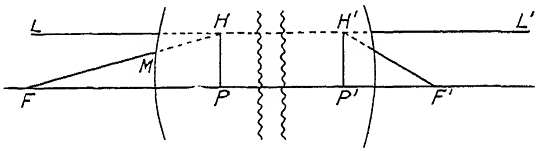

FIG. 22

first is characterized by the case of the pinhole camera, which gives an " upside down " *and* " right-to-left " reversal; the image formed by a plane mirror is a case of the " reverse " mode, since, for example, images in a vertical mirror exhibit a right-to-left reversal, but no inversion.

These geometrical and analytical discussions have a considerable academic interest, but so far as applied optics is concerned they are not essential, and the main results can be obtained with facility (if not by rigorous argument) by the simple geometrical treatment which follows.

A Perfect Optical System. Let us postulate for a beginning a " perfect " optical system having one axis of symmetry. A ray LH (Fig. 22), parallel to the axis, will, in general, after passing through the system, be inclined at an angle to the axis, and will pass through the axial point F′. All rays parallel to the axis in the object space will therefore pass through F′, since they may be regarded as derived from one point at an infinite distance. The point F′ is the *second principal focus* of the system.

Produce the line LH to L′; let it cut the final direction of the refracted ray in the point H′.

In the object space there must be some axial point F from which the rays, after refraction by the system, are parallel to the axis in the image space; let F represent this point, and let the line FMH represent a ray which, after refraction, takes the final path represented by the same line HL′. These rays must now lie all in one axial plane.

Referring now to Maxwell's first condition, the point H represents the crossing point of two rays in the object space, and the point H′ is the corresponding point of the image space. Dropping perpendiculars HP, H′P′ to the axis, we obtain the traces of the so-called *principal planes*. **HP and H′P′ may be regarded as object and image, and the magnification is evidently unity.**

The distances PF and P′F′ are the *focal lengths* of the system; they will be denoted by f and f' respectively.

The most valuable property of the principal planes is that any ray of the object space, passing through a point H of the first plane

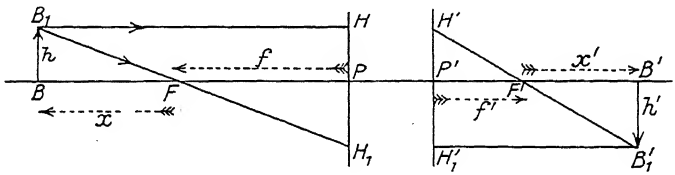

FIG. 23

at a particular distance y from the axis, must pass through the conjugate image point H′ in the second principal plane (in the image space); since the magnification is unity, H′ will be at the same distance y from the axis.

Construction to Find the Image. The principal planes and focal points are supposed to be given. Referring to Fig. 23, the construction is shown by which the image in the plane through B′, corresponding to the object at B, can be found. It is evidently sufficient to trace two rays from the object space into the image space. The first one is parallel to the axis, and intersects the first principal plane in the point H; after refraction it must leave the second principal plane from the point H′ (where P′H′ = PH) and pass through the second principal focus F′. The other ray passes through the first principal focus F, as shown, and is parallel to the axis after refraction; its distance from the axis in the image space is found from the distance at which it intersects the first principal plane. Note that PH = h and $P'H'_1 = h'$, where h and h' are the heights of object BB_1 and image $B'B_1'$, respectively.

We had $$PF = f, \quad P'F' = f'$$

magnification is unity is evident from the possibility of choosing one, and only one, pair of conjugate planes to give any real value, positive or negative, of magnification.

The Abbe theory of general optical systems is available in English[2]; in the present book the main results will first be obtained in a more geometrical discussion.

The analytical relations between collinear or homographic spaces have been applied to the general theory of image formation by Czapski. The forms of the expressions giving the correlation of the two spaces lead at once to the equations of two planes of discontinuity which appear in the rôles of the focal planes. When these planes are chosen as reference planes, the equations giving the relations between co-ordinates of the object and image spaces can be put into specially simple forms. The general cases of image formation are comprised by the *obverse* and the *reverse* modes; the

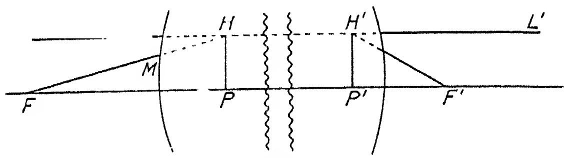

Fig. 22

first is characterized by the case of the pinhole camera, which gives an " upside down " *and* " right-to-left " reversal; the image formed by a plane mirror is a case of the " reverse " mode, since, for example, images in a vertical mirror exhibit a right-to-left reversal, but no inversion.

These geometrical and analytical discussions have a considerable academic interest, but so far as applied optics is concerned they are not essential, and the main results can be obtained with facility (if not by rigorous argument) by the simple geometrical treatment which follows.

A Perfect Optical System. Let us postulate for a beginning a " perfect " optical system having one axis of symmetry. A ray LH (Fig. 22), parallel to the axis, will, in general, after passing through the system, be inclined at an angle to the axis, and will pass through the axial point F′. All rays parallel to the axis in the object space will therefore pass through F′, since they may be regarded as derived from one point at an infinite distance. The point F′ is the *second principal focus* of the system.

Produce the line LH to L′; let it cut the final direction of the refracted ray in the point H′.

In the object space there must be some axial point F from which the rays, after refraction by the system, are parallel to the axis in the image space; let F represent this point, and let the line FMH represent a ray which, after refraction, takes the final path represented by the same line HL′. These rays must now lie all in one axial plane.

Referring now to Maxwell's first condition, the point H represents the crossing point of two rays in the object space, and the point H′ is the corresponding point of the image space. Dropping perpendiculars HP, H′P′ to the axis, we obtain the traces of the so-called *principal planes*. **HP and H′P′ may be regarded as object and image, and the magnification is evidently unity.**

The distances PF and P′F′ are the *focal lengths* of the system; they will be denoted by f and f' respectively.

The most valuable property of the principal planes is that any ray of the object space, passing through a point H of the first plane

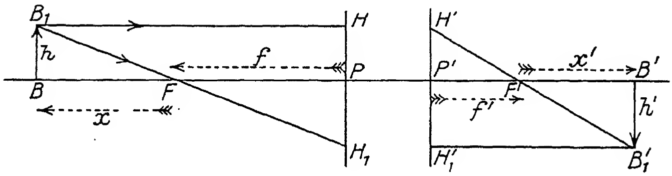

FIG. 23

at a particular distance y from the axis, must pass through the conjugate image point H′ in the second principal plane (in the image space); since the magnification is unity, H′ will be at the same distance y from the axis.

Construction to Find the Image. The principal planes and focal points are supposed to be given. Referring to Fig. 23, the construction is shown by which the image in the plane through B′, corresponding to the object at B, can be found. It is evidently sufficient to trace two rays from the object space into the image space. The first one is parallel to the axis, and intersects the first principal plane in the point H; after refraction it must leave the second principal plane from the point H′ (where P′H′ = PH) and pass through the second principal focus F′. The other ray passes through the first principal focus F, as shown, and is parallel to the axis after refraction; its distance from the axis in the image space is found from the distance at which it intersects the first principal plane. Note that PH = h and $P'H'_1 = h'$, where h and h' are the heights of object BB_1 and image $B'B_1'$, respectively.

We had $$PF = f, \quad P'F' = f'$$

Let $$\mathrm{FB} = x, \quad \mathrm{F'B'} = x'$$

(Note that " FB " means the distance measured *from* F *to* B, and similarly.) It will be found that the equations below are in accordance with the sign conventions now in use (page 17).

Then, from the similar triangles in the figure

$$\frac{h}{h'} = -\frac{x}{f} \qquad (12)$$

$$\frac{h'}{h} = -\frac{x'}{f'} \qquad (13)$$

and by multiplying corresponding sides of the two equations we obtain

$$xx' = ff' \qquad (14)$$

This relation was known to Newton, in a special form, and is sometimes called after his name.

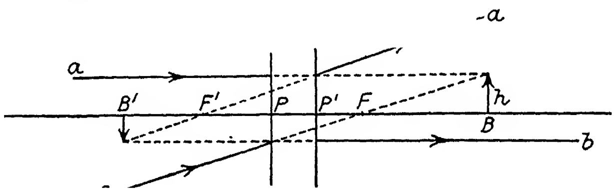

FIG. 24

It is to be noted that these equations are not dependent upon the particular positions assigned to the principal planes and focal planes; the form of the equations remains the same if, for example, P is shown to the left of F, although the diagrams then look different.

The student should himself draw the diagram for the case when F and F′ interchange the positions they have in Fig. 23; this will correspond in practice to the case typified by a double concave lens which causes a parallel bundle to diverge after transmission. It is recommended that the rays of the image space shall be drawn in red in order to distinguish them. When this is done it will be evident that the object space interpenetrates the image space; an object or a virtual object may be situated in *any* position relative to an optical system. Fig. 24 shows the construction when the object is virtual and is situated to the right of such a " diverging " system; the image is found also to be virtual and situated to the left of the system. The equations are still valid.

To Trace any Ray from the Object Space into the Image Space. Let P, F, P′, F′, be the axial points of the principal and focal planes

in the object and image spaces. Let (*a*), Fig. 25, be any ray in the object space; it is desired to find its direction in the image space.*

Draw the ray (*b*) in the object space passing through F and parallel to (*a*). These parallel rays will meet in one point of the second focal plane. The distances at which they cross the second principal plane are known, for these are determined by the distances in the first

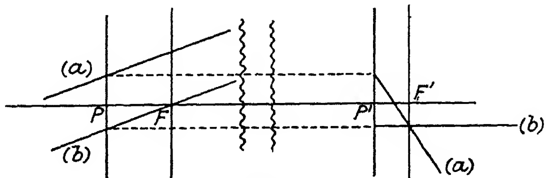

FIG. 25

principal plane. The path of ray (*b*) is completely known, since it travels parallel to the axis in the image space; hence the point at which it cuts the second focal plane is known, and this is the second of the two required points on the path of ray (*a*) in the image space.

A similar method is obviously possible for a ray not lying in an axial plane.

Relation between Positions of Conjugate Planes. Fig. 26 illustrates a simple graphical method of exhibiting the relations between the

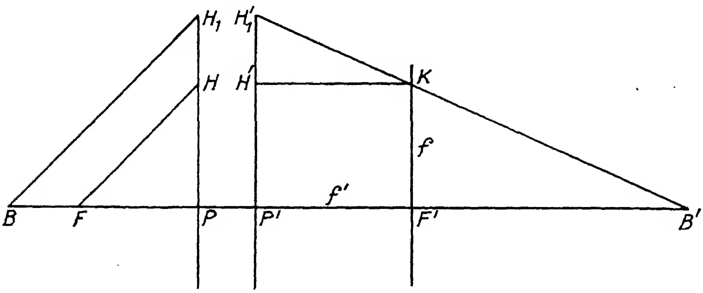

FIG. 26

positions of axial object and image points B and B′ respectively. PH is made equal to FP, and BH_1 is drawn parallel to FH. The path of these "rays" in the image space is then determined; both pass through the point K in the second focal plane, of which the co-ordinates with respect to the axes P′F′ and P′H′ are numerically

* Fig. 25 may appear unfamiliar, but it is useful to practise changing the relative positions of principal and focal planes. The student should draw the figure for the more usual case.

equal to f' and f respectively. Hence the construction to find the image point is to make $P'H_1' = BP$, join $H_1'K'$ and produce to meet the axis in B′.

The Nodal Points of an Optical System. The focal points and principal planes of an optical system are shown, as before, in Fig. 27. It is desired to find under what conditions a point on the axis can be found in the object space so that a ray directed towards it will, after transmission by the system, leave the conjugate point in the image space at an equal angle with the axis.

Start by taking any point K in the second focal plane through which the ray H′K travels parallel to the axis. The path of the corresponding ray in the object space is FH; the rays cut the principal planes in the points H and H′ at the same distance from the axis.

Through K draw the line $KN'H_1'$ parallel to FH, cutting the axis in N′ and the second principal plane in H_1'; taking H_1 in the first

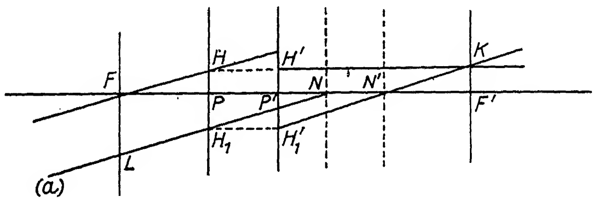

FIG. 27

principal plane so that $PH_1 = P'H_1'$, draw the line LH_1N parallel to $H_1'K$, cutting the first focal plane in L, the first principal plane in H_1, and the axis in N. Then FH and LH_1 may represent parallel rays of the object space meeting in K after transmission, and the ray LH_1N is one for which the paths before and after transmission are parallel.

We have thus obtained a system with two points N and N′ fulfilling the condition required above; it remains to examine the location of N and N′. They are the *Nodal Points* of the system.

Since the figure $NH_1H_1'N'$ is a parallelogram, $H_1H_1' = PP' = NN'$. Again, since $FL = HH_1 = H'H_1'$, it will be clear from the construction that the triangles FLN and $H'H_1'K$ are equal in all respects, and hence $FN = H'K = P'F'$, showing that N is a fixed point independent of the inclination of the ray LN.

It is also seen from the triangles FPH and N′F′K that $F'N' = PF$, showing that N′ is also fixed with regard to the other points of the system.

From the above equations it follows that

$$\frac{\mathrm{FP}}{\mathrm{FN}} = \frac{\mathrm{F'N'}}{\mathrm{F'P'}} = -\frac{f}{f'}$$

The Nodal Planes. Since N and N′ are axial conjugate points, the planes perpendicular to the axis passing through these points are conjugate planes. An object in the first has an image in the second. The magnification is obtained from equation (13),

$$\frac{h'}{h} = -\frac{x'}{f'} = -\frac{\mathrm{F'N'}}{f'} = -\frac{\mathrm{PF}}{f'} = -\frac{f}{f'}$$

It follows at once from the equations above that in cases when the two focal lengths are numerically equal, and $f' = -f$, the nodal and principal planes will coincide, and the "magnification" will be unity.

Longitudinal Magnification. The formula,

$$xx' = ff'$$

when differentiated gives

$$x' + x \cdot \frac{dx'}{dx} = 0 \quad \text{or} \quad \frac{dx'}{dx} = -\frac{x'}{x}$$

Dividing equation (13) by (12)

$$\frac{x'}{x} = \left(\frac{h'}{h}\right)^2 \cdot \frac{f'}{f}$$

Hence, $$\frac{dx'}{dx} = -\left(\frac{h'}{h}\right)^2 \cdot \frac{f'}{f} \qquad . \quad . \quad . \qquad (14)^*$$

This formula throws light on the relation between the space representation in the axial direction as compared with the representation of dimensions perpendicular to the axis. In the case of an undistorted presentation, $\frac{dx'}{dx}$ would be directly proportional to the magnification $\left(\frac{h'}{h}\right)$ instead of to the square of this ratio.

Combination of Two Systems. The next step is the investigation of the position of the principal and focal planes of a combination of two systems for which the data are known and which are co-axial.

Fig. 28 represents the focal and principal planes of two co-axial

* It will be proved below that $-\left(\frac{f'}{f}\right) = \frac{n'}{n}$ where n' and n are the refractive indices of object and image spaces; hence, $\frac{dx'}{dx} = \left(\frac{h'}{h}\right)^2 \frac{n'}{n}$.

systems, a and b (*met by the light in the order* a, b), of which the "adjacent" focal points are situated so that

$$F_a'F_b = g$$

There is no restriction as to the media in which the systems are placed, but of course there must be no change of medium between the two systems. Since it must be granted from the general theory that the principal and focal planes of the combination exist, it is simple to proceed by finding that axial point of the object space, a ray from which is rendered parallel to the axis in the final image space after the double transmission.

Any ray passing through the first focal point F_b of the system (b) must fulfil this condition; such a ray is shown in the diagram by $H_a'F_bH_b$, and it cuts the second focal plane of system (a) in the point J. What was its course before refraction by (a)?

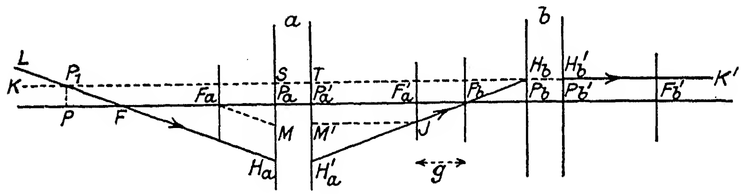

FIG. 28

If the ray M'J', parallel to the axis and cutting the second principal plane of (a) in the point M' be drawn, its course before transmission by system (a) must pass through both F_a and M, where M lies in the first principal plane so that $P_aM = P_a'M'$. Now since there are two rays which meet in the point J in the second focal plane of (a), their courses must have been parallel before transmission by (a), and the required path LH_a becomes known; it cuts the axis in the point F, which is recognized as the first focal point of the combination.

If the *final* path $H_b'K'$ of this same ray be produced backwards to K it will intersect the initial path LH_a in the point P_1. Wherever the second principal plane of the combination is situated, the intersection height of the final path of the ray with this plane must be equal to H_bP_b in the diagram, and this is equal to P_1P where P is the foot of the perpendicular dropped from P_1 to the axis.

The initial path of a ray entering a system intersects the first principal plane at the same height from the axis as that with which the final path intersects the second principal plane. Hence P_1P must lie in the first principal plane of the combination, since P_1

is (in general) the only point on the incident ray at the required distance from the axis.

From the above construction the following relations are derived—

$$\frac{P_1P}{PF} = \frac{P_aM}{F_aP_a} \qquad (a) \text{ and } \frac{F_bP_b}{H_bP_b} \quad \frac{F_a'F_b}{F_a'J}$$

From the second of these relations, putting $F_a'J = P_aM$, and $H_bP_b = P_1P$, we obtain

$$\frac{F_bP_b}{P_1P} = \frac{F_a'F_b}{P_aM} \quad . \quad . \quad . \quad . \quad . \quad . \quad . \qquad (b)$$

Multiplying corresponding sides of (a) and (b), we then obtain

$$\frac{F_bP_b}{PF} = \frac{F_a'F_b}{F_aP_a} \text{ or } -\frac{f_b}{f} = -\frac{g}{f_a}$$

where f is written for PF, giving

$$f = \frac{f_af_b}{g} \quad . \quad . \qquad (15)$$

Let the separation of "adjacent" principal points, $P_a'P_b = d$. If the line KK′ parallel to the axis cuts the first and second principal planes of (a) in the points S and T respectively,

$$\frac{F_a'F_b}{P_a'P_b} = \frac{P_a'M'}{TH_a'} = \frac{P_aM}{SH_a}$$

Also $$\frac{P_aF_a}{P_aP} = \frac{P_aM}{SH_a}$$

whence $$\frac{P_aF_a}{P_aP} = \frac{F_a'F_b}{P_a'P_b}, \text{ or } \frac{f_a}{P_aP} = \frac{g}{d}, \text{ or } P_aP = \frac{f_ad}{g} \qquad (16)$$

In a similar manner it may be shown that

$$f' = -\frac{f_a'f_b'}{g} \qquad (17)$$

and $$P_b'P' = \frac{f_b'd}{g} \qquad (18)$$

The student should draw the necessary diagrams and work out the two last formulae for himself.

The above formulae are sufficient for the calculation of the positions of the focal and principal planes of combinations with more than two members, since they can be combined in pairs till the constants of the whole system are obtained.

Application of the General Theory. The discussion of cases of

refraction at curved surfaces, which led up to the formulae concerning the thin lens, and the general relations between the object and image spaces for a single refraction when narrow pencils are dealt with, indicated that the Maxwellian conditions of perfect imagery are likely to be generally valid only in so far as rays are confined to the paraxial region, and images are comparatively small. While this is true, there are many cases in which useful approximations can be obtained by the theory.

The inquiry may first be made under what circumstances the focal lengths of a system will differ numerically. In Fig. 29 the focal and principal planes of a "perfect" system are shown, but the angles of the rays with the axis are large. *The diagram can best be regarded as representing a possible case of the action of a real lens system, if it be assumed that all distances shown perpendicular to the axis are represented on a greatly enlarged scale;* in fact, this applies

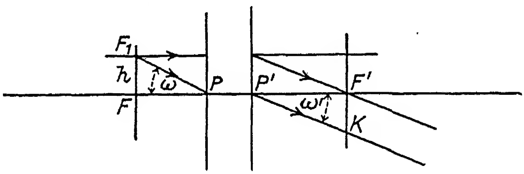

FIG. 29

to the great majority of the cases in which such diagrams are employed.

F_1 represents, then, a point very near the axis in the first focal plane; the ray F_1P is traced through the system by the usual method. According to our conventions, the geometry of the figure allows us to write for the angles ω and ω' which the ray makes with the axis at P and P'

$$\tan \omega = -\frac{h}{f} \text{ and } \tan \omega' = \frac{h}{f'}$$

where $h = FF_1 = KF'$; when ω and ω' are very small these relations give

$$f\omega = -f'\omega'$$

But the Lagrange relation (9), $nha = n'h'a'$, applied to the present case, gives $nh\omega = n'h'\omega'$ where the h and h' refer to the sizes of object and image in the conjugate planes represented by the axial crossing points of one ray; in the case above, these points are P and P', the axial points of the unit planes where $h = h'$. Hence, in this case

$$n\omega = n'\omega'$$

and since $$f\omega = -f'\omega'$$

$$\frac{n}{f} = -\frac{n}{f'} \quad . \quad . \quad . \quad . \quad (19)$$

A system will have numerically different focal lengths, then, when the initial and final media are not the same; a typical case is the human eye, for which the anterior focal length in air may be taken as $-16 \cdot 8$ mm., while the posterior focal length is $22 \cdot 4$ mm., the object space being filled with the "vitreous humour," of refractive index about $1 \cdot 33$.

Power of a Series of Optical Systems or Surfaces. Fig. 27 shows a pair of parallel rays entering an optical system at an angle ω (say) with the axis. One of them passes through the first focal point. They intersect in the second focal plane at a distance h' from the axis where

$$h' = f \tan \omega$$

In the "reduced" notation, equation (8) becomes

$$h\,\overline{\mathscr{L}} = h'\,\overline{\mathscr{L}}'$$

and this equation can be applied to any series of refracting surfaces or optical systems, so that

$$\frac{h_1'}{h_1} = \frac{\overline{\mathscr{L}}_1}{\overline{\mathscr{L}}_1'}, \quad \frac{h_2'}{h_2} = \frac{\overline{\mathscr{L}}_2}{\overline{\mathscr{L}}_2'}, \text{ etc.}$$

and since $h_2 = h_1'$ being identical, we have for k elements

$$m = \frac{h_k'}{h_1} = \frac{\overline{\mathscr{L}}_1 \times \overline{\mathscr{L}}_2 \times \qquad \overline{\mathscr{L}}_k}{\overline{\mathscr{L}}_1' \times \overline{\mathscr{L}}_2' \times \qquad \overline{\mathscr{L}}_1'} = \prod_0^k \frac{\overline{\mathscr{L}}}{\overline{\mathscr{L}}'}$$

If the original object is at an infinite distance then we can imagine two stars, one on the axis, the other sending a parallel beam into the system at an angle ω with the axis. The images are found in the final focal plane at a distance $h_k' = f \tan \omega$ where f is the first focal length of the whole combination.

For the corresponding image size formed by the first element we have

$$h_1' = f_1 \tan \omega$$

and hence the final h_k' is given by

$$h_k' = f_1 \tan \omega \prod_2^k \frac{\overline{\mathscr{L}}}{\overline{\mathscr{L}}'} = f \tan \omega$$

Hence, if we calculate the values of $\overline{\mathscr{L}}$ and $\overline{\mathscr{L}}'$ arising in the refraction of a paraxial ray (originally parallel to the axis) through

the system we can find the focal length of the combination by the relations

$$f = f_1 \prod_2^k \frac{\overline{\mathscr{L}}}{\overline{\mathscr{L}'}}$$

By tracing light through the system in the opposite direction in an exactly similar manner we could obtain the second focal length

$$f' = f_k' \prod_{k-1}^{1} \frac{\overline{\mathscr{L}}}{\overline{\mathscr{L}'}}$$

but otherwise it is easily calculated by equation (19). The paraxial trace gives also, on a final result, the position of the second focal point. The position of the second principal point is found at a distance of $-f'$ from the second focal point.

Numerical Example. Schematic Eye. Gullstrand has given figures for a simple optical system intended closely to imitate the optical action of the human eye. (A more complex arrangement is detailed in Chapter V.) This " schematic eye " has three refracting surfaces of which the first is the convexity of the cornea, and the second and third enclose the crystalline lens, imagined as embedded in a single medium. The lengths are given in metres.

$r_1 = 0{\cdot}0078.$ Humour: $n = 1{\cdot}336,\quad d_1 = 0{\cdot}0036$

$r_2 = 0{\cdot}01.$ Crystalline: $n = 1{\cdot}4130,\ d_2 = 0{\cdot}0036$

$r_3 = -\,0{\cdot}0060.$ Humour: $n = 1{\cdot}336$

The calculation for the vergencies and focal lengths is shown on page 49.

From the table $\overline{\mathscr{L}_3}' = 78{\cdot}75$, whence $l_3' = 1{\cdot}336/78{\cdot}75$ m. $=$ 16·97 mm.

Therefore the distance of the second focal point from the cornea $= 16{\cdot}97 + d_1 + d_2 = 24{\cdot}17$ mm. The focal length

$$f = f_1 \prod_2^3 \frac{\overline{\mathscr{L}}}{\overline{\mathscr{L}'}} = -\,23{\cdot}22 \times 0{\cdot}8634 \times 0{\cdot}8370 = -\,16{\cdot}78 \text{ mm.}$$

$$f' = -\frac{n'}{n} f = 1{\cdot}336 \times 16{\cdot}78 = 22{\cdot}42 \text{ mm.}$$

The second principal point is found at a distance from the cornea

$$= 24{\cdot}17 - 22{\cdot}42 = 1{\cdot}75 \text{ mm.}$$

$$\text{Power of eye} = \frac{1}{{\cdot}01678} = \frac{1{\cdot}336}{{\cdot}02242} = 59{\cdot}59 \text{ diopters.}$$

FORMULAE: $\overline{\mathscr{L}}' = \overline{\mathscr{L}} + \mathscr{F}$ $\quad \overline{\mathscr{L}}_2 = \dfrac{\overline{\mathscr{L}}_1'}{1 - \bar{d}\,\overline{\mathscr{L}}_1'} = \dfrac{1}{\left(\dfrac{1}{\overline{\mathscr{L}}_1'} - \bar{d}\right)}$

	1st Surface		2nd Surface		3rd Surface	
	Number	Logarithm	Number	Logarithm	Number	Logarithm
n	1·0000		1·3360	·1258	1·4130	0·1501
r	0·0078	$\bar{3}$·8921	0·0100	$\bar{2}$·0000	− 0·0060	$\bar{3}$·7782n
n'	1·3360	0·1258	1·4130	·1501	1·3360	0·1258
d	0·0036	$\bar{3}$·5563	0·0036	$\bar{3}$·5563		
$\bar{d}$	0·002694	$\bar{3}$·4305	0·002548	$\bar{3}$·4062		
$n' - n$	0·3360	$\bar{1}$·5263	0·0770	$\bar{2}$·8865	- 0·0770	$\bar{2}$·8865n
$\mathscr{R}$	128·2	2·1079	100·0	2·0000	− 166·67	2·2218n
$\mathscr{F}$	43·07	1·6342	7·70	0·8865	12·83	1·1083
f (mm.)	− 23·22	1·3658n				
f' (mm.)	31·02	1·4916				
$\overline{\mathscr{L}}$	0		48·71	1·6876	65·92	1·8190
$\overline{\mathscr{L}}'$	43·07	1·6342	56·41	1·7514	78·75	1·8963
$1/\overline{\mathscr{L}}$	0·02322	$\bar{2}$·3658	0·01772	$\bar{2}$·2486	0·01269	$\bar{2}$·1037
$1/\overline{\mathscr{L}}' - \bar{d}$	0·02053	$\bar{2}$·3124	0·01517	$\bar{2}$·1810		
$\overline{\mathscr{L}}'/(1 - \bar{d}\overline{\mathscr{L}}')$	48·71	1·6876	65·92	1·8190		
$\overline{\mathscr{L}}/\overline{\mathscr{L}}'$			0·8634	$\bar{1}$·9362	0·8370	$\bar{1}$·9227

Equation for Distances of Conjugate Foci from Principal Points of a Lens System. Let a ray passing through an axial object point intersect the 1st principal plane at unit height, then if l is the distance measured from the first principal point to the object, and l' the distance from the second principal point to the image,

$$\alpha = \frac{1}{l} \quad \text{and} \quad \alpha' = \frac{1}{l'}$$

The Lagrange relation gives

$$\frac{h'}{h} = \frac{n\alpha}{n'\alpha'}$$

and by equation (13), $\dfrac{h'}{h} = -\dfrac{x'}{f'}$

Then $$\frac{n\alpha}{n'\alpha'} = \frac{nl'}{n'l} = -\frac{x'}{f'}$$

Subtract unity from each side, then

$$\frac{nl' - n'l}{n'l} = -\frac{(x' + f')}{f'} \quad -\frac{l'}{f'}$$

$$nl' - n'l = -\frac{n'll'}{f'}$$

The final form is

$$\frac{n'}{l'} - \frac{n}{l} = \frac{n'}{f'} = -\frac{n}{f} \tag{20}$$

This formula may be compared with the similar one for a single surface, in which the principal points are coincident at the vertex.

Two Coaxial Lenses in Air. Let each lens be treated as "thin," then the principal planes of such a thin lens are no longer separated.

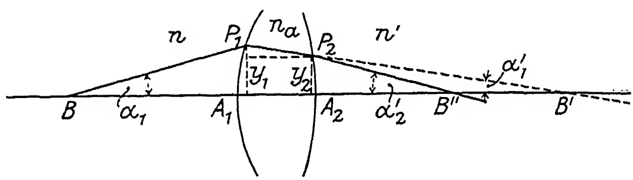

FIG. 30

Let d be the separation of the lenses, then if (as before) $F_a'F_b = g$, we obtain $d = f_a' + g - f_b = f_a' + f_b' + g$ if the lenses are in air.

We obtained $f = \frac{f_a f_b}{g}$, and this formula is convenient in some cases; alternatively

$$f' = -\frac{f_a' f_b'}{} \quad -\frac{f_a' f_b'}{f_a' + f_b' - d}$$

so that

$$\frac{1}{f'} = \frac{1}{f_a'} + \frac{1}{f'_b} - \frac{d}{f_a' f_b'} \tag{21}$$

The application of equations (16) and (18) to this case give

$$P_aP = \frac{f'd}{f_b'}, \text{ and } P_bP' = -\frac{f'd}{f_a'}; \text{ or } = \frac{f'd}{f_a}$$

Refraction by Two Coaxial Spherical Surfaces. In Fig. 30, B and B′ are axial conjugate points for the spherical surface A_1P_1. Their distances l and l' from A_1 are connected by the relation

$$\frac{n_a}{l'} - \frac{n}{l} = \mathscr{F}_1$$

where the refractive indices of the media on the object and image sides of A_1P_1 are n and n_a respectively.

Let BP_1 be a paraxial ray which intersects the surface at a height y_1; multiplying the above equation by y_1, we obtain

$$\frac{n_a y_1}{l'} - \frac{n y_1}{l} = \mathscr{F}_1 y_1$$

and, remembering the limitations of the paraxial region, this may be written

$$n_a \alpha_1' - n \alpha_1 = \mathscr{F}_1 y_1$$

since α_1, the angle made by the ray BP_1 with the axis, is given by $\dfrac{y_1}{A_1B} = \dfrac{y_1}{l}$, and similarly for α_1', the angle of inclination of the ray after the first refraction.

It is convenient now to introduce the so-called "reduced inclinations" typified by

$$\bar{\alpha} = n\alpha$$

when the ... on becomes

$$\ldots - \bar{\alpha}_1 = \mathscr{F}_1 y_1 \quad . \quad . \quad . \quad . \quad (a)$$

Let the ... s considered above meet a second surface of power ... d" distance $\bar{d}$ from the first.

Let the ... een the feet of the perpendiculars from P_1 and P_2 ... δ; then, strictly,

$$\ldots = y_1 - \delta \tan \alpha_1'$$

Remembering, however, that y_1 and y_2 are both very small, we may neglect the difference between δ and the length $A_1A_2 = d$, the separation of the surfaces, and since α_1' is also very small, the equation may be written with sufficient accuracy

$$y_2 = y_1 - d\alpha_1', \quad \text{or} \quad y_2 = y_1 - \bar{d}\,\bar{\alpha}_1' \quad . \quad . \quad . \quad (b)$$

where $\bar{d} = \dfrac{d}{n_a}$, and $\bar{\alpha}_1' = n_a \alpha_1'$.

We can add to equations (*a*) and (*b*) above,

$$\bar{\alpha}_2' = \bar{\alpha}_1' + \mathscr{F}_2 y_2$$

giving the final reduced inclination of the ray after refraction at the second surface.

Eliminating y_2 and $\bar{\alpha}_1'$, we obtain

$$\bar{\alpha}_2' = y_1(\mathscr{F}_1 + \mathscr{F}_2 - \mathscr{F}_1 \mathscr{F}_2 \bar{d}) + \bar{\alpha}_1 (1 - \mathscr{F}_2 \bar{d})$$

Subtract unity from each side, then

$$\frac{nl' - n'l}{n'l} = -\frac{(x' + f')}{f'} = -\frac{l'}{f'}$$

$$nl' - n'l = -\frac{n'll'}{f'}$$

The final form is

$$\frac{n'}{l'} - \frac{n}{l} = \frac{n'}{f'} = -\frac{n}{f} \qquad (20)$$

This formula may be compared with the similar one for a single surface, in which the principal points are coincident at the vertex.

Two Coaxial Lenses in Air. Let each lens be treated as "thin," then the principal planes of such a thin lens are no longer separated.

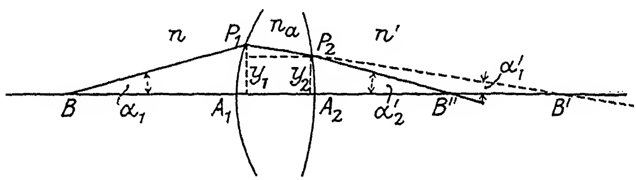

FIG. 30.

Let d be the separation of the lenses, then if (as before) $F_a'F_b = g$, we obtain $d = f_a' + g - f_b = f_a' + f_b' + g$ if the lenses are in air.

We obtained $f = \frac{f_a f_b}{g}$, and this formula is convenient in some cases; alternatively

$$f' = -\frac{f_a' f_b'}{g} = \frac{f_a' f_b'}{f_a' + f_b' - d}$$

so that

$$\frac{1}{f'} = \frac{1}{f_a'} + \frac{1}{f'_b} - \frac{d}{f_a' f_b'} \qquad (21)$$

The application of equations (16) and (18) to this case give

$$P_aP = \frac{f'd}{f_b'}, \text{ and } P_bP' = -\frac{f'd}{f_a'} \text{ or } = \frac{f'd}{f_a}$$

Refraction by Two Coaxial Spherical Surfaces. In Fig. 30, B and B′ are axial conjugate points for the spherical surface A_1P_1. Their distances l and l' from A_1 are connected by the relation

$$\frac{n_a}{l'} - \frac{n}{l} = \mathscr{F}_1$$

where the refractive indices of the media on the object and image sides of A_1P_1 are n and n_a respectively.

Let BP_1 be a paraxial ray which intersects the surface at a height y_1; multiplying the above equation by y_1, we obtain

$$\frac{n_a y_1}{l'} - \frac{n y_1}{l} = \mathscr{F}_1 y_1$$

and, remembering the limitations of the paraxial region, this may be written

$$n_a a_1' - n a_1 = \mathscr{F}_1 y_1$$

since a_1, the angle made by the ray BP_1 with the axis, is given by $\frac{y_1}{A_1B} = \frac{y_1}{l}$, and similarly for a_1', the angle of inclination of the ray after the first refraction.

It is convenient now to introduce the so-called " reduced inclinations " typified by

$$\bar{a} = na$$

when the previous equation becomes

$$\bar{a}_1' - \bar{a}_1 = \mathscr{F}_1 y_1 \quad . \quad . \quad . \quad . \quad (a)$$

Let the refracted ray as considered above meet a second surface of power $\mathscr{F}_2$ at a " reduced " distance $\bar{d}$ from the first.

Let the distance between the feet of the perpendiculars from P_1 and P_2 to the axis be δ; then, strictly,

$$y_2 = y_1 - \delta \tan a_1'$$

Remembering, however, that y_1 and y_2 are both very small, we may neglect the difference between δ and the length $A_1A_2 = d$, the separation of the surfaces, and since a_1' is also very small, the equation may be written with sufficient accuracy

$$y_2 = y_1 - d a_1', \quad \text{or} \quad y_2 = y_1 - \bar{d}\,\bar{a}_1' \quad . \quad . \quad . \quad (b)$$

where $\bar{d} = \frac{d}{n_a}$, and $\bar{a}_1' = n_a a_1'$.

We can add to equations (a) and (b) above,

$$\bar{a}_2' = \bar{a}_1' + \mathscr{F}_2 y_2$$

giving the final reduced inclination of the ray after refraction at the second surface.

Eliminating y_2 and $\bar{a}_1'$, we obtain

$$\bar{a}_2' = y_1(\mathscr{F}_1 + \mathscr{F}_2 - \mathscr{F}_1\,\mathscr{F}_2\,\bar{d}) + \bar{a}_1\,(1 - \mathscr{F}_2\,\bar{d})$$

Dividing by $\bar{\alpha}_1$

$$\frac{\bar{\alpha}_2'}{\bar{\alpha}_1} = \frac{\bar{y}_1}{\bar{\alpha}_1}(\mathscr{F}_1 + \mathscr{F}_2 - \mathscr{F}_1\mathscr{F}_2\bar{d}) + (1 - \mathscr{F}_2\bar{d})$$

Remembering the meaning of the "reduced" distances and inclinations now being employed, and the Lagrange relation ($h\bar{\alpha} = h'\bar{\alpha}'$ in this notation), we find for the height h' of the image of the object (height h)

$$\frac{h}{h'} = \frac{A_1B}{n}(\mathscr{F}_1 + \mathscr{F}_2 - \mathscr{F}_1\mathscr{F}_2\bar{d}) + (1 - \mathscr{F}_2\bar{d});$$

writing $\mathscr{F} = \mathscr{F}_1 + \mathscr{F}_2 - \mathscr{F}_1\mathscr{F}_2\bar{d}$. (22)

we have $\dfrac{h}{h'} = \dfrac{\mathscr{F}}{n}\left(A_1B + \dfrac{n(1 - \mathscr{F}_2 d)}{\mathscr{F}}\right)$

Assuming the validity of the general theory and comparing this equation with the equation (12)

$$\frac{h}{h'} = -\frac{x}{f}$$

We may write $\dfrac{\mathscr{F}}{n} = -\dfrac{1}{f}$, and $x = FB = A_1B + \dfrac{n(1 - \mathscr{F}_2\bar{d})}{\mathscr{F}}$

whence $-\dfrac{n}{f} = \dfrac{n'}{f'}$ . . . . . . (23)

(writing n and n' for the refractive indices of the first and last media).

For the distance ($FA_1 = FB - A_1B$) from the first principal focus to the first surface of the system we obtain

$$FA_1 = \frac{n(1 - \mathscr{F}_2\bar{d})}{\mathscr{F}} \qquad (24)$$

In a similar way it can be shown that the distance of the second principal focus from the apex of the second surface is given by

$$A_2F' = \frac{n'(1 - \mathscr{F}_1\bar{d})}{\mathscr{F}} \quad . \quad . \quad . \quad . \quad . \qquad (25)$$

The ordinary case of a thick lens in air is represented by putting $n = n' = 1$.

These results can be used to calculate the positions of the focal and principal planes of lenses of finite thickness, as for the spectacle lenses of Fig. 164, Chapter VIII. Thus

$$A_2P' = A_2F' - f' = \frac{n'(1 - \mathscr{F}_1\bar{d})}{\mathscr{F}} - \frac{n'}{\mathscr{F}} = -\frac{n'\mathscr{F}_1\bar{d}}{\mathscr{F}}$$

Compare this result with that of equation (18). Also work out an expression for A_1P, i.e. $A_1P = \dfrac{n\mathscr{F}_2\bar{d}}{\mathscr{F}}$

It must not be forgotten that $\bar{d}$ in the above equations is the reduced thickness, i.e. $\dfrac{d}{n_a}$, where n_a is the refractive index of the lens.

Vertex Powers. The so-called "vertex powers" of a system in air are of some importance in the theory of spectacles. Thus we have for a thick lens in air (see also page 274),

$$\text{Front vertex power} = \frac{1}{FA_1} = \frac{\mathscr{F}}{1 - \mathscr{F}_2\bar{d}}$$

$$\text{Back vertex power} = \frac{1}{A_2F} = \frac{\mathscr{F}}{1 - \mathscr{F}_1\bar{d}}$$

It is not usual to make any distinction in sign between the front and back vertex powers. The back vertex power will be written

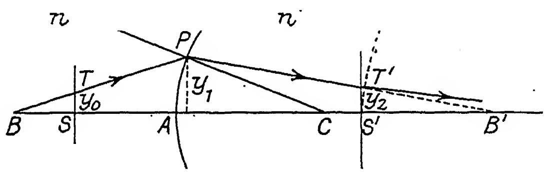

FIG. 31

$\mathscr{F}_v$. Note that the form of the expressions for the corresponding powers of a system of two thin lenses will be the same, with the exception that the reduced distance $\bar{d}$ will be replaced by the true distance d.

Analytical Discussion. It may be of some service for those who wish to go more fully into the theory, to read the following simplified discussion, which is on the lines of the Gaussian method.

In Fig. 31, B and B′ are paraxial conjugate points for the refracting spherical surface AP.

Let AB $= k$ and AB′ $= k'$. These distances are connected, then, by the relation

$$\frac{n'}{k'} - \frac{n}{k} = \mathscr{F}_1$$

Let BP be a ray refracted through the surface at a very small distance, AP $= y_1$, from the axis, then multiplying the above equation through by y_1 we have

$$\frac{n'y_1}{k'} - \frac{ny_1}{k} = \mathscr{F}_1 y_1$$

If α_1' and α_1 are the angles made by the ray with the axis after and before refraction, the above equation may be written

$$n'\alpha_1' - n\alpha_1 = \mathscr{F}_1 y_1$$

Draw a normal plane through the axial point S in the object space, and another through S′ in the image space. Let the ray path intersect these, as shown, in the respective points, T and T′ where ST $= y_0$ and S′T′ $= y_2$. Let AS $= b$ and AS′ $= d$. Then, remembering the paraxial limitations, and neglecting only small quantities of the second order,

$$y_1 = y_0 + b\alpha_1 \quad = y_0 + \frac{b}{n} \cdot n\alpha_1$$

$$y_2 = y_1 - d\alpha_1' = y_1 = \frac{a}{n'} \cdot n'\alpha_1'$$

but in order to simplify the appearance of the equations in which the reduced quantities only will appear we shall put $\boldsymbol{b}$ instead of $\bar{b}$; $\boldsymbol{\alpha}$ instead of $\bar{\alpha}$; $\boldsymbol{d}$ instead of $\bar{d}$, merely using thicker type.

Then
$$y_1 = y_0 + \boldsymbol{b\alpha}_1$$
$$y_2 = y_1 - \boldsymbol{d\alpha}_1'$$
and (from above)
$$\boldsymbol{\alpha}_1' = \boldsymbol{\alpha}_1 + \mathscr{F}_1 y_1$$

Eliminating y_1 from these equations, we obtain

$$\boldsymbol{\alpha}_1' = \mathscr{F}_1 y_0 + \boldsymbol{\alpha}_1(1 + \mathscr{F}_1\boldsymbol{b})$$
$$y_2 = (1 - \boldsymbol{d}\,\mathscr{F}_1)y_0 + \boldsymbol{\alpha}_1(\boldsymbol{b} - \boldsymbol{d} - \boldsymbol{bd}\,\mathscr{F}_1)$$

These equations are of the form

$$\left.\begin{aligned} \boldsymbol{\alpha}_1' &= Ay_0 + B\boldsymbol{\alpha}_1 \quad . \\ y_2 &= Cy_0 + D\boldsymbol{\alpha}_1 \end{aligned}\right\} (a), \text{ where } \left\{\begin{aligned} A &= \mathscr{F}_1, \quad B = 1 + \\ C &= 1 - \boldsymbol{d}\mathscr{F}_1, D = \boldsymbol{b} - \boldsymbol{d} - \boldsymbol{bd}\mathscr{F}_1 \end{aligned}\right.$$

and by multiplying the co-efficients it is found that $BC - AD = 1$.

As before, let us introduce a second refracting surface with its apex at S′, and of power $\mathscr{F}_2$; the ray will be refracted at this surface and will intersect a new plane (situated at a reduced distance $\boldsymbol{b}'$ from S′) at a height of y_3 (say). Then

$$\boldsymbol{\alpha}_2' = \boldsymbol{\alpha}_1' + \mathscr{F}_2 y_2$$
$$y_3 = y_2 - \boldsymbol{b}'\boldsymbol{\alpha}_2'$$

and we may proceed to eliminate y_2 and $\boldsymbol{\alpha}_1'$ from equations (a) and the last two, obtaining

$$\left.\begin{aligned} \boldsymbol{\alpha}_2' &= y_0(A + \mathscr{F}_2 C) + \boldsymbol{\alpha}_1(B + \mathscr{F}_2 D) \quad . \quad . \quad . \quad . \quad . \\ y_3 &= y_0\{C - \boldsymbol{b}'(A + \mathscr{F}_2 C) + \boldsymbol{\alpha}_1\{D - \boldsymbol{b}'(B + \mathscr{F}_2 D)\} \quad . \quad . \end{aligned}\right\} (b)$$

These equations are of the same form as (a) above, and may be written

$$\boldsymbol{\alpha}_2' = A'y_0 + B'\boldsymbol{\alpha}_1$$
$$y_3 = C'y_0 + D'\boldsymbol{\alpha}_1$$

If we evaluate $B'C' - A'D'$ we find that $B'C' - A'D' = BC - AD = 1$. Thus, it appears that the form (a) is a most general one for the effect of refraction of a ray at a series of coaxial spherical surfaces.

Let surface "$n + 1$" be a plane reference surface situated in the medium beyond the nth surface of a system. Then we can find relations of the general form

$$\alpha_n' = Ay_o + B\alpha_1$$
$$y_{n+1} = Cy_o + D\alpha_1$$

where A, B, etc. are new constants.

Now let the two reference surfaces denoted by "o" and "$n + 1$" be brought into coincidence with surfaces "1" and "n." These latter must be *fixed* in relation to the system; for example, they may be the first and last refracting surfaces; then the above equations give

$$\alpha_n' = Ay_1 + B\alpha_1$$
$$y_n = Cy_1 + D\alpha_1$$

and it is evident that equations of the same type as above connect α_n' and y_n with α_1 and y_1. A, B, C, and D are now definite constants of the system.

Take a plane at a *reduced distance* $\boldsymbol{l}$ from the first surface above; then let the entrant ray intersect this plane in B_1 at a height h from the axis.

Take a second plane at a *reduced distance* $\boldsymbol{l}'$ from the last surface, and let the emergent ray intersect this in a point B_1' at a distance h' from the axis.

Then
$$y_1 = h + \boldsymbol{l}\alpha_1$$
$$h' = y_n - \boldsymbol{l}'\alpha_n'$$

Eliminating y_1 and y_n, the following equations are found

$$\alpha_n' = hA + \alpha_1 (A\boldsymbol{l} + B)$$
$$h' = h(C - \boldsymbol{l}'A) - \alpha_1 (A\boldsymbol{l}\boldsymbol{l}' + B\boldsymbol{l}' - C\boldsymbol{l} - D) . \quad . \quad . \quad (c)$$

The form of these equations can be recognized as the same as before. The conditions for image formation will be clear. If the points B_1, B_1' are object and image, the ratio of h' to h will be independent of α_1, the inclination of the incident ray. Then

$$A\boldsymbol{l}\boldsymbol{l}' + B\boldsymbol{l}' - C\boldsymbol{l} - D = 0 \quad . \quad . \quad . \quad . \quad . \quad (d)$$

is a general equation connecting the reduced distances of conjugate planes from two planes fixed in reference to the instrument; the position of the latter planes determines the constants B, C, and D.

The relation

$$A\boldsymbol{l}\boldsymbol{l}' + B\boldsymbol{l}' - C\boldsymbol{l} - D = 0$$

yields when multiplied by A

$$A^2\boldsymbol{l}\boldsymbol{l}' + AB\boldsymbol{l}' - AC\boldsymbol{l} - AD = 0$$

and since $BC - AD = 1$

$$(A\boldsymbol{l} + B)\,(C - A\boldsymbol{l}') = 1$$

The magnification of the sharp image is given by

$$\frac{h'}{h} = (C - \boldsymbol{l}'A) = \frac{1}{(A\boldsymbol{l} + B)}$$

The positions of the unit planes are given by putting the magnification equal to unity, obtaining

$$C - l_1'A = 1,\ Al_1 + B = 1\ . \qquad . \qquad . \qquad . \qquad (e)$$

The position of the first principal focus is found by putting equation (*d*) into the form

$$A + \frac{B}{l} - \frac{C}{l'} - \frac{D}{ll'} = 0$$

Then, if $l' \quad \infty,\ A + \dfrac{B}{l_f} = 0$, or $l_f = -\dfrac{B}{A}$

if $l = \infty,\ A - \dfrac{C}{l_f'} = 0 \qquad\qquad l_f' = +\dfrac{C}{A}$

The *reduced* distances f and f' of the focal planes from the principal planes therefore appear as

$$f = l_f - l_1 = -\frac{B}{A} - \frac{(1-B)}{A} = -\frac{1}{A}$$

and

$$f' = l_f' - l_1' = \frac{C}{A} - \frac{(C-1)}{A} \quad \frac{1}{A}$$

Relations between the Distances of Conjugate Planes. It will appear from the form of equation (*d*) that the more familiar forms of the optical equations connecting the distances of conjugate foci from certain reference points are merely particular cases of the general relation given by (*d*).

Reference to Principal Planes. To refer the conjugate distances to the unit planes, introduce into (*d*) the values of B and C obtained from (*e*). Then

$$All' + (1 - Al_1)l' - (1 + Al_1')l - D = 0$$

This equation must become an identity when $l = l_1$ and $l' = l_1'$, thus giving

$$D = -(Al_1'l_1 - l_1' + l_1)$$

Substituting this into the above form it reduces to

$$\frac{1}{(l' - l_1')} - \frac{1}{(l - l_1)} = A = \frac{1}{f'}$$

Now $(l' - l_1')$ is the reduced distance of the image plane from the second principal plane, while $(l - l_1)$ is the reduced distance of the object plane from the first principal plane.

Thus,

$$\frac{n'}{l'} - \frac{n}{l} = A = \frac{n}{f'},$$

where l' and l stand for real distances now measured from the principal planes, is the simplified form useful in the present case.

Reference to Focal Planes.

Let

$$l - l_f = x \text{ and } l' - l_f' = x'$$

or

$$l = x - \frac{B}{A} \text{ and } l' = x' + \frac{C}{A}$$

The equations c now assume the form

$$\alpha_n' = hA + \alpha_1 A\mathbf{x}$$
$$h' = h(-A\mathbf{x}') - \alpha_1\left(A\mathbf{x}\mathbf{x}' + \frac{1}{A}\right)$$

The relation between reduced object and image distances measured from the focal planes is therefore

$$\mathbf{x}\mathbf{x}' = -\frac{1}{A^2} = \mathbf{f}\mathbf{f}'$$

or in ordinary distances

$$\frac{x}{n}\cdot\frac{x'}{n'} = \frac{f}{n}\cdot\frac{f'}{n'}; \text{ or } xx' = ff'$$

Also, the magnification will be

$$\frac{h'}{h} = -A\mathbf{x}' = -\frac{\mathbf{x}'}{\mathbf{f}'}$$

the form being again the same when ordinary distances are denoted.

Relations between the Gaussian Constants and the Composition of the Instrument. (Use of Differential Notation.)

The method adopted is to assume the existence of a group of coaxial spherical refracting surfaces for which the equations

$$\left.\begin{aligned} \alpha'_{n-1} &= Ay_1 + B\alpha_1 \quad . \quad . \quad . \quad . \\ y_{n-1} &= Cy_1 + D\alpha_1 \quad . \quad . \quad . \quad . \end{aligned}\right\} \quad (f)$$

give the final values of α'_{n-1}, y_{n-1}, in terms of α_1 and y, where y_1 and y_{n-1} are the heights at which the ray crosses the first and last surfaces respectively. Then let a new coaxial surface of power $\mathscr{F}_n$ be placed at a reduced distance $\mathbf{d}'$ from the last refracting surface, and let y_n be the height at which the ray crosses it, and α_n' the reduced inclination after refraction. Then

$$y_n = y_{n-1} - \mathbf{d}'\alpha'_{n-1}$$
$$\alpha_n' = \alpha'_{n-1} + y_n\mathscr{F}_n$$

Eliminating y_{n-1} and α'_{n-1} we obtain

$$\alpha_n' = y_1\{A + \mathscr{F}_n(C - \mathbf{d}'A)\} + \alpha_1\{B + \mathscr{F}_n(D - \mathbf{d}'B)\}$$
$$y_n = y_1(C - \mathbf{d}'A) + \alpha_1(D - \mathbf{d}'B).$$

These equations are of the usual form, and the new constants are

$$A_1 = A + \mathscr{F}_n(C - \mathbf{d}'A)$$
$$B_1 = B + \mathscr{F}_n(D - \mathbf{d}'B)$$
$$C_1 = C - \mathbf{d}'A$$
$$D_1 = D - \mathbf{d}'B$$

Let the power A_1 be written $\mathscr{F}$, then the following relations are found

$$A_1 = \mathscr{F}, \quad C_1 = \frac{\partial\mathscr{F}}{\partial\mathscr{F}_n}, \quad D_1 = \frac{\partial B_1}{\partial\mathscr{F}_n}$$

Imagining the whole system to be reversed, left to right, the values of the y's will be unchanged, but the inclinations will change sign.

The equations (*f*) above give (by simple algebra, remembering that $BC - AD = 1$)

$$-\alpha_1 = Ay_{n-1} + C(-\alpha'_{n-1})$$
$$y_1 = By_{n-1} + D(-\alpha'_{n-1})$$

where $-\alpha_1$ and $-\alpha'_{n-1}$ are the reduced inclinations of the reversed ray. Thus it is seen that the functions of B and C are now interchanged and we can obtain

$$B_1 = \frac{\partial \mathscr{F}}{\partial \mathscr{F}_1}, \text{ and } D_1 = \frac{\partial C_1}{}$$

from the second of which $D = \dfrac{\partial^2 \mathscr{F}}{\partial \mathscr{F}_1 \partial \mathscr{F}_n}$

Successive applications of the equation $A_1 = A + \mathscr{F}_n(C - \mathbf{d}'A)$, enable us to find the expressions for the powers of groups of refracting surfaces.

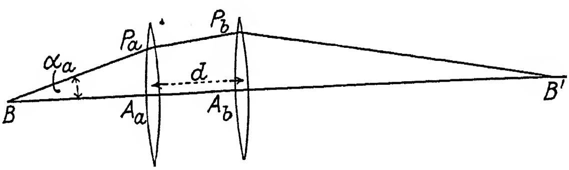

FIG. 32

For a single surface $\mathscr{F} = \mathscr{F}_1$, and $B = C = 1$.

For two surfaces $\mathscr{F}_1$ and $\mathscr{F}_2$ separated by a reduced distance $\mathbf{d}_1$,

$$\mathscr{F} = \mathscr{F}_1 + \mathscr{F}_2(1 - \mathbf{d}_1\mathscr{F}_1)$$

whence $B = \dfrac{\partial \mathscr{F}}{\partial \mathscr{F}_1} = 1 - \mathbf{d}_1\mathscr{F}_2$, and $C = \dfrac{\partial \mathscr{F}}{\partial \mathscr{F}_2} = 1 - \mathbf{d}_1\mathscr{F}_1$

For three surfaces,

$$\begin{aligned} \mathscr{F} &= \mathscr{F}_1 + \mathscr{F}_2(1 - \mathbf{d}_1\mathscr{F}_1) + \mathscr{F}_3[C - \mathbf{d}_2\{\mathscr{F}_1 + \mathscr{F}_2(1 - \mathbf{d}_1\mathscr{F}_1)\}] \\ &= \mathscr{F}_1 + \mathscr{F}_2 + \mathscr{F}_3 - \mathbf{d}_1\mathscr{F}_1\mathscr{F}_2 - (\mathbf{d}_1 + \mathbf{d}_2)\mathscr{F}_1\mathscr{F}_3 - \mathbf{d}_2\mathscr{F}_2\mathscr{F}_3 \\ &\quad + \mathbf{d}_1\mathbf{d}_2\mathscr{F}_1\mathscr{F}_2\mathscr{F}_3 \quad . \quad . \end{aligned} \tag{26}$$

Refraction by a Series of Coaxial Thin Lenses. The form of the results which have been obtained for refraction at a series of coaxial refracting surfaces is much the same as that of the equations for refraction by a series of thin coaxial lenses; for the ordinary equation

$$\frac{1}{l'} - \frac{1}{l} = \mathscr{F}_a$$

when multiplied by $y_a = A_aP_a$ (see Fig. 32), the intersection height of a ray BP_a in the first lens gives

$$\frac{y_a}{l'} - \frac{y_a}{l} = \mathscr{K}_a y_a$$

If we write α_a, α_a' for the angles of inclination of the ray before and after refraction by lens a, then

$$\alpha_a' - \alpha_a = \mathscr{K}_a y_a, \qquad \text{where } y_a = A_aB \,.\, \alpha_a$$

Also $$y_b = y_a - d\alpha_a',\text{*}$$

and $$\alpha_b' - \alpha_b = \mathscr{K}_b y_b.$$

The form of these equations is identical with those which were given in connection with refraction at two spherical surfaces with

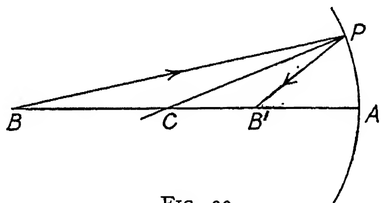

FIG. 33

the exception that the axial distances now appear as true lengths not as " reduced " lengths.

We thus obtain for a pair of lenses (as in equation (21))

$$\mathscr{K} = \mathscr{K}_a + \mathscr{K}_b - \mathscr{K}_a\mathscr{K}_b d \quad . \quad . \quad . \quad (27)$$

also $$FA_a = 1 - \mathscr{K}_b d \qquad (28)$$

and $$A_bF' = 1 - \atop \mathscr{K} \qquad (29)$$

The form of the results for three lenses is the same as that of equation (26).

Spherical Reflecting Surface. Let AP, Fig. 33, be the trace of a spherical reflecting surface with centre C, and let B be an object point on the axial line BCA. An incident ray BP in the axial plane is reflected so as again to intersect the axis at B′. Then

$$\frac{PB}{\sin \widehat{BCP}} = \frac{CB}{\sin \widehat{BPC}} \quad \text{and} \quad \frac{PB'}{\sin \widehat{B'CP}} = \frac{B'C}{\sin \widehat{CPB'}}$$

* Note that α_a' is shown in Fig. 32 as an angle which would numerically be negative.

Since $\widehat{BCP}$ and $\widehat{B'CP}$ are supplementary angles, and the angle of reflection is equal to the angle of incidence, the "sines" disappear when one of the above equations is divided by the other, leaving

$$\frac{PB}{PB'} = \frac{CB}{B'C}$$

When the point P is very close to A, the length BP becomes very nearly equal to BA, and B′P to B′A. Hence, under paraxial restrictions

$$\frac{AB}{AB'} = \frac{CB}{B'C}$$

If lengths are measured from the apex A of the surface, as usual, the last equation may be written

$$\frac{l}{l'} = \frac{l-r}{r-l'}$$

and, by a simple transformation

$$\frac{1}{l'} + \frac{1}{l} = \frac{2}{r}$$

The mirror has one principal focus, given by

$$f = \frac{r}{2}$$

The numerical "power" of the surface is therefore given by $\frac{2}{r}$.

Reflection as a Particular Case of Refraction. It is worth noting that if the usual expressions for the laws of reflection and refraction be compared (see Appendix, page 312, and Fig. 195),

$$i = -i'$$

$$n \sin i = n' \sin i'$$

The second is transformed into the first if we put $n' = -n$. Thus, the law for paraxial refraction at a spherical surface

$$\frac{n'}{l'} - \frac{n}{l} = \frac{n'-n}{r}$$

is at once reduced to the form given above for a reflection. This device is always adopted in the trigonometrical computing of systems involving reflection and involves no change in the form of the standard computing schedule, although it is naturally essential to remember the reversed direction of the light after reflection.

The graphical construction for "object and image" will be

obvious; it involves one focal plane and one principal plane, and is illustrated in Fig. 34. The Abbe equations, now becoming

$$\frac{h'}{h} = -\frac{x'}{f} = -\frac{f}{x}, \text{ and } xx' = f^2$$

are valid in this case, and the ordinary forms (page 40) will further hold for any combination of refractions and reflections.

Combinations of Refracting and Reflecting Surfaces. Owing to the fact that the paraxial rays have generally to pass back into the same medium after transmission through any system of coaxial refracting surfaces combined with *one* reflecting surface, there can only be one principal focus for such a system, and the same considerations show that there can be only one focal length and therefore one principal plane. The system will therefore be equivalent (so far as paraxial relations are concerned) to a single mirror

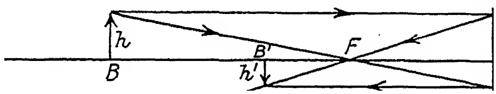

FIG. 34

which must be the image, formed by the refracting system, of the actual reflecting surface. This image clearly acts as the principal plane of the system. Also the apparent centre of curvature and the real centre of curvature will be corresponding conjugate points with regard to the refracting system.

The use of the methods previously outlined for finding the constants of a series of optical surfaces needs some care. It may be imagined for simplicity* that the path of the ray after reflection in such a case is continued onwards in the " left to right " sense, as if a " plane mirror " image of the ray paths were formed, as suggested in Fig. 35, which illustrates the case of one reflecting and one refracting surface. The ray may be considered to be subject to the effect of three surfaces of powers $\mathscr{F}_1$, $\mathscr{F}_2$, $\mathscr{F}_3$, at distances d' and d'', which become equal to the thickness d in the paraxial case. We need not then bother about negative refractive indices.

In applying this method, note that the " power " of the reflecting

*A more systematic discussion of the method of dealing with this case on the basis of a reversal of the sign of the refractive index for the right to left direction is given in the Appendix, p. 311, *et seq.*

surface will be of the positive or converging type when the radius is negative. Also in analogy with the general equation

$$\frac{n'}{l'} - \frac{n}{l} = \frac{n' - n}{r} = \mathscr{F}$$

where the power is connected with the difference of the *reduced* lengths, the power of the reflecting surface must appear in connection with the reduced lengths also. Thus when $n' = n_1$

$$-\frac{n}{l'} - \frac{n}{l} = n\left(-\frac{2}{r}\right) = \mathscr{F}$$

It will be realized that a reflecting concave surface will have a power which depends upon the medium in which it is situated if we think of a thin plano-convex lens with a silvered back. The effective power of

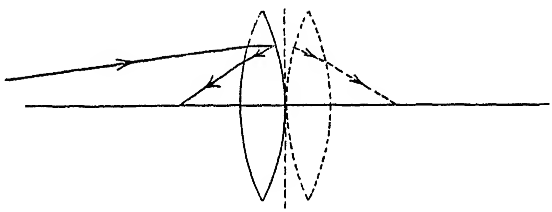

FIG. 35

the system is n times that of the reflecting surface alone, although the power of the plane glass surface is zero.

Case of One Refracting and One Reflecting Surface. Let r_g, r_m be the radii of the refracting and reflecting surfaces respectively. The refractive index is n outside, and n' between the surfaces The distance l_c of the apparent centre of curvature from the refracting surface is given by

$$\frac{n'}{r_m + d} - \frac{n}{l_c} = \frac{n' - n}{r_g} = \mathscr{F}_1$$

where d is the distance between the surfaces, while the distance l_p of the virtual image of the reflecting surface formed by refraction at the first surface is given by

$$\frac{}{d} - \frac{}{l_p} \qquad n' - n$$

Hence, using the relation $r_m = -\dfrac{2n'}{\mathscr{F}_2}$ and employing the reduced distances, we obtain by simple algebra

$$\bar{l}_c = \frac{-2 + \bar{d}\mathscr{F}_2}{2\mathscr{F}_1 + \mathscr{F}_2 - \bar{d}\mathscr{F}_1\mathscr{F}_2}, \quad \bar{l}_p = \frac{\bar{d}}{1 - \bar{d}\mathscr{F}_1}$$

The apparent radius of curvature is the distance to the apparent centre from the apparent principal point or surface, i.e. $l_c - l_p$

$$\bar{l}_c - \bar{l}_p = \frac{-2}{2\mathscr{F}_1 + \mathscr{F}_2 - 2\bar{d}\mathscr{F}_1\mathscr{F}_2 - 2\bar{d}\mathscr{F}_1^2 + \bar{d}^2\mathscr{F}_1^2\mathscr{F}_2}$$

The quantity in the denominator is therefore the effective power.

The ordinary equations can be applied to this problem (see equation 26). For a combination of three surfaces see also Appendix, p. 314.

$$\alpha_3' = y_1\{\mathscr{F}_1 + \mathscr{F}_2 + \mathscr{F}_3 - \mathscr{F}_1\mathscr{F}_2\mathbf{d}_1 - \mathbf{d}_1\mathscr{F}_1\mathscr{F}_3 - \mathbf{d}_2\mathscr{F}_3(\mathscr{F}_1 + \mathscr{F}_2 - \mathscr{F}_1\mathscr{F}_2\mathbf{d}_1)\}$$
$$+ \alpha_1(1 - \mathscr{F}_2\mathbf{d}_1 - \mathbf{d}_1\mathscr{F}_3 - \mathbf{d}_2\mathscr{F}_3 + \mathscr{F}_2\mathscr{F}_3\mathbf{d}_2\mathbf{d}_1)$$

or
$$\alpha_3' = y_1A + \alpha_1B$$

where
$$B = \frac{\partial A}{\partial \mathscr{F}_1}$$

Now when $\mathscr{F}_1 = \mathscr{F}_3$ and $\mathbf{d}_2 = \mathbf{d}_1$

$$A = 2\mathscr{F}_1 + \mathscr{F}_2 - 2\mathscr{F}_1\mathscr{F}_2\mathbf{d}_1 - 2\mathscr{F}_1^2\mathbf{d}_1 + \mathbf{d}_1^2\mathscr{F}_1^2\mathscr{F}_2$$

which is the power as obtained directly above; and

$$B = 1 - \mathscr{F}_2\mathbf{d}_1 - 2\mathbf{d}_1\mathscr{F}_1 + \mathbf{d}_1^2\mathscr{F}_1\mathscr{F}_2$$

The distance from the refracting surface to the first focal point will be $l_f = -\dfrac{B}{A}$.

Let the effective powers, in diopters, of the surfaces for refraction and reflection in the above problem be $\mathscr{F}_1 = +2$, $\mathscr{F}_2 = +4$. If the system is thin, the total power is $(2 \times 2) + 4 = 8D$. (The actual power of a reflecting surface of the same curvature in air would be $\dfrac{4}{n'}$. If $n' = 1{\cdot}5$, $\mathscr{F}_2$ (air) $= 2{\cdot}6$ and $r = -0{\cdot}75$ m.) If the actual thickness $= d = 3$ cm. $= 0{\cdot}03$ metres, the reduced thickness $\bar{d} = 0{\cdot}02$ metres.

The power $A = 7{\cdot}5264$

$$B = 0{\cdot}8432$$

$$l_f = -\frac{B}{A} = -0{\cdot}112 \text{ metres.}$$

Gaussian Constants.

If we imagine, *first*, an object in the first surface of a system, and its corresponding image formed by the system, we obtain (page 55) $h'/h = C$. Again if an object is so placed that its image is formed in the last surface of the system, we obtain $h/h' = B$ and $D = -lc$. These formulae give a means of finding the constants useful in certain cases, such as the above.

REFERENCES

[1] *Dioptrische Untersuchungen*, Gottingen, 1841.

[2] Conrady, *Applied Optics and Optical Design* (Oxford University Press, 1929).

CHAPTER III

THE PHYSICAL STUDY OF LIGHT

Wave-motion. Before actually dealing with the phenomena of light, and the hypotheses which have been advanced to explain them, it is proposed to discuss a few conceptions relating to " wave-motion " and to explain some of the formulae commonly used.

The most familiar type of wave-motion is that of the surface of water when disturbed. At the seashore we observe waves which are straight and are propagated at right angles to the lines of the crests. If we drop a stone into a pond we observe ripples which are propagated outwards in all directions; since the ripples are circular, we infer a uniform velocity of propagation in all directions.

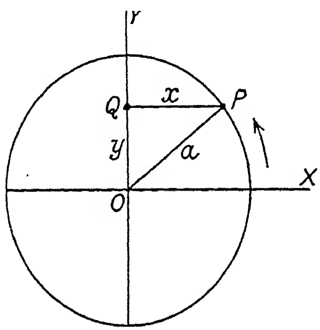

FIG. 36

If we hold one end of a light rope, say thirty feet in length, fastened at the other extremity, we can cause a pulse or disturbance to pass along the cord by giving a sharp jerk to the end we are holding, and we may even observe the reflection of the pulse from the fixed end. Again, if we give a regular up-and-down movement to the end we hold, a series of " waves " will be seen to travel along the cord, each point of the cord repeating in its turn a similar movement of " vibration " to that of the hand.

The study of sound has shown that the air in the neighbourhood of a very rapidly vibrating body is itself also in vibration, and that it is the vibrations of the air which convey the " sound " to the ear.

The first step in the study of wave-motion, then, is the study of " vibration."

Let the point P, Fig. 36, move in a circular path with uniform angular velocity ω.* The centre of the circle is at O, the origin of the co-ordinate axes of X and Y. The co-ordinates of P are x, y.

The point Q found at the foot of the perpendicular dropped from P to the axis of Y will now possess a " Simple Harmonic Motion."

* The angular velocity ω is the quotient of $\frac{2\pi}{T}$ where T is the time taken to move through an angle 2π.

If the time t be reckoned as zero when P crosses the axis of X, then

$$y = a \sin \omega t, \text{ or } y = a \sin 2\pi \frac{t}{T}$$

Differentiating with regard to t*

$$\frac{dy}{dt} = \omega a \cos \omega t, \text{ and again } \frac{d^2y}{dt^2} = -\omega^2 a \sin \omega t$$
$$= \omega x \qquad\qquad\qquad\qquad = -\omega^2 y$$

The velocity $\frac{dy}{dt}$ of the point Q is therefore greatest when passing the central position O and is zero when at the extreme points. The acceleration $\frac{d^2y}{dt^2}$ is greatest at the extreme points, and is always an acceleration towards the centre; it is proportional to the displacement. Evidently it is the type of motion characteristic of a body subject to a restoring force proportional to the displacement, and of which the motion is not otherwise hindered. We shall speak of the angle between the radius vector OP and the X axis as the "Phase Angle." The constant "a" is the "amplitude" of the vibration.

Now consider the expression†

$$y = a \sin 2\pi \left(\frac{t}{T} - \frac{x}{\lambda}\right) \quad . \quad . \quad . \quad . \quad (30)$$

as applied to the co-ordinates of a series of points which, when $a = o$, lie in the straight line $y = o$, i.e. the axis of x.

If x is constant while t varies, then the particle at any point x_1 will experience a simple harmonic vibration; on the other hand, if we examine the conditions along the line at any instant by putting $t = t_1$ and allowing x to vary, we obtain a "sine curve," Fig. 37. If t be changed by $\pm T$ while x is constant, or x be changed by λ while t is constant, we shall obtain precisely the same numerical value of y, and also the same velocity and acceleration; we shall have vibrations for which the phase angle will be the same or, in other words, the vibrations will be "in the same phase."

The length λ between the normal positions of points vibrating in

* Students not familiar with the calculus should accept these results as a simple expression of the velocity $\frac{dy}{dt}$ and the acceleration $\frac{d^2y}{dt^2}$ of the point Q.

† The corresponding expression $y = a \cos 2\pi\left(\frac{t}{T} - \frac{x}{\lambda}\right)$ equally represents a wave-train; the phase difference as compared with that of equation (30) evidently being 90° or $\frac{\pi}{2}$.

the same phase is called the " wave-length." The " crests " of such a wave motion represent regions of similar phase.

The appearance of the wave motion is as if a line bent thus into a sine curve were being bodily moved. Actually, each particle is performing a vibration similarly with all the others, but with a difference of phase from those near it. We note that by increasing the time t, we can produce the same variation in y as by diminishing x, for each operation would increase the quantity within the bracket.* Hence, the equation represents a wave-train moving in the positive x direction; while $y = a \sin 2\pi \left(\frac{t}{T} + \frac{x}{\lambda}\right)$ would represent a wave-train moving in the reversed direction.

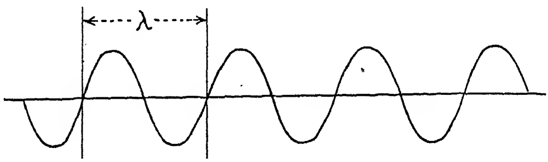

FIG. 37

In time T a " crest " moves through a distance λ. Hence, in unit time a crest moves through a distance $\frac{\lambda}{T}$, and this distance is the velocity V. Hence

$$\lambda = VT \qquad . \quad . \quad . \quad . \quad . \qquad (31)$$

If N is the " frequency," we shall evidently find N complete wave-lengths in a distance V, since N waves travel out from the source in unit time, and the initial disturbance is propagated to a distance V.

Hence $V = N\lambda$, and $T = \frac{1}{N}$; the latter equation is obvious, since T is the time to send out one complete wave, and N are sent out per second.

If the position of a point in space are given by its Cartesian co-ordinates x, y, z, then the equation (30) above can be interpreted as representing a group of plane waves travelling through space in the direction of the x axis; the value of the variable displacement from the normal position (represented by the sine term) is clearly independent of y and z.

In the case of the vibrations of " sound," the motion of the parts of the medium are *not* at right angles to the direction of propagation

* At any one point, after the lapse of a given time, we find the phase characteristic previously of a smaller value of x.

as in the case we have been considering, but are parallel to it. They are waves of condensation and rarefaction. On the other hand, waves with transverse vibrations can be produced in various elastic media and their properties studied.

It can be proved in the case of all these mechanical vibrations that the energy of a wave motion passing through unit area normal to the direction of propagation is proportional to the square of the amplitude. Suppose, then, that we have a source of wave motion

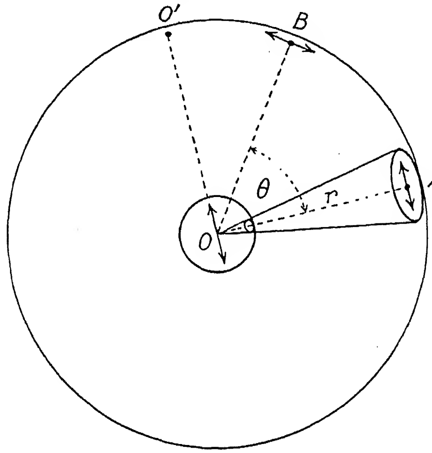

FIG. 38

O, of negligible dimensions, at the centre of two spheres of radii "unity" and "r" respectively (see Fig. 38).

Draw a cone of very small solid angle $d\varphi$ with its apex at O, marking off areas $d\varphi$ and $r^2 d\varphi$ respectively from the two spheres. *If we may assume that the direction of energy propagation is in straight lines*, all the energy passing through the area $d\varphi$ must pass through the other area $r^2 d\varphi$.

Let I_1 and I_r be the energy per unit area at the two radii

then $I_1 = ka_1^2$ where a_1 is the amplitude at unit radius

and $I_r = ka_r^2$,, a_r ,, ,, ,, radius r

The conservation of energy is expressed by $I_1 d\varphi = I_r r^2 d\varphi$ or $ka_1^2 d\varphi = ka_r^2 r^2 d\varphi$.

Hence
$$a_r = \frac{a_1}{r} \tag{32}$$

Polarization. As mentioned above, the vibrations of sound are in the direction of propagation, but in transverse vibrations such as

those which we can set up in a single cord, or as waves in an elastic solid medium, the direction of the motion is important. If we shake the end of the cord in a vertical plane all the other parts will move in a vertical plane also, and so on. In Fig. 38 we may imagine the direction of displacement of the mechanical vibrations of the source in an elastic solid to be in the line OO′. The movement propagated to O′ can there have no component parallel to the surface of the sphere, but the maximum tangential displacement in the surface will be in the equator perpendicular to OO′. If a point in the equator, such as A, has the surface component of amplitude $\frac{a_1}{r}$, the surface amplitude at another point B, where OB makes an angle θ with the equatorial plane, will be $\frac{a_1}{r}$ multiplied by some function of θ which diminishes as θ increases. The direction of the vibrations at any point of the surface will be in a plane containing OO′.

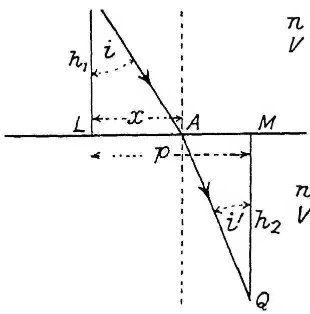

FIG. 39. FERMAT'S PRINCIPLE

The Nature of Light. The Greek speculations regarding the nature of light have already been referred to, and the "emission" or corpuscular theory was generally accepted until the seventeenth century. In 1637 Descartes published his essay on *Dioptrics* (in which he formulated the law of refraction) expressing the view that light is a pressure which is transmitted by an infinitely elastic medium pervading space. His attempted theoretical explanation of the law of refraction led to the conclusion that light would pass more readily through a more highly refracting medium. This was in opposition to the theory of Fermat (1604–1665) that light would travel from one point to another by such a route that the time is a minimum. In conjunction with the law of refraction, the necessary condition implied in Fermat's idea is that the velocity should vary inversely as the refractive index, as will be seen below.

The principle of the rectilinear propagation of light and the law of reflection at a plane surface have already been shown to agree with Fermat's principle. For the case of refraction consider Fig. 39. Let the velocities of light above and below the separating surface be V and V′. The points P and Q are on the incident and refracted rays, and PL, QM are perpendicular to the plane of the refracting surface; A is the point of refraction.

The time (t) for the disturbance to travel from P to Q is

$$t = \frac{PA}{V} + \frac{AQ}{V'}$$

Let PL = h_1, MQ = h_2, LA = x, LM = p, then the equation becomes

$$\frac{(h_1^2 + x^2)^{\frac{1}{2}}}{V} + \frac{\{h_2^2 + (p-x)^2\}^{\frac{1}{2}}}{V'}$$

If this time is a minimum, then $\frac{dt}{dx} = 0$, i.e.

$$\frac{x}{V(h_1^2 + x^2)^{\frac{1}{2}}} - \frac{(p-x)}{V'\{h_2^2 + (p-x)^2\}^{\frac{1}{2}}} = 0$$

or

$$\frac{\sin i}{V} - \frac{\sin i'}{V'} = 0$$

This gives

$$\frac{\sin i}{\sin i'} = \frac{V}{V'}$$

Hence

$$\frac{\sin i}{\sin i'} = \frac{n'}{n} = \frac{V}{V'}, \text{ and } n'V' = nV \tag{33}$$

Hence, Fermat's principle is in accordance with the law of refraction if the above equation is fulfilled; in spite of the somewhat irrelevant arguments on which it was first stated, this principle is one of the most fundamentally important ideas in optics, and will be discussed more fully later.

Although the minimum value of the optical path is seen to hold in some cases, it may be alternatively a maximum, or may have a stationary value. Thus it will be shown that various optical paths, through a lens, between an object and image point, may have a constant value, so that disturbances starting in the same phase and travelling by different paths may yet arrive in the same phase.

In 1676, Römer's observations on the eclipses of Jupiter's satellites showed that light had, in fact, a finite through very great velocity. His estimate was 192,000 miles per second. Modern researches have given a revised estimate of 299,860 km., or about 186,000 miles per second.

About the time when Newton's researches on "Dispersion" were in progress, a book by Grimaldi was published in 1665, two years after the death of its author. In it was described his work on *diffraction*. He had found that the boundaries of shadows were *not* exactly determined by the paths of possible rays between the source of light and the screen on which the shadows were observed; light might appear within a region which (if the path of light in one medium were always precisely straight) should remain in darkness; conversely, certain dark shadows appeared larger than their strictly geometrical limits. These observations were taken up and further investigated by Newton, who also described the colours due to

successive reflection of light at the surfaces of thin films, such colours as are seen in ring form at the point of contact between a convex lens and a glass plate when pressed together.*

Great as were Newton's services to experimental optics, his opposition to the wave-theory of light carried great weight against it after it had been propounded by Huygens in 1678. (Huygens' *Traité de la Lumière* was published later, in 1690.)

Huygens conceived that light is composed of pulses propagated with a definite velocity through a space-pervading medium which could be thought of as consisting ultimately of small elastic spheres in contact. Hence, any motion of one such sphere would tend to impart a motion to all those with which it was in contact, more especially those in the line of its displacement.

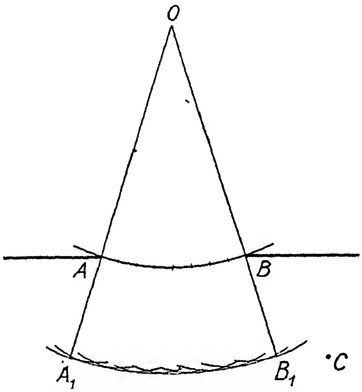

FIG. 40. HUYGENS' PRINCIPLE

His explanation of the rectilinear propagation of light will illustrate the theory. In Fig. 40, AB represents an opening in a screen. A pulse or "wave" of light, having spread with uniform velocity from O, is represented by the arc AB. Now each particle in the wave-front becomes a source of disturbance, and wavelets spread out from each such particle as centre. The envelope to such a series of wavelets will be an arc A_1B_1 with O as centre. In the immediate region of the arc A_1B_1 the density of the wavelets will be greatest, but at any point C outside the lines OA_1, OB_1, the wavelets will only arrive at different times, and their effects will be comparatively small. It is to be noted that the idea does not involve the propagation of a regular series of vibrations through the medium, as in the case of sound, but rather assumes the disturbance to consist of arbitrary pulses of no definite period.

The case of refraction at a plane surface was dealt with as follows. AB, Fig. 41, represents the trace of a plane "wave" incident on the surface AB′ separating media of refractive indices n and n'. The normal to the wave lies in the plane of the diagram.

When the wave reaches the point A in the surface, this point becomes the centre of a secondary wavelet spreading out in the second medium. Suppose the velocity in the first medium is V

* The theory is given in Chapter VI.

and in the second V′, then, by the time that the part of the incident wave at B has travelled to B′ the radius of the wavelet will be $BB' \cdot \frac{V'}{V}$. The envelope of all the secondary wavelets will be found by drawing a tangent from B′ to the wavelet. Regarding the ray as the normal to the wave-surface, it is easy to see that BAB′ is the angle of incidence and A′B′A the angle of refraction.

$$\text{Then } \frac{\sin \widehat{BAB'}}{\sin \widehat{A'B'A}} = \frac{BB'}{AA'} = \frac{V}{V'} = \frac{n'}{n}, \text{ as before.}$$

Huygens also applied this type of " construction " to deal with the phenomenon of " double refraction " in substances such as

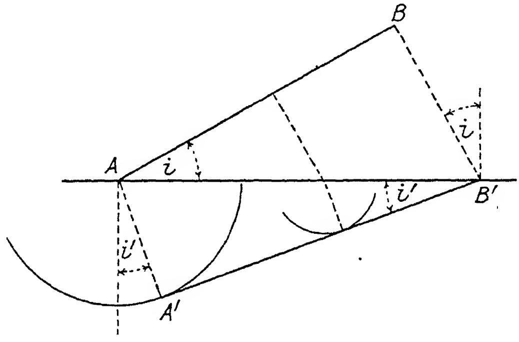

FIG. 41. HUYGEN'S CONSTRUCTION FOR REFRACTION

Iceland spar or quartz; in this case the " wave " is assumed to spread out in two sheets or surfaces, one spherical, the other ellipsoidal. In this way he was able to explain the variation of direction between the " ordinary " and " extraordinary " rays, which generally result on refraction of a single ray by a doubly refracting body. (See Chapter VI.)

For the purposes of the present book, the development of the simple wave-theory of light into the electro-magnetic theory of the nature of the wave-displacements must be left without comment. Nor is it possible to comment on modern views of the phenomena of energy transference by the waves of light. For the proper discussion of the theory of instruments it will, however, be necessary to follow some developments in the early growth of the wave-theory.

Young's Experiment. It is not possible to follow the full history of the investigations on the nature of light, but the corpuscular

theory was very generally accepted during the eighteenth century, as, for example, by Robert Smith, whose *Compleat System of Opticks* appeared in 1738. At the beginning of the nineteenth century, Thomas Young, physician and physicist, took up the wave theory and showed how it could be used to explain some of the phenomena described by Grimaldi and Newton. He abandoned the idea of single irregularly emitted pulses, and put forward the idea of continuous vibrations. Although Newton had not relinquished the idea of the corpuscular theory of light, he had been driven to postulate a periodicity in light in order to explain the thin film phenomena. Young ascribed colour variations to differences of frequency and hence to differences of wave-length. The essential features of his contribution to the theory of optics can best be explained in the discussion of one of the experiments which he described.

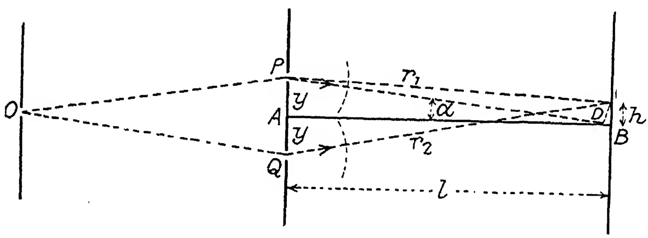

FIG. 42. TO ILLUSTRATE YOUNG'S EXPERIMENT

Light from a very small origin O, Fig. 42, diverges to a screen A wherein are two small apertures P and Q; these apertures become origins of light spreading to the region beyond A, and this is suggested by the dotted arcs, which are intended to suggest divergent wave-fronts spreading from P and Q. Thus the illumination of the further screen B is due to both sources.

The *principle of superposition* enunciated by Young states that if the displacements at any instant at a point such as C in the plane B, due to P and Q respectively, are s_1 and s_2, then the resultant displacement is

$$S = s_1 + s_2$$

In order that the algebraic addition may be valid, the direction of the displacements must be identical; in other words, they must be polarized in the same direction.

Similarly, if there were more than two sources, the displacement would be $s_1 + s_2 + s_3 +$ etc.

Let it be assumed that P and Q are single sources emitting simple harmonic waves of the same frequency and in the same phase, and

let PC $= r_1$ and QC $= r_2$. Also assume that the displacements arriving at C can be added in accordance with the above principle, then if the amplitude at C due to P is a_1 and that due to Q is a_2, we may express the resultant displacement of the two simple harmonic wave-trains as

$$S = s_1 + s_2 = a_1 \sin 2\pi\left(\frac{t}{T} - \frac{r_1}{\lambda}\right) + a_2 \sin 2\pi\left(\frac{t}{T} - \frac{r_2}{\lambda}\right) \quad . \qquad (34)$$

Putting $\delta_1 = \dfrac{2\pi r_1}{\lambda}$ and $\delta_2 = \dfrac{2\pi r_2}{\lambda}$ the expression becomes

$$S = a_1 \sin\left(\frac{2\pi t}{T} - \delta_1\right) + a_2 \sin \frac{2\pi t}{T} - \delta_2$$

Expanding the brackets and separating the terms, we obtain

$$S = \sin\frac{2\pi t}{T}(a_1\cos\delta_1 + a_2\cos\delta_2) - \cos\frac{2\pi t}{T}(a_1\sin\delta_1 + a_2\sin\delta_2)$$

If possible, let us find an angle Δ such that

$$A\cos\Delta = a_1\cos\delta_1 + a_2\cos\delta_2 \quad . \quad . \quad . \qquad (a)$$

$$A\sin\Delta = a_1\sin\delta_1 + a_2\sin\delta_2 \quad . \quad . \quad . \qquad (b)$$

$$\text{Then } S = A\sin\frac{2\pi t}{T}\cos\Delta - A\cos\frac{2\pi t}{T}\sin\Delta = A\sin\left(\frac{2\pi t}{T} - \Delta\right.$$

which would represent a simple harmonic vibration of the same frequency, but with a new phase term Δ and a new amplitude A, In order to find the significance of A and Δ, square and add the equations (a) and (b) above.

Then $A^2 = a_1^2 + a_2^2 + 2a_1a_2(\cos\delta_2\cos\delta_1 + \sin\delta_2\sin\delta_1)$

or $$A^2 = a_1^2 + a_2^2 + 2a_1a_2\cos(\delta_2 - \delta_1) \qquad (35)$$

and, on dividing (b) by (a)

$$\tan\Delta = \frac{a_1\sin\delta_1 + a_2\sin\delta_2}{a_1\cos\delta_1 + a_2\cos\delta_2} \quad . \quad . \qquad (35a)$$

If P and Q are acting as sources of the same intensity, and r_1 is only slightly different from r_2, equation 32 indicates that a_1 and a_2 will be very nearly equal. Supposing them actually equal, as they will be at certain points,

$$A^2 = 2a_1^2(1 + \cos\overline{\delta_2 - \delta_1}) = 2a_1^2\left\{1 + \cos\frac{2\pi}{\lambda}(r_2 - r_1)\right\}$$

Hence, when $r_2 = r_1$, $A^2 = (2a_1)^2$. When $(r_2 - r_1)$ is an odd number of half wave-lengths) the value of A^2 will be zero. In mechanical

in monochromatic light thus gives a means of determining the *wave-length* by using the formula given above. If white light is used to produce the interferences, the fringes in the various spectrum colours are found to be apparently superposed; though the central fringe may appear white, those on each side will show coloured borders, and the difference of spacing is such that comparatively few fringes can be observed as compared with the number that can be seen when really monochromatic light is employed.

Before dealing with the other methods of exhibiting interference, however, it is necessary to inquire into the conditions obtaining in the actual experiment as compared with those assumed in the theoretical treatment given above.

First the origin of light O is of very finite size. The wave-length of light for the middle of the spectrum is about $0{\cdot}5 \times 10^{-3}$ mm., often written $0{\cdot}5\mu$, and modern knowledge of the structure of matter has taught us to regard the origins of wave-trains of light

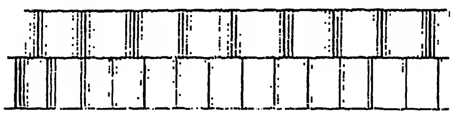

FIG. 44. RELATIVE SPACING OF FRINGES

as being comparable at most with the dimensions of an atom, which is very much smaller still, and is, in fact, of the order of 10^{-8} cm.

Hence, even if we put a flame very close to the opening O in order to make it practically self-luminous, we should still have a " source " which could be regarded as possibly consisting of millions of separate sources of light.

Again, the apertures at P and Q are of very finite dimensions and similar considerations apply to them; how then can the observed interference phenomena be explained?

Before going more fully into the discussion of the actual experiment suggested by Young, we may describe an arrangement due to Fresnel. Referring to Fig. 45, OA and OB are the traces of two plane mirrors (imagined perpendicular to the diagram) inclined at a small angle, while ab is a small source of light the images of which, a_1b_1 and a_2b_2, formed by reflection in the two mirrors, illuminate the screen s. It is evident that corresponding points in these images lie on a circle with O as centre, struck through the corresponding point of the object, and that the angle between the images subtended at the centre O is twice the angle between the mirrors. The two reflected beams overlap in the shaded portion of the diagram. In

practice the source is a small pinhole brightly illuminated and placed close to the plane of the mirrors which, when inclined at a very small angle, produce a pair of images which are very close together. The fringes are observed by an eyepiece. The mirrors must be optically polished; if they are of glass the reflection from the back surfaces must be prevented by blackening the latter or using dark "smoke" glass.

If we could regard the source of light as a point source, the two images must correspond to two equal sources emitting light in the same phase, and the theoretical treatment of page 73 would be applicable. But since they are actually of finite size we can regard them as divided into a great number of corresponding elementary areas sufficiently small to be treated as origins of waves. Thus pairs

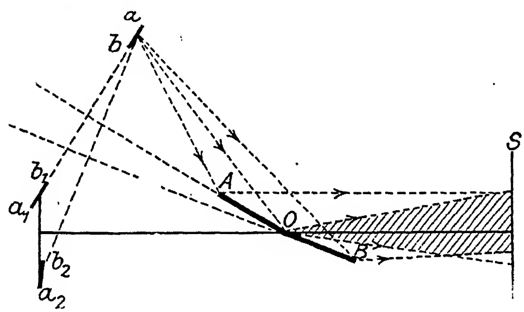

FIG. 45

of areas a_1 and a_2 would produce a set of fringes, and also b_1 and b_2, but the second set would overlap the first. In order to see how the overlapping occurs it is evident that the central fringe for a_1a_2 lies on the line which bisects a_1a_2 at right angles and passes through O; similarly, the central fringe for b_1b_2 lies on the line bisecting b_1b_2 at right angles and passing through O. Hence, the amount of overlapping of the fringes depends on the angle subtended by the source at O.

The condition which must be fulfilled by the source, then, is that it shall subtend a very small angle at the mirrors; provided this condition is fulfilled, its actual size is of no importance. Thus Fresnel was able easily to observe the fringes when a star was used as the source.

For the fuller discussion of Young's experiment it is necessary to return to a conception based upon Huygens' principle.

Fig. 46 represents the source of light O, and the two apertures P and Q as possessing a finite size. The effect at any point C on the screen B must be due to the action of all the disturbances derived from P and

Q. Let us suppose that P and Q are similar, and equal in area; it would thus be possible to divide up these areas P and Q into any number of pairs of elementary areas a and b, a' and b', symmetrically disposed with regard to the axis of symmetry AB between P and Q. Then if a and b could be regarded as a pair of elementary sources vibrating with the same frequency, they would give rise to a set of interference fringes overlying those produced by a' and b' etc. There will, however, be no visible fringes unless the vibrations from the separate points have sufficient agreement in phase so that the light and dark fringes from different pairs occupy similar positions.

The vibrations derived from a and a', b and b', may first be imagined to be derived from a single elementary source such as e situated in the

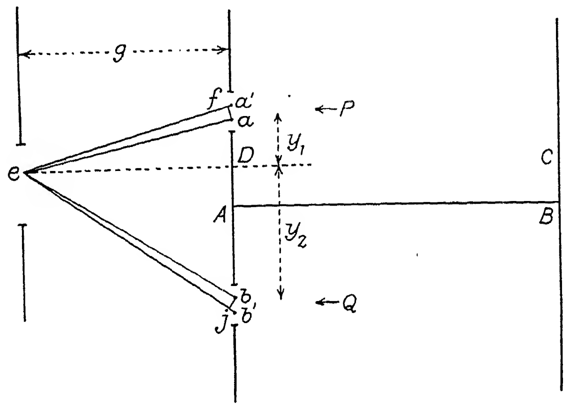

FIG. 46

aperture O; the disturbances originating from this point e will have a difference of phase at a and b

$$\frac{2\pi}{\lambda}(ea - eb)$$

while those at a' and b' will have a difference

$$\frac{2\pi}{\lambda}(ea' - eb')$$

In each case the centre of the interference fringe system will be found at the point where the disturbances arrive in the same phase. Since the disturbances at a and b are not in the same phase, the centre fringe will be displaced from B; likewise for a' and b'.

Then the net relative displacement of the centres of the interference fringes for the two systems will be such as to correspond to a phase difference (p) given by

$$p = \frac{2\pi}{\lambda}(ea' - eb') - \frac{2\pi}{\lambda}(ea - eb)$$

or

$$p = \frac{2\pi}{\lambda}\{(ea' - ea) - (eb' - eb)\}$$

Drop a perpendicular af from a on ea', and bj on eb', then, within a small second order error, $ef = ea$ and $ej = eb$

$$\therefore p = \frac{2\pi}{\lambda}\{fa' - jb'\} = \frac{2\pi}{\lambda}\left\{\frac{aa' . \mathrm{D}a}{e\mathrm{D}} - \frac{bb' . \mathrm{D}b}{e\mathrm{D}}\right\} \text{ sufficiently nearly}$$

Writing $\mathrm{D}a = y_1$, $\mathrm{D}b = y_2$, $e\mathrm{D} = g$

$$p = \frac{2\pi}{\lambda}\frac{aa'}{g}(y_1 - y_2), \text{ if we take } aa' = bb'$$

We shall only find large variations in $(y_1 - y_2)$ when we deal with different points in the aperture O when this is large; the confusion of the fringes will thus be minimized by keeping aa' small (restricting the diameters of P and Q), by increasing the value of g, the distance of O from the plane of P and Q, and by restricting the diameter of O itself; i.e. as in Fresnel's experiment its angular diameter must be kept small.

We may regard the " fringes " actually seen under experimental conditions as the resultant of many overlying systems with maxima and minima of brightness more or less in the same regions; if the

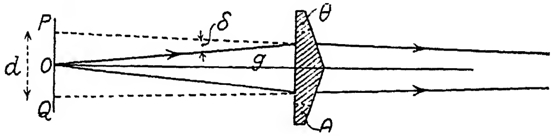

FIG. 47. THE BI-PRISM

maxima become too widely spread, however, the fringes cease to be visible.

It was because of the somewhat complex considerations underlying Young's experiment that Fresnel was led to devise his double mirror arrangement. In Young's experiment the interference takes place between diffracted beams, and it was thought that diffraction might involve some change in the properties of light.

The Bi-prism and Other Methods. There are a number of other methods of producing interference fringes. Fresnel's bi-prism is very useful. Its mode of action will be evident from Fig. 47. The bi-prism produces two images, P and Q, of the small aperture at O. These act as the sources of interfering beams. The deviation produced in a ray by transmission through a prism of small angle θ can be shown to be $\delta = (n - 1)\theta$. Hence, d, the distance between the images will be

$$d = 2g\delta = 2g(n - 1)\theta = g(n - 1)(\pi - \mathrm{A})$$

where A is the angular measure of the obtuse angle of the bi-prism. It is to be noted that the distance between the images is dependent on the refractive index. For the comparatively high refractive

index characteristic of the shorter wave-lengths, the images will be farther apart; hence, the fringes will be more closely spaced on this account, as well as on account of the diminished wave-length. The distance from the central minimum to the first dark maximum for a given wave-length is naturally calculated by the formula derived in discussing Young's experiment

$$h = \frac{\lambda l}{2d}$$

Billet has used the two halves of a converging lens cut across a diameter and mounted so that the distance between them can be adjusted. Each half can thus be made to project the image of a small source of light, and the two images can be made to approach very closely.

Lloyd has produced interferences between light derived from a small source and from its image formed by reflection in a single mirror, but the central band of zero path difference cannot be directly obtained.

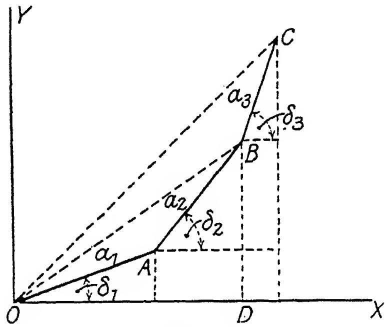

FIG. 48

Graphical Interpretation of the Superposition Formulae. Equations (35) and 35*a*) can be illustrated graphically, as indicated in Fig. 48.

Let O be the origin of co-ordinates. Draw the line OA of length a_1, and making an angle δ_1 with the axis of x. From its extremity draw AB of length a_2 and making an angle δ_2 with the axis of x.

The line OB then represents the amplitude of the sum of the vibrations by its length; the phase angle is represented by the angle it makes with the axis of x; for we see from the triangle OAB that

$$OB^2 = a_1{}^2 + a_2{}^2 + 2a_1\, a_2 \cos(\delta_2 - \delta_1),$$

since $(\delta_2 - \delta_1)$ is the exterior angle between AB and OA produced, and $\tan \widehat{BOX} = \dfrac{a_1 \sin \delta_1 + a_2 \sin \delta_2}{a_1 \cos \delta_1 + a_2 \cos \delta_2}$, which is easily seen by taking the projections of a_1 and a_2 on the axes of x and y.

If, now, a third component

$$s_3 = a_3 \cos \left(\frac{2\pi t}{T} - \delta_3\right)$$

is added to the sum, we shall easily see that it is done graphically by drawing BC of length a_3, and at an angle of δ_3 with the axis of x; as before, OC represents the length and phase angle of the resultant. We see that, generally, if there are several components, then A the amplitude of the resultant is given by

$$\begin{aligned} A^2 &= (a_1 \sin \delta_1 + a_1 \sin \delta_2 + a_3 \sin \delta_3 + \text{etc.})^2 \\ &\quad + (a_1 \cos \delta_1 + a_2 \cos \delta_2 + a_3 \cos \delta_3 + \text{etc.})^2 \\ &= (\Sigma\, a \sin \delta)^2 + (\Sigma\, a \cos \delta)^2 \end{aligned}$$

and $$\tan \Delta = \frac{(\Sigma\, a \sin \delta)}{(\Sigma\, a \cos \delta)}$$

Diffraction. Fresnel extended the ideas of Huygens by considering that each point in a surface coincident with a wave-front can be treated as the origin of a *vibratory* disturbance (as distinct from mere arbitrary pulses) spreading out in all directions. Thus, if O, Fig. 49, represents a point source, the locus of points vibrating in the same phase (i.e. the wave-front) will be a circle such as AP struck with O as centre, and radius a.

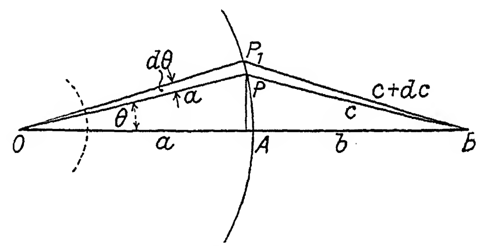

FIG. 49

Let the amplitude at unit radius from the centre be A_1, then the amplitude in the locus AP will be $\frac{A_1}{a}$, and the displacement will be

$$\frac{A_1}{a} \sin 2\pi \left(\frac{t}{T} - \frac{a}{\lambda}\right.$$

Take a point P on the locus, join PB, and call this length c. Then the amplitude ds_1 produced at B by the action of a very small area $d\sigma$ situated on the surface at P must be directly proportional to the area, and to the amplitude in the surface, and inversely proportional to the distance PB; i.e.

$$ds_1 = \frac{KA_1 d\sigma}{ac} \sin 2\pi \left(\frac{t}{T} - \frac{a+c}{\lambda}\right.$$

(where K is a constant), since the disturbance has to travel a total distance $(a + c)$ from O to B, via P.

In order to obtain the total amplitude effect at B, it would be necessary on the super-position principle to find the sum

$$A^2 = (\Sigma a_1 \sin \delta_1)^2 + (\Sigma a_1 \cos \delta_1)^2$$

for the whole of the surface, adding up the effects of all the elementary areas and taking account of the relative phases of the disturbances from them. In order to integrate, the surface may conveniently be divided into annular circular areas surrounding A as centre.

Let $\widehat{AOP} = \theta$; draw OP_1 so that $\widehat{AOP_1} = \theta + d\theta$. Join P_1B and call it $c + dc$. Imagine that $d\theta$ and dc are very small.

Now $c^2 = a^2 + (a + b)^2 - 2a(a + b) \cos \theta$

Differentiating with regard to θ (remembering that a and b are constants)

$$2cdc = 2a(a + b) \sin \theta d\theta \quad . \quad . \quad . \quad . \qquad (a)$$

Now, if we rotate the diagram about the axis OA, the arc PP_1 will strike out an annular area of amount $d\sigma$.

$$d\sigma = 2\pi a \sin \theta \,.\, a d\theta$$

$$= \frac{2\pi acdc}{a + b}, \text{ from equation } (a) \text{ above.}$$

Hence, the expression for the effect at B of this elementary annular area becomes

$$ds_1 = \frac{KA_1}{ac}\left\{\frac{2\pi acdc}{(a+b)}\right\} \sin 2\pi \left(\frac{t}{T} - \frac{a + c}{\lambda}\right)$$

$$= \frac{2\pi KA_1 dc}{(a + b)} \sin 2\pi$$

We could now take a point P_2 such that $P_2B = P_1B + dc = PB + 2dc$; the effect of the annular strip P_1P_2 would then be

$$ds_2 = \frac{2\pi KA_1 dc}{a + b} \sin 2\pi \left(\frac{t}{T} - \frac{a + c + dc}{\lambda}\right)$$

If we take a number of rings with equal steps of "dc" we shall obtain zones which can contribute the same amplitude to the effect at B, provided K remains constant, but the phases of the contributions will vary *in equal steps*. The result will be of the type (n terms in each series)

$$A^2 = m^2[\{\sin p + \sin (p + \delta) + \sin (p + 2\delta) + \ldots . + \sin (p + \overline{n - 1}\, \delta)\}$$

$$+ \{\cos p + \cos (p + \delta) + \cos (p + 2\delta) + \qquad + \cos (p + \overline{n - 1}\,\delta)\}^2]$$

where m represents the contribution of an elementary ring.

The sums of these series are well-known.* The expression becomes

$$A^2 = m^2 \left[\left\{ \frac{\sin \{p + \frac{1}{2}(n - 1)\delta\} \sin \frac{1}{2}n\delta}{\sin \frac{1}{2}\delta} \right\}^2 + \left\{ \frac{\cos \{p + \frac{1}{2}(n - 1)\delta\} \,.\, \sin \frac{1}{2}n\delta}{\sin \frac{1}{2}\delta} \right\}^2 \right]$$

$$m^2 \sin^2 \frac{\quad}{2}$$

$$\sin^2$$

or evidently
$$A = \frac{m \sin \frac{n\delta}{2}}{\sin \frac{\delta}{2}} \quad . \quad (36a)$$

If now n is very great but $n\delta$ is still finite and equal to D, say,

$$A = m \frac{\sin \frac{D}{2}}{\sin \frac{D}{2n}} = m \cdot \frac{\sin \frac{D}{2}}{\frac{D}{2n}}$$

$$= nm \frac{\sin \frac{D}{2}}{\frac{D}{2}} \quad . \quad (36b)$$

The coefficient nm is the total amplitude which would be contributed if the contributions of all the zones were in the same phase.

The required constancy of "K" is evidently a doubtful point. The contribution of a zone to the amplitude at B might be diminished as the angle made by PB with the normal to the surface increased. But evidently if we restrict the problem to finding the effect of a narrow area surrounding A, it will be justifiable to try the effect of regarding K as constant.

Suppose we first take a circular zone such that $PB = AB + \frac{\lambda}{2}$,

* See any book on higher trigonometry.

and find the whole effect; then the amplitude m contributed by an elementary ring is

$$m = \frac{2\pi KA_1 dc}{a+b}, \text{ and thus } nm = \frac{2\pi KA_1 ndc}{a+b} = \frac{2\pi KA_1\left(\frac{\lambda}{2}\right)}{a+b}$$

The total phase difference D is $\frac{2\pi}{\lambda}\left(\frac{\lambda}{2}\right) = \pi$

Hence, a_1, the amplitude due to the whole zone as defined above, will be

$$a_1 = \frac{\pi\lambda KA_1}{(a+b)} \frac{\sin\frac{\pi}{2}}{\frac{\pi}{2}}$$

$$= \frac{2\lambda KA_1}{(a+b)} \quad . \quad . \quad . \quad . \quad (37)$$

To find the phase of the resultant we may evaluate

$$\tan\Delta = \frac{\sin p + \sin\overline{p+\delta} + \ldots + \sin(p + \overline{n-1}\delta)}{\cos p + \cos\overline{p+\delta} + \ldots + \cos(p + \overline{n-1}\delta)}$$

and from the sums of the series appearing in the expression above, we find

$$\tan\Delta = \tan\left\{p + \frac{n-1}{2}\delta\right\}$$

and thus evidently $\qquad \Delta = p + \frac{n-1}{2}\delta$

This equation shows that the phase of the resultant in such a case is the mean of the phases of the first and last "contributions"; this is otherwise obvious from considerations of symmetry. Hence, the phase of the resultant of the whole zone considered above where $PB = AB + \frac{\lambda}{2}$ would be $\frac{\pi}{2}$ behind that of the disturbance arriving from the centre, if we consider the secondary waves from points such as P to start out with the same phase as the vibrations in the wave-surface. The expression for the displacement is therefore

$$s = \frac{2\lambda KA_1}{(a+b)} \cos 2\pi\left(\frac{t}{T} - \frac{a+b}{\lambda}\right)$$

the cosine appearing instead of the sine.

If, now, we take a wider zone given by making PB $= AB + \frac{\lambda}{2}$ and AB $+ \lambda$ for the limits, the amplitude a_2 produced at B may be slightly smaller numerically than that from the first zone; on the same suppositions the phase would be $3\frac{\pi}{2}$ behind that of the disturbance from A, and therefore the amplitude contributions, being in exactly opposite phases, can be subtracted to find the resultant of both.

Amplitude from first two zones $= a_1 - a_2$ (and similarly the resultant amplitude for any number of zones will be $a_1 - a_2 + a_3 - a_4 +$ etc. . . .).

With respect to $(a_1 - a_2)$, this will be very small in comparison with either a_1 or a_2, and it thus appears that if we screen off the outer parts of the surface so as to allow only the first two zones to send light to B, the illumination should be much smaller than when only the first zone is allowed to act. If the aperture is opened so as to admit the third zone there will again be a maximum illumination. Such "zones" were used for the discussion of diffraction problems by Fresnel, and are often termed Fresnel zones.

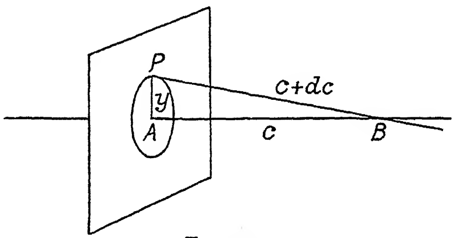

FIG. 50

For finding the general effects of the first few zones it is quite legitimate to use formula (36).

Suppose it is desired to find the effect, at a point on the axis of symmetry, of the diffraction of a plane wave-train at a circular aperture, assuming that the incident wave-fronts are parallel to the plane of the aperture.

In Fig. 50, the aperture has centre A and radius AP $= y$. B is a point on the axis, so that AB $= c$ and PB $= c + dc$.

Then $y^2 + c^2 = (c + dc)^2 = c^2 + 2cdc$, if dc is small of the first order, so that $(dc)^2$ can be neglected.

Then $y^2 = 2cdc$ and $dc = \frac{y^2}{2c}$.

The difference of phase between disturbances arriving at B from A and P is therefore

$$D = \frac{2\pi}{\lambda}\left(\frac{y^2}{2c}\right) = \frac{\pi y^2}{\lambda c}$$

In formula (36), *nm* appears as the total amplitude which would result if all the elementary zones gave their contributions at B in the same phase. It is evidently proportional to the area of the aperture, and inversely proportional to the distance of B from the point A. Hence (36) becomes in this case, writing $\mathcal{K}$ as a constant of proportionality,

$$A = \mathcal{K}\frac{\pi y^2}{c}\,\frac{\sin\left(\dfrac{\pi y^2}{2\lambda c}\right)}{\left(\dfrac{\pi y^2}{2\lambda c}\right)} = 2\mathcal{K}\lambda \sin\frac{\pi y^2}{2\lambda c} = K_1 \sin\left(\frac{K_2}{c}\right)$$

where K_1 and K_2 are constants for a given aperture and wave-length. The values of A are plotted against c in Fig. 51.* As we

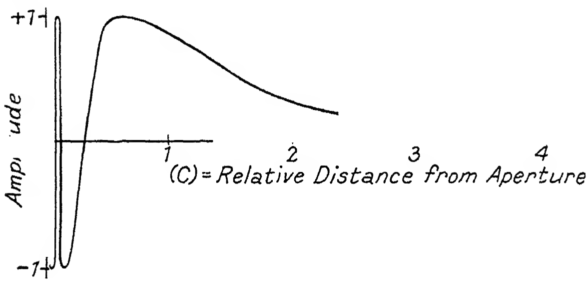

FIG. 51. AMPLITUDE AND RELATIVE DISTANCE FROM APERTURE

approach the point A from a distance which is very great in comparison with the radius, the amplitude on the axis slowly increases to a maximum; it then falls through zero and becomes negative, going thus through a series of maxima of alternate sign the more rapidly as the distance from the aperture decreases. The *intensity*, which is proportional to the square of the amplitude, can naturally show no changes of sign, but varies between zero and a more or less uniform maximum value. The accuracy of the expression diminishes as the distance c becomes shorter.

The discussion just given is only applicable to points on the axis, but we may gain some idea of the distribution of intensity away from the axis by the following argument. Let us consider the plane of B, where, as we approach A, the first maximum on the axis is found. From the expression above we shall then have

$$\frac{\pi y^2}{2\lambda c} = \frac{\pi}{2}, \text{ or } y^2 = \lambda c,$$

* K_1 and K_2 are taken as unity, to exhibit the form of the curve.

the sine term then becoming unity. The aperture then includes the first of the Fresnel zones mentioned above, and $PB - AB = \frac{\lambda}{2}$.

Imagine that LMNP, Fig. 52, is a portion of the plane wave-front *unobstructed by a screen*, and let B_1 be a point in the plane of observation so that B_1B is perpendicular to AB, and is equal, say, to $\frac{y}{2}$.

If we draw the first Fresnel zone for the point B_1 we shall obtain a circular area suggested by the dotted line. Now imagine the screen replaced in the original position with respect to B. As far as B_1 is concerned the aperture obviously includes a part only of the first Fresnel zone, and also a portion of the second. The radii

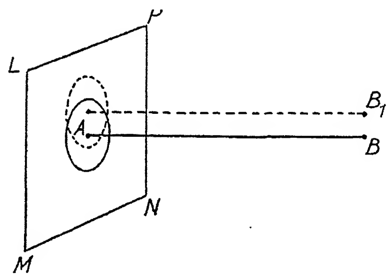

FIG. 52

of successive zones, enclosing rings of equal area, are 1, $\sqrt{2}$, $\sqrt{3}$, etc., so that a small portion of the third begins to appear. Clearly the illumination is very much lower than at the axial point, and we may therefore infer a concentration of light at B of which the dimensions are comparable with the aperture itself. Exact calculation shows that the effective concentration is even smaller than the aperture; a " focus " can be found where the bright *axial spot* has only one-third of the diameter of the aperture.

The Pinhole Camera. Calculation will show that the ratio $\frac{y}{c}$ must be very small if the first Fresnel zone only is to be included. If c is 50 cm. and we assume $\lambda = 0{\cdot}5 \times 10^{-3}$ mm., the radius of the zone is 0·5 mm.

Fig. 53 shows a set of photographs of the diffraction effects at a circular aperture. As the aperture is approached the concentration of light becomes more definite and a dark ring begins to appear surrounding it. The illumination at the centre falls, and a dark spot appears (the first two Fresnel zones are now included); further

inwards still, a dark ring appears to grow out of the centre while a bright spot increases to a maximum on the axis.

It is owing to the comparatively great concentration of light which appears when the first Fresnel zone is included by the aperture, that the pinhole camera can be used to produce quite well-defined photographs. Further diminution of the size of the pinhole causes the image patch to become more and more diffuse.

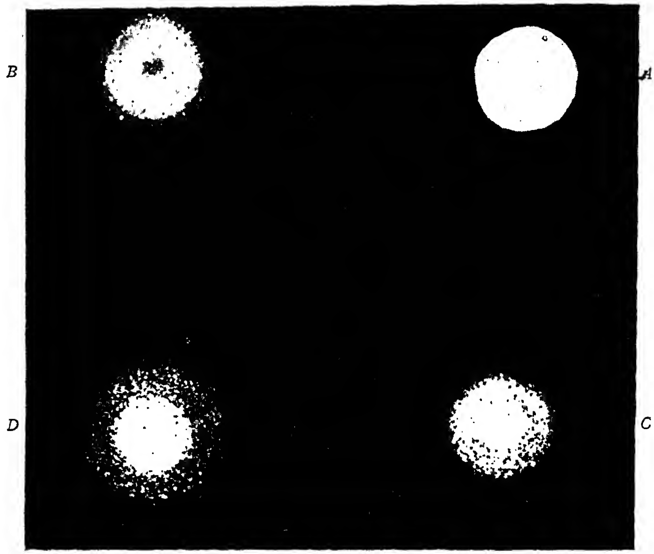

FIG. 53

A. Circular aperture
B. Diffraction pattern when the aperture includes two Fresnel zones
C. Pattern when the aperture includes the first Fresnel zone only
D. Pattern at a still greater distance

The main disadvantage of the photographs is that when wide-angle views are taken the effective area of the aperture varies with the obliquity; this factor adversely affects both the illumination and definition towards the margin.

Results of Advanced Theoretical Studies of Diffraction. The effect at the point B, Fig. 49, of the disturbances due to the whole wave-front is

$$a_1 - a_2 + a_3 - a_4 + \text{etc.}$$

If the successive terms are of slowly diminishing magnitude, the

higher ones being comparatively small, it is easy to show that the sum of the series must be very nearly $\left(\frac{a_1}{2}\right)$*.

Now $$\frac{a_1}{2} = \frac{\lambda K A_1}{(a+b)} \quad . \quad . \qquad \text{from (37)}$$

On the other hand, the displacement at B can be calculated directly; it is

$$\frac{A_1}{(a+b)} \sin 2\pi\left(\frac{t}{T} - \frac{a+b}{\lambda}\right)$$

Hence, if we put $K = \frac{1}{\lambda}$ in our equation for the use of Huygens' principle, the correct value of the amplitude will be obtained.

There is a difficulty regarding the phase, however, for if it be assumed that the effect at B is simply half that of the first Fresnel zone, this would be

$$\frac{A_1}{(a+b)} \cos 2\pi\left(\frac{t}{T} - \frac{a+b}{\lambda}\right)$$

In order to find the correct phase by the application of Huygens' principle we must therefore assume that the secondary disturbances start with a phase $\frac{\pi}{2}$ in advance of the vibrations in the wave-front, or that the length of the optical path is diminished by a quarter of a wave-length.

* The sum
$$S = a_1 - a_2 + a_3 - a_4 + \; . \; . \; . \; . \; - a_{n-1} + a_n$$
can be written
$$S = \frac{a_1}{2} + \left(\frac{a_1}{2} - a_2 + \frac{a_3}{2}\right) + \left(\frac{a_3}{2} - a_4 + \frac{a_5}{2}\right) + \text{etc. to} \; . \; . \; . \; .$$
$$+ \left(\frac{a_{n-2}}{2} - a_{n-1} + \frac{a_n}{2}\right) + \frac{a_n}{2}$$
$$= a_1 - \frac{a_2}{2} - \left(\frac{a_2}{2} - a_3 + \frac{a_4}{2}\right) - \left(\frac{a_4}{2} - a_5 + \frac{a_6}{2}\right) - \text{etc. to} \; . \; . \; . \; .$$
$$- \left(\frac{a_{n-3}}{2} - a_{n-2} + \frac{a_{n-1}}{2}\right) - \frac{a_{n-1}}{2} + a_n$$
If the terms a_1, a_2, a_3 only decrease in magnitude very slowly, we may conclude that the terms in the brackets would probably all be positive or all negative. The sum is seen to lie between
$$\frac{a_1}{2} + \frac{a_n}{2} \text{ and } \left\{\left(a_1 - \frac{a_2}{2}\right) - \left(\frac{a_{n-1}}{2} - a_n\right)\right\}$$
and therefore cannot differ greatly from $\frac{a_1}{2} + \frac{a_n}{2}$ or from $\frac{a_1}{2}$ if $\frac{a_n}{2}$ can be neglected.

Suppose we have a source of light O emitting radiation, and a point B at which the total effect is to be found, a permissible modification of Huygens' principle is to imagine a surface surrounding B which, while the waves are passing, will clearly be a seat of disturbances of various amplitudes and phases. With certain restrictions we may find the effect at B by adding up the contributions derived from all points of this surface which are capable of sending them, taking account of their amplitudes and relative phases on arrival. A little consideration will, however, make it appear that the disturbances arriving at B in any instant must be regarded as having

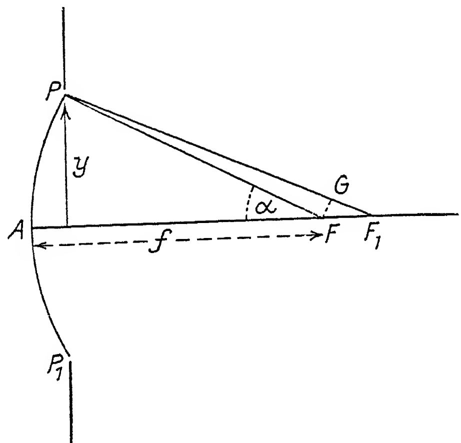

FIG. 54

been possibly derived from *all points in the space surrounding B* and arriving with the phases which were characteristic of these points at a time $\frac{r}{V}$ before arrival (where r is the distance of a point from B and V is the velocity). This latter method is clearly the most general, and it is possible to obtain a mathematical solution of the problem as to the conditions under which the effect of the *surface* can be regarded as equivalent to the effect of the *space*. The results confirm those which have already been obtained tentatively above, and show that we must not regard the modified Huygens' principle as a physical description of the mechanism of these diffraction phenomena, but rather as a helpful " short cut " to be applied with due reservations in order to escape considerations of a much more complex character.

Diffraction Phenomena with Convergent Light. *Effects on the*

Axis. Let a convergent wave-train with spherical wave-fronts be limited by a circular diaphragm symmetrically placed with respect to the axis. The case is represented in Fig. 54, and the radius of the diaphragm is shown as y, that of the wave-front is f. The trace of the wave-front is AP, and the axial "focus" where all disturbances from the wave-front arrive in the same phase is F. The angle $\widehat{AFP} = \alpha$.

Let F_1 be an axial point such that FF_1 is a small distance δf; the geometrical path difference of disturbances reaching F_1 from A and P will be

$$AF_1 - PF_1 = (AF + FF_1) - (PG + GF_1)$$

where G is a point on PF_1 at the foot of a perpendicular dropped from F to PF_1. Then, if δf is small, $PF = PG$ with sufficient accuracy, and $AF_1 - PF_1 = FF_1 - GF_1 = \delta f\ (1 - \cos\alpha.)$

A familiar expansion in trigonometry gives

$$\cos\alpha = 1 - \frac{\alpha^2}{2} + \frac{\alpha^4}{4} - \text{etc.}$$

and if α is small, $\frac{\alpha^4}{4}$ and higher terms may be neglected, and $AF_1 - PF_1 = \delta f \,.\, \frac{\alpha^2}{2}$

It will sometimes be convenient to write $\delta p =$ (increase of marginal path *minus* increase of axial path).

Then, in cases where f is large in comparison with y, which will often be the case with actual optical instruments

$$\delta p = -\frac{\delta f}{2}\left(\frac{y}{f}\right)$$

If the medium be not air the equation for the optical path difference becomes

$$\delta p' = -n'\frac{\delta f}{2}\left(\frac{y}{f}\right)^2 \quad . \quad . \quad . \quad . \quad (38)$$

where n' is the refractive index.

When δp is $\pm\lambda$ it will be seen that the surface includes two Fresnel zones and the intensity on the axis will be zero. From the investigation on page 82, which is valid for the present case, it appears that the zones will be equal in area, and for any elementary ring in the first zone there will be another of equal area in the second zone which gives an amplitude contribution equal in magnitude but opposite in sign. Hence, there will be a series of maxima and

minima, practically symmetrically spaced along the axis on each side of the focus.

Effects in the Focal Plane. It is worth while to examine the effects in the plane of the focus at right angles to the axis, but an easy discussion is only possible when the aperture is rectangular. This case is represented in Fig. 55, where F is the centre of curvature of the wave-front, LMNO is a portion of the wave-front supposed to be transmitted by a rectangular aperture symmetrically placed, and A is the central point. Take $FF_1 = h$, parallel to one side of the aperture and perpendicular to AF. The line P_1AP is a mid-line of the rectangle. Let $P_1A = AP = y$.

The conditions are such that we might imagine FF_1 a portion of the axis of a globe on which LM, ON were parallels of latitude.

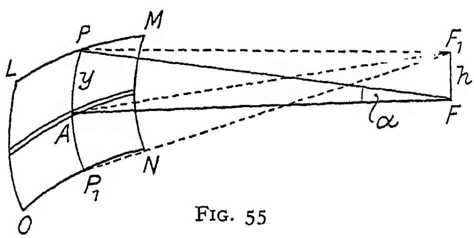

FIG. 55

The point F_1 is equidistant from all points on such lines, and consequently the phase contribution from a whole strip parallel to LM will be the phase of the contribution from its mid-point.

From the similar case encountered in discussing Young's experiment we find

$$P_1F_1 - PF_1 = 2h \sin \alpha, \text{ or } AF_1 - PF_1 = h \sin \alpha.$$

Evidently when $AF_1 = PF_1 + \frac{\lambda}{2}$, we shall always be able to find a pair of horizontal strips in the sections above and below A which give their contributions in opposite phases, so that the results neutralize. It may be inferred that there will then be a minimum illumination at F_1 when

$$\frac{hy}{f} = \frac{\lambda}{2}$$

or

$$h = \frac{f\lambda}{2y}$$

(taking $\sin \alpha = \frac{y}{f}$ approximately), and there will be additional minima when $h = \frac{3f\lambda}{2y}, \frac{5f\lambda}{2y}$, and etc.

The conditions when the aperture is circular are not so easily dealt with, but it can be shown that the first minimum will be found when

$$h = \frac{0{\cdot}61\lambda}{\sin\,\alpha} \quad . \quad . \quad . \quad . \qquad (39)$$

or by an allowable approximation

$$0{\cdot}61\,\frac{\lambda_0}{n'}\frac{f}{y}. \qquad (39a)$$

$\frac{\lambda_0}{n'}$ being now written for λ, the actual wave-length of the light; λ_0 is the wave-length in air and n' the refractive index.

In this case there will be central symmetry, the minima are represented by dark rings, and the general appearance of the concentration in the focal plane is shown by Fig. 56. The central condensation of light is called the "Airy disc," since the distribution of light in the image was first worked out by Sir George Airy in 1834.

FIG. 56.
PHOTOGRAPH OF THE AIRY DISC

Intensity near the Focus. General Method for Circular Aperture.* Let F in Fig. 57 represent a point on the axis of a circular aperture limiting a symmetrical, spherical, convergent wave-train. FF_1 is a line of small height h perpendicular to the axis OF. Imagine a spherical reference surface (with centre F) limited by the aperture; then the circular ring ACBD is drawn in the surface with *its centre* O in the axis, having a radius y. The diameter CD is parallel to, and the diameter AB perpendicular to, FF_1. The surface is the seat of disturbances in various phases.

Take the point P in the ring so that $\widehat{COP} = E$. Join PF_1, PF and HF, having drawn PH perpendicular to AO and F_1G perpendicular to PF as shown.

* This section is given for students who can follow the necessary mathematics. Others should omit it. Those who are not acquainted with Bessel Functions should note that the integrals can be evaluated by "mechanical integration." (See Conrady, *R.A.S.*, "Monthly Notices," 79 (1919), 575.)

If h is a small quantity of the first order, PG = PF_1 within a small error of the second order. Hence, if $\text{PF}_1 = r$, and PF = R

$$r = \text{R} - h \sin \widehat{\text{GF}_1\text{F}}$$

It will appear from the diagram that the points P, H, F_1, F, and G are all in one vertical plane, and that $\widehat{\text{GF}_1\text{F}} = \widehat{\text{PFH}}$. Hence,

$$r = \text{R} - h \sin \widehat{\text{PFH}} = \text{R} - h\frac{\text{PH}}{\text{R}} = \text{R} - \frac{hy \cos \text{E}}{\text{R}}$$

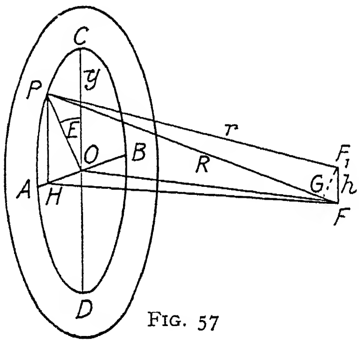

FIG. 57

The area of an element of surface at P is $yd\text{E}dy$. Hence, by Huygens' principle the displacement at F_1 produced by this element is

$$ds = \frac{\text{A}}{\lambda r}(yd\text{E}dy) \sin \left\{2\pi\left(\frac{t}{T} - \frac{r}{\lambda}\right) + \delta\right\}$$

where δ represents a term to express the phase of the disturbance in the element and A is the amplitude in the surface.

The total displacement is therefore

$$s = \frac{\text{A}}{\lambda\text{R}}\iint \sin \left[2\pi \left\{\frac{T}{t} - \frac{\text{R} - hy\left(\frac{\cos \text{E}}{\text{R}}\right)}{\lambda}\right\} + \delta\right] yd\text{E}dy$$

in which the approximation of writing R for r in the denominator of the co-efficient outside the integral has been introduced; the integration is to be performed over the whole surface. The expression may be simplified by writing it

$$s = \frac{\text{A}}{\lambda\text{R}}\iint \sin\left\{x + \frac{2\pi hy \cos \text{E}}{\lambda\text{R}}\right\} yd\text{E}dy$$

$$= \frac{\text{A}}{\lambda\text{R}}\iint \sin (x + \text{W} \cos \text{E})\, yd\text{E}dy$$

where
$$W = \frac{2\pi hy}{\lambda R} \tag{40}$$

Writing in the limits,
$$s = \frac{A}{\lambda R}\int_{E=o}^{E=2\pi}\int_{y=o}^{y=y_1}(\sin x \cos \overline{W \cos E} + \cos x \sin \overline{W \cos E})\, ydEdy$$

In integrating with respect to E, the elements of the integral involving sin (W cos E) will cancel each other in pairs if δ (which is contained in the term x) is independent of E, since for every one value of E there will be another for which the cosine is numerically equal and opposite in sign.

The integral therefore reduces to
$$s = \frac{A}{\lambda R}\int_o^{2\pi}\int_o^{y_1}\sin x \cos W \cos E\, ydEdy\,,$$
$$= \frac{A}{\lambda R}\int^{1} \sin x \left\{ 2\pi\, J_o\left(\frac{2\pi hy}{\lambda R}\right)\right\} ydy$$

where J_o is the Bessel function of the zero order.* If now x is independent of y, which will be the case of a spherical wave-front with centre in F, the expression is integrable, and becomes
$$s = \frac{Ay_1}{h} J_1\left(\frac{2\pi hy_1}{\lambda R}\right) \sin x$$

The sin x is the periodic term; the other part represents the amplitude. Hence the intensity is given by
$$I = \text{constant}\ \frac{Ay_1}{h} J_1\left(\frac{2\pi hy_1}{\lambda R}\right)$$

This subject will be continued in Chapter IV (see page 123). The form of the above expression, when plotted, is shown in Figs. 67 and 74.

The Properties of Radiation. *Experimental Methods.* We have already summarized the results of Newton's famous experiments on the dispersion of light, from which it was considered to be proved that white light was in reality a mixture of monochromatic radiations. Wollaston first observed the dark lines in the spectrum of sunlight, but Fraunhofer, who discovered them independently, made the fullest use of this convenient way of determining particular

* Tables of these "Bessel functions" are available, and thus it is convenient to express results in terms involving them.

radiations for "dispersion" measurements, or the variation of refractive index with "colour," but since that time a vast range of experimental methods for quantitative and qualitative study of dispersion and dispersed radiation has been built up.

Fig. 58 illustrates the optical parts of a simple form of spectroscope. The collimator contains a slit, usually of variable width, placed in the focal plane of the lens L_1 so that light radiating from the centre of the slit will give a beam which is parallel on emergence from L_1.

The telescope consists of the object glass L_2 and the eyepiece, carried together in a tube which is pivoted so as to rotate about the vertical axis of the instrument. It is usual to have the optical axes of telescope and collimator horizontal, while the axis of rotation

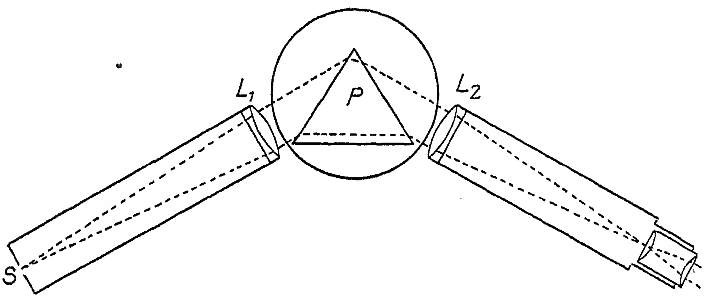

FIG. 58. PLAN OF SPECTROMETER

is vertical. A small circular table furnished with levelling screws, and usually mounted so as to be capable of rotation about the same axis, is placed so as to hold a prism or diffraction grating placed between the telescope and collimator. It is a convenience to have divided circles and verniers to measure any rotation of the table or the telescope.

If the telescope is turned so as to be coaxial with the collimator, the lens L_2 projects an image of the slit into the focal plane, where it may be brought to coincidence with the crossing point of the "cross wires," usually spider threads or the finest silk fibres, with the aid of the eyepiece or magnifier by which both image and cross wires are observed.

Applying the law of refraction

$$n \sin i = n' \sin i'$$

to the refraction of a ray at the two faces of a prism, it can be shown that the total horizontal deviation produced by the prism (with its refracting edge vertical) is a minimum when the passage of the ray

is symmetrical. When this is the case we have, writing A for the angle of the prism and δ for the deviation (Fig. 59),

$$2(90^\circ - i') = 180^\circ - A \quad \text{or } A = 2i'$$
$$\text{and } \delta = 2i - 2i'$$

whence the law of refraction gives

$$n' = \frac{\sin i}{\sin i'} = \frac{\sin\left(\frac{A+\delta}{2}\right)}{\sin\left(\frac{A}{2}\right)}$$

the minimum deviation method is a familiar method of finding the refractive index of a prism.

Emission and Absorption Spectra. If a sodium flame is placed in front of the slit, and the latter is made very narrow, a double image

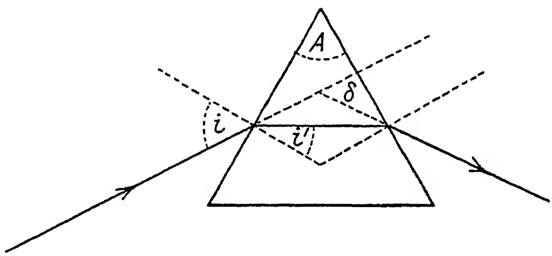

FIG. 59

of the slit can be observed by the eyepiece when the light is refracted through the prism, and the images will have the characteristic orange-yellow colour of the sodium flame. They represent the "sodium lines." Each "line" corresponds to light of a definite frequency, on which frequency the refractive index, and hence the deviation, depends. Sometimes it may be more accurate to make measurements with a wider slit with a thread stretched down its centre. With sodium light a double thread image will be seen, but each dark thread image will be partially illuminated by light from another portion of the slit.

Line emission spectra of more or less complexity are yielded when the salts of other alkali metals are vaporized in a Bunsen flame (or, better, an oxy-hydrogen flame), and a very wide range of "line" spectra can be obtained by vaporizing chemical substances with the aid of the electric arc or spark.

The arc may be formed between poles of the actual substance if it be metallic, and the flame of the arc is the source of light. It is

usually convenient first to place the arc A (Fig. 60) on the axis of the collimator by using a very wide slit, and observing the patch of light projected into the centre of the collimator lens when alignment is obtained. A condensing lens of sufficient aperture to utilize the whole aperture of the collimator lens should then be placed in position, so as to project the image of the illuminant on to the plane of the slit.

The electric spark is another important agent in the production of line spectra, more especially when it is oscillatory. An induction coil or a transformer is used with a condenser of suitable capacity in parallel with the spark gap. Thus for ordinary spectroscopic purposes a 6 in. or 10 in. coil run by a mercury or electrolytic break may be used with two or three Leyden jars, in parallel, connected across the spark terminals. The condensed discharge is quite different from that obtained without the condenser; it volatilizes

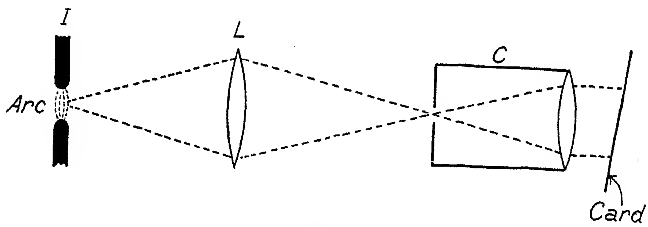

FIG. 60

much greater amounts of the substances of the poles; it is also necessarily much shorter. Spectra of the same substance excited by the flame, arc, and spark may have certain lines in common, but there are, in general, important differences owing to the greater atomic disturbances which are produced in the arc and spark.

Another important method of exciting spectra is that of a high-tension discharge through gases at low pressure contained in a vacuum tube. The discharge may be made to pass through a capillary portion of the tube, and a reasonably great intensity of brightness can be obtained with a small induction coil run from two or three accumulators. The hydrogen and helium spectra obtained in this way are of great importance in refractometry, i.e. the measurement of refractive indices.

Another special source of great utility, giving a bright line spectrum, is the mercury arc, in which the discharge takes place in a tube of glass or quartz through an "atmosphere" of mercury vapour, one or both electrodes being a surface of mercury. The small sealed lamps in fused quartz suffer from the disadvantage that the rising

pressure and temperature inside the tube have an adverse effect on the homogeneity of the light. Each spectrum line is "broadened," and gives a small range of frequencies instead of one frequency. This destroys the value of the light for certain interference experiments.

In marked contrast to the line spectra are the continuous spectra yielded by light from hot bodies such as, for example, the crater of the carbon arc, or the tungsten ball of a pointolite lamp.* The appearance yielded in the spectroscope is a band of rainbow colours from red to violet. Spectra of any kind seem to fade away towards each end when observed visually, but radiations can be detected beyond each end of the visible spectrum if suitable means are employed. Fig. 61 shows the construction of a "spectrograph," in which the spectrum falls on a photographic plate. Since the

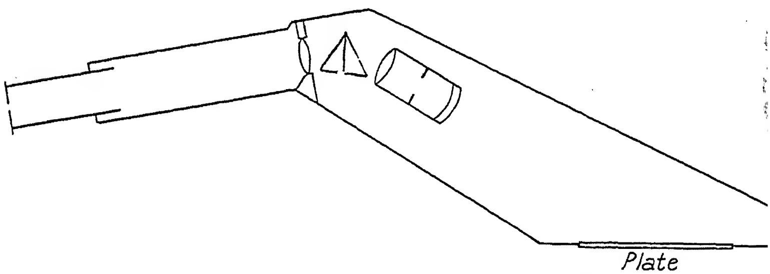

FIG. 61. DIAGRAM OF QUARTZ SPECTROGRAPH

refractive index of the material of the lens is higher for the shorter wave-lengths, these will be brought to a focus nearer the lens. Hence, the plate is inclined as shown. Photography shows that the visible radiations occupy only a part of the photographic range of the spectrum. In the ultra-violet (the region of wave-lengths shorter than the violet) it is necessary to use a substance like quartz which transmits the shorter wave-lengths better than glass.

Ordinary photographic plates are not sensitive to the red end of the spectrum, but they may be sensitized to these radiations, and to a range of still longer wave-lengths (the infra-red region) by bathing with suitable dyes and subsequent drying in darkness before exposure.

The range of radiation which can be detected photographically is, however, short in comparison to the full range which can be recognized if the energy of the radiation is detected by thermometric

* The "pointolite" lamp is a convenient vacuum tungsten arc manufactured by Messrs. Ediswan, Ltd.

means. Fig. 62 shows the construction of a typical instrument used in the investigation of the infra-red, in which the " collimator " and telescope lenses used in the visual spectroscope are replaced by concave mirrors M_1, M_2, thus avoiding the effects of different focusing distances for different wave-lengths as encountered in the quartz spectrograph. Instead of the photographic plate, a thermopile or a delicate resistance thermometer (bolometer) is used to find the energy falling in different spectral regions. It is usual to place

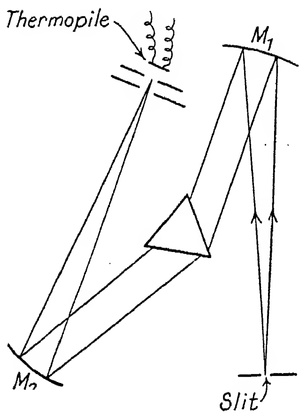

Fig. 62. Apparatus for Investigation of the Infra-red Spectrum

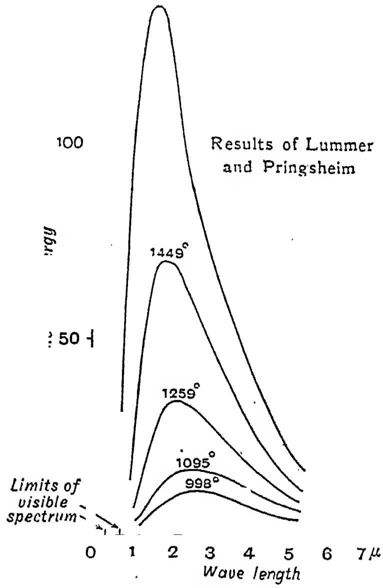

Fig. 63

a screen with a slit parallel to the spectrum lines in the plane of the spectrum, using the thermopile just behind the slit. The energy of the radiation is absorbed by the blackened surface of the thermopile and transformed into heat. The heating effect may be taken as a measure of the energy passing into the range of wave-length determined by the width of this-slit in the spectrum. When corrections are made for the width of both collimator and spectrum slits, it is possible to derive the distribution of energy in the spectrum, i.e. the *relative* values of the heating effects which would be found for different parts of the spectrum, if both slits were made indefinitely narrow.

The wave-length and frequency of the radiation passing through

the second slit can be found when necessary by the use of a diffraction grating method.

The distribution of energy in the spectrum of hot bodies giving continuous spectra is a function of the temperature. The total emission of energy is proportional to the fourth power of the absolute temperature; the ideally efficient radiator (the "black body" of radiation theory; charcoal comes fairly close to the ideal) has an energy distribution at various temperatures represented by Fig. 63. It will be noticed that the visible spectrum occupies a comparatively restricted region in the diagram; most of the energy of hot bodies at the temperatures shown is found in the long-wave heat radiations. As the temperature rises the maximum energy is found at shorter and shorter wave-lengths. In applied optics, the distribution of energy for various sources is of some importance, and Fig. 64 gives curves for various natural and artificial sources of light. The sun's radiation corresponds roughly to that of a "black body" at 5000° C., a temperature unattainable in practical sources of artificial light; the light from a blue sky has an even greater *relative* energy in the violet end of the spectrum. See Fig. 64.

Planck has given an expression for the distribution of energy in the spectrum of a black body—

$$E = \frac{c_1\lambda^{-5}}{\left(e^{\frac{c_2}{\lambda T}} - 1\right)} \quad . \quad . \quad . \quad . \quad (42)$$

where c_1 and c_2 are constants, e is the natural base of logarithms and T is the absolute temperature. For the region of the visible spectrum and shorter wave-lengths, the formula of Wien

$$E = c_1\lambda^{-5}\, e^{\overline{\lambda T}} \qquad (43)$$

is sufficiently accurate.

The distribution of energy in the lines of emission spectra is receiving much attention at the present time, but the subject is mainly of theoretical importance.

Absorption of Radiation. When radiation passes from one medium into another, the phenomena of reflection and refraction are, in general, to be observed at the surface. Many homogeneous media have the property of absorbing radiation as it passes through them, and the absorbing power usually varies with the wave-length. When the variation occurs within the range of the visible spectrum, then some of the radiations which may be looked upon as the constituents of "white" light are absorbed while others are transmitted, and the phenomena of colour usually appear.

As the radiation passes through a homogeneous absorbing medium the intensity of a parallel beam is reduced in accordance with the "exponential" law

$$I = I_0 e^{-\alpha t} \quad . \quad . \quad . \quad . \quad . \quad (44)$$

where α is the absorption coefficient and t is the thickness.

The shortest wave-length radiations which can be photographed in the ultra-violet are easily absorbed by air, which necessitates the use of the vacuum spectrograph for investigations in the regions

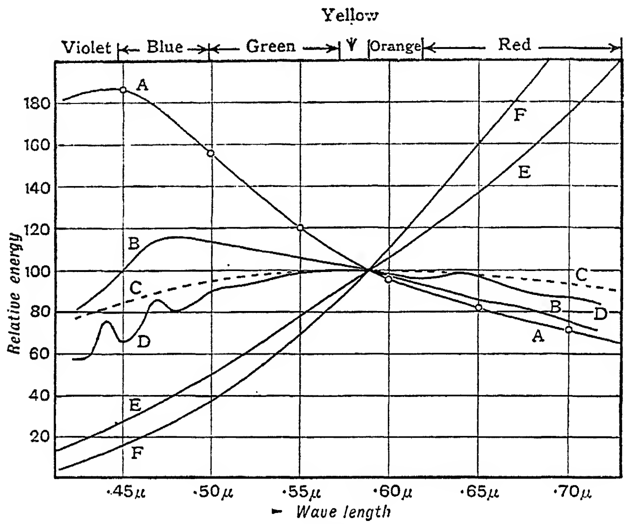

FIG. 64

below 0·180μ. Quartz transmits down to $\lambda = 0{\cdot}18\mu$ approximately, while ordinary glass transmits down to about 0·295μ. The question of the ultra-violet absorption of glass is one of considerable moment in connection with photography.

On the long wave-length side glass transmits well only as far as 5μ, even in ordinary thickness, say 2 mm. Rock-salt is much more transmissive and will pass radiations as far as $\lambda = 20\mu$ and beyond. There are, however, ranges of wave-length in which absorption takes place for most substances.

It is well established now, that X-rays and the γ-rays of radium are of the same nature as "light," only with very short wave-lengths; at the other extreme appear the heat radiations and the long wave-length radiations employed in wireless telegraphy and telephony.

The following table will give some idea of the distribution of some known radiations in terms of wave-length and frequency.

Wave-length (in microns)	Wave-number (reciprocal of wave-length expressed in cm.)	Characteristic of Radiation
(Approx) ·00001	10^{10} to 10^{8}	Gamma rays (from radium).
·00001 to ·005	10^{9} to 10^{7}	Röntgen or X-rays of varying "hardness."
0·1 to 0·2	10^{5} to 5×10^{4}	Extreme ultra-violet region explored by Schumann.
0·12	$8{\cdot}4 \times 10^{4}$	Short wave-length limit of transmission of fluorite.
0·185	$5{\cdot}9 \times 10^{4}$	Short wave limit for quartz. Air becomes relatively opaque for shorter waves.
0·2 to 0·39	$5{\cdot}0$ to $2{\cdot}54 \times 10^{4}$	Ordinary ultra-violet region. Chemically and physiologically active radiation.
0·39 to 0·77	$2{\cdot}54$ to $1{\cdot}3 \times 10^{4}$	Visible radiation.
0·39 to 0·43	$2{\cdot}54$ to $2{\cdot}32 \times 10^{4}$	Violet.
0·43 to 0·47	$2{\cdot}32$ to $2{\cdot}13 \times 10^{4}$	Blue.
0·47 to 0·5	$2{\cdot}13$ to $2{\cdot}00 \times 10^{4}$	Blue-green.
0·5 to 0·53	$2{\cdot}00$ to $1{\cdot}89 \times 10^{4}$	Green.
0·53 to 0·56	$1{\cdot}89$ to $1{\cdot}79 \times 10^{4}$	Yellow-green.
0·56 to 0·59	$1{\cdot}79$ to $1{\cdot}69 \times 10^{4}$	Yellow.
0·59 to 0·62	$1{\cdot}69$ to $1{\cdot}61 \times 10^{4}$	Orange.
0·62 to 0·77	$1{\cdot}61$ to $1{\cdot}30 \times 10^{4}$	Red.
0·77 to 1·0	$1{\cdot}30$ to $1{\cdot}00 \times 10^{4}$	Near infra-red. Can be explored by photography.
1·0 to 20	$1{\cdot}00$ to $0{\cdot}05 \times 10^{4}$	Infra-red or "heat" radiations. Spectrum explored by thermopile or bolometer.
20 to 500	$0{\cdot}05 \times 10^{4}$ to 20	Radiations studied by special thermometric methods.
500 to 10 kilometres or beyond.	20 to 10^{-6}	Waves detected by electrical methods.

Emission and Absorption Spectra. If the prism and collimator of an ordinary spectroscope be fixed, the divided circle for the telescope can be calibrated in terms of wave-length; the "Hilger" wave-length spectrometers permit the direct reading of the wave-lengths of visible lines. The characteristic spectrum lines for different elements are listed in wave-length tables such as Watt's *Index of*

Spectra and in Kayser's *Handbuch der Spektroskopie*. A convenient modern table is Kayser's *Tabelle der Hauptlinien*. Much useful information is contained in Messrs. Adam Hilger's booklets, *Wave-length Tables for Spectrum Analysis* and *Visual Lines for Spectrum Analysis*. Emission spectra are shown (as photographed) in Eder and Valenta's *Atlas typischer Spektren*. A characteristic method in the so-called " Spectrum Analysis " is to place a small quantity of an unknown substance between the poles of a carbon arc; the presence of the characteristic " lines " of an element in the arc spectrum is strong evidence of its presence in the unknown substance; the method is valuable but difficult to make quantitative, although progress in this direction has been made.*

Absorption spectra may be divided into two classes; the first is typified by the solar spectrum with its dark lines. Light from the carbon arc passed through a sodium flame will exhibit a pair of *dark* sodium lines in the orange-yellow region of the spectrum; the sodium vapour in the flame is capable of absorbing radiation of the same wave-length as those which it emits. In the solar spectrum the absorbing gases are those of the cooler layers of the solar atmosphere; they produce the characteristic dark lines in the continuous spectrum of the light emitted by the deeper layers.

The second class of absorption spectra are those which result from the selective absorption of various transparent materials at ordinary temperatures. The quantitative investigation of the absorption is one of the principal aims in " spectro-photometry," now of great industrial importance.

In applied optics, the study of absorption spectra is of importance in connection with " colour filters." Solutions of various inorganic salts and of organic compounds, especially the " dyes," are very useful in isolating the light from various limited ranges of the spectrum. An *Atlas of Absorption Spectra* has been published by Uhler and Wood; a great many measurements on absorption have been made by Mees.

A convenient method of using the various dyes is to employ them as the colouring agent in gelatine films; the latter may be mounted between plates of glass. A convenient range of " colour filters " of this kind is manufactured by Messrs. Kodak, Ltd., and full information as to their transmission is published by that firm.

Dyes are of importance in microscopy and especially in bacteriology. Bacterial preparations are commonly stained with a basic aniline dye in alcoholic solution, using phenol, aniline, or an alkali as a mordant; the absorption of the more frequently used dyes such

* More especially in relation to spark spectra, by Barratt.

as gentian violet should be considered in regard to the achromatism of microscope objectives intended for this work.

The absorption spectrum of an organic compound in solution may contain bands characteristic of certain radicals. The spectra of the alkaloids have been examined by Hartley in this connection and a great deal of work on the infra-red absorption of organic compounds is due to Abney and Festing.

CHAPTER IV

THE OPTICAL IMAGE AND ITS DEFECTS

THE distribution of light near the focus of a convergent spherical wave-train has been shown to depend upon the ratio of the aperture to the focussing distance. Hence the study of the limitations of the image-forming pencils of light is a matter of the greatest importance.

Fig. 65 represents in a conventional way the optical system of centered lenses which is forming the image B′ of an axial object B. All the lenses are mounted in circular mounts which limit their

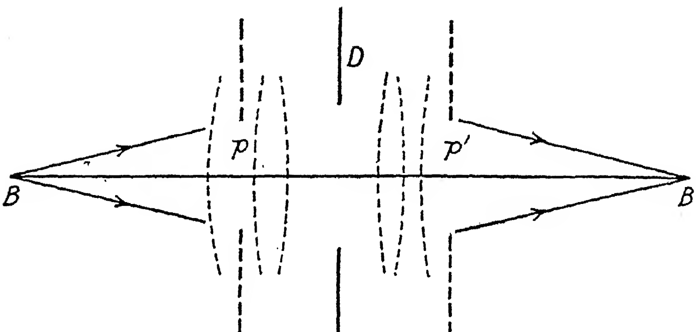

FIG. 65

diameters and, in addition, the system may comprise circular diaphragms, such as D, introduced at various points to limit the beams. An eye placed at B and looking into the system might observe (under proper illumination) the images of a number of the lens boundaries and diaphragms; thus the mount limiting the nearest lens of the system would be "seen" directly; others *might* appear under a smaller angle, and spaced at various distances. The limitation of the rays which pass quite through the system is evidently performed by that diaphragm the *image* of which subtends the smallest angle at B. This image is the *entrance pupil.* If the rim of the first lens or a diaphragm in front of the system subtends the smallest angle, it will itself constitute the entrance pupil.

Thus, to find the entrance pupil theoretically it would be necessary for each lens mount or diaphragm in turn, to construct the image of it formed by that part of the lens system lying to the left of it, imagining for this purpose light to be travelling from right to left. That diaphragm image which subtends the smallest angle at the

object point will be the entrance pupil. The image of the *same diaphragm*, formed by the part of the system lying to the right, is called the *exit pupil*. These pupils are evidently in conjugate planes with respect to the lens system; their radii will be denoted by p and p'.

It is not the case that the exit and entrance pupils are necessarily constant for all positions of the object; this will be understood from Fig. 66, in which 1, 2, 3, represent diaphragm images formed as set forth above. An axial object point B will have (1) as its effective entrance pupil; the point B_1 will have (3).

The limitations of the pencils from extra-axial object points at finite distances from the axis may be of a complex character, as indicated in the diagram; the approximately conical pencil trans-

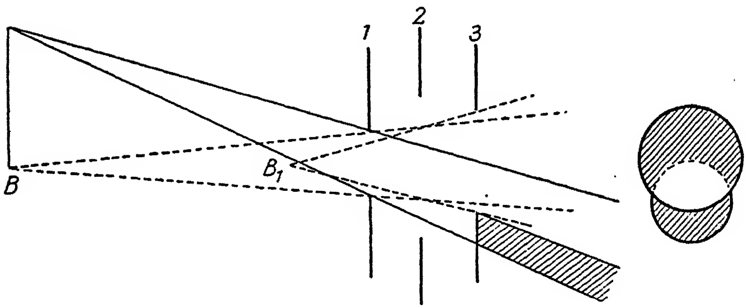

FIG. 66

mitted by (1) will be partly cut off by (3). Hence it is to be remembered in discussing extra-axial images that the effects characteristic of a circular aperture cannot always be assumed to be present.

Resolving Power. As already mentioned, the distribution of light in the focal plane of a "spherical" wave-train was calculated by Airy with the results of the type shown by the full-line in Fig. 67. In order to compute the ability of the system to form distinct images of close point sources, we assume that each of the sources has an image giving the characteristic distribution of light. Since the light from the two object points will be mutually incoherent there will be no visible interference effects between their images. Hence the intensity along the line through the image centres will be represented by the sum of the ordinates of the intensity curve for each. There will be a decided dip when the maximum of one falls on the first minimum of the next, but when the images are a trifle closer this dip will vanish, and it is approximately in this condition that it would begin to be difficult to detect the double nature of the image, when it is registered by a photographic plate or other means.

Although it is not a conception which is necessarily optically exact, the limit of resolution is conventionally accepted as that when the centre of one Airy disc falls upon the first dark minimum of the other. The separation h' of the centres of the two images is thus given by equation (39),

$$h' = \frac{0{\cdot}61\lambda'}{\sin\,\alpha'}$$

where α' is the angular semi-aperture of the convergent cone from the boundary of the circular diaphragm to the centre of each image point, and λ' is the wave-length of light in the image space.

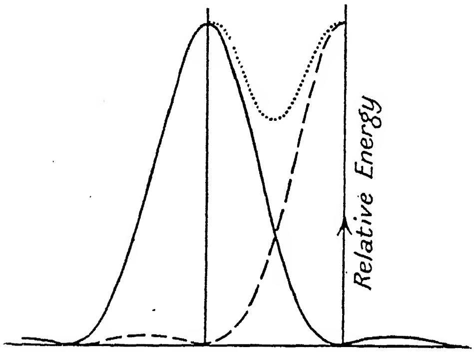

FIG. 67

Full line = Airy disc energy distribution
Broken line = Second image with maximim coincident with first dark minimum of airy disc
Dotted line = Sum of ordinates

In actual practice there may be possibilities of resolution beyond the above limit, as will be seen below.

Fermat's Theorem. We have already discussed the conception of the optical image as the meeting point of congruent rays originating from the object point; our discussion of the diffraction effects of a convergent wave by a circular aperture has prepared us for the concept of the image as being the point where vibratory disturbances from the object point meet in the same phase. If the wave surface is spherical and converging to its central point we can visualize the " rays " as being the normals to the wave-surface.

Following Huygens' principle it is seen generally that a wave-surface must spread along lines normal to its own direction, i.e. along the rays, and this leads to a very general theorem regarding the path of a ray, which has already been justified for the particular cases of reflection and refraction.

The path of a "ray" of light from one point to another is such that the time taken in the journey by a disturbance has no more than an infinitesimal difference from the time which would be occupied in travelling along other very close adjacent paths between the same points.* (The adjacent path must lie everywhere close to the ray path within a distance which is small of the first order, and must similarly make only very small angles with the ray path.

Thus the time may be either a minimum or maximum or genuinely stationary; the minimum property was shown to hold for reflection and refraction at plane surfaces. The more formal proof of the general theorem will be found in textbooks of theoretical optics.

An optical example of a stationary optical path is found in the case of Fig. 68, in which F and F′ are the two foci of an ellipsoid of

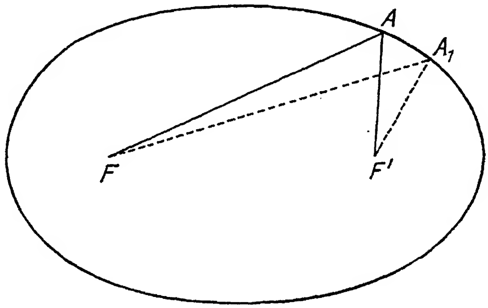

FIG. 68. SECTION OF ELLIPSOIDAL SURFACE: FOCI *F* AND *F′*

revolution having a smooth inner reflecting surface. By a well-known property of the ellipse $FA + AF' = FA_1 + A_1F'$ where A and A_1 are any two points on the surfaces. It will also be remembered that FA and AF′ make equal angles with the normal to the surface at A; hence we have a case in which the total path of a reflected beam between two points is really stationary. Reflection at a plane surface tangential at A would have given a minimum path. A more highly curved surface than that of the ellipsoid, tangential to the latter at A, would have provided an example in which FA + AF′ represented a maximum path.

Analytical Statement of Fermat's Theorem. Let the length of path of light in a medium "*a*" be dl_a and let the refractive index be n_a. Let the velocity in the medium be V_a and the velocity in vacuo be V_o. Then

$$V_o = n_a V_a$$

* I.e. as compared with the total time of the journey.

$$\text{The time occupied} = \frac{dl_a}{V_a} = \frac{dl_a n_a}{V_o}$$

Hence, the total time occupied in traversing media a, b, c, etc., will be

$$t = \frac{1}{V_o}(n_a dl_a + n_b dl_b + n_c dl_c)$$

Hence, if the time is to have a stationary value, then

$$\Sigma ndl$$

must also have a stationary value for the same conditions, i.e. under the very small variations of path between two points as contemplated in Fermat's theorem.

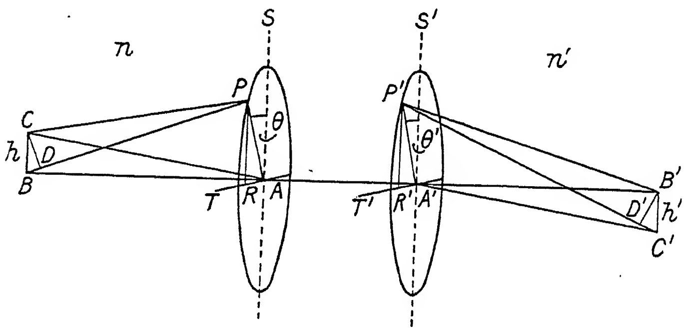

FIG. 69

The Optical Sine Relation. In Fig. 69, BC and B′C′ represent a very small object and image respectively, perpendicular to the axis BAA′B′ of a centered optical system.

Imagine a circle drawn on a plane touching the first refracting surface of the system so that its centre is on the axis, and P to be a point through which we can track a ray BP to its final destination, which we will assume to be the image point B′. It will pass through the point P′ which we can imagine to lie on a similar circle on a plane touching the last surface.

The general condition that B′ may be the image of B is that (Σndl for the actual path BP . . . P′B′) = (Σndl for BA . . .A′B′). Consider now the formation of the image C′. We can track the rays CP and CA through the system to their final destination, which will be one point C′ if the system is properly designed, but the points of intersection of the last surface may *not* exactly coincide

with P′ and A′; Fermat's theorem allows us, however, to calculate the optical lengths of these paths as

$$(\Sigma ndl \text{ for CP} \ldots \text{P}'\text{C}') \text{ and } (\Sigma ndl \text{ for CA} \ldots \text{A}'\text{C}')$$

where the paths (P to P′) and (A to A′) *are taken as the same as those for the disturbances from* B. This is because these "paths" are adjacent paths to the actual ones, lying everywhere very close to them and making only small angles with them at any point.

Let the refractive indices of the object and image spaces be n and n' respectively, then if disturbances are to meet in the same phase at C′ as well as at B′

$$n \,.\, \text{CP} + (\text{P to P}') + n' \,.\, \text{P}'\text{C}' = n \,.\, \text{CA} + (\text{A to A}') + n' \,.\, \text{A}'\text{C}',$$

and $n \,.\, \text{BP} + (\text{P to P}') + n' \,.\, \text{P}'\text{B}' = n \,.\, \text{BA} + (\text{A to A}') + n' \,.\, \text{A}'\text{B}'.$

Subtracting, we find

$$n(\text{BP} - \text{CP}) + n'(\text{P}'\text{B}' - \text{P}'\text{C}') = n(\text{BA} - \text{CA}) + n'(\text{A}'\text{B}' - \text{A}'\text{C}').$$

If h and h' are assumed to be small of the first order, then

$$\text{CA} = \text{BA}, \text{ and A}'\text{B}' = \text{A}'\text{C}', \text{ sufficiently nearly.*}$$

This will make the right-hand side of the above equation vanish, and we then have

$$n(\text{BP} - \text{CP}) = n'(\text{P}'\text{C}' - \text{P}'\text{B}') \quad . \quad . \quad . \quad (a)$$

We may draw AS and A′S′ in the reference planes parallel to BC and B′C′. Let the angle $\widehat{\text{PAS}} = \widehat{\text{P}'\text{A}'\text{S}'} = \theta$. (Note that P and P′ must lie in the same axial plane if the system is centered). Draw also AT, A′T′, at right angles to AS and A′S′ respectively in the reference planes, and drop perpendiculars PR, P′R′ to AT, A′T′. Also draw CD perpendicular to BP and B′D′ perpendicular to P′C′.

The points C, B, D, P, R, are evidently in one vertical plane. Imagining the line BR to be drawn we see

$$\widehat{\text{BCD}} = \widehat{\text{RBP}}$$

Now, if h is small of the first order CP = DP within a small quantity of the second order; hence

$$\text{BP} - \text{CP} = \text{BD} = h \sin \widehat{\text{BCD}} = \text{h} \sin \widehat{\text{RBP}} = h \,.\, \frac{\text{PR}}{\text{BP}}$$

$$= h\left(\frac{\text{AP}}{\text{BP}}\right)\cos\theta$$

* Note that $\text{CA}^2 = h^2 + \text{BA}^2$, whence

$$\text{CA} = \text{BA}\left(1 + \frac{h^2}{\text{BA}^2}\right)^{\frac{1}{2}} = \text{BA}\left(1 + \tfrac{1}{2}\left(\frac{h}{\text{BA}}\right)^2 - \tfrac{1}{8}\left(\frac{h}{\text{BA}}\right)^4 + \text{etc.}\right)$$

If h is taken sufficiently small in comparison with BA, it will be seen that the terms beyond the first in the expansion can be neglected, since $\frac{h^2}{2\text{BA}^2}$ will be extremely small even in comparison with h.

Let the angle $\widehat{ABP}$ be α, as usual, then

$$BP - CP = h \sin \alpha \cos \theta$$

Note that $\sin \alpha$ and $\cos \theta$ are not very small quantities. Hence, the difference between BP and CP is not negligible in comparison with h, as was the difference between CA and BA.

Similarly, it may be shown that

$$P'C' - P'B' = h' \sin \alpha' \cos \theta$$

whence $nh \sin \alpha \cos \theta = n'h' \sin \alpha' \cos \theta$, from equation ($a$) above, or

$$nh \sin \alpha = n'h' \sin \alpha' \quad . \quad . \quad . \quad . \quad (45)$$

This is the " optical sine relation " evidently an extended form of the Lagrange relation (see equation (9)). The above proof is due to Conrady.

The so-called " sine condition " is derived from it. Provided that the system is free from spherical aberration (see below), so that the disturbances from all zones of the system meet in the same phase in the axial image point, the " sine condition " is the law which the rays through the optical system should fulfil if the disturbances from all zones are similarly to meet in the same phase in image points away from the axis. Thus, if the ratio of h' to h is to be the same for all zones, *then the ratio* $\dfrac{\sin \alpha}{\sin \alpha'}$ *must be constant for all zones also*. This will free the system from the defect known as coma.

A case in which it has already been encountered is in the " aplanatic " refraction at a spherical surface. See the footnote on page 20, Chapter I. The term " aplanatic " signifies freedom both from spherical aberration and coma.

Resolving Power in the Object Space. The separation h' of the centres of two images placed at the least distance for conventional resolution was shown to be

$$h' = \frac{0{\cdot}61\ \lambda'}{\sin \alpha'}$$

If the refractive index of the medium of the image space is n' then the wave-length in the image space will be $\dfrac{\lambda_0}{n'}$ where λ_0 is the wave-length in a medium of refractive index unity. Hence, the above equation becomes

$$h' = \frac{0{\cdot}61\ \lambda_0}{n' \sin \alpha'}$$

whence $$0{\cdot}61\lambda_0 = n'h' \sin \alpha'$$
$$= nh \sin \alpha$$

by the optical sine relation, where h is the corresponding separation of the object points in the object space. This gives

$$h = \frac{0{\cdot}61\,\lambda_o}{n \sin \alpha} \qquad . \quad . \quad . \quad . \quad (46)$$

This is a very general equation and one of great importance in connection with the theory of the microscope. The minimum separation of two object points for possible resolution is thus directly proportional to the wave-length, and inversely proportional to the refractive index of the object space and to the sine of the semi-apical angle of the cone of rays entering the optical system from the object.

Refraction at a Spherical Surface Discussed on the Wave Theory. Referring to Fig. 70, let it be supposed that disturbances travelling along the directions LP and MA would meet in the same phase at

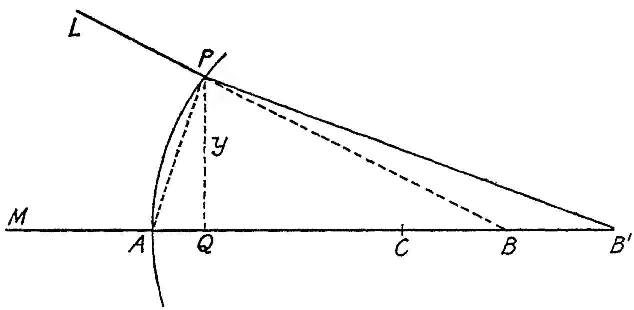

FIG. 70

the point B, provided they are unhindered. Introduce now a spherical refracting surface so situated that its centre falls on the line MAB. We may consider that the disturbances meet the surface in the points P and A, and that these points become the origins of disturbances which will meet in various phases at different points; let us investigate the optical path difference with which the disturbances will meet at a new axial point B′. The refractive indices of object and image spaces are n and n', as usual.

The increase in path for the marginal disturbance

$$= n' \,.\, \mathrm{PB}' - n \,.\, \mathrm{PB}$$

while the increase in path for the axial disturbance

$$= n' \,.\, \mathrm{AB}' - n \,.\, \mathrm{AB}$$

Hence, the net increase (marginal *minus* axial) will be

$$\begin{aligned}\Delta p &= (n' \,.\, \mathrm{PB}' - n \,.\, \mathrm{PB}) - (n' \,.\, \mathrm{AB}' - n \,.\, \mathrm{AB})\\ &= n'(\mathrm{PB}' - \mathrm{AB}') - n(\mathrm{PB} - \mathrm{AB})\end{aligned}$$

We can next calculate a simple expression for (PB′ − AB′), and a similar one for (PB − AB).

From P drop PQ perpendicular to AB and let the length be y. Let AB, AB′ be l, l' respectively, and let r be the radius of the spherical surface.

If we imagine Fig. 70 completed by drawing the semicircle, with centre C_1 above the axis, and remember that the angle in a semicircle is a right angle, it is easily seen that

$$AP = 2r \cos \widehat{CAP}$$

$$\text{Since } AQ = AP \cos \widehat{CAP}$$

$$\text{then } AQ = \frac{AP^2}{2r}$$

$$\text{Now } PB^2 = AP^2 + AB^2 - 2\,AP\,.\,AB \cos \widehat{CAP}$$

$$= AP^2 + AB^2 - 2\,AQ\,.\,AB$$

$$= AB^2 + AP^2\left(1 - \frac{AB}{r}\right)$$

Writing AB $= l$ we obtain the formula (still free from approximation for our case)

$$PB = l\left\{1 + \frac{AP^2}{l'}\left(\frac{1}{l} - \frac{1}{r}\right)\right\}^{\frac{1}{2}}$$

In cases which we shall consider the value of AP will be small in comparison with r, so that we may make the approximation of writing y for AP, where y represents the incidence height of the ray.

$$PB = l\left\{1 + \frac{y^2}{l}\left(\frac{1}{l} - \frac{1}{r}\right)\right\}^{\frac{1}{2}}$$

$$= l\left\{1 + \frac{y^2}{2l}\left(\frac{1}{l} - \frac{1}{r}\right) - \frac{y^4}{8l^2}\left(\frac{1}{l} - \frac{1}{r}\right)^2 + \frac{y^6}{16l^3}\left(\frac{1}{l} - \frac{1}{r}\right)^3 - \text{etc.}\right\}$$

if we consider that the rays considered make only small angles with the axis, so that y is small in comparison with l, then the fourth term in the expansion, containing the factor y^6 will tend to be small in comparison with the third; we will only discuss the cases in which it may be neglected. If the direction PB is more steeply inclined, then the higher order terms become of increasing importance.

In a similar manner we easily obtain (neglecting the terms in y^6 and y^8 etc.)

$$PB' = l' \left\{ 1 + \frac{y^2}{2l'} \left(\frac{1}{l'} - \frac{1}{r} \right) - \frac{y^4}{8l'^2} \left(\frac{1}{l'} - \frac{1}{r} \right)^2 \right\}$$

then, since $AB = l$, and $AB' = l'$, the previously obtained equation for the optical path difference—

$\Delta p = n'(PB' - AB') - n(PB - AB)$ becomes

$$\Delta p = \left\{ \frac{n'y^2}{2} \left(\frac{1}{l'} - \frac{1}{r} \right) - \frac{n'y^4}{8l'} \left(\frac{1}{l'} - \frac{1}{r} \right)^2 \right\} - \left\{ \frac{ny^2}{2} \left(\frac{1}{l} - \frac{1}{r} \right) - \frac{ny^4}{8l} \left(\frac{1}{l} - \frac{1}{r} \right)^2 \right\}$$

$$= \frac{y^2}{2} \left\{ n' \left(\frac{1}{l'} - \frac{1}{r} \right) - n \left(\frac{1}{l} - \frac{1}{r} \right) \right\} + \frac{y^4}{8} \left\{ \frac{n}{l} \left(\frac{1}{l} - \frac{1}{r} \right)^2 - \frac{n'}{l'} \left(\frac{1}{l'} - \frac{1}{r} \right)^2 \right\}$$

This equation shows that if y is so small that the second term above can be neglected, the optical path differences become zero at the values of l and l' given by

$$n \left(\frac{1}{l} - \frac{1}{r} \right) = n' \left(\frac{1}{l'} - \frac{1}{r} \right)$$

This shows that if we restrict the region considered to the paraxial region, imagined as a very narrow thread-like space surrounding the axis, then if the disturbances start out from an axial object point at a distance l from the surface, they will arrive in the same phase at the corresponding paraxial focus point. On the other hand, when the aperture is finite, and we may picture the image forming rays as inclined at a few degrees to the axis, then the disturbances arriving at the paraxial focus (where the " y^2 " term is zero) from various zones of the refracting surface will have optical path differences (zonal path *minus* axial path) approximately proportional to the fourth power of the radius of the zone. This is the simplest case of *spherical aberration* and is called " Primary."

When the rays have larger inclinations to the axis, the above expression for PB does not become accurate until more terms in the expansion are included. By taking in the y^6 term we obtain the expression for the " secondary " spherical aberration. Even terms in y^8 (and higher) may be needed to express the law of optical path differences accurately under some conditions.

Spherical Aberration of a Thin Lens. The optical path difference (marginal path *minus* axial path) arising at the *paraxial focus* after a single refraction is

$$\Delta p = \frac{y^4}{8} \left\{ \frac{n}{l} \left(\frac{1}{l} - \frac{1}{r} \right)^2 - \frac{n'}{l'} \left(\frac{1}{l'} - \frac{1}{r} \right)^2 \right\}$$

Since $n\left(\frac{1}{l}-\frac{1}{r}\right) = n'\left(\frac{1}{l'}-\frac{1}{r}\right)$ at the paraxial focus,

$$\triangle p = \frac{y^4}{8}\left[\frac{n}{l}\left(\frac{1}{l}-\frac{1}{r}\right)^2 - \frac{1}{n'l'}\left\{n'\left(\frac{1}{l'}-\frac{1}{r}\right)\right\}^2\right]$$

$$= \frac{y^4}{8}\left\{n^2\left(\frac{1}{l}-\frac{1}{r}\right)^2\left(\frac{1}{ln}-\frac{1}{l'n'}\right)\qquad n'^2\left(\frac{1}{l'}-\frac{1}{r}\right)^2\left(\frac{1}{ln}-\frac{1}{l'n'}\right)\right\}$$

In the case of a thin lens with surfaces 1 and 2, we shall put $n_1 = n_2' = 1$ and $n_1' = n_2 = N$, and the sum of the path differences arising at the two surfaces (the same value for y is valid at each, since the lens is assumed " thin ") is therefore

$$\frac{y^4}{8}\left\{\left(\frac{1}{l_1}-\frac{1}{r_1}\right)^2\left(\frac{1}{l_1}-\frac{1}{Nl_1'}\right)+\left(\frac{1}{l_2'}-\frac{1}{r_2}\right)^2\left(\frac{1}{l_2N}-\frac{1}{l_2'}\right)\right\} = \frac{y^4}{8}\{A\}$$

The value of the coefficient A can best be expressed as a function of the power of the lens $\mathscr{P}$, the vergence of the rays from the object $\mathscr{L}_1 = \frac{1}{l_1}$ and the curvature $\mathscr{R}_1 = \frac{1}{r_1}$ of the first surface.

Since we have

$$\mathscr{L}_1' = \frac{\mathscr{L}_1 + (N-1)\,\mathscr{R}_1}{N} = \mathscr{L}_2$$

$$\mathscr{L}_2' = \mathscr{P} + \mathscr{L}_1$$

$$\mathscr{R}_2 = \mathscr{R}_1 - \frac{\mathscr{P}}{N-1}$$

$$A = (\mathscr{L}_1 - \mathscr{R}_1)^2\left\{\mathscr{L}_1 - \frac{\mathscr{L}_1 + (N-1)\mathscr{R}_1}{N^2}\right\} + \left\{\mathscr{P} + \mathscr{L}_1 - \mathscr{R}_1 + \frac{\mathscr{P}}{N-1}\right\}^2\left\{\frac{\mathscr{L}_1 + (N-1)\,\mathscr{R}_1}{N^2} - \mathscr{P} - \mathscr{L}_1\right\}$$

After somewhat lengthy algebraical reductions the value of the coefficient proves to be (writing n for the refractive index of the lens in place of N)

$$A = -\left\{\mathscr{P}^3\left(\frac{n}{n-1}\right)^2 + \mathscr{P}^2\mathscr{L}_1\left(\frac{3n+1}{n-1}\right) - \mathscr{P}^2\mathscr{R}_1\left(\frac{2n+1}{n-1}\right) - \mathscr{P}\mathscr{R}_1\mathscr{L}_1\left(\frac{4n+4}{n}\right) + \qquad \frac{n+2}{n}\right.$$

The most instructive manner to deal with this equation is to assume a set of values for n, $\mathscr{P}$, and $\mathscr{L}$, then to plot graphically the aberration coefficient as a function of the curvature $\mathscr{R}_1$ of the first surface for

different cases. This will be done in connection with the discussion of telescope object glasses in Part II of this book.

The equation can be applied without serious difficulty to the second lens of a "thin" telescope object glass and the spherical aberration of the combination can then be found. Graphical methods permit of finding the "bendings"* of two lenses which will remove the spherical aberration when used together.

It is not, however, within the scope of the present book to discuss the subject of the correction of aberrations at length. Reference should be made to Conrady's *Applied Optics and Optical Design.*[1] The above equation is also discussed in *The Formation of Images in Optical Instruments*[2] (Von Rohr).

It leads to the conclusion that no bending of an ordinary glass lens will entirely remove the spherical aberration or change its sign when used with incident parallel light, but where a meniscus converging lens is placed in convergent light it may be freed from aberration, as has already been shown (in the discussion of aplanatic refraction, Chapter I), and the sign of the aberration may even be reversed.

The minimum spherical aberration form for a double convex converging lens in parallel light is the "crossed lens." Assuming a refractive index of about 1·51, the curvature of the front surface is about 6·4 times the curvature of the second.

Relations between Geometrical and Physical Expressions of Aberration. Referring to Fig. 71, AQT represents a portion of a spherical surface with centre at B. If this represents the locus of a wave-front, all disturbances will arrive at B in the same phase; but if, however, there are phase differences depending on the zonal radius, the wave-front subject to spherical aberration will have a trace represented by some other curve APR. If it be supposed that B is the paraxial focus, then the actual wave-front has the same curvature as the spherical surface at the centre, but it diverges towards the margin. The actual cases considered will be those in which the divergence is not large, amounting perhaps to a few wavelengths of light.

Whatever be the shape of the wave surface, consider a zone of radius y, marked by the point P. Take another point R on the same trace very close to P and drop perpendiculars PQ, RT to the spherical surface; then the difference between RT and PQ represents

* The term "bending" as applied to a lens denotes the process (carried out on paper) of altering the shape without altering the power. Thus, one might add a power of + 4D to the first surface, and a power of − 4D to the second.

the extra path which a disturbance from R will have to travel on its way to the centre B, as compared with the disturbance from P. The optical path difference discussed above is seen in the distortion of the wave surface. The focus for a very narrow zone, at P of the actual wave-front, is found by drawing PD perpendicular to the wave-front and cutting the axis in D; this represents a "*ray*," and if the point B is the paraxial focus, then the intercept BD is a measure of the "longitudinal spherical aberration,"* in the geometrical sense, of the chosen zone.

The ray intercepts a plane through B, perpendicular to the axis, in the point E; then BE is a measure of the "*lateral* aberration."

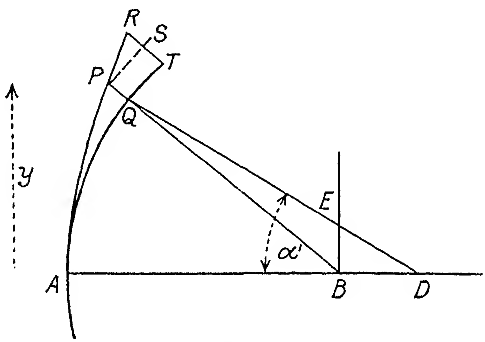

FIG. 71

If we draw PS parallel to the short intercept QT of the spherical surface (the intercepts are considered so short as to be practically straight) and call PR $= \delta\rho$ (a short segment of the wave-surface), RS $= \frac{\delta p}{n'}$ (δp representing an element of *optical* path difference so that the linear path difference is obtained by dividing by n'), then

$$\widehat{\mathrm{RPS}} = \frac{1}{n'}\frac{\delta p}{\delta\rho}$$

but since PD and QB are perpendicular to PR, PS respectively, $\widehat{\mathrm{RPS}} = \widehat{\mathrm{BQD}}$ (a measure of the "angular aberration"), and hence, if the angles are small

$$\frac{\delta p}{\delta\rho} = \frac{n'\,\mathrm{BE}\cos\alpha'}{\mathrm{QB}} = \frac{n'\,\mathrm{BD}\sin\alpha'}{\mathrm{QB}}$$

* The early discussions of "Aberration" were all given in terms of the intercepts between the crossing points of such rays from chosen zones of the wave-front.

Now, if the investigation is confined to small values of the zonal radius, the segment of the wave-surface PR can be represented by δy instead of $\delta \rho$ with sufficient accuracy.* Also we will write

$$BD = \delta l',\ QB = l',\ \text{and } \sin \alpha' = \frac{y}{l'}.$$

Hence,
$$\frac{\delta p}{\delta y} = \frac{n'\delta l' y}{l'^2}$$

When δp and δy are vanishingly small, their ratio becomes equal to the differential coefficient and we obtain

$$\delta l' = \frac{l'^2}{n'y}\left(\frac{\partial p}{\partial y}\right) \quad . \quad . \quad . \quad . \quad . \quad . \quad (47)$$

The equation involving the lateral intercept of the ray, which may be written T′, now becomes

$$\frac{\partial p}{\partial y} = \frac{n'}{l'}(T') \cos \alpha'$$

and if the angle α' is not large it will be sufficiently accurate to assume $\cos \alpha' = 1$, whence

$$\frac{\partial p}{\partial y} = \frac{n'}{l'} T'$$

and
$$p = \frac{n'}{l'}\int_0^Y T' dy \quad . \quad . \quad . \quad . \quad . \quad . \quad . \quad (48)$$

the integration to be performed over the whole radius Y, say. If p is positive the marginal path will be greater than the axial. Note that p is the " marginal " path *minus* axial path calculated for a zone of radius Y, which may be the marginal or any intermediate zone.

If by any means, then, we can measure or calculate the lateral intercepts of the rays from different zones, these can be plotted as abcissae against y as ordinates, as in Fig. 72. The area between the curve and the lines $x = 0$ and $y = Y$ is proportional to the optical path differences between disturbances arriving at the focus from zones $y = 0$ and $y = Y$.

For another focus at a distance m from B, the transverse or lateral intercept becomes T'_m, where

$$T'_m = T' - \frac{my}{l'}$$

* $\delta \rho$ will be practically equal to δy, the increase of radius y in the length PR.

Hence, the path differences at the new focus are

$$p_m = \frac{n'}{l'}\int_0 \left(\mathrm{T}' - \frac{my}{l'}\right) dy$$
$$= \frac{n'}{l'}\left\{-\frac{m\mathrm{Y}^2}{2l'} + \int_0^{\mathrm{Y}} \mathrm{T}'dy\right\} \quad . \quad . \quad . \quad . \quad (49)$$

The term $\frac{m\mathrm{Y}^2}{2l'}$ represents the triangular area included between the same two lines mentioned above and the line

$$x = \frac{my}{l'}$$

Therefore, in a case of a lens system which gives large path differences for one focus, the condition of affairs might evidently be greatly improved by choosing another focus which would make the above areas for curve and triangle equal; this would make the optical path difference between central and marginal disturbances disappear, and the residual path differences for other paths would be much smaller.

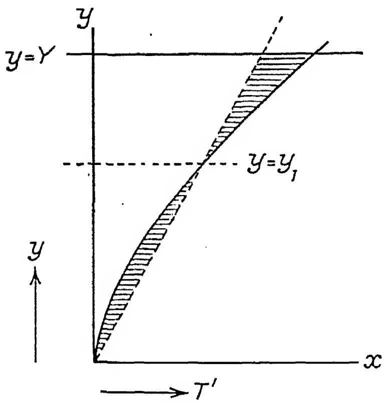

FIG. 72

Note that the path difference between a marginal and axial disturbance, arising through a change of focus, is given by the first term in equation (49).

Thus, δp_m = (increase of marginal path *minus* increase of axial path arising through a displacement " m " of the focus point considered) is given by

$$\delta p = -\frac{n'm}{2}\left(\frac{\mathrm{Y}}{l'}\right)^2$$

Compare this equation with (38).

Primary Spherical Aberration. *General Case.* In the case of the thin lens considered above, the aberration at the paraxial focus expressed in terms of optical path, was given by

$$\frac{\mathrm{A}}{8}y'^4$$

The effect of a change of focus on the path difference as expressed above was proportional to y^2. Hence, the general expression for the path difference (marginal disturbance *minus* axial disturbance) *near* the paraxial focus of a thin lens is

$$p = c_1 y^2 + c_2 y^4$$

where c_1 and c_2 are constants obtainable from the formulae already given. It can be shown that a similar formula will suffice to express the aberration at the focus of a more complex optical system; the y values may, in fact, be the intersection heights of rays in any surface of the system, or, for example, in some other suitable reference plane such as the exit pupil. As previously indicated, terms of higher order may be included to represent the *higher aberration*, where necessary.

Distribution of Ray Paths in Primary Spherical Aberration. Equation (47)

$$\delta l' = \frac{l'^2}{n'y}\left(\frac{\delta p}{\delta y}\right)$$

combined with the expression for primary spherical aberration,

$$p = c_1 y^2 + c_2 y^4$$

gives

$$\delta l' = \frac{l'^2}{n'}(2c_1 + 4c_2 y^2)$$

If $\delta l'$ is measured with respect to the paraxial focus, for which $c_1 = o$, the axial aberration is evidently proportional to the square of the zonal radius. Similarly, it can be shown that the transverse or lateral aberration is proportional to y^3.

The case is represented diagrammatically in Fig. 73. B_p is the paraxial focus and B_m the marginal focus. The rays from a zone $\frac{Y}{2}$ come to a focus at the point C where the distance $B_pC = \frac{(B_pB_m)}{4}$. The rays coming to a focus at the mid-point between B_p and B_m come from the zone $\frac{Y}{\sqrt{2}} = 0{\cdot}707Y$.

Focus with Minimum Residuals of Path Differences. Using the notation of the previous section and referring to Fig. 72, let us represent the variation of m by differing slopes of the dotted line passing through the origin. The area between the curve and between the lines $x = o$ and $y = y_1$ (say), *less* the corresponding triangular area, represents the optical path difference between disturbances arriving at the focus m from the zone given by $y = y_1$ and from the

centre. It is easily seen that the area of "curve *minus* triangle" (in our figure) reaches a maximum negative value at about $\frac{Y}{2}$ while at Y the whole difference is very small. On the other hand, the path differences between disturbances from $y = \frac{Y}{2}$ and $y = Y$ will have reached a positive amount of about the same numerical value as the negative maximum. The maximum residuals are clearly least when the two shaded areas are equal, and this means that the total

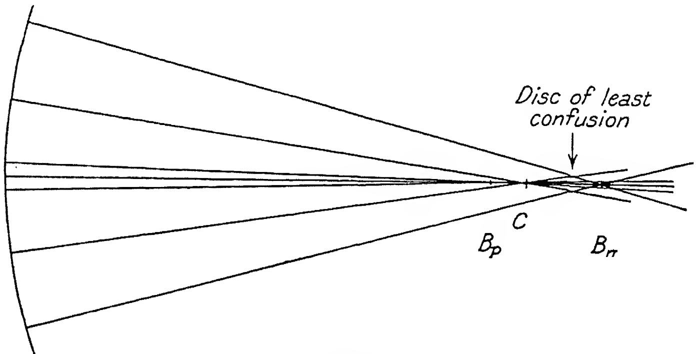

FIG. 73

areas for curve and triangle are equal, the path difference for the margin then being zero—

$$p_Y = c_1 Y^2 + c_2 Y^4 = 0.$$

If we assume that $Y = 1$, then $c_2 = -c_1$, and the general equation will become: $p = -c_2 y^2 + c_2 y^4$, a form which holds only for the special focus which makes $p = 0$ for $y = 1$.

The radius for the maximum optical path difference at this special focus is found by differentiating the expression for p and equating the result to zero, giving

$$\frac{dp}{dy} = -2c_2 y + 4c_2 y^3 = 0$$

whence $y = \frac{1}{\sqrt{2}}$. As we have seen, the rays from this zone intercept the axis half-way between the paraxial and marginal foci. The value of p for this focus $\left(y = \frac{1}{\sqrt{2}}\right)$ proves to be $\frac{-c_2}{4}$.

The maximum path differences at the paraxial focus are found

between disturbances from the centre and from the extreme margin. At the paraxial focus

$$p = c_2 y^4$$

and the maximum path difference is therefore c_2.

Remembering that a ray is the normal to the wave surface, the criterion for the marginal focus is that

$$\frac{\delta p}{\delta y} = 0 \text{ for } y = 1$$

i.e.
$$\frac{\delta p}{\delta y} = 0 = 2c_1 y + 4c_2 y^3$$

whence $c_1 = -2c_2$. The maximum path differences are now $-c_2$. Hence at the mid-focus we find a point where the residual path differences are only one-quarter of those existing at either the marginal or paraxial foci.

Numerical Calculations for the Distribution of Light in the Neighbourhood of an Image. In Chapter III the method of calculation of the distribution of light was worked out for points in the focal plane. To obtain numerical results in the general case it is convenient to divide up the spherical reference surface, which may be assumed to be of unit radius, into a series of annular zones of equal areas. Thus the bounding radii may be $\sqrt{\frac{1}{n}}$, $\sqrt{\frac{2}{n}}$, etc. Each narrow ring will thus produce a numerically equal effect of amplitude at the centre, but at a point such as F_1 (Fig. 57) the contribution of one ring will be proportional to

$$\int_0^{2\pi} \cos \overline{W \sin E}\, dE$$

where W has the significance of the previous investigation, i.e. it is the difference of phase at F_1 with which a disturbance from C, Fig. 57, meets one derived from A or B; it is half the maximum difference of phase between disturbances arriving from the zone considered, the extreme difference being for C and D. In presenting the results it is convenient to specify the distance FF_1 by that maximum value of W which relates to the outermost ring in the surface. Thus the W value for intermediate zones will be

$$W_m \quad \sqrt{\frac{1}{n}},\ W_{max} \times \sqrt{\frac{2}{n}},\ \text{etc.}$$

and the contributions of the various zones can easily be computed by evaluating the integral. If the contributions of amplitude are all in the same phase they can be added directly; this was the case for points in the focal plane, for the phase of the resultant at F_1 for any one ring must be the phase of the elements derived from A or B, and this will be identical for all zones when we deal with a spherical *wave-surface*.

It is otherwise if the various rings of the reference surface give contributions which arrive at the focus with differences of phase. The relative phases of the resultants arriving at F_1 may be considered to be

essentially the same as at F. Let the phase for one ring be " δ " and the amplitude contribution be " a," then the final intensity will be found by evaluating, as shown in Chapter III, the equivalent of

$$\{\Sigma a \sin \delta\}^2 + \{\Sigma a \cos \delta\}^2$$

The actual integration must, however, be carried out by mechanical quadratures in order to obtain the requisite accuracy. Full details of the method will be found in Prof. Conrady's original paper.*

For points away from the paraxial focal plane the phase differences for various rings will be expressed sufficiently nearly in the absence of aberration (from equation (38)) by

$$\frac{}{\lambda}\,\delta p = -\frac{2\pi}{\lambda}\cdot\frac{\delta f}{2}\left(\frac{y}{f}\right)^2 = C_1 y$$

In the presence of primary spherical aberration we have seen that the general expression for the optical path differences for disturbances was

$$p = c_1 y^2 + c_2 y^4$$

Hence, $$= \frac{2\pi p}{\lambda} = C_1 y^2 + C_2 y^4$$

The results of numerical computation are shown in Figs. 74 and 75. The vertical scale for intensity is given for the lowest curve. The radius of the marginal zone is taken as unity.

In Fig. 74 (no aberration) C_1 is given the values 0°, 45°, 90° . . . 540°, the light intensities being calculated for W = 0°, 40°, 80° . . . 600° in all the corresponding planes. There will be symmetry of the results on each side of the focus (the symmetry is not *absolute* with real systems).

The case of primary spherical aberration is shown in Fig. 75. The maximum radius is again assumed to be unity, and C_2 is given the value 360°, while C_1 varies in steps of 90° from $-1080°$ to 0°. From foregoing results we have—

$C_1 = 0$: paraxial focus
$C_1 = -720°$: marginal focus
$C_1 = -360°$: focus with least residuals of phase.

At $C_1 = -360°$ the outstanding phase residuals are $\frac{C_2}{4} = 90°$.

The positions of the limiting rays are shown in the diagrams. Let k be the distance, measured perpendicular to the axis, between a point on the limiting ray (from the zone of radius y) and the axis at an axial distance δf from the axial crossing point of the ray. Then if f has the same meaning as before,

$$k = \delta f\frac{y}{f} = -2\frac{\delta p' f}{y} \quad \text{(from equation (38), taking } n' = 1\text{)}$$

Hence, W_k, the value of W† for a displacement k at the point fixed by δf is given by

$$W_k = \frac{360°}{\lambda}\cdot\frac{ky}{f} = -\frac{360°}{}\,2\delta p$$

* *Monthly Notices, R.A.S.*, 79 (1919), 575.

† The optical phase difference $360° \frac{(AF_1 - CF_1)}{\lambda}$ (Fig. 57).

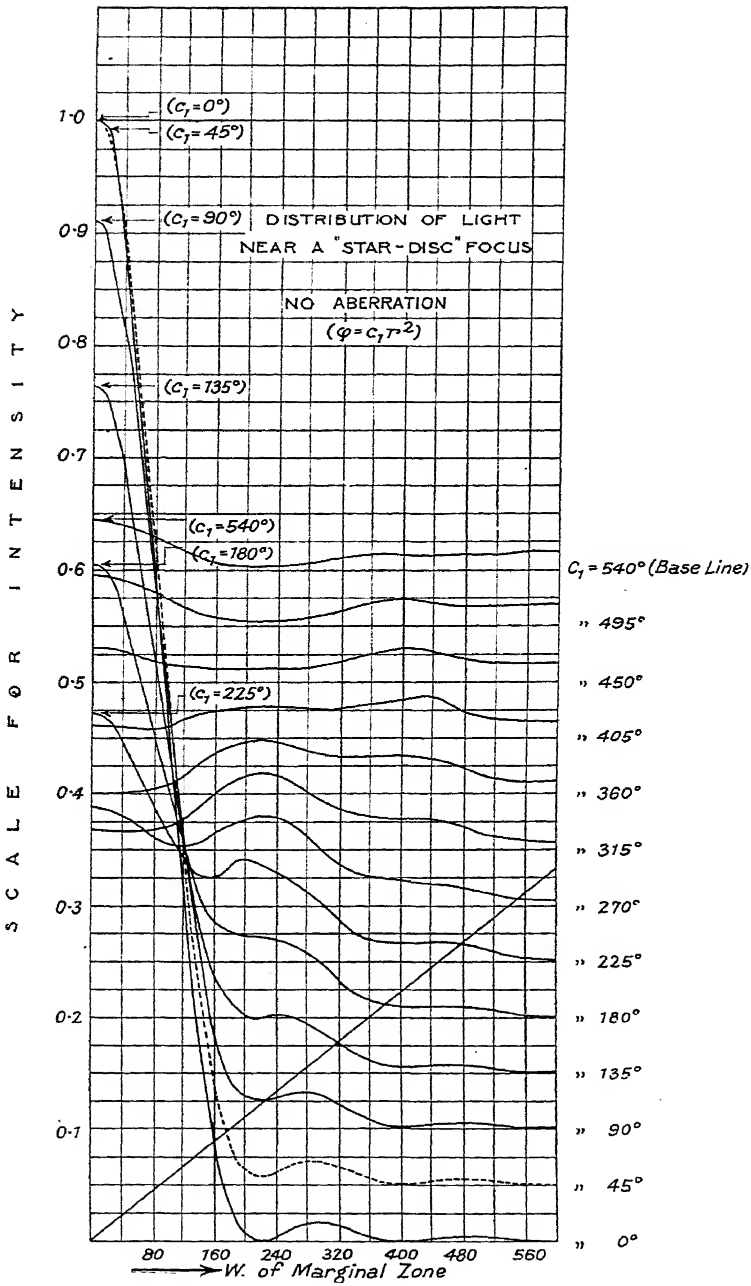
DISTRIBUTION OF LIGHT NEAR A "STAR-DISC" FOCUS
NO ABERRATION
($\varphi = c_1 r^2$)
($c_1 = 0°$)
($c_1 = 45°$)
($c_1 = 90°$)
($c_1 = 135°$)
($c_1 = 540°$)
($c_1 = 180°$)
($c_1 = 225°$)
SCALE FOR INTENSITY
1·0
0·9
0·8
0·7
0·6
0·5
0·4
0·3
0·2
0·1
$C_1 = 540°$ (Base Line)
" 495°
" 450°
" 405°
" 360°
" 315°
" 270°
" 225°
" 180°
" 135°
" 90°
" 45°
" 0°
80
160
240
320
400
480
560
→W. of Marginal Zone

FIG. 74

from which it is seen that W is numerically equal to twice the phase difference (for marginal path *minus* axial path) calculated for the zone of radius y arising from a shift of the axial focussing point through a distance δf.

In the case of primary spherical aberration the geometrical " circle of least confusion " through which all rays pass, lies at three-quarters of the distance from the paraxial to the marginal focus, and is bounded by the intersection of the ray from the opposite mid-zone of half radius and the marginal ray (see Heath's *Geometrical Optics*, p. 113). The extreme marginal ray is easily drawn through the marginal focus, by means of the above relation $W_k = 2d\omega$,* while the other mid-zone ray is drawn through its axial intersection point (one-quarter of the distance from the paraxial to the marginal focus) at an angle the tangent of which is numerically one-half that of the marginal ray. The radius of the " circle of least confusion " is thus found, the corresponding W value being 360°.

In the case of no aberration, the maximum central intensity is unity, but when $C_1 = 90°$ (corresponding to a path difference of a quarter of a wavelength) the actual intensity is still 0·8102, but as the first dark ring of the Airy disc is almost filled with light, the loss of definition in a complex image would probably just be noticeable. Hence, a total " permissible depth of focus " corresponding to a path difference of not more than $\pm \frac{\lambda}{4}$ may be inferred. The corresponding focal depth in the object space of a lens system could be calculated. The symmetry of the diffraction effects on each side of the focus has already been noted.

In the case of primary spherical aberration the diffraction patterns are found to be markedly dissimilar on the two sides of the focus. On the one side is a very pronounced set of ring systems, but on the other side a gradually weakening patch of light appears. The intensity at the focus giving least residuals of phase (90° in this case) is still 0·8 of the greatest intensity possible when no aberration is present, but the first dark ring here is not completely devoid of light, and the first bright ring has double the intensity of that surrounding the ideal Airy disc. The *radius* of the first dark ring (W = 220°) at this point is practically identical with that of the aberration-free image. It is thus much smaller than the geometrical " disc of least confusion," and does not lie in the same plane as the latter.

Higher Aberration. In actual practice, spherical aberration of more complex character is often encountered, in which the effects must be represented by such an expression as

$$p = c_1y^2 + c_2y^4 + c_3y^6 + c_4y^8$$

the contributions of the terms in y^6, y^8, and so on, being known as the higher aberrations. For further details see papers by Prof. Conrady[3] and the author[4]. It frequently occurs that one or more

* In Fig. 75, the marginal focus is found at $C_1 = -720°$ (see scale on right-hand of figure). On going to $C_1 = -540°$, the change of phase $d\omega$ between axial and marginal disturbances is 180°. The W value is therefore 360°. We thus obtain two points on the ray from the extreme margin.

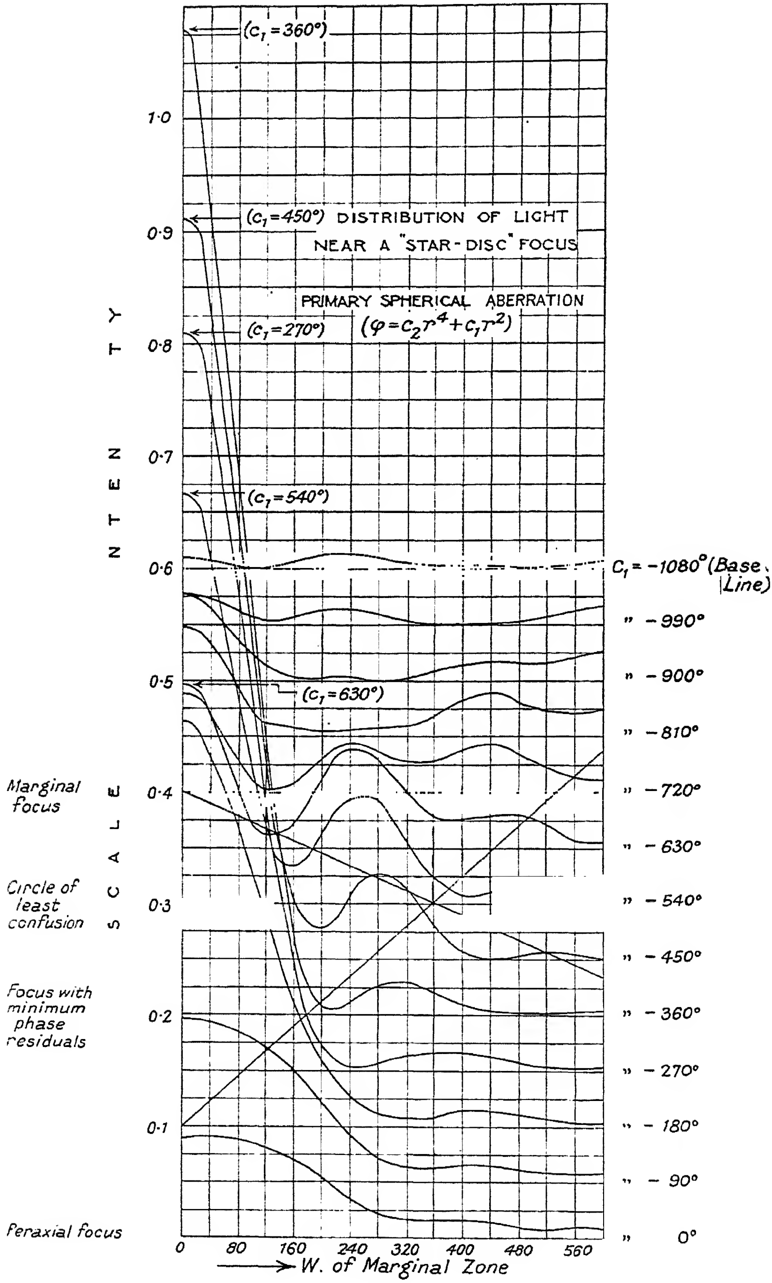

DISTRIBUTION OF LIGHT NEAR A "STAR-DISC" FOCUS
PRIMARY SPHERICAL ABERRATION
$(\varphi = c_2 r^4 + c_1 r^2)$
$(c_1 = 360°)$
$(c_1 = 450°)$
$(c_1 = 270°)$
$(c_1 = 540°)$
$(c_1 = 630°)$
INTENSITY SCALE
1·0
0·9
0·8
0·7
0·6
0·5
0·4
0·3
0·2
0·1
$C_1 = -1080°$ (Base Line)
" −990°
" −900°
" −810°
" −720°
" −630°
" −540°
" −450°
" −360°
" −270°
" −180°
" −90°
" 0°
Marginal focus
Circle of least confusion
Focus with minimum phase residuals
Peraxial focus
0
80
160
240
320
400
480
560
W. of Marginal Zone

FIG. 75

of the constants in the equation above have different signs, and cases are thus represented in which the wave surface has a double bend so that there is a zone of maximum or minimum focussing distance (Zonal Spherical Aberration).

Nothing is more remarkable, however, than the persistence, at some focus, of a concentration closely resembling the Airy disc, even in the presence of considerable spherical aberration. It may be surrounded by more or less "haze" when the aberration is large, but its size, as given by the diameter of the first dark ring, can usually be calculated very closely from equation (39*a*), Chapter III, although it may even be smaller, if anything, under some conditions. *It is seen that mere resolution or sharpness of detail in an image is no criterion of the optical perfection of the system, unless the good definition is accompanied by the maximum possible contrast.*

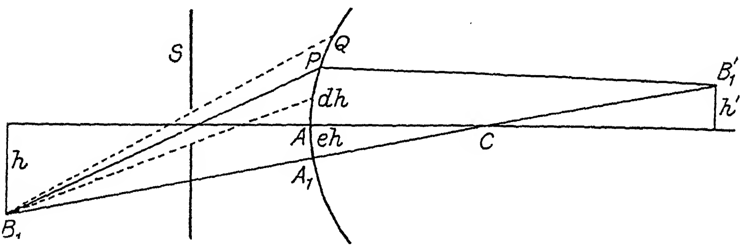

FIG. 76A

Distribution of Light in Extra-axial Images. The foregoing investigations have related to the simpler case when the convergent wave-front has an axial symmetry, as is secured when we have an axial object point and an axially symmetrical optical system.

It is now necessary to inquire as to the variations of optical path which arise when the object and image are no longer on the axis of symmetry.

We will consider first of all a single spherical refracting surface with a stop, as shown in Fig. 76A; then the results so obtained can be extended without difficulty to a system containing a number of coaxial spherical surfaces.

The circular stop is located in the diaphragm S, while B_1 is the object point situated at a distance h from the axis of symmetry passing through the centre C of the refracting surface.

The *principal ray* is the one which passes through the centre of the stop; it intersects the refracting surface in the point P, and the outer limiting rays intersect the surface in an approximately circular figure shown in end-view in Fig. 76B.

The restrictions applied to the present discussion are that h is a small quantity of the first order, and also that the radius of the stop is small. Hence, if we draw the line B_1C through the centre of curvature (cutting the surface in A_1), the perpendicular distance of any point on the circle of intersection just mentioned from the line B_1C will be assumed to be small. The inclination of any ray to the axis is also assumed to be small.

If we drop a perpendicular from P to B_1C the portions of the perpendicular lying above and below the line AC will be seen to be both proportional (within allowable approximation) to h. This perpendicular distance can be represented with sufficient accuracy under the limitations of the inquiry by the length of the line PA_1, Fig. 76B. If Q be any point on the circle of intersection, QA_1 will be, in a similar way, a sufficiently accurate measure of the perpendicular distance of Q from the line B_1A_1C.

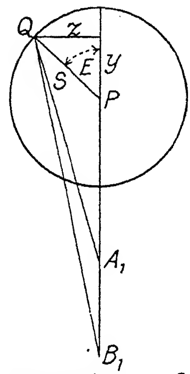

Enlarged View of End Projection

FIG. 76B

Produce the line B_1C to B_1', the "paraxial focus"* which would be realized in the absence of the stop; then the optical path difference with which the disturbance from the point P would meet the "paraxial" disturbance at B_1' would be given by

$$p_P = c_2(A_1P)^4$$

since the above restrictions make it possible to assume the presence of primary aberration only.

Similarly, the optical path difference with which the disturbance from Q would arrive at the "paraxial" focus B_1' would be

$$p_Q = c_2(A_1Q)^4$$

It is convenient to represent the co-ordinates of Q, Fig. 76B, in the circle by y and z, as shown. Hence, we find

$$(A_1Q)^2 = (A_1P + y)^2 + z^2$$

But A_1P is proportional to $h = Mh$, say.

Hence $$A_1Q^4 = \{(Mh + y)^2 + z^2\}^2$$

The net optical path difference between disturbances arriving at the "paraxial" focus discussed above from Q and P will therefore be

$$p = c_2[\{(Mh + y)^2 + z^2\}^2 - (Mh)^4]$$

* Regarding, for the moment, the line $B_1A_1CB_1'$ as the axis.

On expansion this expression reduces to

$$p = c_2\,[(y^2 + z^2)^2 + 4My(y^2 + z^2)h + 2M^2(3y^2 + z^2)h^2 + 4M^3yh^3]$$

If there are a number of such surfaces, each one will produce an optical path difference of this type with its own values of c_2 and M. The value of h at the various surfaces will vary according to the original position of the object point and to the magnification of the intermediate image which is presented as the object to any surface; but for any one surface it may be written as $q_r h$, say, for the rth surface, where h represents the value in some definite stage, preferably the h' for the final image.

Similarly, the y and z co-ordinates of a ray vary as the pencil passes through successive refracting surfaces, but for any one ray path they will bear a sufficiently constant ratio to each other in the various surfaces; denoting their values in the exit-pupil by y and z, their values in the rth surface will be given sufficiently accurately by

$$y_r = p_r y, \quad z_r = p_r z$$

Substituting these values for h, y, and z, and adding up all the optical path differences arising at successive surfaces, the total optical path difference for a disturbance passing along the principal ray, and one which passes through the edge of the " stop " to the final image, will be given by an expression of the form

$$p = a_1(y^2 + z^2)^2 + a_2 y(y^2 + z^2)h + a_3(3y^2 + z^2)h^2 + a_5 yh^3 \quad . \quad (50)$$

The terms of the above equation represent four kinds of aberration which may arise in an optical system, and their characteristics will be discussed below. They correspond to four of the five " aberrations " deduced by von Seidel*[5] in 1856 and often called after his name. They are, in succession, characteristic of

Seidel's
1. Spherical Aberration.
2. Coma.
3. Astigmatism.
5. Distortion.

No. 4 of Seidel's aberrations is the " Curvature of Field " of the surface containing the sharp image found when the first three aberrations are not unduly obtrusive. Referring again to Fig. 76A, we see that in the case of a single refracting surface, a spherical object surface concentric with C would have a corresponding

* Seidel discussed the aberrations in terms of geometrical intercepts between the crossing points of rays, and not, as above, in terms of optical path.

image surface also concentric with C. If the object surface has a different curvature, it is possible (see below) to calculate the curvature of the image surface for one surface, imagining image formation to be effected by narrow pencils passing through the centre of curvature; this is done one by one for all the surfaces of the system and the curvature of a final " image " surface can thus be found. A little consideration will show that the foregoing investigation must relate to the optical path differences arising in this particular surface.

The matter was first investigated by Coddington and later, independently, by Petzval. The above surface is usually known as the " Petzval surface," but it may not contain the physical image.

It is natural to find that the above equation contains no reference to the curvature of field, in view of the particular assumptions on which it was derived. A discussion of the magnitude of the curvature of the field, and its dependence on the optical properties of the system, will be found below.

Discussion of the Aberrations in Terms of Ray Intercepts. The optical designer tests his designs by the method of tracing " rays " through the system, using the method described briefly in Chapter I. It used to be thought that the distribution of light in the image plane could be predicted fairly accurately from the relative concentration of ray intersections, but exact inquiry has now shown this to be erroneous. A case of the discrepancy between the magnitude of the calculated " least disc of confusion " and the actual " Airy disc " patch in the presence of spherical aberration, has been already met with. In one case[1] of " zonal spherical aberration " the size of the ray diffusion patch was eight times that of the actual concentration of light in the Airy disc, even though the residual differences of phase between disturbances arriving in the image from all zones amounted to no more than 90°.

Nothing is more important than for the designer to understand these facts, and to be able ultimately to interpret the ray intercepts, which are obtained as the direct results of ray tracing, in terms of optical path differences.

From the equation above (48)

$$T'_z = \frac{l'}{n'}\left(\frac{\partial p}{\partial z}\right)$$

where T_z' is the lateral aberration in the focal plane, measured in the z direction. The corresponding equation,

$$T_y' = \frac{l'}{n'}\left(\frac{\partial p}{\partial y}\right.$$

gives the lateral intercept in the y direction in the focal plane. Thus the point of intersection of the ray in the focal plane (or rather, the part of the focal surface near the axis) can be calculated.

Differentiating equation (50) with regard to y and z we find

$$y \text{ displacement} = T'_y = \frac{l'}{n'}[4a_1y(y^2+z^2) + a_2h(3y^2+z^2) + 6a_3h^2y + a_5h^3]$$

$$z \text{ displacement} = T'_z = \frac{l'}{n'}[4a_1z(y^2+z^2) + 2a_2hyz + 2a_3h^2z]$$

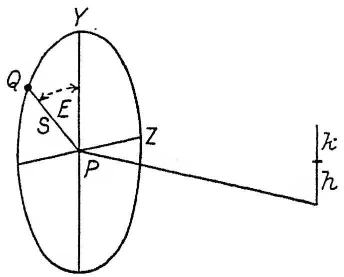

FIG. 77

The easiest way of discussing the equations is to use polar co-ordinates. Put

$$y = S\cos E,\ z = S\sin E,\ y^2+z^2 = S^2$$

taking E as the angle made with the y axis by the radius vector PQ, which is of length S. Whence

$$T'_y = \frac{l'}{n'}[4a_1S^3\cos E + a_2hS^2(2+\cos 2E) + 6a_3h^2S\cos E + a_5h^3]$$

$$T'_z = \frac{l'}{n'}[4a_1S^3\sin E + a_2hS^2\sin 2E + 2a_3h^2S\sin E]$$

The terms involving the various coefficients $a_1 \ldots a_5$ may now be discussed. Note that h is the radial distance of intersection, in the focal surface, of the ray from the centre of the exit pupil. Equation (50), when expressed in polar co-ordinates, becomes

$$p = a_1S^4 + a_2S^3h\cos E + a_3S^2h^2(2+\cos 2E) + a_5Sh^3\cos E \quad . \quad . \quad . \quad (51)$$

Spherical Aberration. The terms in a_1 indicate an optical path difference proportional to the fourth power of the distance from the central axis at which the ray leaves the exit pupil, or a lateral

aberration proportional to S^3. This is characteristic of primary spherical aberration and this type of aberration, therefore, if present on the axis, will exist also in the other parts of the field in the same magnitude.

Coma. The terms in a_2 give the components of the displacement for the ray intersection as

$$T'_y = \frac{l'}{n'}(2a_2hS^2 + a_2hS^2 \cos 2E)$$

$$T'_z = \frac{l'}{n'}(a_2hS^2 \sin 2E)$$

and they are shown as a circle for a given value of S in Fig. 78. For smaller values of S the figure will be similar and the circle will

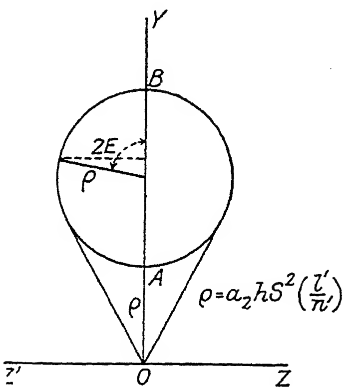

FIG. 78

still lie within the same tangential lines. The point A of the circle nearest the origin lies at a distance $(a_2hS^2)\left(\frac{l'}{n'}\right)$ from it.

Now a displacement of amount $(+ k)$ (see Fig. 77) parallel to the y direction produces an optical path difference between the central disturbance from P and the marginal disturbances from the point Q given by

$$p_1 = \frac{n'kS \cos E}{l'} = \text{(increase of axial path } \textit{less} \text{ increase of marginal path)}$$

(compare the expression derived on page 111). When

$$k = (a_2hS^2)\left(\frac{l'}{n'}\right)$$

$$p_1 = a_2hS^3 \cos E$$

but this is the optical path difference due to coma which is shown by the second term in equation (51). When $\frac{\partial p}{\partial y}$ and $\frac{\partial p}{\partial z}$ are reckoned positive, it signifies a greater marginal than axial path. Hence, the

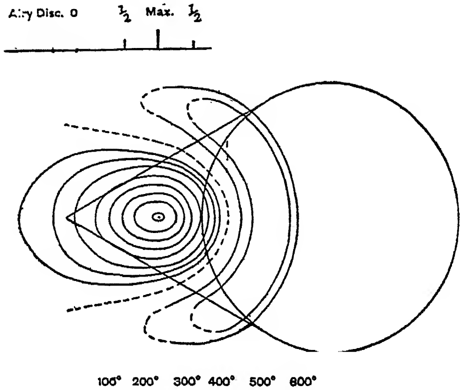

FIG. 79A. CONTOURS OF LIGHT INTENSITY IN THE PRESENCE OF COMA, COMPARED WITH THE OUTLINE OF THE GEOMETRICAL COMA FIGURE

disturbances from the entire ring of the exit pupil of radius S meet in the same phase at the point A of the coma figure (Fig. 78). The point A can thus be looked upon as the physical focus of the corresponding ring of the wave surface, and the foci for intermediate rings are distributed between O and A at distances proportional to S^2. After what has been said above it will be appreciated that while the ray intersections with the focal surface may be distributed round the complete circle AB, the physical focus for the ring of the wave surface may be at the one point A.

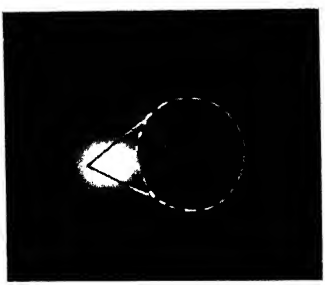

FIG. 79B. PHOTOGRAPH OF STAR IMAGE EXHIBITING SLIGHT COMA
The corresponding geometrical figure is drawn in outline

When the focussing points for all zones of the surface are identical, the magnification is the same for all zones; thus the sine condition is fulfilled and "coma" disappears. Provided that spherical aberration is absent, the "offence against the sine condition" is thus a measure of the coma present.

When the optical path differences are not large, the great proportion of the energy is concentrated into the region of these physical focal points. Fig. 79 shows the results of some calculations of the energy distribution in comparison with the figure showing the boundaries of the patch into which the rays are distributed. The great discrepancies between the distribution of energy calculated from physical theory and that which might be inferred from a corpuscular theory are obvious. In the case shown, the optical path differences for the extreme marginal zone amounted to $\pm$ one wavelength. It is not until the aberration amounts to several wavelengths that more resemblance to the geometrical "coma patch" figure begins to be found in the image.

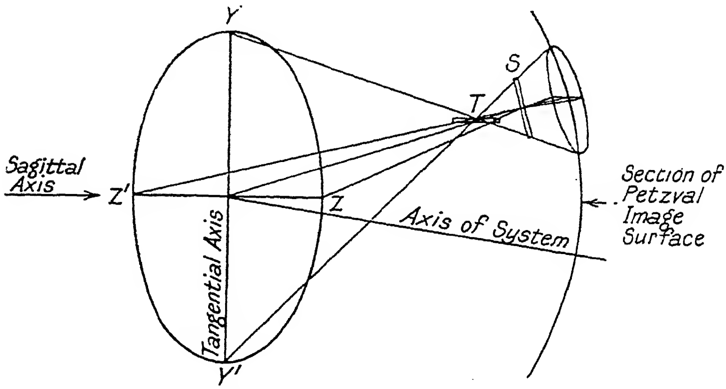

FIG. 80. TANGENTIAL AND SAGITTAL FOCAL LINES

Astigmatism. The terms in a_3 in the displacement equations,

$$T_y = (6a_3h^2S \cos E)\frac{l'}{n'}$$

$$T_z = (2a_3h^2S \sin E)\frac{l'}{n'}$$

show that the figure representing the ray intersections in the Petzval surface from a zone of radius S, is an ellipse with a y axis having three times the length of the z axis (Fig. 80 shows a case in which the lateral intercepts are negative). The rays from the extremity of the Y diameter (the direction of the image point from the centre of the field represents the Y direction) therefore intersect at a distance from the Petzval surface three times the distance of those from the extremity of the Z diameter. The former

focus is the focus of the "tangential" pencil, the latter is that of the "sagittal" pencil; both these foci lie on the same side of the

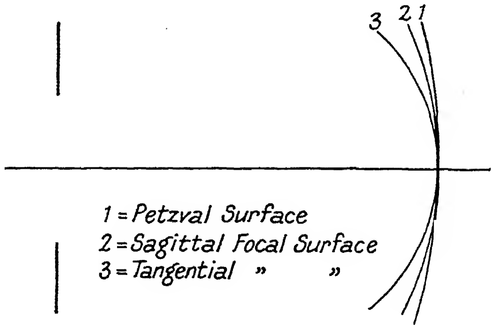

FIG. 81

Note that the distance of the tangential focal surface from the Petzval is three times that of the sagittal surface

Petzval surface. We thus have the tangential and sagittal focal *surfaces*, as suggested in Fig. 81.* The contours for light distribution in the presence of astigmatism have also been worked out in one

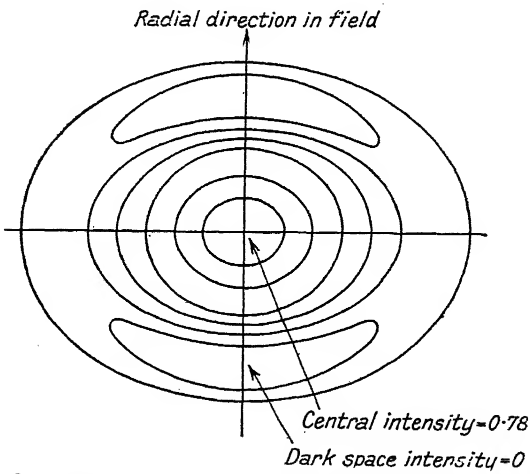

FIG. 82. LIGHT DISTRIBUTION CONTOURS IN THE ELEMENTARY IMAGE NEAR THE TANGENTIAL IMAGE SURFACE

The amount of aberration corresponds to the Rayleigh limit. (See page 141)

or two cases. Typical results are shown in Fig. 82 in which the results of calculation have been supplemented by observation. The

* The power of a thin lens in an oblique direction is worked out on pages 144 *et seq.* Also see section on Astigmatic Refraction in Chapter VIII.

geometrical theory leads to the conclusion that all the rays from a given zone pass through two mutually perpendicular focal *lines*. These are suggested in Fig. 80. The line at the "tangential" focus is perpendicular to the radial direction of the image point in the field; the sagittal line is parallel to this radius.

Actually in cases where the astigmatism may be present in combination with other aberrations, the sagittal line for any zone will not in general lie perpendicular to the principal ray from the centre of the aperture, but will lie in the plane containing the principal ray and the axis of the system, at an angle with the principal ray, depending on the values of the astigmatism and coma.

It will be understood that if the lens system suffering from the astigmatism of oblique pencils is being employed to form an image of any object, any one point of the object away from the axis will be imaged as a short line, tangential in the tangential surface, radial in

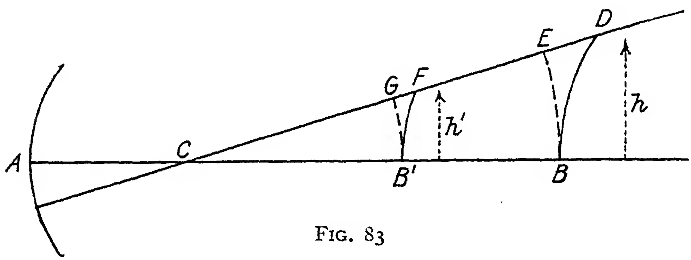

FIG. 83

the sagittal. Thus a diagram consisting of circles concentric with the axis would be imaged as reasonably sharp circles in the tangential focal surface, while radial lines would be imaged as apparently sharp radial lines in the sagittal focal surface, even though the image of an object *point* would appear as a line in either case.

Curvature of Field. Imagine a lens, and a plane object perpendicular to the axis. The image formed by refraction at the first surface of the lens will have a definite curvature. Hence, in order to calculate the final curvature of the image field formed by the whole lens we must be able to deal with the general case of a curved "object field" such as is presented to the second surface of the lens.

Having given the radius of curvature R_i of the object field (which is assumed to be centred on the axis of the lens system) it is required to find the corresponding radius R'_i of the image field. A single refracting surface is first considered, and the image formation is assumed to be effected by pencils passing through the centre of curvature.

In Fig. 83, the dotted arcs BE and B'G with centres at C represent

surfaces which are conjugate with respect to each other, B and B′ being conjugate points on the axis ACB′B (see Chapter I, page 26, for a similar case). The actual object field passes through B, but it has a radius of curvature R_i; it is indicated by the trace BD; similarly, the trace of the image field is shown by B′F. The points C, G, F, E, and D lie on a straight line passing through the centre of curvature C. Hence the intercept GF is the "image" of the intercept ED.

Let h and h' be the object and image heights, then by dropping perpendiculars from E and D to the axis and applying the "spherometer formula" to find the intercepts between the foot of each perpendicular and the point B we shall find—

Distance between feet of perpendiculars = ED very nearly when h' and h are small

$$= \frac{h^2}{2(l-r)} + \frac{h^2}{2R_i}$$

where $l = \mathrm{AB}$ and $r = \mathrm{AC}$, the radius of curvature of the refracting surface. Similarly

$$\mathrm{GF} = \frac{h'^2}{2(l'-r)} + \frac{h'^2}{2\mathrm{R}_i'}$$

But the formula (14) for axial magnification gives

$$\frac{dx'}{dx} = \left(\frac{h'}{h}\right)^2 \frac{n'}{n}, \text{ hence } \frac{\mathrm{GF}}{\mathrm{ED}} = \left(\frac{h'}{h}\right)^2 \frac{n'}{n}$$

$$\text{Hence} \quad \frac{h'^2}{2}\left(\frac{1}{l'-r} + \frac{1}{\mathrm{R}'_i}\right) = \left(\frac{h'}{h}\right)^2 \frac{n'}{n} \times \frac{h^2}{2}\left(\frac{1}{l-r} + \frac{1}{\mathrm{R}_i}\right)$$

$$\text{Whence} \quad \frac{1}{n'\mathrm{R}'_i} - \frac{1}{n\mathrm{R}} = \frac{1}{n(l-r)} - \frac{1}{n'(l'-r)}$$

In order to simplify the right-hand side of the expression we make use of equation (6)

$$\frac{(l-r)l'}{(l'-r)l} = \frac{n'}{n}$$

and obtain

$$\frac{1}{n'\mathrm{R}'_i} - \frac{1}{n\mathrm{R}_i} = \frac{1}{n(l-r)} - \frac{1}{n(l-r)\left(\frac{l'}{l}\right)}$$

$$= \frac{1}{n(l-r)}\left\{1 - \frac{l}{l'}\right\}$$

Equation (7*b*), $\frac{n'}{l'} - \frac{n}{l} = \frac{n' - n}{r}$, gives

$$l \qquad \frac{nr + (n' - n)l}{n'r}$$

Substituting,

$$\frac{1}{n'R'_i} \quad \frac{}{nR_i} - \frac{}{n(l - r)} \left\{ 1 - \frac{nr + (n' - n)l}{n'r} \right\}$$

$$\frac{(n' - n}{nn'r}$$

The equation may be applied successively to any number of refracting surfaces; if n^* and R^*_i are the final values of refractive index and curvature of field we have

$$\frac{1}{n^*R^*_i} - \frac{1}{nR_i} = \Sigma\left(\frac{n - n'}{nn'} \cdot \frac{1}{r}\right) \quad . \qquad (52)$$

Applying the equation to the two surfaces of a thin lens in air, and writing n for the refractive index of the lens, we obtain, assuming R_i infinite (plane object)

$$\frac{1}{R^*_i} = - \frac{1}{nf'} \quad . \quad . \quad . \quad . \quad . \quad . \qquad (53)$$

This equation was first given by Coddington. For a number of coaxial thin lenses

$$\frac{1}{R^*_i} \qquad \frac{1}{nf'}$$

It should be noted that the curvature of the field of a lens system is independent of the relative aperture and also of the object distance.

This discussion, then, enables us to find the curvature of the surface referred to above as the "Petzval surface."

Distortion. The term in a_5 shows a displacement of the image point along the radius of that point drawn from the centre of the field. It is independent of S, and therefore occurs, however small the stop may be which limits the optical system. It is proportional to the cube of the radius of the image point.

It is to be noted, however, that the distortion usually of interest in practice is that which is found in a plane image surface, not generally the curved Petzval surface.

The general result is that the scale of the image presentation is not constant over the field, and, moreover, the displacement is exaggerated the greater the distance from the centre. In the case

where the distortion is inwards, the scale of representation for the peripheral object is too small, this giving barrel-type distortion; in the other case, the scale points are too great, giving pincushion distortion. These effects are shown in Fig. 84, which is self-explanatory.

The subject of distortion will be discussed in greater detail in the chapter on Photographic Lenses, Vol. II.

General Remarks on the Aberrations. The Seidel aberrations arise with monochromatic light and are quite independent of the chromatic aberrations arising through variations of refractive index with wavelength, except in the sense that chromatic variations of the Seidel aberrations are usually experienced to some extent.

It should be noticed that the aberrations of *spherical aberration*, *coma*, and *astigmatism* affect the *definition* of the image point, those of *curvature of field* and *distortion* affect its position.

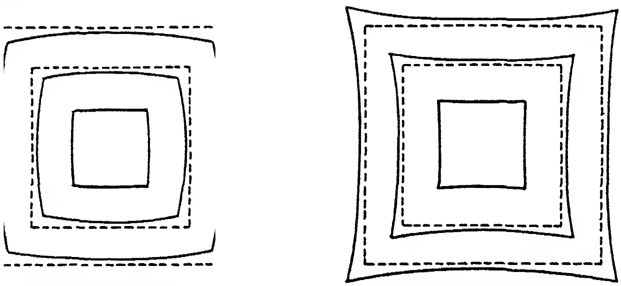

(a) Barrel Type (b) Pincushion Type

FIG. 84. TYPES OF DISTORTION

The laws of the aberrations discussed above are a useful guide in many cases, though no relation has been worked out here between the amounts of these aberrations and the construction of the systems; this is a subject belonging to the province of optical designing and computing.

With large apertures, we saw (page 126) how the spherical aberration becomes more complex; there is a corresponding complexity in the extra-axial aberrations affecting the outer parts of the field, but although it is possible to discuss the higher order aberrations on the lines adopted above, the investigation will not be attempted here. The theory already developed will suffice for a general understanding in many cases and will be referred to in the discussion of various instruments.

Tolerances for Aberration. The somewhat inviting method of ray tracing by the law of refraction, and the application of the results to estimate the distribution of light in the image, has been shown to

be by no means always reliable. The ideal type of image characteristic of spherical convergent waves has been examined, and also the variation from this type consequent on the presence of aberration. The late Lord Rayleigh was the first to show in particular cases that when the disturbances met in the image with optical path differences exceeding one-quarter of a wavelength, the deterioration of the image would begin to be noticeable. This has led to an extremely useful general guide for designers of optical systems by which to test the merits of their designs; a rule which, however, has to be applied with discretion. In cases where the highest definition is required, as in the images formed by the objective of a telescope or microscope, the optical path differences in the image should not be allowed to exceed this " Rayleigh limit " of one-quarter of a wavelength. In other cases, such as photographic lenses, much larger aberrations must be tolerated in order to obtain other ends such as the covering of a large field with reasonably good definition.

Depth of Focus in the Image. From a study of the results of integration of the effects of light from all parts of a finite lens aperture, it appears that it is possible to travel in the axial direction from the centre of an axial image till the optical path difference (extreme marginal path *minus* axial path) of the disturbances reaches $\pm\frac{\lambda}{4}$, before a serious deterioration in the concentration of light begins. This is in agreement with the " Rayleigh limit," and is a very useful approximation.

The optical path difference between marginal and axial disturbances caused by a shift δf along the axis is, under certain conditions,

$$\delta p = -\frac{n'}{2}\,\delta f\left(\frac{y}{f}\right)^2$$

This is obtained from equation (38).

If this may reach a value of $\pm\frac{\lambda}{4}$ the value of δf may be

$$\delta f = \pm\frac{\lambda}{2n'}\left(\frac{f}{y}\right)^2 \quad . \quad . \quad . \quad (54)$$

where λ is, of course, the value of the wavelength of light in a medium of unit refractive index. The total focal depth is therefore

$$\frac{\lambda}{n'}\left(\frac{f}{y}\right)^2$$

This equation is only valid where the focal depth so calculated is small in comparison with the value of f. A fuller discussion of focal depth

will be given in connection with photographic lenses. In practice, it is found, for example, that an eyepiece of a telescope or microscope may be pushed in or withdrawn through a definite interval corresponding to this depth of focus without the manifestation of any serious deterioration of the image. There is, however, no *very* sharply-marked limit.

Chromatic Defects of the Image. The fuller discussion of chromatic aberration and its correction in "achromatic" systems must be postponed till the properties of optical glass are discussed. Considering two wavelengths "D" and "F," the simple formula for a thin lens gives—

$$\frac{1}{f'_D} = (n_D - 1)\,\mathcal{R}$$

$$\frac{1}{f'_F} = (n_F - 1)\,\mathcal{R}$$

Whence $$\frac{f'_F - f'_D}{f'_F f'_D} = (n_D - n_F)\,\mathcal{R}$$

By dividing the last equation by the first—

$$-\frac{(f'_D - f'_F)}{f'_F} = \frac{-\delta f}{f'_F} = \frac{\delta n}{(n_D - 1)} \quad . \qquad (55)$$

Hence, for a given change of wavelength, the fractional change of focal length is given by the expression on the right of the equation, and is thus proportional to the change of refractive index. In a simple lens, therefore, which is forming an image of an axial point source, the foci for the different wavelengths are drawn out along the axis.

Chromatic Variation of the Focal Point. The chromatic variation of the focal point in the above sense causes coloured haloes around the focus. It is easy to arrange a spectacle lens to form the image of a distant but bright source of light, and to examine this image by a suitable eyepiece, mounted coaxial with the lens. As the star focus of such a simple lens is approached, the red focus is first found, which is surrounded by a halo of green and an outer one of violet. Further inwards, the central spot appears whitish from the superposition of radiations, but it is surrounded by a reddish-violet halo which becomes more strongly red as the point of observation shifts inwards to the violet focus, where surrounding rings of green and red are seen.

Chromatic Difference of Magnification. In addition to this axial shift of the focal point with wavelength, there are frequently found

chromatic differences of magnification which may arise through variation of the "focal length" with wavelength. In such a case the star image in the outer parts of the field formed by the optical system, is drawn out into a short spectrum lying in a direction radial from the centre of the field. These two are the most important types of chromatic aberration, but in addition, there is usually a certain degree of chromatic variation in the other aberrations of a complex system. Thus, spherical aberration, even when corrected for one wavelength, may be found in another, and so on.

Tolerance for Chromatic Axial Shift of the Focal Point. As seen above, the "focus" of any homogeneous component of the radiation may be regarded as a concentration of energy in a finite region of

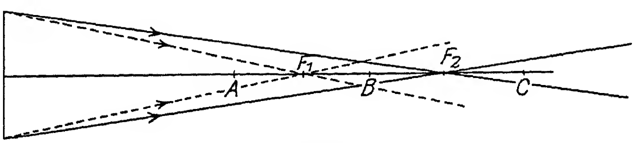

FIG. 85

space. The depth of focus in the image up to the optical path difference of $\pm \frac{\lambda}{4}$ is (in air)

$$\pm \frac{\lambda}{2}\left(\frac{f'}{y}\right)^2$$

Hence, if the full and dotted lines in Fig. 85 respectively indicate the foci of two homogeneous radiations (each having a definite wavelength), their depth of focus may be shown by AB and BC. At the point B there will just be a reasonable concentration of each of them, and a better concentration for all intermediate wavelengths.

Suppose for a moment that these wavelengths were those of the extreme red and violet radiations of the visible spectrum, then the point B would have a reasonable concentration of all wavelengths. Thus, the distance F_1F_2 = the sum of half the total focal depths for each wavelength.

$$\delta f = F_1F_2 = \tfrac{1}{2}(\lambda_1 + \lambda_2)\left(\frac{f'}{y}\right)^2$$

Combining this with equation (55) in the form

$$\delta f = -f' \frac{dn}{n - 1}$$

we obtain

$$\frac{f'}{y} = 2\frac{y\,dn}{(n-1)(\lambda_1 + \lambda_2)}$$

(numerically, disregarding the sign).

In practice, with ordinary crown glass, $\frac{dn}{(n-1)}$ might amount to something like $\frac{1}{80}$. Take $y = 4$ cm., say, and $\lambda_1 + \lambda_2 = \cdot 00004 + \cdot 00007$ cm. $= \cdot 0001$ cm. sufficiently nearly, then

$$f' \quad \frac{2 \times 4}{80 \times \cdot 0001} = \frac{8}{\cdot 008} = 1000$$

Hence, f' required for a colour-free image $= 4{,}000$ cm. This is of course an extreme estimate; in practice, the whole range of visible radiation need not be brought within the focal range (perhaps half would suffice), so that the f' might be brought down to 20 metres for an aperture of 8 cm. From this investigation, the reason for the extraordinarily long astronomical telescopes employed before the invention of the achromatic lens can be understood. The small aperture and long focal length were essential to obtain reasonably colour-free images.

Achromatic Lens. In the case of an ordinary doublet achromatic lens the axial spreading of the colours is greatly reduced. Apple-green ($\lambda = \cdot 000055$ cm.) is found nearest the lens, while red and blue are superimposed at a distance of about $\frac{1}{2000}$ of the focal length beyond. Since the extreme ends of the spectrum are relatively faint, it may be assumed that none of the components should arrive with path differences greater than $\lambda/2$, a doubled tolerance. This is expressed by

$$\delta f_1 + \delta f_2 = \frac{f}{2000} = (\lambda_1 + \lambda_2)\left(\frac{f}{y}\right)^2$$

Assuming $\lambda_1 = \cdot 000055$, and $\lambda_2 = \cdot 000048$ cm., this gives very nearly: $f = 5y^2$, where f and y are to be given in centimetres. Conrady, who first drew attention to the importance of this limit of tolerance, uses a similar expression to show that the majority of big telescopes have focal lengths which are too short in relation to their diameters to obtain the above requirement, and their images probably suffer in consequence.

The Power of a Tilted Lens. A thin lens receives a plane wave-train travelling parallel to the axis. A plane PAQ (Fig. 85A) is the locus of points vibrating in the same phase. The disturbances passing through centre and margin meet in the same phase in the principal focus F. The time that they have taken to travel between passing PQ and arriving at

F is the same. The same condition is expressed by the equality of the "optical paths" i.e. P to F and A to F. Optical paths $= \Sigma ndl$ where n is the refractive index and dl an element of geometrical path.

If the disturbances had not encountered the lens they would have taken equal time to travel to the line RFS also perpendicular to the axis. The extra optical path for the marginal route is

$$PF - PR = \frac{y^2}{2f'}$$

sufficiently nearly if y is small in comparison with f' (see page 85). Note that $AP = AQ = y$, and the thickness of the lens is zero at P and Q.

The *extra* optical path for the axial route is

$$(n - 1)t$$

where t is the thickness of the lens. Applying the spherometer formula twice

$$t = \frac{y^2}{2}\left(\frac{1}{r_1} - \frac{1}{r_2}\right)$$

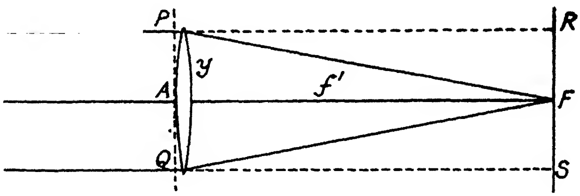

FIG. 85A

Hence equating the extra optical path for centre and margin

$$\frac{y^2}{2f'} = (n-1)\,\frac{y^2}{2}\left(\frac{1}{r_1} - \frac{1}{r_2}\right)$$

$$\text{or } \frac{1}{f'} = \left(n - 1\right)\left(\frac{1}{r_1} - \frac{1}{r_2}\right), \text{ a familiar result.}$$

The student should devise a similar method of obtaining the formula

$$\frac{1}{l'} - \frac{1}{l} = \frac{1}{f'}.$$

When the lens is tilted through an angle θ (Fig. 85B) we consider the disturbances passing through the margin and through the centre of the lens. The latter follows the route of the principal ray shown in the diagram as passing through A and B, and making an internal angle with the lens axis equal to φ. The "focus" for the disturbances through M and B is now F_t.

As before, the optical paths up to the line RF_t would have been equal. The extra path for the marginal route is

$$MF_t - MR = \frac{(MK)^2}{2(KF_t)} = \frac{(y\cos\theta)^2}{2(f'_t - y\sin\theta)}$$

where f'_t is the distance from the lens to the new "focus" F_t.

The extra optical path for the central disturbance is (refractive index of lens) × (path in lens) *minus* (perpendicular distance between parallels through A and B taken parallel to RF_t)

This is expressed by

$$\frac{nt}{\cos\varphi} - \frac{t\cos(\theta-\varphi)}{\cos\varphi}$$

and remembering that $\sin\theta = n\sin\varphi$, this becomes

$$t(n\cos\varphi - \cos\theta).$$

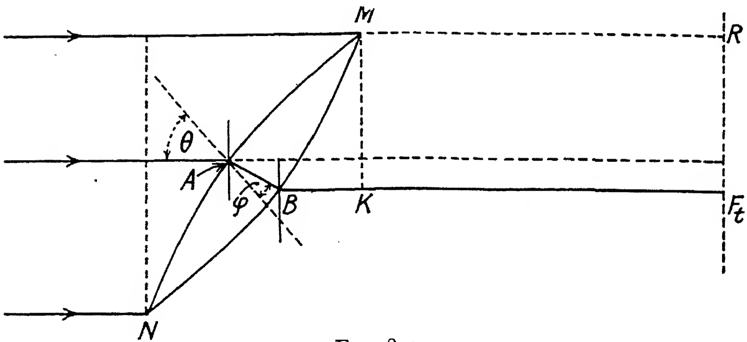

FIG. 85B

Hence, equating the extra paths as before

$$\frac{y^2\cos^2\theta}{2(f'_t - y\sin\theta)} = \frac{y^2}{2}\left(\frac{1}{r_1}-\frac{1}{r_2}\right)\left(n\cos\varphi - \cos\theta\right)$$

$$= \frac{y^2\,(n\cos\varphi - \cos\theta)}{2(n-1)f'}$$

$$\text{and } \frac{1}{f'_t - y\sin\theta} = \frac{1}{f'}\cdot\frac{(n\cos\varphi - \cos\theta)}{(n-1)\cos^2\theta}$$

The equation for the disturbance through N will give a similar expression evidently with a positive sign in the left-hand denominator. It is evident, however, that by taking small values of y we can make the value of both fractions differ very little from $\frac{1}{f'_t}$, and then :—

$$\frac{1}{f'_t} = \mathcal{F}_t = \mathcal{F}\,\frac{n\cos\varphi - \cos\theta}{(n-1)\cos^2\theta}$$

$$= \mathcal{F}\,\frac{n\left(1-\dfrac{\sin^2\theta}{n^2}\right)^{\frac{1}{2}} - (1-\sin^2\theta)^{\frac{1}{2}}}{(n-1)\,(1-\sin^2\theta)}$$

Expanding by the Binomial theorem and neglecting powers of sin θ above the second.

$$\mathscr{P}_t = \mathscr{P}\frac{\left(1 + \dfrac{\sin^2\theta}{2n}\right)}{(1 - \sin^2\theta)}$$

$$= \mathscr{P}\left(1 + \frac{2n+1}{2n}\sin^2\theta\right)$$

This evidently gives the power of the lens the "tangential" focus. The corresponding treatment for disturbances passing through the margin in the axis of tilt, i.e. those which meet in the sagittal focus, will be very similar. The extra optical path for the margin will, however, be

$$\frac{y^2}{2f_s}$$

while the extra optical path for the centre is the same as above.

Hence we find

$$\frac{1}{f'_s} = \frac{1}{f'}\frac{n\cos\varphi - \cos\theta}{(n-1)}$$

$$\text{and } \mathscr{P}_s = \mathscr{P}\left(1 + \frac{\sin^2\theta}{2n}\right)$$

It appears that the power in a tangential direction will be greater than in the sagittal direction, the difference being to this approximation

$$\mathscr{P}_t - \mathscr{P}_s = \mathscr{P}\sin^2\theta$$

and that both the tangential and focal surfaces will have a radius of curvature which is shorter than the focal length and opposite in sign. Compare this result with Fig. 81.

Since we find directly from the earlier equations

$$\frac{f'_s}{f'_t} = \frac{\mathscr{P}_t}{\mathscr{P}_s} = \frac{1}{\cos^2\theta}, \text{ we have}$$

$$\frac{\mathscr{P}_t - \mathscr{P}_s}{\mathscr{P}_s} = \frac{1 - \cos^2\theta}{\cos^2\theta} = \tan^2\theta.$$

Hence $\qquad \mathscr{P}_t - \mathscr{P}_s = \mathscr{P}_s \tan^2\theta.$

References

1. Conrady: *Optical Designing and Computing* (Oxford Unversity Press, 1929). Von Rohr: *The Formation of Images in Optical Instruments* (H.M. Stationery Office, 1920).
2. Conrady: *Monthly Notices, R.A.S.*, 79 (1919), 575.
3. Conrady; *Monthly Notices, R.A.S.*, 79 (1919), 575.
4. Martin: *Trans. Opt. Soc.*, XXVII (1925–26), 249.
5. *Ast. Nach.*, 43, Nos. 1027–1029.

CHAPTER V

THE EYE, AND PHYSIOLOGICAL OPTICS

THE majority of optical instruments function as direct aids to vision, hence it is most important for the optician to understand the action of the human eye, its capabilities, its limitations, and the conditions which govern its efficiency. Its mode of action was unknown to the ancients, and it was left for *Kepler* to show that the refracting parts of the eye produce a clear image upon the retina. Descartes describes, in Chapter V of the *Dioptrice*, an experiment in which a freshly-excised eye is placed in a hole cut in a window shutter. The opaque membranes at the back of the eye being removed, a sharp image of external objects is found on a piece of paper held against the retina. Although we shall not deal with binocular vision in this chapter, it must be remembered throughout that two eyes are concerned in ordinary "seeing." Some special considerations regarding binocular instruments and vision will be dealt with in Vol. II of this book.

Anatomy of the Eye. The eyeball is an approximately spherical body about 1 in. in diameter; the front, however, exhibits the protrusion of the *cornea*, a spherical segment of smaller radius. while the posterior is somewhat flattened. The *cornea* in front and the *sclerotic* behind are the coats which enclose the media of the eye; the general shape is preserved by the internal pressure in the eyeball, which is equivalent to 20–30 mm. of mercury.

The eyeball is situated within the *orbit*, the funnel-shaped bony cavity which is usually called the socket; it is held in position at the rear by the lymph-filled elastic sheath known as the capsule of Tenon, and is protected at the front by the inner surfaces of the lids, i.e. a part of the *conjunctiva*; its movements are controlled by the group of muscles comprising the four *recti* and two *obliques*.

The eyeball is rotated round a vertical axis by the action of the two horizontal recti; the vertical recti rotate it about the transverse axis, which lies in a horizontal plane and intersects the vertical axis in the centre of rotation. The transverse axis is inclined at about 70° to the optic axis.

The *oblique* muscles rotate the eye about the oblique axis, which also lies in a horizontal plane; it makes an angle of about 35° with the optic axis. The oblique axis also passes through the centre of rotation. This centre of rotation is a point of great importance, and

is situated about 15·5 mm. behind the cornea and 9 mm. in front of the retina; it is about 1·5 mm. to the nasal side of the visual axis for horizontal rotations.

Fig. 86 shows a section of the eyeball; passing from front to rear the *cornea* is first encountered, a transparent, horny layer, of thickness about 0·5 mm.,* which is kept moist and transparent by a surface-tension film of lachrymal fluid constantly distributed by the involuntary action of the lids in winking. The

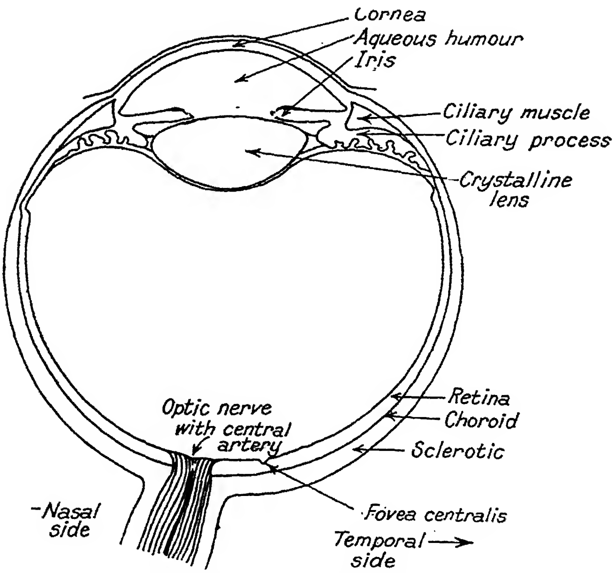

FIG. 86. HORIZONTAL SECTION OF RIGHT EYE

diameter of the cornea is about 12 mm. horizontally and 11 mm. vertically, the remainder of the eye being covered by the opaque *sclerotic*. Several layers of the cornea can be distinguished, but for these and other details works on physiology must be consulted.

Behind the cornea is found the *anterior chamber*, which is filled with a watery, slightly saline fluid of refractive index 1·336, the *aqueous humour*. The axial thickness of the anterior chamber is about 3·1 mm.

At the back of the anterior chamber is the *crystalline lens* on the anterior surface of which the *iris* rests. The central opening of the iris is known as the *pupil*. The heavy pigmentation of the iris renders it practically opaque. The diameter of the pupil, which is

* The thickness at the pole is somewhat less than at the sides.

immediately controlled by the action of radial and circular muscular fibres in the iris, depends (through reflex action) both on the accommodation and on the amount of stimulation of the retinae of the two eyes; it determines the effective aperture of the optical system of the eye. In ordinary light the diameter may be 3 to 4 mm.; in excessive light it may shrink to 2 mm., but after some time in darkness it may rise to 8 mm. It will contract in three or four seconds on re-exposure to light. Blanchard[1] and Reeves have published results, shown in Fig. 87, in which the diameters of the pupil in millimetres are plotted as ordinates against the logarithms of the corresponding field brightnesses as abcissae. It must always be remembered that

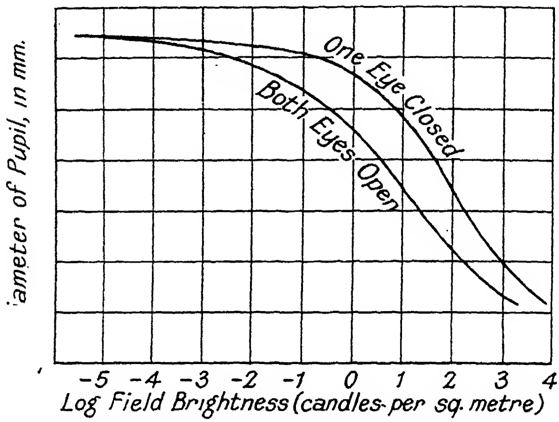

FIG. 87. VARIATION OF THE DIAMETER OF THE PUPIL

the pupil shrinks when the eye is accommodated for near objects. The *crystalline lens* is bi-convex in form, the normal radii of front and back surfaces being about 10 mm. and 6 mm. respectively, and the thickness about 3·6 mm. It is built up of successive fibrous layers, and the refractive index of the material rises from the outer parts, where it is about 1·38, to the inner nuclear portions where it is about 1·41. The anterior covering, or capsule, of the lens has a maximum thickness about 3 mm. from the pole; the thin posterior capsule is thickest at the periphery. The lens is held in position by the *suspensory* ligament, which is attached to the *ciliary body* (see below).

At the back of the lens is found the *vitreous humour*, transparent, and of jelly-like consistency (refractive index 1·336), which occupies the main volume of the eyeball between the lens and the *retina*.

The retina is a coat of several layers which constitutes the receiving

screen of the eye; it will be more fully described below. Immediately behind the retina is situated the *choroid*, a "vascular" layer of tissue richly supplied with dark brown pigment cells and blood vessels; together with the retina it extends over all the inner surface as far as the ciliary body, and it is concerned with the nourishment of the retina. Finally, the tough outer coating of the eyeball (the sclerotic) is encountered; it is about 1 mm., thick, opaque, and usually white in colour; it merges into the transparent cornea in the region of the ciliary body.

Accommodation. The *ciliary body* lining the inner surface of the sclerotic near its junction with the cornea contains both circular and radial muscle fibres; the *suspensory ligament* attaches it to the capsule or outer sheath of the crystalline lens.

It is well established that the lens itself is in youth highly elastic and deformable, and it is also well-known from optical observations of reflected images that accommodation, or change in power of the optical system of the eye, is accompanied by the variation of curvature of the anterior surface of the lens, and not by any variations in the curvature of the cornea or in the optical length of the eye. The precise mechanism is, however, still the subject of discussion. According to Helmholtz's theory, the effect of accommodation is obtained by an action of the muscles which relieves the normal outward radial tension exerted by the suspensory ligament; the lens therefore takes up its natural more highly-curved figure, the anterior apex of the crystalline moving slightly outwards. On the other hand, Tscherning correctly observed that the act of accommodation is accompanied by a relative increase of curvature of the polar part of the anterior surface and a flattening of the peripheral part; the changes in the posterior surface (which is not displaced at the pole during accommodation) are slighter. In order to account for the lenticonous of the anterior surface, Tscherning at one time maintained that an outward radial pull of the ciliary muscle in accommodation made manifest the bulging of the denser central nucleus. Later he supposed that the action of the ciliary muscle is to press the vitreous forward upon the posterior parts of the lens while the outward tension of the suspensory ligament is maintained; this was expected to produce a depression in the periphery of the posterior surface and a bulging of the pole.

Observations by Hess, Graves, and others have, however, established that the radial tension of the suspensory ligament is relaxed during accommodation, thus confirming the theory of Helmholtz. The phenomenon of non-sphericity of the surfaces is, according to Fincham,[2] explainable by the variable thickness of the anterior

capsule, which has its greatest thickness in a mid-zone of the surface, and is thus capable of relieving the relative tension of the membrane at the pole and allowing a bulging effect in that region.

The crystalline lens loses its elasticity with advancing years, and accommodation usually vanishes entirely by the age of 75, see page 263.

The Retina. The optic nerve enters the eye at the rear, its centre being up to 3·5 mm. from the posterior pole of the axis of symmetry. The sclerotic is continuous with the lining of the nerve channel. Debouching from the entrance of the channel, the nerve fibres run in all directions over the inner surface of the retina. Since the various media have practically the same refractive indices, such fibres remain transparent; they are not themselves sensitive to light, but they convey the impulses derived from the special sensitive elements of the retina. The various structures of the retina have been the subject of much microscopical study; differentiation of the various parts is effected by the use of selective staining by appropriate dyes which have been found to colour some parts of the structure more strongly than other parts. Some ten layers of the retina are distinguished (Fig. 88)—

1. Internal limiting membrane.
2. Nerve layer.
3. Ganglion layer.
4. Inner synapse layer.
5. Inner nuclear layer.
6. Outer synapse layer (much arborization).
7. Outer nuclear layer.
8. External limiting membrane.
9. Rod and cone layer.
10. Pigment cell layer (*pigmentum epithelium*).

In explanation of the above list, the nerve layer (2) contains the nerve fibres connected with the main nerve channel mentioned above. A single nerve fibre does not usually traverse the thickness of the retinal layers down to the rods or cones which are the receptive organs, but may enter a "ganglion" cell in the third layer. Each of these ganglion cells has a number of fine processes or extensions which again split up into fine branches (arborization); there are corresponding arborizations of the nerve fibres which come up to meet them. There is another double arborization in layer 6; the nature of the structure is suggested by the diagram.

While the details of the "mechanism" are not fully understood, it is suggestive of the possibility that a single nerve fibre may, under

some conditions, collect the impulses from several of the sensitive elements; on the other hand, a specially strong impulse from a single element might be distributed into several nerve channels. There are certain experimental facts of vision which lend support to such suppositions.

The rod and cone layer is the sensitive region in which light energy is transformed into the nervous impulse, probably electrical in

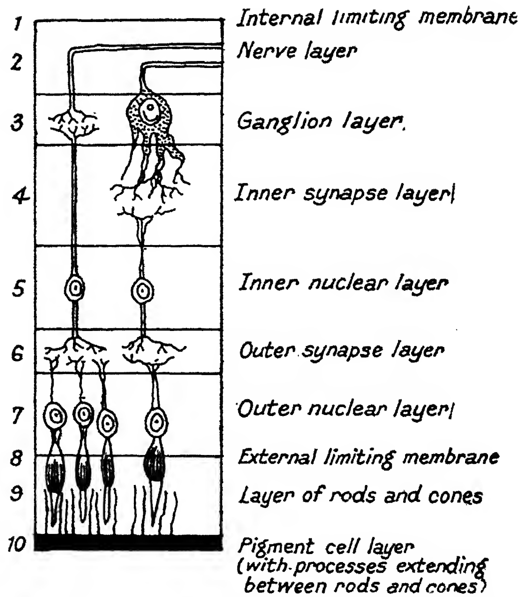

FIG. 88. STRUCTURE OF RETINA (DIAGRAMMATIC)

character. The general shape of the " rods " and " cones " is shown in the diagram.

The region where the optic nerve enters the eye is from 2·0 to 2·5 mm. in diameter, and is seen as the " optic disc " when the retina is examined with the ophthalmoscope. Radiation falling on some part of this area gives rise to no sensation of light. Draw two small crosses 3 in. apart on a sheet of paper. Observing the left-hand one with the right eye only when both are on a level with the eye, bring the paper gradually closer to the face. The right-hand cross will vanish in a certain range of positions in which its image falls on the blind spot. The " blind spot " subtends 5° horizontally and 7° vertically at the posterior nodal point.

On the temporal side of the pole is found the *macula lutea*, a round

or slightly elliptical area about 2 mm. in diameter, in which region the retina is covered with a yellow pigment. In the central region of this yellow spot is found a rod-free area in which the cones are the only percipient elements; this area measures about 0·8 mm. A still smaller region can be distinguished in the centre, where the thinning out of the retina forms a small elliptical depression (the horizontal and vertical diameters are 0·3 and 0·2 mm.) called the *fovea centralis*; the retinal structures here consist only of cones and ganglion cells. The *fovea centralis* is the seat of most distinct vision; visual acuity rapidly diminishes outwards from the central region. The thick ends of the cones in the fovea are closely packed; photo-micrographs show them to possess hexagonal sections. These cones are, however, considerably elongated, and are more rod-like in character than the cones in the peripheral portions of the retina. The rods in the periphery become comparatively numerous, exceeding the cones in the proportion of 10 : 1. It is said that the thin ends of the cones contract and thicken when stimulated by light.

The distance between the centre of the optic disc and the fovea is about 4·75 mm. The "pole" varies somewhat in different eyes, but is usually a little to the nasal side of the fovea, perhaps 1·25 mm.

Various measurements of the diameters of the foveal cones show some considerable variations, and the figures given range from 2μ to $5{\cdot}4\mu$; the figure most frequently given is about 2μ to 3μ. The outer cones are considerably coarser than those at the fovea. According to Fritsch the diameter of foveal cones varies between different persons.

The rods have the peculiarity of secreting a purple fluid known as the visual purple or rhodopsin; spectroscopic observations show that the region of maximum absorption in the spectrum is at wave-length $\cdot 50\mu$ in the green. This substance is bleached by light (see below, page 162), and is considered by some authorities to play an important part in the visual process. It is not definitely known whether a similar substance occurs in small quantity *in* the rod-like cones of the fovea or whether, as suggested by Edridge-Green, the rhodopsin diffuses among them from the surrounding regions of the retina.

The pigment layer which forms the outer parts of the retina contains closely-packed cells of hexagonal section containing dark brown pigment; these have numerous fine "processes" or extensions passing up amongst the rods and cones. Stimulation of the retina by light causes an elongation of these processes, and this action plays an extremely important part in the *adaptation* of the retina to different degrees of light intensity. It is estimated that

there are altogether about three million cones and eighteen million rods.

The nerves from each eye, having passed through an aperture at the back of the orbit, meet in the *chiasma* at the base of the brain, and the fibres from the nasal side of each retina cross over at this point to the opposite part of the brain, while those from the temporal side exhibit no such crossing. This phenomenon is known as *decussation*. Each optic nerve contains approximately one million recognizable fibres which are probably capable of conveying separate impulses. It is noteworthy that the number of fibres is apparently much less than the receptor elements.

Optical Properties of the Eye. The axis of symmetry passing from the anterior pole in the cornea intersects the retina at a point close to the nasal boundary of the macula.

The determination of the radii of curvature, separations of surfaces, and refractive indices of the media of the human eye as they exist during life is a matter of considerable difficulty, since only limited observations are possible on the living organ, and important changes may be encountered in an eye which is opened up after death. Evidence on any point has to be collected from various sources.

The variations of refractive index in the crystalline lens present some difficulties, but attempts have been made to represent its performance by the action of a theoretical lens composed of an outer portion of refractive index 1·386 and an inner core (double convex) of refractive index 1·406. The data given by Gullstrand in his Appendix to the English translation of Helmholtz's *Physiological Optics* show the constants of a "schematic" eye which would closely represent the optical working of an average real human eye with completely relaxed accommodation. The data for a simpler scheme also due to Gullstrand have been given in Chapter II.

SCHEMATIC EYE

Refractive Index

Cornea	1·376
Aqueous and vitreous humours	1·336
Lens (outer part)	1·386
Core of lens	1·406

Positions, measured in mm. along the axis from the anterior pole

Anterior surface of cornea	0
Posterior ,, ,, ,,	0·5
Anterior ,, ,, lens	3·6
,, ,, ,, core	4·146
Posterior ,, ,, ,,	6·565
,, ,, ,, lens	7·2

Radii of Curvature in mm.

Anterior	surface	of cornea	. . .	7·7
Posterior	,,	,, ,,	. . .	6·8
Anterior	,,	,, lens	. . .	10·0
,,	,,	,, core	. . .	7·911
Posterior	,,	,, ,,	. . .	− 5·76
,,	,,	,, lens	. . .	− 6·0

Under these conditions, the equivalent optical system of the complete eye can be calculated, with the following results—

COMPLETE SYSTEM OF EYE

Refracting power	58·64 diopters
Position of first principal point . .	1·348 mm. from anterior pole
,, ,, second principal point . .	1·602 ,, ,, ,, ,,
,, ,, first focal point . . .	− 15·707 ,, ,, ,, ,,
,, ,, second focal point . .	24·387 ,, ,, ,, ,,
First focal length	− 17·055 mm.
Second focal length	22·785 ,,
Position of *fovea centralis* . . .	24·0 mm. from anterior pole
Axial " refraction " (see Chapter VIII) .	1·0 diopter

The second focal length being 22·785 mm., the distance from the second nodal point to the second principal focus will be obtained by dividing 22·785 by 1·336, giving 17·055 (i.e. the distance of the first focal length). Thus, the second nodal point will be situated at 7·332 mm. from the anterior pole; the distance for the first nodal point is 7·078 mm. Under the above conditions the image of an infinitely distant object would be formed just behind the retina; slightly increased accommodation would be needed to obtain a sharp focus.

Owing to the closeness of the two principal and the two nodal points it is sufficient for general purposes to consider each pair as one point and a simplified schematic eye or " reduced " eye (due to Laurance) is shown in Fig. 89. The distances, in millimetres, are: AP = 2·2, PF = − 15, PF′ = 20, AN = 7·2, NF′ = 15, AF′ = 22·2, AF = − 12·8. The " round numbers " for PF and PF′ adopted in this scheme are sufficiently accurate for most purposes, and are convenient for quick calculations. In a normal eye viewing infinitely distant objects, the retinal point B′ will coincide with the second principal focus F′.

A simple scheme, adapted by Emsley from Listing's proposal, takes as the starting point an eye having one refracting surface, of power 60 D, separating air from a medium for which $n = 4/3$. The radius of this equivalent surface is 5·55 mm. $f = -16{\cdot}65$ mm. and $f' = 22{\cdot}22$ mm. The equivalent surface is taken 2 mm. back from the cornea. The total axial length of the Gullstrand reduced eye, quoted in Chapter II, was 24·17 mm., and the figures just given correspond closely to the focal lengths, etc., there calculated.

The *visual axis* may be considered to pass from the fovea through the nodal point to the fixation point. It makes an angle (the "angle α") of about 5° to 6° with the optic axis; the direction is such that if the right eye "fixes" the centre of a clock face normal to the line of sight, the optic axis is deviated approximately in the four o'clock direction. The visual axis does not, therefore, pass out through the true centre of the cornea, or the anterior pole, but on the nasal side and slightly upwards. The angle between visual and optical axes may vary with the anatomical construction of the eye.

The *pupillary axis* of the eye is the line passing through the centre of curvature of the corneal surface and the centre of the pupil. The *optic axis* is conceived as the central axis of symmetry of the globe, and passing through the centre of the cornea, but it cannot be located with the same experimental certainty as the pupillary axis if the two do not coincide. The angle κ (kappa) is the angle between the pupillary and visual axes.

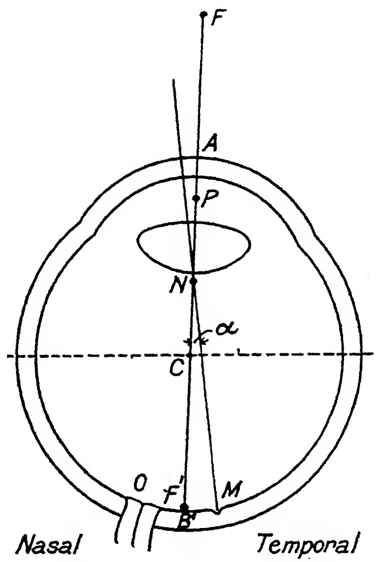

FIG. 89. REDUCED EYE

Another angle denoted by γ (gamma) has been defined as the angle between the optic axis and the "*line of fixation*" joining the centre of rotation of the eyeball to the object viewed by the eye.

Energy and Light. Quantitative Units. When energy radiated in wavelengths between approximately $\cdot 4\mu$ and $\cdot 7\mu$ reaches the retina of the eye, a sensation of "light" is produced. In the measurement of quantities of light, as distinct from quantities of energy, the valuation must take account of the sensation produced.

The "standard candle" unit (once represented by a candle fulfilling a certain specification, but now fixed by standardized electric lamps) is the unit source of light having unit "luminous intensity"; the quantity of light radiated by this unit source into unit solid angle is the unit quantity of light, called the *Lumen*.

The unit of illumination is the *foot-candle*; it represents the illumination given by unit source at a distance of 1 ft. (Another unit sometimes used is the metre-candle.)

The *brightness* in a given direction of a surface emitting light is the quotient of the luminous intensity (candle-power) measured in that direction, by the area of this surface projected on a plane perpendicular to the direction considered. The practical expression will be in " candles per square foot " or per square metre, etc.

The properties of radiating surfaces are of considerable importance in photometry. A " uniformly diffusing " surface is such that if the candle-power of an element of the surface in the normal direction is J, the candle-power in a direction at an angle θ to the normal will be J cos θ. This property is a close approximation to the truth in the case of most self-luminous smooth surfaces (such as of red-hot or white-hot objects). It is also nearly true of many " matt " reflecting surfaces such as those of blotting-paper, chalk, etc., and it may be shown that if the above law is fulfilled, the surface will " look " equally bright when viewed from any direction.

The sensation of " brightness " can be differentiated from that of colour, and it is possible to make reasonably consistent photometric matches between white and coloured fields. Hence, it is possible to establish a photometric unit of brightness for any coloured light by comparison with a standard which may approximate to white.

Another unit of brightness sometimes employed is that of a perfectly reflecting and diffusing surface on which the normal illumination is one foot-candle; the brightness of a surface is often given thus in " equivalent foot-candles."

Still another practical unit is the " Lambert," i.e. the brightness of a perfectly diffusing surface which reflects or radiates one lumen per square centimetre. The thousandth part of this unit, the milli-lambert, is more convenient. If the relation between the foot-candle and the milli-lambert be computed (allowing for the change of units of length) it will be found that 1 equivalent foot-candle = 1·076 milli-lamberts = 3·426 candles per square metre = 0·3183 candles per square foot.

The Perception of Light. In order that a sensation of light may be perceived at all, the stimulation of the retina must be of sufficient intensity and duration. The luminous surface employed as the visual object may be called the stimulus source. It has been shown by Ricco[3] and others that, with steady illumination for the macular region of the retina, the condition that a luminous sensation may just be perceived is that the total quantity of light (proportional to area of source *times* brightness) must reach a definite value; this law holds for sources subtending angles up to nearly one degree (50′ to be more exact). Hence, the brightness required for a small circular disc would be inversely proportional to the square of the diameter. These experiments were confirmed by the present writer,[4] who also found that for disc objects subtending angles above 1° (up to 4°) the threshold brightness is approximately inversely proportional to the diameter of the disc.

The " threshold brightness " found in such a way with a source of constant size varies, however, with the portion of the retina used and the " state of adaptation " of the eye. It is found that the regions just outside the fovea are more sensitive to light, a maximum sensitiveness being reached at about 5° to 6°. As the eye is kept free from light, or adapted to a lower degree of illumination, the sensitiveness rapidly increases; the " threshold " thus falls for upwards of an hour, but most rapidly in the first few minutes.

Fig. 90 shows the variation of the threshold with time as the " light-adapted " eye is subjected to re-adaptation to darkness.

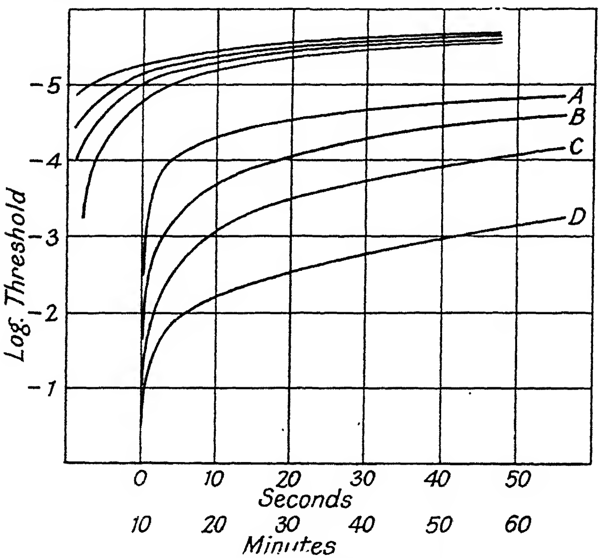

FIG. 90. PROGRESS OF DARK ADAPTATION

The initial steady states of adaptation, determined by the brightness of the so-called sensitizing field, are given by A = 0·3, B = 3·0, C = 30·0, and D = 300 candles per square metre (approx.) (Blanchard[5]).

It is on this process of adaptation that we depend for the capacity of the eye to function comfortably as it does, over a range of relative brightness values of the order of a million to one. The elongation of the processes of the pigmentary layer is intimately concerned in the process of adaptation to increasing intensities of light.

Fig. 91 shows the variation of the threshold energy with wavelength. The ordinates represent the logarithms of the energy. The experiments were made by Abney and Watson, using parts of

the retina at various angular distances from the fovea, and it is interesting to see that the wavelength for minimum threshold energy is shorter away from the fovea. It will be seen that the greatest sensitiveness was found at 5° from the fovea.

As far as foveal vision is concerned, the initial sensation, as the stimulus intensity rises through the threshold value, is said to be

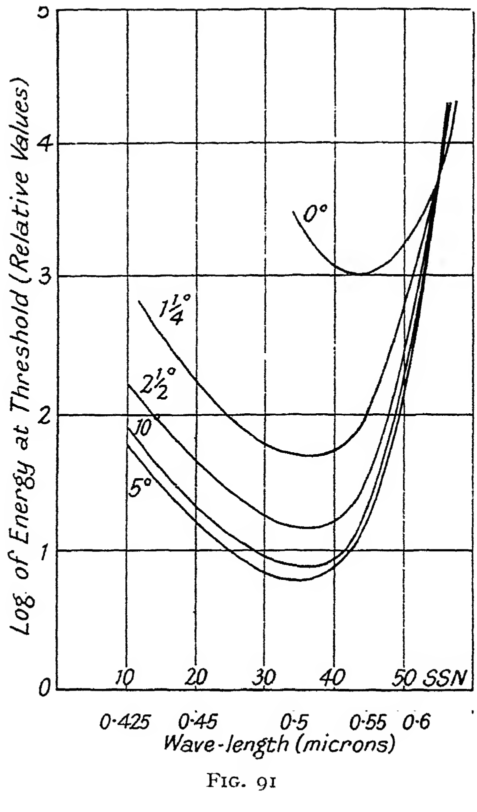

FIG. 91

"colourless" for all spectral colours except the red. There is thus in general an interval in which no hue is apparent (the "photochromatic interval") which is greatest for the shorter wavelengths.

The Visibility of Radiation. It was mentioned above that it is possible by various means to make photometric matches between white and coloured fields, and thus to establish a photometric scale for light of any colour.

When the eye views a "continuous" spectrum of some suitable source, a band of coloured light is seen which has maximum brightness in some intermediate part and sinking to zero at each end. Physical means enable an observer to measure the relative quantity of energy for different regions of the spectrum, and photometric experiments determine the relative brightness of the corresponding parts of the spectral band.

The "visibility" of the radiation is defined as the quotient of

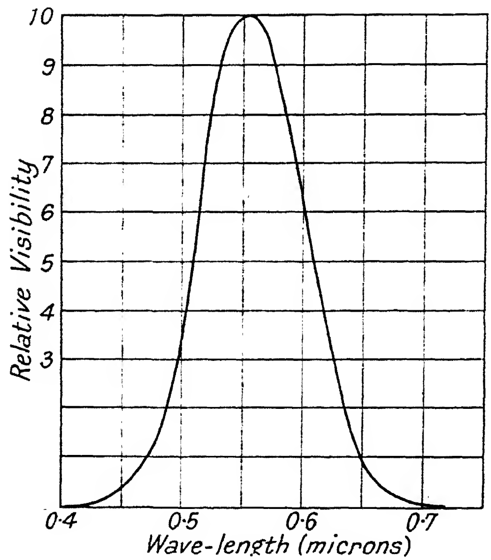

FIG. 92. ADOPTED VISIBILITY CURVE FOR "NORMAL EYE"

the brightness by the energy, and this is a function of great importance in colorimetry and photometry.

The visibility curve has been determined for a great number of observers with normal vision and the mean result,[8] now accepted as a standard, is shown in Fig. 92. (See Table, page 162.)

The results are modified when the visibility curve is re-determined for lower degrees of brightness,[9] say below 0·1 foot-candle. The maximum of the visibility curve is moved towards the shorter wavelengths. This means that if red and a blue field have the same brightness when the intensity is great, the blue will appear the brighter when the energy reaching the eye from each source is reduced in the same proportion for each. This is known as the Purkinje[10] effect.

The chief change occurs between external field brightness of about 1 equivalent foot-candle (when the peak of the visibility curve is at about 0·555μ) and about ·001 foot-candles,* when the peak has moved to about 0·505μ, much farther towards the blue.

It is interesting and suggestive that the human scotopic† luminosity curves for the spectrum corresponds closely to the rates of bleaching effected by the dispersed radiation in visual purple from the frog (Trendelenburg[11]).

TABLE

VISIBILITY OF RADIATION

Wavelength in μ	Visibility	Wavelength in μ	Visibility
0·400	0·0004	0·600	·631
·41	·0012	·61	·503
·42	·0040	·62	·381
·43	·0116	·63	·265
·44	·023	·64	·175
·45	·038	·65	·107
·46	·060	·66	·061
·47	·091	·67	·032
·48	·139	·68	·017
·49	·208	·69	·0082
·50	·323	·70	·0041
·51	·503	·71	·0021
·52	·710	·72	·00105
·53	·862	·73	·00052
·54	·954	·74	·00025
·55	·995	·75	·00012
·56	·995	·76	·00006
·57	·952		
·58	·870		
·59	·757		

* When experiments on retinal sensitiveness are made, the data given should be sufficient to determine the *retinal* illumination. The results are sometimes reduced to those which would be obtained with a standard pupillary aperture of 1 sq. mm. In this case, the unit of retinal illumination is the "photon," i.e. the illumination of the retina produced when the brightness of the object observed is 1 candle per square metre and the aperture of the pupil 1 square millimetre. However, for ordinary purposes, it is useful to know the apparent external brightness levels at which the visual changes occur. White paper illuminated by sunlight may have a brightness of about 1,000 apparent foot-candles or higher. Indoor day illumination may be of the order of 100 foot-candles, while good reading illumination by artificial light may be about 4–10 foot-candles. Fair-sized print can be read, although with difficulty, at 0·05 foot-candles. At this stage the pupillary aperture may be of the order of 50 sq. mm. One apparent foot-candle = 3·43 candles per square metre, so that 0·01 apparent foot-candles would correspond to 0·034 × 50 = 1·7 photons, very approximately, and 0·05 foot-candles to 8·5 photons.

† Scotopic = referring to conditions of weak illumination.

The Perception of Form. Visual Acuity. Taking the distance from the double nodal point to the retina as 15 mm., we find that an intercept of 1 mm. on the retinal surface subtends an angle of 3° 48′, say 4° approximately, at the nodal point. From the properties of the nodal point we see that an object which subtends about 4° in the field of vision will give a retinal image of length 1 mm. The minimum diameter of a foveal cone, ·002 mm., subtends an angle of $\frac{\cdot 002}{15}$ radians, or 28 seconds of arc. The fovea centralis subtends a visual angle of 55′ to 70′, while the entire macula subtends from 4° to 12°.

The possible fineness of the detail of a retinal image must be dependent, as with any optical system, on the factors, *inter alia*, of the aperture ratio of the system and the wavelength of light, although there may, of course, be reasons why the optical system fails to realize the theoretical possibilities. Assuming an aperture of the pupil of 4 mm. diameter, an average size, and a focal distance of 21 mm., assuming also an optical system without aberration, the radius of the Airy disc may be calculated by formula (39*a*), written in the form

$$h' = 0{\cdot}61 \frac{\lambda_o}{n'} \frac{f'}{y}$$

When $\lambda_o = 0{\cdot}5\mu$, $n' = 1{\cdot}34$, $y = 2$, and $f' = 21$ mm., we find $h' = {\cdot}0025$ mm. This length would subtend an angle of 34″ of arc approximately. A 2 mm. pupil produces a disc with a radius subtending 68″ of arc. Now, from our experience of image formation it is certain that the centres of two independent Airy discs can only approach each other just a little closer than the length of the radius before the possibility of resolution ceases. The presence of moderate spherical aberration does not prevent the formation of an image disc which approximates closely to the Airy disc (in fact, even slightly smaller concentrations may be obtained[12]), but it is necessary to consider both the presence of irregularities in the lens, and the chromatic aberrations of the eye (which is *not* chromatically corrected), in order to judge whether the limiting factor is the wave-nature of light or the defects of the system.

The irregularities of the lens and the edge of the pupil are doubtless the cause of the radiating streaks which are characteristic of the usual appearance of a star, and it is only necessary to screen a part of the pupil when looking at the bars of a window (with bright sky behind them) to become aware of chromatic effects in the visual image.

It has been calculated that the chromatic aberrations of the eye are practically the same as those of a single spherical refracting surface with the refractive index of water, having a radius of 5·125 mm. (Listing reduced eye[13]). Assuming the proper refractive indices for water for the extremes of the spectrum, violet and red, the positions of the corresponding foci, given incident parallel light and a 4 mm. pupillary diameter, are separated by approximately 0·43 mm. Assuming that the retina is placed at the position where the patch of confusion of the rays is least (Fig. 93), the diameter of the latter can be calculated to be 0·04 mm., which is twenty times the diameter of a cone. The visible concentration of light is, however, very much more compact. There are the following facts to remember. First, the high relative luminosity of the brightest parts

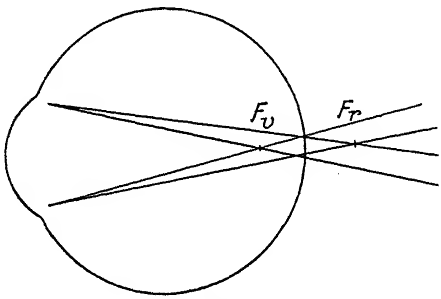

FIG. 93

of the spectrum as compared with the end regions; secondly, that the relatively lower dispersion in the longer wavelengths draws the red focus closer to that for brightest light than the violet focus, and also that there is a physical depth of focus (see page 141) which is 0·04 mm. with a 4 mm. pupil. Although it is only one-tenth of the geometrical axial chromatic aberration, this focal depth or range will include a great deal of the spectrum in the region of brightest light. A concentration comparable with the Airy disc is valid for the depth of focus. Subjectively, the concentration of the image is very great, and the faint purple border which must be present in the retinal image is not seen in ordinary vision.

It is interesting to note in passing that the length of the foveal cones is of the same order (0·04 mm.) as the physical depth of focus or maximum concentration of light. This suggests that the origin of the stimulus of light may occur anywhere in the length of the organ.

Experiments by Luckiesh[14] with homogeneous light derived from

a mercury lamp with a green filter have shown that the visual acuity (see below) is increased about 15 per cent by the use of this illumination, which naturally entirely obviates chromatic aberration. It may be concluded, however, that chromatic aberration cannot be responsible for a very serious loss of visual acuity.

Spherical aberration, and irregular aberrations arising, perhaps, from the lack of homogeneity in the crystalline lens, produce some effect on acuity, but any attempt at obtaining measurements of such aberration meets with considerable difficulty.[15] The main method is the subjective examination of " out of focus " images of small sources of light and their variation with accommodation. The presence of such aberration may be responsible for the diminution in acuity which occurs when the diameter of the pupil increases above 5 mm. Lister and Cobb found a practically constant acuity between 5 mm. and 3 mm., but a decrease for diameters above or below this range. The retinal illumination was kept constant in Cobb's experiments.

The work of Gullstrand has indicated that the anterior surface of the cornea is usually to be regarded as aspherical. The spherical aberration of the system is likely to be of the zonal type in which the axial focus of some intermediate zone falls closest to the lens. The marginal focus may lie within or beyond the paraxial focus according to the pupilliary aperture.

The considerable magnitude of the zonal errors is illustrated by the 4 dioptre difference of power between the paraxial zone and a zone of 2 mm. radius, which is established by many observations by Gullstrand.

Hooke first pointed out in 1671, that the resolving power of a normal eye for such an object as a double star is just about one minute of arc. Thus, in spite of chromatic and monochromatic aberrations, the optimum acuity of the eye is not far removed from the limits imposed by the nature of light, for pupillary diameters of 3 to 4 mm. The decrease in acuity for smaller pupillary diameters must be ascribed to the lower physical resolving power of the optical system.

It is remarkable that the fineness of the mosaic of retinal receptors in the fovea is of the order required to do justice to the resolving power of the optical system of the eye for two close point objects. It has been, in fact, held that the visual condition for " resolution " must be the presence of a relatively unstimulated cone between two others in which more energy is received. Hence, the closest approach for the centres of two images would correspond, on this supposition, to the double cone diameter, subtending about 56

seconds of arc in the visual field, and this was imagined to set a limit to the possible acuity of vision. It is doubtful, however, whether the supporters of this theory have taken sufficient account of the physical distribution of energy in the image on the one hand, and the remarkable facts of contour acuity on the other.

The realization of this optimum acuity of vision is, of course, entirely dependent on the capacity of the retinal receiving apparatus. A great deal of experimental work on the influence of *illumination* on visual acuity has been performed, with illumination increasing from very low values. There is a rapid rise in acuity up to about 5 equivalent foot-candles when viewing a black-and-white test chart; the rate of increase then diminishes and a more or less steady optimum state is reached at about 20 foot-candles and upwards.

In such work it is necessary to allow time for the *adaptation* of the eye to any given condition of illumination. If an eye adapted to, say, 0·1 foot-candle is suddenly exposed to 1,000 times this brightness there is at first a sensation of discomfort and glare, with practically a total loss of fine discrimination in vision. This, however, rapidly passes away and the eye begins again to function normally, delicate details of form and contrast coming again into view.

Of course, an overwhelming intensity of light may result in permanent physical damage to the retina; experiments at a very high brightness level are subject to difficulty and uncertainty on this account.

Measures of Acuity. The simplest measure of "acuity" or sharpness of vision from the theoretical standpoint is the minimum angular separation which permits of resolution for two point objects. As mentioned above, the value for the normal eye is approximately 1 minute of arc. Other criteria sometimes discussed are: the minimum dimensions for seeing a line or point, and the minimum separable for lines or sets of lines arranged as a grating.

Another criterion of acuity is the minimum distinguishable change of contour, which concerns the power to distinguish the displacement between two parts of a line, as in reading a vernier where the apparent continuity of vernier and scale divisions must be examined. This is called the "contour" or "vernier" acuity.

The minimum dimensions for a distinguishable line or point are quite indeterminate if the object is self-luminous, and mainly depend on the amount of light radiated by the object, which must simply exceed the threshold of vision valid for the case in question. The object may, however, be exhibited black on a white ground or vice versa, as by using objects of paper. Aubert[16] found that a

square of white paper on a black ground could be seen when the side of the square subtended 18 seconds of arc. For a black square

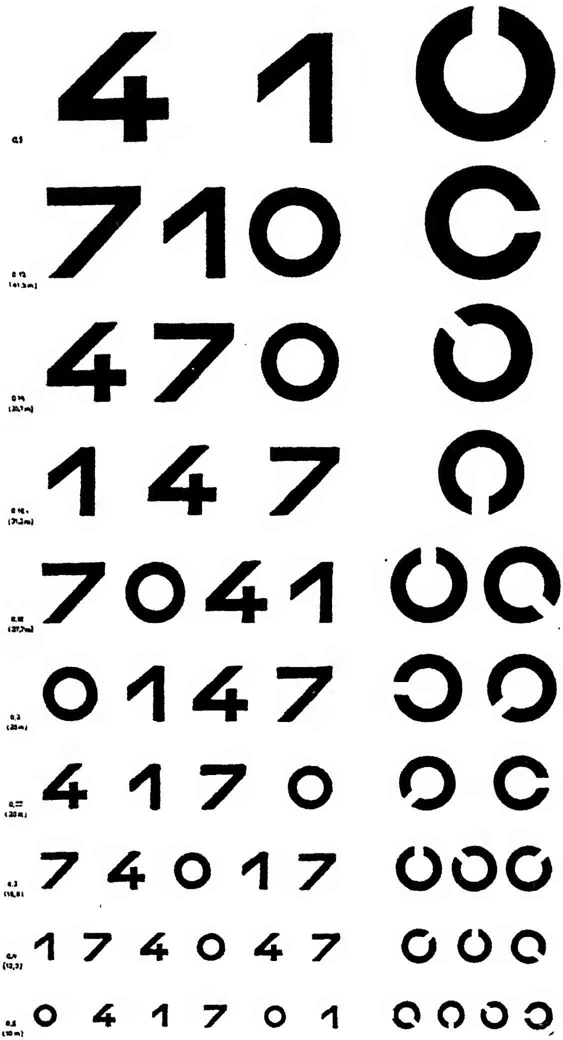

FIG. 94A. TEST CHART (ZEISS)

on a white ground the angle had to exceed 35 seconds. With all such objects, the contrast between the parts of the field to be

distinguished is of the first importance. A grating may consist of opaque black wires seen against a light ground, thus producing a maximum contrast. The lines may then be distinguished under a much smaller angle than with a grating in which the lines are grey on white.

Irregularities of the eye such as axial astigmatism are likely greatly to affect the measurements of acuity of the unaided eye, according to the nature and position of the object.

The "page of type" naturally employed as a test object in selecting spectacles must have suggested the employment of a graduated series of test letters. Donders suggested to Dyer and Snellen that the 1 minute subtense characteristic of the *minimum*

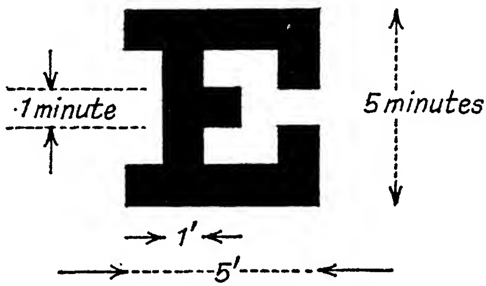

FIG. 94B. TO ILLUSTRATE THE PRINCIPLE OF CONSTRUCTION OF A TYPICAL TEST-CHART LETTER

Subtending 5 minutes at the standard distance; the width of the stroke subtends 1 minute

separabile for points should form the basis of construction of test letters, and in 1862 Snellen's optotypes were published. In these a number of rows of letters are printed. Each letter in one row has a diameter subtending 5 minutes of arc at a certain distance (marked on the chart against the row), and the stroke or limb of the letter has a width subtending 1 minute; the spaces between the adjacent limbs of each letter also subtend 1 minute. It is considered that a person of normal vision should be able to read the letters of any row at the distance marked above it. A chart showing figures in a similar way is illustrated in Fig. 94A, this chart being one published by Zeiss. Fig. 94B shows the details of the construction of a typical test-chart "letter."

Vision is usually tested at 6 metres or about 20 ft. The types are provided for distances of 2 metres to 60 metres. Imagining that a patient being tested at 6 metres can just read line No. 12 (readable by the normal eye at 12 metres), the visual acuity thus found for the patient would be expressed as $V = \frac{6}{12}$.

Tested in this way, many persons of good eyesight will find an "acuity" greater than $\frac{6}{6}$.

The chart illustrated in Fig. 94A is one-quarter of the size of a normal chart for use at 5 metres. Hence it would be used at 1·25 metres to obtain the correct angular subtense of the letters. Only part of the chart is reproduced; the bottom line is labelled 0·5 (10 m.) These types have been arranged by A. Hegner on the basis of data due to Hess, and the originals are published by Messrs. Carl Zeiss.

The conditions of the test need some care in arrangement; the illumination should be adequate, i.e. above 5 foot-candles, and glare must be avoided. No reflection from a "shiny" surface can be tolerated. If the results of tests made at successive times are to be comparable, the illumination must be equal in both cases. Hence, artificial light is usually employed.

It is almost invariably found that some letters are read more easily than others, and, though this may even be a convenience when using the chart for finding the power, etc., of spectacles to correct eyesight, it is confusing when a reliable measure of visual acuity is required. The "broken ring" of Landolt[17] (see Fig. 94) aims at providing a test less variable than that of the letters. The ring has a diametrical subtense of 5 minutes at the standard distance, while the line and the gap have each a subtense of 1 minute. The observer must be able to recognize the position of the gap in any relative position. Although the measurement of acuity by such a "broken ring" or "broken square" may be rendered more difficult in the presence of uncorrected visual astigmatism, a greater consistency can be obtained in tests with such standardized objects.

A recent test chart, due to Emsley, avoids the use of open letters like L, T, V, etc., and only retains those in which lines and spaces can be standardized to one-minute angular substance.

Vernier or Contour Acuity. The investigation of the causes underlying the 1 minute value found for the *minimum separabile* naturally includes the answering of the question "What is the least retinal image displacement which gives a mental impression of a change of position of the object?" The sense of vision is endowed, in the language of physiology, with a specially sensitive "local signature."

The question of the space image in binocular vision and the general question of the perception of "direction," are too complex to be discussed at present, but the perception of relative position is very

important; it is much more delicate than the resolving power of the eye for close double images would seem to suggest.

Wülfing[18] and many others have examined the contour or vernier acuity of the eye in experiments in which human subjects of normal vision are asked to place the separated parts of a line (Fig. 95) in exact alignment. The lines may be drawn on two cards, one movable relatively to the other along the line of separation. Such experiments show that the minimum separation detectable to unaided vision is as low as 10-12 seconds of arc, and with practice the lines can be adjusted by many persons within a probable error perhaps as small as 3 or 4 seconds.

The recent experiments of Langlands[19] show that there is distinct ability to make a good judgment of relative position with similar objects, even with flash illuminations of extremely short duration

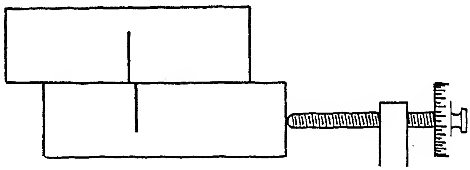

Fig. 95. Diagram of Apparatus for Investigating "Contour Acuity"

(Spark $< 10^{-3}$ second), but the accuracy improves as the duration of the illumination rises above about $\frac{1}{10}$th second, showing apparently that the finest degree of discrimination may depend on a movement of the images over the foveal cones. These experiments were carried out on "binocular acuity" depending on the perception of depth through the stereoscopic sense.

No finally satisfactory explanation of the extraordinarily great acuity of the human eye in observations of this type has yet been suggested. One of the best-known theories was advanced by Hering,[20] and the class of argument which he put forward is illustrated by Fig. 96. In (*a*) we see the retinal mosaic on which an imaginary image with a broken line of separation between light and dark portions is shown. It is assumed that any one cone or row of cones has its own "local sign," i.e. the passage of stimulation from one cone or row of cones to another causes a definite apparent displacement of the image. In the upper portion the row *n* of the cones is stimulated, but in the lower portion no cone in this row receives light. Hence, a break in the line would be perceived, even though the actual discontinuity might be small in comparison with the diameter of a cone. In part (*b*) the image has been slightly

shifted and no discontinuity would be perceived; hence, we see why slight retinal movements might be helpful in discrimination, Hering's discussion covered other cases.

The physical facts of the retinal image call, however, for a more thorough-going treatment when it is remembered that the radius even of the monochromatic Airy disc corresponding to an elementary image is of the same order as the diameter of one cone, and the spreading of an image of a luminous area bounded by a straight edge would certainly be of the same order of magnitude.

The experiments of Hartridge,[21] moreover, would indicate that a very high order of accuracy in "coincidence" settings of the

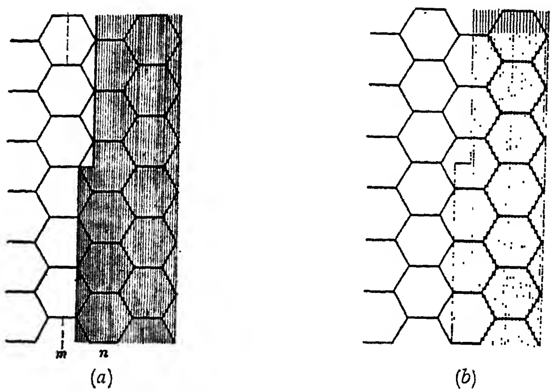

FIG. 96. TO ILLUSTRATE HERING'S THEORY OF THE RETINA

above type is possible not only when the lines (the parts of which are to be brought into alignment) are sharp or bounded by sharp edges, but also when they are very diffuse. Hartridge conducted his experiments with apparatus which presented a spectrum divided into two parts by a line of separation perpendicular to the spectrum lines themselves; the diffuse lines were, actually, absorption bands. The setting consisted in making a consistent alignment of the two halves of a "band." The question of acuity of vision as regards form is therefore intimately connected with the capacity of the retina to register fine differences of stimulation or simultaneous contrast between contiguous regions, and is probably connected with "fine-grained" effects of induction and inhibition.

Perception of Movement. A similar delicacy exists in the perception of the minimum displacement in the perception of movement. Such movements may be slow, regular movements to and fro, of time-period about $\frac{1}{2}$ second. Volkman,[22] Stern,[23] and others have

made measurements which indicate, as an average, a possibility of recognition of a displacement of 10 seconds of arc or even less. Such conditions assume the presence of a fixed reference object in the field.

When the movement is continuous, the minimum angular velocity in the visual field which allows of a perception of movement is 1 to 2 minutes of arc per second.

Peripheral Vision. The power of the visual apparatus to impart

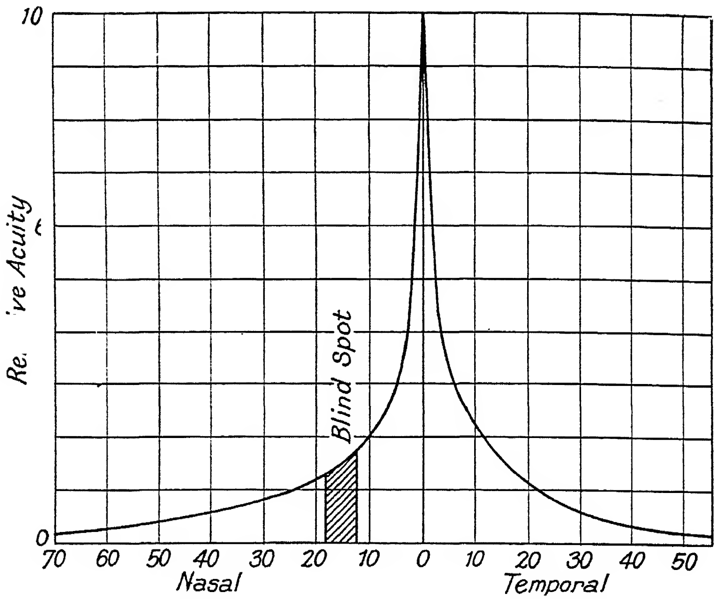

FIG. 97. VARIATION OF ACUITY WITH ANGULAR DISTANCE FROM FOVEA

the mental impression of a sharply-defined " point " image rapidly diminishes as the image moves away from the fovea, and the power to discriminate the independence of two close images rapidly falls. Fig. 97 shows the visual acuity and its variation at various angles in the visual field (Wertheim[24]) ; at 5° from the fovea it falls to one-third of the maximum. Similarly, the power of the retina to register " displacement " or " movement " diminishes from the fovea outwards, as shown by Ruppert.[25] The results of his experiment showed, however, that the perception of displacement by the periphery of the retina is more sensitive than that of movement. Sensitiveness to movement is equivalent to a high sensitiveness to changes of

illumination; the sensitiveness to flicker in the dark-adapted eye is greater in the outer regions of the retina than at the centre. In some respects, the retinal periphery must be regarded as specially adapted for the perception of movement. The lack of discrimination of form away from the fovea can be associated with the arborization of the nerve fibres referred to above, through which several rods and cones may transmit impulses to a single bi-polar cell, which several bi-polar cells may connect to a single ganglion cell. Hence, two separated images on the retina may give rise to a single visual impression.

Perception of Contrast. It is not difficult to present to the eye a photometric field of two equal portions in which the relative " brightness " can be quantitatively adjusted. If the brightness of one part is B and the other $B + dB$, where dB is the least *perceptible* difference in brightness, then the fraction

$$\frac{dB}{B}$$

(often called the " Fechner fraction ") can be measured under various conditions. In experiments on direct vision, the size of the matching field is restricted to 2°, so that the image may fall within the area of the retina which is more or less uniformly pigmented. Measurements of this type have been made by König, Brodhun,[26] Nutting,[27] and others, and tables of their results show that for monochromatic or white stimuli the value of the fraction is approximately uniform over a wide range of absolute brightnesses corresponding to those encountered in ordinary vision, but its value rises greatly when the retinal illumination sinks below 30 photons or thereabouts (external field brightness of the order of one-fifth equivalent foot-candles).

König and Brodhun's results for orange-red ($0{\cdot}605\mu$) and violet ($0{\cdot}43\mu$) are shown in Fig. 98. There is some little doubt as to the effective value of the unit of brightness employed,* but it will be seen that the Fechner fraction is plotted as ordinate against the logarithm of the field brightness. The eye is more sensitive to contrast changes in the shorter wavelength regions for equal apparent field-brightness under conditions of low illumination.

Photometric Scales. Addition of Luminosities. Given monochromatic light of a single wavelength, the photometric measure of quantity of light is proportional to the energy. Let e_1, e_2, e_3, etc., be the relative energy of the monochromatic components of a mixed

* König and Brodhun used an " artificial pupil " for observation, so that the values of the field brightness are truly proportional to the retinal illumination.

radiation, and v_1, v_2, v_3, their visibility coefficients, then the photometric "quantity of light" will be proportional to

$$e_1v_1 + e_2v_2 + e_3v_3 = \text{F, say.}$$

The additive property of the "luminosities," e_1v_1, e_2v_2, etc., is a very important one; it has been established by the work of Abney and Ives. Luminosity, in fact, appears as an experience, regarding any stimulus, of a unique and separable character.

If now the relative energy of all the components is increased in

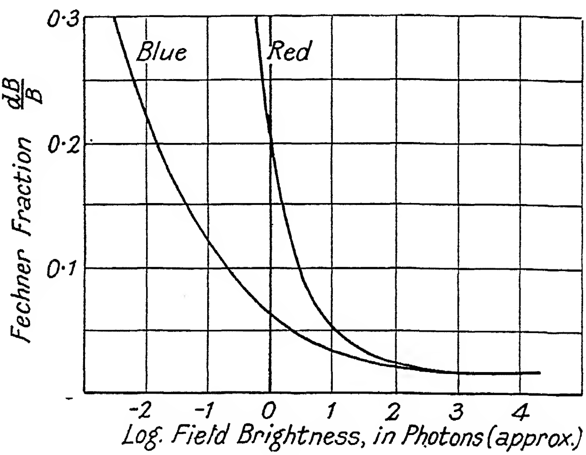

FIG. 98

the same ratio, K, say, the quantity of light in the photometric sense will now be

$$\text{K}(e_1v_1 + e_2v_2 + e_3v_3) = \text{KF}.$$

If the *relative* amounts of energy of the components in the mixed radiation vary, the quantity of *light* will no longer be proportional to the total energy. The photometric scale is only related to the energy scale for light of constant composition.

Weber's "law" states that the least perceptible increase of the stimulation of a sensation is proportional to the intensity of the original stimulus. Mathematically—

$$\frac{d\text{I}}{\text{I}} = \text{constant.}$$

König and Brodhun's results have shown how far this law is obeyed.

It may be assumed that the just perceptible steps, ds, of sensation are equal steps in the quantity of the sensation (Fechner[28]), then

$$ds = K\frac{dI}{I}.$$

In order to obtain a measure of the increase of sensation resulting from an increase of the stimulus from I_0 to I we may integrate, thus obtaining

$$s - s_0 = K \log \left(\frac{I}{I_0}\right)$$

for the range in which K may be considered constant.

Hence, the sensation scale of brightness is very different from the practical photometric scale. To illustrate this it is possible to prepare a series of grey papers which have reflection coefficients increasing in arithmetic progression from 0·1 to 0·9, say. The higher steps, i.e. between 0·7 and 0·8, and 0·8 and 0·9, appear exceedingly small differences of contrast as compared with the steps 0·1 to 0·2, 0·2 and 0·3. On the other hand, a series with the reflection coefficients increasing in geometric progression appears to possess practically equal steps of contrast.

Colour Vision. The briefest summary of a few outstanding phenomena of colour vision must suffice for the present purpose. Colour is a sensation. The colour variables are those of hue, brightness, and saturation. Hue is a property of colour which varies with changes in the frequency of the stimulating light, but colours may retain the same hue while containing a greater or less admixture of white. The smaller the white constituent, the greater the "saturation."

Now we may illuminate one side of a photometric field by any colour we please, and the other by an *additive* mixture of three spectral colours such as red, green, and blue, in their pure condition. (An "additive" mixture would be secured, in one way, if the same screen were illuminated by red, green, and blue lanterns.) Then it is a most remarkable fact that by a variation of the relative proportions of these three "primaries" in the mixture we can secure all possible changes of hue, and we can further match most colours which can be put into the other field (with the exception of certain ranges of the most highly-saturated colours). If the brightness of the test colour and of the three primaries can be varied in known numerical proportions, then the amount of the primaries necessary

to match any test colour can be found. A "colour equation" results—

$$mC = aR + \beta G + \gamma B$$

where m is the amount of the test colour C and a, β, γ, are the amounts of red, green, and blue respectively, measured on some convenient scale established for each colour on a photometric basis. One possible scale is that of "luminosity," see page 174. A suitable adjustment of the primaries enables us to match a definite amount of a *white* test colour.

Let it be supposed that we are now given a colour C_1, which is too saturated to be matched by a mixture of the three primaries alone. Then we can secure a match in one of two ways; either by adding a small amount of one of the primaries to it, so that its saturation is reduced and we obtain a match represented by

$$m_1C_1 + \beta_1G = a_1R + \gamma_1B,$$

or we can reduce the saturation of the test colour by mixing it with white, thus getting an equation of the type

$$m_2C_1 + n_2W = a_2R + \beta_2G + \gamma_2B$$

This can be combined with the equation for white

$$n_2W = a_3R + \beta_3G + \gamma_3B$$

so that in either case we can obtain an *equation* representing the test colour, no matter what its saturation.

(The primaries may be, theoretically, any three different colours, but in order directly to match a wide range of colours, it is necessary to have them as pure or fully saturated as possible, and spaced as far as possible from each other in the spectrum; thus red, green, and blue, or red, green, and violet, are usually selected.)

These remarkable experimental facts led Thomas Young[29] to suggest that a visual colour sensation was, in general, a mixture of three primary sensations. This is an enormous simplification of the theory of colour vision. Springing directly from the experimental work of Newton and expressed thus by Young, the question was taken up and put on a sound experimental and theoretical basis by Maxwell and Helmholtz.

Whether or no the "trichromatic" theory is in harmony with all the phenomena of colour vision is still undecided. The "hue" sense must be regarded as a part only of the visual process. Moreover, no satisfactory anatomical evidence of any triply differentiated structure of the retinal or cortical visual apparatus has yet been

adduced; thus the relative parts played by this trichromatic apparatus (supposing its existence in any form) and by the remainder of the visual equipment are hard to differentiate.

Colour Blindness. Various individuals differ amongst themselves in the amounts of the three primaries, red, green, and blue, which they require to effect colour matches, especially in the blue end of the spectrum, and many such variations are attributable to variations in the amount of macular pigmentation. Other individuals are found, however, who can match any spectral hue with two primaries only, red and blue, or green and blue. Such often cannot distinguish the hues of red and green, and they may sometimes be blind to some range at the extreme red end of the spectrum. Other individuals, again, are totally unable to perceive any "hue," their sensations being of relative brightness and darkness only. Their "spectral luminosity" measurements correspond to those effected in normal vision under scotopic conditions.

Field of Vision for Colours. Under normal conditions for normal sight, the power of distinguishing hue is confined to certain regions of the retina surrounding the fovea. Green may be indistinguishable beyond a zone from 20° to 30° from the centre, but blue and red may have larger fields. With increased intensities, however, the limits of the hue perceiving areas are greatly extended.

Time Relations in Vision. When a dark adapted retina is suddenly stimulated by exposure of the eye to a field of steady brightness, the sensation rapidly rises to a maximum which is the sooner reached the greater the intensity of the stimulus. The sensation thereafter sinks somewhat until a fairly steady state is reached for a time at least. (Long-continued stimulation of the retina may result in a state of abnormal visual action in which the field of vision disappears.) The chief investigators have been Exner,[30] and Broca and Sulzer. The main features of their results are indicated in Fig. 99, from which it will be seen that the blue stimulus causes a sharp rise of sensation to a maximum not shown in the diagram, but which is at least five times the final value. The action is least marked with the green stimulus. The maximum is reached in under one-seventh of a second.

On the other hand, the sensation does not immediately disappear when the stimulus is removed, but takes a finite time to sink below the limit of perception.

The effect of the finite rates of growth and decay of sensation when the stimulus is suddenly applied or removed, enables the eye to "integrate" the brightness of a rapidly-varying source, provided that the total cycle of variations is regular and of sufficiently great

frequency. If I is the apparent photometric brightness and t the total period of the complete cycle, while i is the actual photometric brightness,

$$It = \int_0^t i\,dt$$

Put into words, the principle states that the impression produced by a light undergoing rapid regular periodic variations of sufficiently

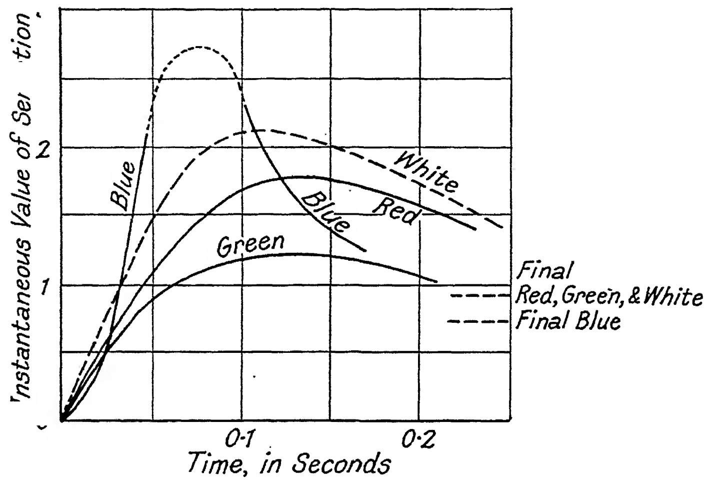

FIG. 99

great frequency, is as if the light emitted during each period were distributed uniformly throughout the duration of the period.

This law, which rests on the work of Talbot[31] and Plateau,[32] and has been abundantly verified by Abney and others, shows that the apparent intensity of light transmitted by a sector disc (Fig. 100) in rapid rotation is proportional to the angular opening.* Such a disc transmits a "flickering" light; the flicker, however, is only seen at low frequencies. Porter[33] and Ives[34] showed that for various monochromatic lights the critical frequency at which flicker disappears is a linear function of the logarithm of the photometric brightness of the field. It is interesting that the function may suddenly change at certain brightness levels, although remaining linear.

In the hands of Allen and others the phenomenon of the critical period for flicker has been made the basis for determination of the

* The use of too small an angular opening for the sector should be avoided, as it may lead to inaccuracy.

apparent brightness of the visual field, but this method must be carefully distinguished from the better-known methods of "flicker photometry."

In the flicker photometer, advantage is taken of the fact that "flicker" occurs at slow speeds of alternation between any two

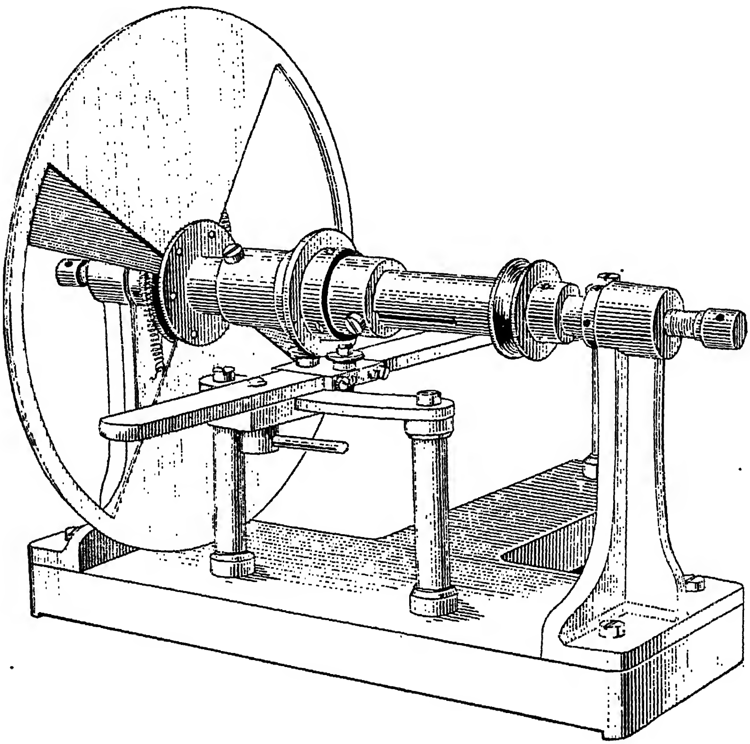

FIG. 100

successions of brightness or colour in the field. However, even when the alternate fields differ in hue, the critical frequency of flicker is a minimum when their apparent photometric brightness is equal. Hence, by adopting a suitable frequency, the flicker may be made to disappear by adjusting the brightness of one of the pair.

Spatial Induction. The retina is by no means a system of independent receptors, for stimulation of one area may profoundly affect the sensitiveness and the action of another part. The most familiar examples of such actions are found in the familiar phenomena of simultaneous contrast both in brightness and colour. A

succession of uniform strips of grey, increasing in darkness from one to the other, give the impression of " flutings " owing to the subjective accentuation of contrast at each boundary. The surprising effects of colour contrast cannot be discussed here.

The retina seems to function best in general when the average brightness level of the whole is near that of the immediate field under observation. Thus Jones[35] found that a kinema picture, a relatively small field surrounded ordinarily by complete darkness, can be better seen if a certain amount of light reaches the periphery of the field. Cobb[36] has investigated the effects on foveal vision produced by stimulation of the peripheral parts of the retina, and has shown that with intensities of the surround field increasing from " darkness " the contrast sensitivity is at first improved, but becomes impaired as the surround intensity rises above that of the central field. Similar experiments by Emerson and Martin[37] investigated these phenomena with monochromatic light. The first increase of sensitiveness (giving a lower contrast " limen ") is followed by a decrease, but more quickly in the longer wavelengths. The experiments were made at wavelengths 0·68, 0·67, 0·56, and 0·48μ. In the case of 0·48μ the brightness of the surround may be increased to nearly three times that of the central field before a decrease of sensitiveness (as compared with the sensitiveness for an entirely dark surround) manifests itself.

Experiments of this kind, and direct trials with instruments, point to the great importance of providing large fields of view in observational instruments such as " night glasses " intended for use under conditions of extremely low illumination. On the other hand, they suggest that under some circumstances it may be desirable to be able to reduce the size of the field.

The phenomenon of " glare " is sufficiently common to be familiar to all. Many attempts have been made to study it systematically. Nutting, Blanchard, and Reeves[38] conducted experiments in which the retina was sensitized to a definite field brightness before flashing on a much brighter field. The intensity of the bright field was increased by trial until it appeared uncomfortably bright when first seen. The three observers agreed very well in their estimates, and found that for a brightness F of the sensitizing field the lower limit of " glare " G is represented by the equation

$$G = 1{,}700\ F^{0 \cdot 32}$$

In addition to work involving such introspective estimations as the above, the effect of a " glaring " stimulus in the field can be

studied in relation to the acuity of vision for form and contrast in other parts of the field.

The question has been studied in relation to the size of the field of view of observational instruments by the writer with T. C. Richards.[39] It was found that in the case of night glasses the largest possible visual field is almost invariably required for best effects *in very weak illumination.* Under these conditions, a small object not discernible against the background in the centre of a small field may come into view easily when the size of the stimulated retinal area is increased. On the other hand, it is frequently the case that the object observed in the central part of the visual field of a telescope in daylight is darker than its bright surroundings. Such conditions were studied by statistical methods of observation, and it has been shown that an improvement in the speed and accuracy of observation could then be obtained by a diminution in the size of the field, which removes the excessive stimulation of the peripheral regions of the retina.

A partial explanation of these various effects is to be found in the variation of the "adaptation level" of the retina due to the various stimuli present in the visual field. Thus, with the telescope field bright in the peripheral portions and dark in the centre, the adaptation level of the central region of the retina is too high and the comparatively weak central stimulus fails to secure the necessary sensitiveness; on the other hand, with a bright central field in surrounding darkness there may be some effect of "glare," because the adaptation level is too low, due to the relatively unstimulated peripheral portions of the retina. However, the relative "adaptation level" is not the only factor in the full explanation of these effects, especially those concerned with feeble stimuli; Nutting[40] has shown, for example, that the increase in size of a weak sensitizing field actually lowers the foveal threshold. This evidently involves an action of another type which might, following the one theory, be concerned with the stimulation of the output of visual purple, effecting a higher sensitization. According to Edridge Green, the rods of the retina are solely concerned with the production of visual purple, which acts as the photo-sensitive substance when diffused among the cones; the latter organs pick up the visual impulse. This, however, is in opposition to the duplicity theory of von Kries, by which the rods are the organs concerned in the reception of faint light.

After-images or Successive Induction. The time relations in vision hitherto mentioned have included the rate of adaptation to darkness and the rate of growth of sensation subsequent to the

commencement of stimulation. Certain phenomena of some importance occur on the removal of a stimulation. If the retina, moderately dark adapted, is exposed for, say, 1 second to stimulation by a bright field, the immediate impression is followed by an image resembling the original in colour and form. If the original stimulus is strong, the hue may change through red, green, and blue phases, even if the original was white. Meanwhile the image gradually loses its form. Such changes have been described by MacDougall[41] and others. The above are the phenomena of the "positive" after-image.

If the eye is turned to a grey field immediately after the first short stimulation, a "negative" after-image is observed which is at first of a hue complementary to the original stimulus. With white stimuli, coloured negative after-images are observed which again exhibit various phases of hue.

References

1. Blanchard: *Phys. Rev.*, 11 (1918), 81.
2. Fincham: *Trans. Opt. Soc.* XXX (1928–29).
3. Ricco: *Ann. di. Ottal.*, VI (1897).
4. Martin: Department of Scientific and Industrial Research, *Bulletin No.* 3.
5. Blanchard: See (1), above.
6. Abney and Watson: *Phil. Trans. Roy. Soc. A.*, 216 (1915), 91.
7. Abney: *Researches in Colour Vision*, Chapter XII.
8. *Receuil des Travaux de la Commission Internationale de l'Eclairage*, 6 (1924), 348.
9. König: *Gesammelte Abh. zur Physiol. Optik* (Leipzig, 1903), p. 144.
10. Purkinje: *Magazin f. d. gesammte Heilkunde, Berlin*, 20 (1825), 199.
11. Trendelenburg: *Centralbl. f. Physiol.*, XVII (1904).
12. Conrady: *Monthly Notices, R.A.S.*, June, 1919.
13. Helmholtz: *Physiol. Optics.*, English translation, Vol. I, p. 176.
14. Luckiesh: *Colour and Its Applications* (New York), 1921, p. 131.
15. Ames and Proctor: *Jour. Opt. Soc. Amer.*, 5 (1921), 22.
16. Aubert: *Physiologie der Netzhaut*, Breslau, 1865.
17. Landolt, E.: *Ann. d'Ocul*, 75 (1876), 207.
18. Wülfing: *Zeit. f. Biol.*, XXIX (1892), 189.
19. Langlands: Medical Research Council, Special Report Series, No. 133.
20. Hering: *Leipzig Berichte* (1900), 16–24.
21. Hartridge: *Phil. Mag.* XLVI (1923), 49.
22. Volkman: *Physiol. Untersuchungen im Gebiete der Optik* (Leipzig), 1863.
23. Stern: *Zeit. f. Psychol.*, VII (1894), 321.
24. Wertheim: *Zeit. f. Psychol.*, VII (1894), 177.
25. Ruppert: *Zeit. f. Sinnesphysiol.*, XLII (1908), 409.
26. König and Brodhun: *Sitz. Akad. Berlin*, July 26, 1888.

27. Nutting: *Bull. Bureau of Standards*, 5 (1908), 285.
28. Fechner: *Leipzig Berichte*, 4 (1859), 455.
29. Young: *Phil. Trans.*, 92 (1802), 12.
30. Exner: *Sitz. d. Weiner Akad.*, LVIII (1868), 2, 601.
31. Talbot: *Phil. Mag*, 5 (1834), 327.
32. Plateau: *Acad. Roy. des Sciences, Brussels, Bull.* 2 (1835), 52.
33. Porter: *Proc. Roy. Soc.*, 63 (1898), 347.
34. Ives: *Phil. Mag.*, 24 (1912), 352.
35. Jones: *Comm. No.* 135, Research Lab., Eastman Kodak Co.
36. Cobb: *Jour. Exp. Psychol.*, 1 (1916), 419, 540.
37. Emerson and Martin: *Proc. Roy. Soc. A.*, 108 (1925), 483.
38. Blanchard: *Phys. Rev.*, 11 (1918), 81.
39. Martin and Richards: *Trans. Opt. Soc.*, 30 (1928–29), 22.
40. Nutting: *Trans. Ill. Eng. Soc. Amer.*, XI (1916), 4.
41. McDougall: *X. N. S.*, 235, 1901.

CHAPTER VI

PHYSICAL OPTICS (CONTINUED): INTERFERENCE BY SUCCESSIVE REFLECTION, POLARIZATION, DOUBLE REFRACTION

Interference Caused by Successive Partial Reflections. Successive reflection of light from two close parallel or nearly parallel surfaces produces two close images of the same small source. In such a case, interference effects can be observed by the eye even when the source of light is very broad.

Consider two parallel reflecting surfaces bounding a layer of refractive index n'. The refractive index of the medium outside the layer is n. Let OA, Fig. 101, be the incident ray which suffers partial reflection at A and at B, the final parallel directions of the reflected rays being AD and CE. Drawing CD perpendicular to these emergent rays and imagining them brought to a common focus P by some optical system (which might be the eye), it is assumed that the relative difference of path with which the disturbances meet in P will be that which they already possess at C and D.

The optical path difference is

$$\begin{aligned}\delta &= n'(\mathrm{AB} + \mathrm{BC}) - n\mathrm{AD} \\ &= \frac{2n't}{\cos i'} - 2nt \,.\, \tan i' \sin i \\ &= 2t\left\{\frac{n' - n \sin i' \sin i}{\cos i'}\right\} \\ &= \frac{2tn'}{\cos i'}\left\{1 - \sin^2 i'\right\} \\ &= 2n't \cos i'\end{aligned}$$

It is found that reflection at a denser medium introduces a phase change of π in the reflected light. Hence, the total path difference arising on reflection will be equivalent to

$$\delta_1 = 2n't \cos i' + \frac{\lambda}{2}$$

If the thickness is zero there will be destructive interference; this

also occurs when $2n't \cos i'$ happens to be equal to any whole number (m) of wavelengths, i.e.

$$2n't \cos i' = m\lambda$$

Interference of this kind can be observed with a telescope under conditions of very great path differences if the two surfaces are *accurately* parallel, and homogeneous light (say, the green light from a mercury lamp) is employed. This effect will be described in the chapter dealing with interferometers.

In the case of a very thin film such as a soap bubble, the eye receives a diverging cone of rays, filling the pupil, from any small elementary area of the film. If BC, Fig. 102, is the broad source of light there will be a definite area of this which contributes light to the image of the film element, but the relative retardations of the different pairs of interfering disturbances will be very nearly equal if the angles of incidence and reflection do not differ greatly. It may be noted that if the eye is focussed on a point P of the film (Fig. 103) the paths of the two disturbances may be different from that shown in Fig. 101, but the change of the calculated path difference will be negligible if the film is of the order of thinness which causes the interference colours to appear. In Fig. 103, the path of one disturbance is distinguished by a dotted line.

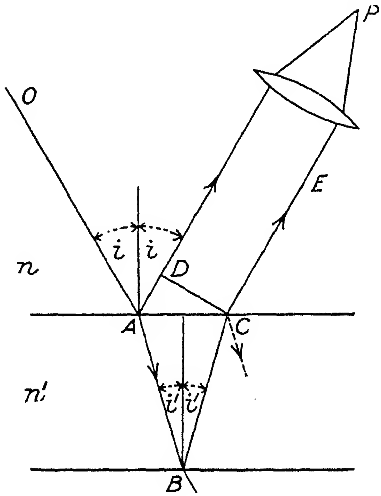

FIG. 101

The conditions for "destructive" interference might, for example, be fulfilled for green light $\lambda = \cdot 555\mu$, say. Neighbouring wavelengths would be subject to more or less reduction of intensity, but the red, $\lambda = \cdot 65\mu$, and the violet, $\lambda = \cdot 45\mu$, would be clearly much less reduced. The reflected light would therefore exhibit a purple coloration owing to the excess of red and violet.

When the thin film interferences are formed in the space near the contact of a plane and a spherical surface, the appearances have a circular symmetry. They were, as previously mentioned, described by Newton.

Let x be the radius of a circular zone, concentric with the point of contact of two spherical surfaces, Fig. 104. The spherometer formula for the sagitta "a" of the surface of radius r is

$$a^2 - 2ra + x^2 = 0$$

from which $a = r - (r^2 - x^2)^{\frac{1}{2}}$.

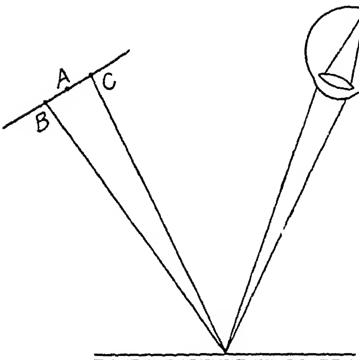

FIG. 102

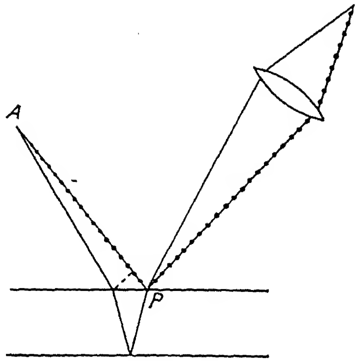

FIG. 103

Developing by the binomial theorem—

$$= \frac{x^2}{2r} + \frac{x^4}{8r^3} + \text{etc.}$$

The region in which interferences are observed will often be very close to the point of contact, where x is small in comparison with r. The second term $\frac{x^4}{8r^3}$ and higher terms can then be neglected.

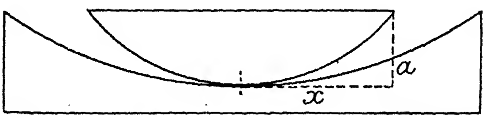

FIG. 104

The separation of two surfaces can therefore be written

$$S = \frac{x^2}{2}\left(\frac{1}{r_1} - \frac{1}{r_2}\right)$$

In the case where light suffers double reflection under practically normal incidence, as will usually be the case when Newton's rings are observed, the retardation in the air film will be

$$2S = x^2\left(\frac{1}{r_1} - \frac{1}{r_2}\right)$$

which will be equal to o, λ, 2λ, etc. for the centre dark spot and successive dark rings.

In measuring the radius of a shallow convex curve by Newton's rings method, the contact between the curve and a flat glass surface is illuminated with the aid of a " vertical illuminator " plate in the measuring microscope. The microscope is focussed on the ring system and the diameter of the first and any other convenient ring measured. Mercury green light is the best illuminant. Let x_1 be the radius of the first ring and x_{21} that of the 21st ring, then

$$r = \frac{x_{21}^2 - \cdot}{20\lambda}$$

(*N.B.* For mercury green line = ·0005461 mm.)

Colours of the Rings. When the interferences are observed with white light, colours appear in the rings, of which only a few are visible. The optical path differences in the film increase more rapidly for the shorter wavelengths which are the soonest restored, and the soonest again extinguished if we think of zones of increasing radius. The order of appearance of the colours is given in a table by Quincke (page 211).

Polarization. The early beginnings of the wave-theory of light were developed with the idea that the displacements or vibrations in the medium were performed in the direction of propagation, in a manner analogous to the case of sound waves in air. The explanation of the phenomena of polarization and double refraction, some of which are dealt with below, can only be given satisfactorily under the assumption that the displacements, whatever their nature, are transverse, or perpendicular to the direction of propagation.

For the systematic and theoretical discussion of this subject, reference must be made to works on physical optics. The present account will be confined to a recapitulation of the main facts of importance in applied optics.

The vibrations in ordinary unpolarized light take place in all directions perpendicular to the direction of propagation. Figs. 105A and 105B suggest the vibration directions in (*a*) ordinary unpolarized light, (*b*) plane polarized light, the direction of propagation being perpendicular to the plane of the paper. In the case of ordinary light the intensity of the components is constant for all directions of vibration, but in " plane polarized " light all the displacements are parallel to one direction.

The simplest way of producing plane polarized light is by oblique reflection at a plane surface of a refracting medium such as glass or water. The angle of incidence has to bear a certain relation to

the refractive index of the medium, which follows from the general equations governing the reflection coefficients of polarized light at a plane reflecting surface.

Imagine a "parallel" beam of polarized light to be incident at an angle i on a plane reflecting surface, and let the angle of refraction be i'. The refractive indices above and below the surface are unity and n' respectively. Let it be supposed that the vibrations of the light take place at right angles to the plane containing any ray and the normal to the surface.*

The development of the electro-magnetic theory has taught us that the "'vibration direction" just mentioned may be regarded as that of the electric forces in the wave-front. (The electric forces

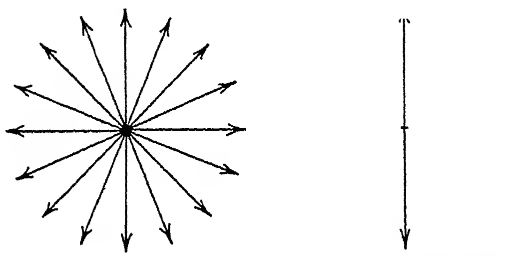

FIG. 105

are accompanied by corresponding magnetic forces perpendicular both to the electric forces and to the direction of propagation, but these need not be considered in the simple account to be introduced here.)

Then, for light polarized in the above sense, the ratio of the amplitude A_1 in the incident light to the amplitude of the reflected light A_1' is given by

$$A_1' = -A_1 \frac{\sin (i - i')}{\sin (i + i')}$$

The corresponding equation for the *intensity* of the reflected light I_1', as compared with the incident, is

$$I_1' = I_1 \frac{\sin^2 (i - i')}{\sin^2 (i + i')}$$

* The light is then said to be polarized in the " plane of incidence," a rather unfortunate convention. The " plane of polarization " was originally defined as the particular plane of incidence in which the polarized light suffers maximum reflection, so the convention was established before the development of the electro-magnetic theory.

When the light is so polarized that its vibration directions are in the plane of incidence containing a ray and the normal, then the formulae are

$$A_2' = A_2 \frac{\tan (i - i')}{\tan (i + i')} \qquad I_2' = I_2 \frac{\tan^2 (i - i')}{\tan^2 (i + i')}$$

When ordinary light is reflected, it is regarded as containing components which are not polarized in either of the above ways, but we may regard any arbitrary displacement OA, Fig. 106, as being the resultant of two displacements OB and OC in directions at right angles. An argument of this kind leads to the assumption that the incident unpolarized light can be regarded as the resultant of two sets of components of equal total intensity, polarized in mutually perpendicular directions, and exhibiting all possible variations of relative phase. This will be more fully understood when circular and elliptical polarization has been explained. Hence, the total intensity of the reflected energy is

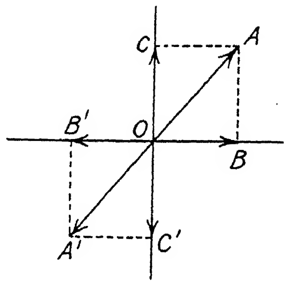

FIG. 106

$$I_1' + I_2' = I \left\{ \frac{\sin^2 (i - i')}{\sin^2 (i + i')} + \frac{\tan^2 (i - i')}{\tan^2 (i + i')} \right\}$$

where the two terms in the right-hand side represent the intensities of the components.

A closer examination of the above formulae for the case when $n' > 1$ will show that with increasing values of i, the value of I_1' steadily increases up to a value of I_1 when $i = 90°$, since whatever the value of i' (less than 90°),

$$\sin (90° - i') = \sin (90° + i')$$

and hence the factor of I_1 is unity.

We also see that $\dfrac{\tan^2 (i - i')}{\tan^2 (i + i')}$ will be unity when $i = 90°$, but the value of I_2' does not regularly increase with increasing angles of incidence owing to the rapid increase of the denominator, which passes through an infinite value when $(i + i') = 90°$.

Since in this case $\sin i = n' \sin i'$

$$= n' \sin (90° - i)$$

$$= n' \cos i$$

we see that the second term in the equation for the total intensity is zero when tan $i = n'$. In this case we have plane polarized light only reflected, in which the vibrations are perpendicular to the plane of incidence. This is applied in the simple reflecting polariscope. For ordinary glass, $i = 57°$ approx. (See page 207.)

For perpendicular incidence the reflection factor is independent

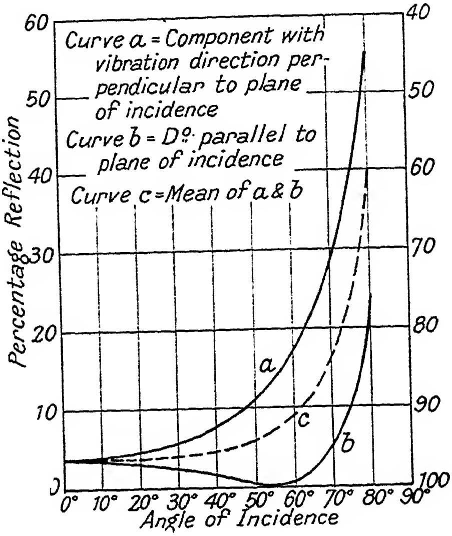

FIG. 107. REFLECTION FROM SURFACE OF GLASS

of the plane of polarization of the light and therefore holds for unpolarized light also. It is

$$I_R = I \frac{(n' - 1)^2}{(n' + 1)^2}$$

Fig. 107 shows the variation of intensity of the two components of the reflected light for glass of refractive index 1·5, the curve drawn as a dotted line indicating the mean of the two. There is a relative phase change of $\frac{\pi}{2}$ for the vibrations parallel to the plane of incidence (lower full-line curve in Fig. 103) on passing through the angle for zero intensity.

Fig. 108 shows, in the same way, the variation of intensity of the two polarized components in the case of silver and steel. The figure

is from results given by von Rohr. There is evidently no possibility of producing plane polarized light by reflection from such surfaces.

Double Refraction. In 1669 Erasmus Bartholinus discovered that near objects seen through a crystal of Iceland spar or calcite appear doubled. The doubling is not noticeable when a very distant object is so viewed;* the *actual* separation of the two images is constant and is therefore not observable when they are at a great distance.

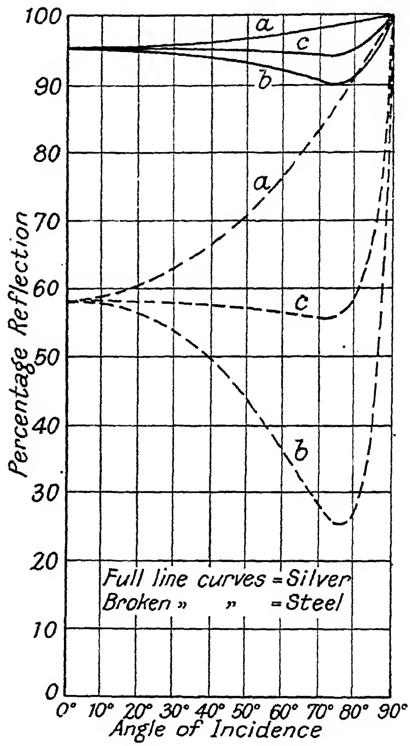

FIG. 108. REFLECTION FROM SILVER AND STEEL

A rhomb of calcite is shown in Fig. 109. The three edges OA, OB, OC make equal angles with each other in the sense that $\widehat{AOB} = \widehat{BOC} = \widehat{COA}$. We can imagine a line entering the rhomb symmetrically through O so that it makes equal angles with the three edges; this line gives the direction of the "optic axis."

If the rhomb of spar is put down on a card pierced by a small hole, the two images formed by "double refraction" are seen to be so situated that the line joining them is apparently parallel to this "optic axis," no matter how the rhomb is placed on the card. If the rhomb is rotated about the direction of view, one image remains stationary while the other moves round it so as to fulfil the above condition. Experiment with a piece of spar soon shows that the double refraction of the light must be in the sense indicated in Fig. 110. One image appears in the original direction, the other displaced with respect to the crystal as indicated, so that the light has suffered a deviation away from the normal in passing through

* Several textbooks of light fall into the error of stating that a distant object appears doubled, but this cannot be the case if a natural rhomb with parallel bounding faces is used for the observation.

the crystal. Since the *actual* separation of the images appears constant, no matter what the distance of the object, it is inferred that the two parts into which the original ray is divided become parallel on emergence.

Interesting experiments may be carried out by supporting a piece of black glass above the rhomb and observing the light, after it has been reflected from the glass at the polarizing angle, for various positions of the calcite. In this way it is not difficult to show that the light from the two images is plane polarized in

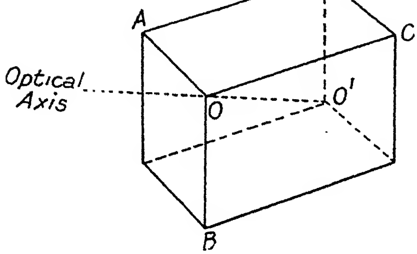

FIG. 109. RHOMB OF CALCITE

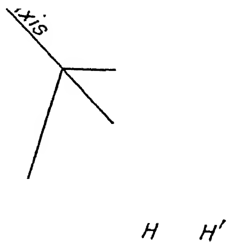

FIG. 110

perpendicular directions. That from the stationary image (called the *ordinary* image) is " polarized in the plane which passes through the two images," which means that the electric forces in the wave-front are perpendicular to that plane, while the light from the rotating image called the *extraordinary* image is polarized in the direction perpendicular to the first.

By cutting and polishing faces perpendicular to the axis of a rhomb of calcite it may be shown that double refraction of this kind does not take place when the light traverses the crystal in the direction of the axis.

Types of Crystals. Through the experiments of Laue, Friedrich, Knipping, and others, carried out since 1911, it has been established that (as was indeed previously suspected) the external form of crystals is a consequence of their atomic structure. This is a regular arrangement of the atoms, in three dimensions, known as a space-lattice. The ordinary molecules lose their identities, the constituent atoms all filling definite places in a continuous arrangement which is an indefinite repetition of a fundamental elementary structure, such as is illustrated in Fig. 111, which represents potassium chloride.

The black dots are the chlorine atoms and the white are the potassium.

It will be realized that there are various planes which are relatively rich in atoms; these represent the possible crystal faces and cleavage planes. The regular structure is capable of producing diffraction effects in X-rays, which are radiations analogous to light but of much shorter wavelength. Just as the number of lines in a diffraction grating can be calculated from the angle of diffraction of light, so the relative spacing of the atoms in a crystal are inferred from the X-ray spectra.

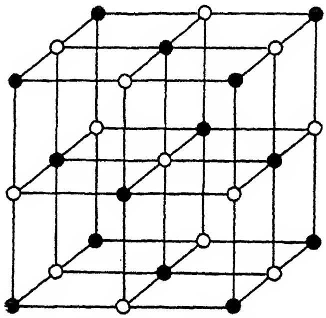

Potassium Chloride
K=O Cl=●
FIG. 111

The classes of crystals are usually defined in relation to the " crystallographic axes " which are to some extent a matter of geometrical convention, but which are most easily employed to express the symmetry and arrangement of the crystal faces if the selected axes are parallel to the edges of the ultimate " cells," of which the structure is composed. Of the seven main classifications of crystals, there are six in which the unit cells are parallelopipeds with various relative lengths of edges and various angles between the edges.

The relative lengths of the edges are determined by important parameters which govern the inclinations of the faces of the crystal. The " law of rational intercepts " due to Haüy, states that any face of a crystal makes intercepts on the axes which may be expressed as rational multiples of the parameters.

Thus, in the table given below, in which the relations of the main

Angles between Edges of Unit Cell	Relative Lengths of Edges of Unit Cell	Classification (Crystallographic)	Optical Classification
Three edges at right angles	$\imath = b =$	Cubic	Not doubly refracting.
	$\imath = b$	Tetragonal	D.R. Uniaxial.
.. .. ..	$\imath \quad b$	Orthorhombic	Biaxial.
Two ,, ,, ,,	$\imath \quad b$	Monoclinic	Biaxial.
None of edges at right angles	$\imath \quad b$	Triclinic	Biaxial.
	$\imath = b =$	Rhombic*	Uniaxial.
		Hexagonal*	Uniaxial.

* The rhombic system may be looked upon as a group of the hexagonal type from the crystallographic standpoint, but the rhombic unit parallelopiped is such that the angles between the edges at two opposite corners are equal. In the hexagonal system there is no unit parallelopiped.

classifications are set out, the axes for the cubic system may be imagined parallel to the ordinary axes of Cartesian co-ordinates. Since the parameters, a, b, and c are equal, we may expect faces with equal intercepts on all three axes. Other faces may have unit

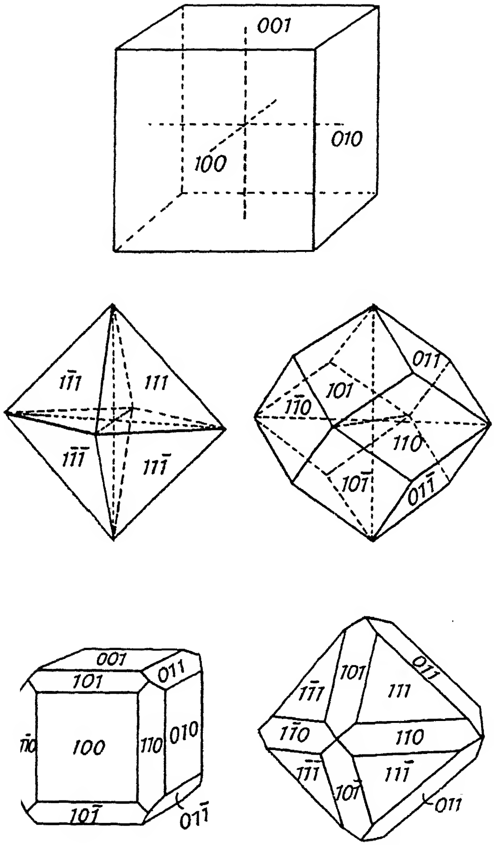

FIG. 112. CRYSTAL FORMS OF THE CUBIC SYSTEM

(a) Cube (fluor-spar, rock salt)
(b) Octahedron (magnetite, spinel)
(c) Rhombdodecahedron (garnet)
(d) Faces characteristic of cube and rhombdodecahedron appearing in the same crystal as in fluor-spar
(e) Rhomdodecahedral and octahedral faces appearing as in magnetite

distance of intercept for one axis and infinite distances for the other two, and so on. These various faces may be developed together in one crystal, as shown in Fig. 112. In the table, D.R. stands for "doubly refracting."

In other cases than the cubic, the parameters may be unequal.

Thus, gypsum is a monoclinic crystal in which $a : b : c = 0{\cdot}690 : 1 : 0{\cdot}42$. In all types of crystals there may arise faces in which the intercepts are of the type pa, qb, rc, where p, q, and r may be simple integers of low value or may be infinite. Thus we might have a face $1a$, $2b$, ∞c. In the Millerian system the indices are proportional to the *reciprocals of the intercepts*. If the intercepts are $1a$, $2b$, ∞c, the Millerian indices would be (2, 1, 0). We may form the reciprocals and multiply the numbers by the least common denominator. Thus ($2a$, $3b$, $4c$) becomes (6, 4, 3,), which is usually written (6 4 3) without parameters or commas between the numbers. If an intercept is on the negative prolongation of an axis through the

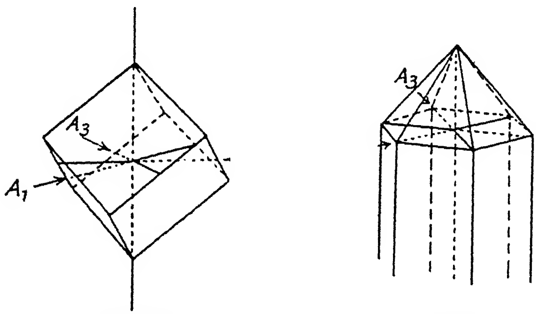

FIG. 113

origin, the intercept figure is distinguished by a bar over the figure, thus: $\bar{3}$.

Theory of Double Refraction. Calcite or Iceland spar and quartz, or rock-crystal can be referred to the hexagonal type of crystallization in which there are three equal horizontal axes at 120° apart and one vertical axis for which the parameter is different. Fig. 113 shows the position of axes 1, 2, and 3 for a cleavage rhombohedron of calcite, and a quartz crystal with prism and pyramid faces. It will be understood that the direction of the vertical axis is a unique direction in a particular sense; it is the optic axis of the crystal. Thus the term " uniaxial " applies to this unique direction and has no reference to the usual crystallographic axes, which are four in number.

If a disturbance travels outwards from a centre in an isotropic medium (in which the optical properties in all directions are uniform) the wave-front takes the form of a sphere. Huygens found that in uniaxial crystals such as calcite, the wave-front travels outwards in two sheets; one is a sphere and the other an ellipsoid of revolution.

The axis of symmetry is the optic axis, and the two surfaces touch each other only in the two points on this axis. In Iceland spar the sphere lies within the ellipsoid; this is the characteristic of *negative* uniaxial crystals. In quartz the ellipsoid lies within the sphere, and this is characteristic of positive uniaxial crystals. Huygens' construction, applied to the problem of finding the two directions of refraction for a beam, explains the deviation of the extraordinary ray from the normal shown in Fig. 110, for suppose in Fig. 114 that the optic axis is in the plane of the diagram, and let parallel light

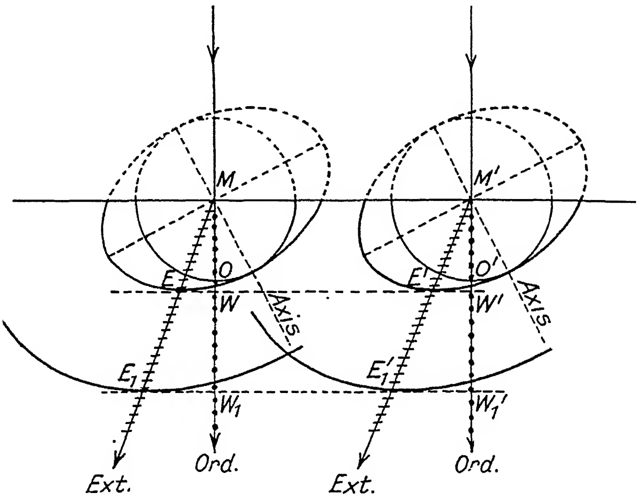

FIG. 114. ILLUSTRATING HUYGENS' CONSTRUCTION FOR THE EXTRAORDINARY WAVE-FRONT AND RAY DIRECTION

fall normally upon the surface of the crystal represented by the line MM′. The disturbances spread in two sheets from M and M′, two spheres and two ellipsoids. The envelope of the ellipsoidal wave-fronts in two positions will be the lines EE′ and E_1E_1'; the extra-ordinary wave-front for the refracted beam is seen to bear away to the left, while the ordinary beam will be undeviated. (The construction for the ordinary wave-front is not shown in the diagram.)

It will be seen that the velocity of the extraordinary wave-surface normal to itself as compared with the ray velocity is represented by the ratio of $\frac{WW_1}{EE_1}$ in the figure. *The velocity of the wave produced by the extraordinary ray is not generally the same as the " velocity of the ray " itself.* The " velocity of the ray " is proportional to the radius vector of the ellipsoid in the direction of the ray.

The *vibration directions* are indicated in the figure. A *principal section* of a uniaxial crystal is one which is parallel to the optic axis, and in the extraordinary ray the vibrations take place in the principal section containing the ray and the axis; in the ordinary ray they are at right angles to this.

The method of construction for various conditions will be understood from the above example, but it may be pointed out that if the optic axis does not lie in the plane of the diagram, the extraordinary ray will in general be deviated above or below the diagram. When the light is normally incident, no change of direction will take place for the extraordinary ray if the optic axis is parallel or perpendicular to the refracting surface. The velocity of propagation

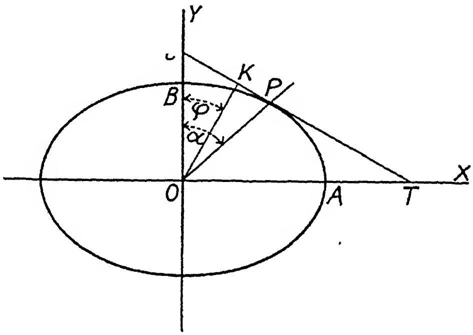

FIG. 115

for the ordinary and extraordinary rays and wave-fronts is identical only in the direction of the axis.

Ray- and Wave-Velocities. In Fig. 115, let the ellipse represent any principal section of the ellipsoid of extraordinary ray-velocity. The semi-axis OA $= a$ represents the maximum ray-velocity, and OB $= b$ represents the minimum ray-velocity in the extraordinary wave-front. The vector OP represents the ray-velocity for some intermediate direction, making an angle α with the Y-axis. The tangent at this point P represents the wave-front (see Fig. 114). The normal OK represents the wave-velocity on the same scale.

The equation to the ellipse is

$$\frac{x^2}{a^2} + \frac{y^2}{b^2} = 1$$

If P is the point (x', y'), while OP $= r$,

$$\sin \alpha = \frac{x'}{r}, \cos \alpha = \frac{y'}{r}$$

and, since x' and y' are on the ellipse,

$$\frac{r^2 \sin^2 \alpha}{a^2} + \frac{r^2 \cos^2 \alpha}{b^2} = 1$$

whence
$$r^2 = \frac{a^2 b^2}{b^2 \sin^2 \alpha + a^2 \cos^2 \alpha} \quad . \quad (55)$$

Again, the tangent at (x', y') is

$$\frac{xx'}{a^2} + \frac{yy'}{b^2} = 1$$

and the intercept on the axes of X and Y are respectively—

$$\mathrm{OT} = \frac{a^2}{x'} \qquad \mathrm{O}t = \frac{b^2}{y'}$$

Let $w = \mathrm{OK}$, then

$$w = \mathrm{O}t \cos \phi = \mathrm{OT} \sin \phi, \text{ where } \widehat{\mathrm{BOK}} = \phi$$

$$w = \frac{b^2}{y'} \cos \phi = \frac{a^2}{x'} \sin \phi.$$

Then, since x' and y' are on the ellipse

$$\left(\frac{a^2 \sin \phi}{w}\right)^2 \frac{1}{a^2} + \left(\frac{b^2 \cos \phi}{w}\right)^2 \frac{1}{b^2} = 1$$

giving
$$w^2 = a^2 \sin^2 \phi + b^2 \cos^2 \phi \quad . \quad . \quad . \quad (56)$$

In order to obtain the relation between α and ϕ, note that

$$\tan \alpha = \frac{x'}{y'} = \frac{a^2 \sin \phi}{b^2 \cos \phi} = \frac{a^2}{b^2} \tan \phi \quad . \quad . \quad (57)$$

Refractive Indices. The maximum and minimum wave-velocities a and b are related to the corresponding "refractive indices" n_a, n_b by the relation

$$a n_a = b n_b = w n = \text{constant } (k, \text{ say})$$

Hence, the above formulae can easily be expressed in terms of the refractive indices if required. Thus (56) becomes

$$n^2 = \frac{n_a^2 \; n_b^2}{n_b^2 \sin^2 \phi + n_a^2 \cos^2 \phi}$$

and (57) becomes

$$\tan \alpha = \frac{n_b^2}{n_a^2} \tan \phi.$$

In the case of negative uniaxial crystals in which the ray-velocity ellipsoid is outside the sphere, the value of n_b coincides with that for the ordinary refractive index; a is greater than b. Hence the ordinary refractive index is the greater.

In quartz, on the other hand, the ellipsoid is within the sphere, and the value of n_a (the lesser) is coincident with the ordinary refractive index.

The conception of the refractive indices of the extraordinary waves is useful in crystal optics because they enable a convenient calculation of the " optical path " to be made for particular directions of transmission in the crystal. *They cannot, of course, be used*

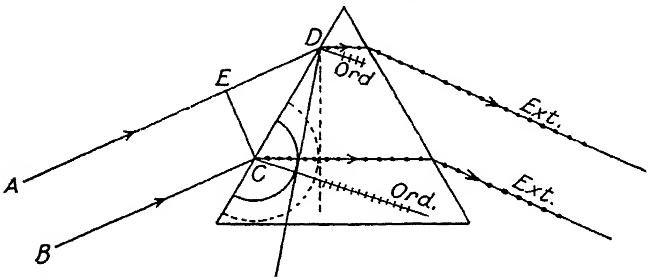

FIG. 116. DETERMINATION OF THE EXTRAORDINARY REFRACTIVE INDEX

The optic axis of the crystal is perpendicular to the diagram. Note the broken semicircle and the full-line semicircle which represent Huygens' construction for the extraordinary and ordinary wave-fronts respectively. The deviation of the ordinary ray is a little exaggerated for clearness of the diagram

in general for the calculation of the directions of the extraordinary ray by the application of the simple law of refraction.

The determination of the refractive index for the ordinary ray can be carried out on a spectrometer with a 60° prism cut in any way from a uniaxial crystal, but in order to measure the extraordinary index on the spectrometer by ordinary methods it is necessary to obtain a prism cut with its refracting edge parallel to the crystal axis, or alternatively to have the axis perpendicular to the refracting edge and bisecting the angle between the prism faces.

The condition obtained in the first case is shown in Fig. 116. Applying Huygens' construction to the case in question (shown in the figure in a section perpendicular to the refracting edge and thus also perpendicular to the crystal axis), the wave-fronts spread out in the two sheets, both having circular sections in the plan. The radius of the extraordinary wave-front section must be taken as $\frac{\text{ED}}{n_e}$ where n_e is the extraordinary refractive index. It is clear that

in this case the ordinary law of refraction is obeyed. Hence, the refractive index is calculable from the usual formula

$$n_e = \frac{\sin \frac{A + D}{2}}{\sin \frac{A}{2}}$$

where A is the angle of the prism and D is the minimum angular deviation of the beam.

With the axis in these directions there is evidently a maximum difference between the directions of the ordinary and extraordinary

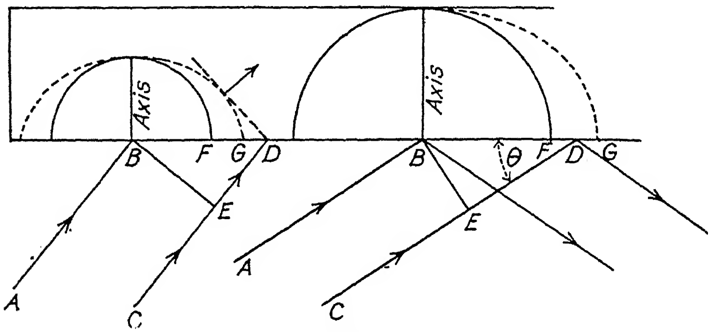

FIG. 117

wave-fronts. The difference is a minimum when the direction of transmission in a prism can take the direction of the axis; if the latter is perpendicular to the refracting edge of the prism and parallel to the base of the equilateral section, the minimum deviation condition will correspond to transmission in the axial direction. For the recognition of the ordinary and extraordinary beams, see below.

Another very convenient method of determining the refractive index of a crystal block is by the total reflection method. Imagine a crystal block cut with its face perpendicular to the axis, and let a parallel beam from an isotropic medium pass into the crystal as indicated in Fig. 117. Let the refractive index of the first medium be n, and let the ordinary and extraordinary indices of the block be n_o and n_e respectively.

Two parallel entrant rays AB and CD meet the surface in B and D respectively. Dropping a perpendicular BE from B to CD, we know that the time taken for the disturbance to travel from E to D is proportional to $n \cdot ED$. During this period the disturbances

originating from B spread out in two sheets, and reach the points F and G in the surface where

$$n \,.\, \mathrm{ED} = n_o\mathrm{BF} = n_e\mathrm{BG}.$$

When F or G pass beyond the point D there can be no refracted ray, but all the energy is totally reflected. With varying angles of incidence there is, in fact, a sudden increase in the reflected energy

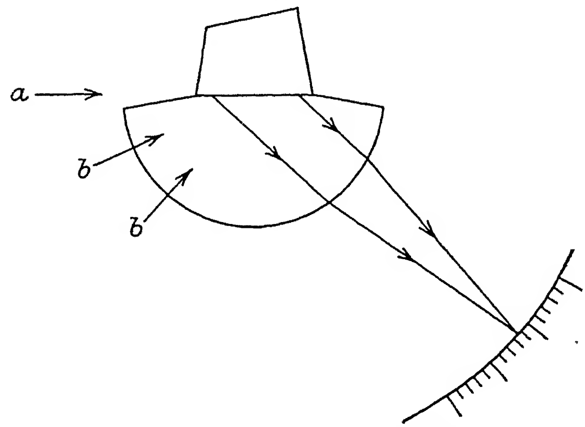

FIG. 118. PRINCIPLE OF CRYSTAL REFRACTOMETER

at the "critical angle," for either the ordinary or extraordinary beam. Suppose G coincides with D, then

$$n_e\mathrm{BD} = n\mathrm{ED}$$

$$\frac{n_e}{n} = \cos \widehat{\mathrm{BDE}} = \sin \phi$$

where ϕ is the angle of incidence.

Alternatively, if a beam be sent along the bounding surface in the crystal block at grazing incidence, no light can emerge into the lower medium except at angles greater than at the critical angle. The equation just quoted shows that n must be greater than n_e in order that ϕ may have a real value in the case considered.

These phenomena lend themselves to the determination of refractive indices by the crystal refractometer, or total reflectometer (Fig. 118), which, in some instruments, employs a hemispherical block of dense glass with a plane face on the top. The crystal specimen is placed in position with a film of liquid between the crystal and top face; the liquid must have a higher refractive index than the crystal in order to save total reflection (at the glass-liquid

face) occurring at angles of incidence smaller than that for the effective critical angle for the crystal; the angle so determined is that which would be found if the glass and crystal were in actual optical contact.

If light (*a*, Fig. 118) can be sent into the crystal so that it is incident at grazing incidence on the bounding surface, the hemispherical surface of the block will produce an image surface in which the direction of the critical angle is registered by a boundary on one side of which all the refracted light is concentrated. If this method is not practicable, the contact face is illuminated diffusely by light (*bb*). The boundary then shows up as a border of contrast of intensity between the partially and totally reflected light.

Provided that the optic axis is perpendicular to the bounding face as shown in Fig. 117, there will be a maximum difference between the critical angles for the extraordinary and ordinary beams. The angle is decreased if the axis has another direction. It is always possible to rotate the block on the hemisphere (or rotate the two together in the instrument) until the crystal axis lies in a plane perpendicular to the plane of incidence. As this is done, the difference of the angles reaches a maximum, and the ordinary and extraordinary indices may again be measured.

Direction of Vibrations. The distinction between the ordinary and extraordinary waves is rendered easy by the recognition of the direction of vibration of the plane polarized light which they give. In Fig. 114 we see that the extraordinary ray's vibration direction is in the plane containing the ray and optical axis, while the ordinary ray vibrates in the direction perpendicular to the ray and the axis. Prof. Cheshire has likened the uniaxial crystal to wood containing a "grain." The elasticity of the medium differs in the grain direction from that found perpendicular thereto; and this would result in a difference of velocities of mechanical wave-motions involving displacements in these respective directions.

The extraordinary ray vibrates in a plane containing the "grain," the ordinary ray *across* the grain. In the axis direction any light propagated must vibrate across the grain; only one velocity is possible. Light propagated perpendicular to the axis, however, may vibrate either across the grain or in a plane containing the grain direction; hence the two velocities for light polarized in these ways.

Polarizing Prisms. Owing to the comparatively wide angular separations of the ordinary and extraordinary rays in calcite, it is possible to remove one of them by total reflection while transmitting the other.

The basis of the Nicol prism is a rhombohedron of calcite about three times as long as it is broad. The Fig. 119 represents a section through the shorter diagonals of the end faces. It is slit diagonally, perpendicular to this section, so that the cut makes an angle of about 22° with the edge AB. The natural angles ADC and ABC are about 70° 53′; it is usual to grind the end faces down until the angles are 68° and they are thus at right angles to the plane of the slit. The new faces are polished and the two separated parts are cemented with Canada balsam.

On entering the prism, a ray splits up into the ordinary and extraordinary rays. With increasing angles of incidence on the interior cemented face, we pass from the condition when both rays

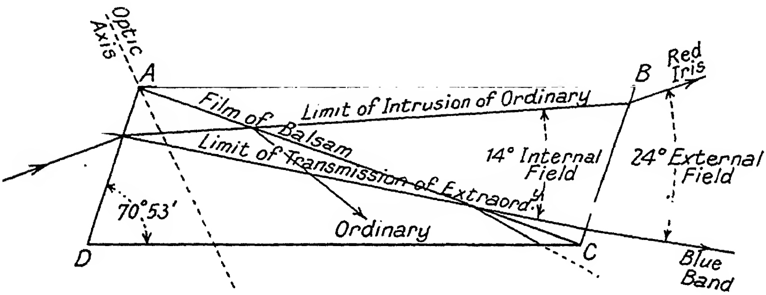

FIG. 119. THE NICOL PRISM

are transmitted to that when the ordinary ray is incident at 67° 53′, and thereafter is totally reflected. The extraordinary ray is still transmitted until its angle of incidence increases to 82° 32′. The external field or angular range for the resulting plane polarized light is 24°.

Different cements may be employed. Canada balsam, balsam of copaiba, linseed oil, and poppy oil are used in various polarizing prisms, and are of assistance in securing the best conditions by choosing a cement of suitable refractive index.

The field of plane polarized light in the untrimmed Nicol as described above is not symmetrical about the direction of the central line parallel to the long edges. The field is limited on one side by a blue band[1] with darkness beyond it, and on the other side by a system of fine coloured fringes beyond which the two beams are transmitted and the light is not polarized; the angular directions of the blue band and the fringes are at about 11° and 3° respectively on each side of the directions parallel to the edge, increased to about 14° and 10° externally. The trimming of the end faces to 68° improves

the symmetry. Many efforts have been made to produce prisms with more symmetrical fields; it is in this connection that the use of various liquids is important. The table below gives some useful indices—

	Refractive Indices			Critical Angle
$\lambda(\mu) =$	0·6708	0·5893	0·3962	(0·5893)
Iceland spar (ordinary ray)	1·6537	1·6586	1·6833	37° 2′ (Spar-air)
,, ,, (extraordinary ray)	1·4842	1·4864	1·4978	42° 16′ ,,
Canada balsam	1·523	1·526	1·553	67° 53′ Spar-medium (ord.)
Linseed oil		1·485		63° 36′ ,, ,,
Poppy oil		1·463		62° 28′ ,, ,,
Balsam of Copaiba		1·549		74° 34′ ,, ,,

The extraordinary refractive indices given in the table above are naturally the minimum values. The actual value of the refractive index and, therefore, the critical angles effective with various media for the extraordinary ray, varies with the direction of transmission with respect to the optic axis. The values can, if required, be calculated from the formulae given above.

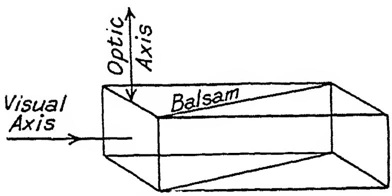

FIG. 120. GLAN-THOMPSON PRISM

There are certain objections to the sloping end faces of the Nicol prism. They diminish the light by reflection and give a lateral displacement to the image of the object unless parallel light is transmitted; there is also some tendency to produce slight "elliptical polarization" of the transmitted light. Hence, in many cases the ends of the "Nicol" are trimmed to be at right angles to the long edges of the prism if the resulting asymmetry of the field can be tolerated.

The Glan-Thompson Prism. This prism is illustrated in Fig. 120, and it will be seen that the end faces are parallel to the optic axis. In one type, the angular breadth of the field for plane polarized light is 41° 50′; the angle between the film and end face is 76° 5′, and the ratio of length to breadth of the prism is 4·16. Linseed oil is used for the cement, with which the extraordinary ray is not totally reflected at any angle of incidence on the film.

The Foucault Prism and Others. Prisms containing a cement such as Canada balsam, do not transmit the ultra-violet. In case a prism is wanted for purposes of ultra-violet polarimetry, the Foucault type, which has a film of air, is employed. The modification due to Hoffman is illustrated in Fig. 121, the air film is at 50° with the axis of vision and the angular field is between 7° and 8° only.

There are a number of other prisms of some interest which are occasionally encountered. Ahren's prism in three parts, and Feussner's prism are perhaps of greatest interest. In the latter the film of doubly refracting material is cemented between two wedges of glass. According to Thompson, "The glass and cement ought to have an index of refraction equal to that of the higher of the two indices of the crystal, and the optic axis of the slice ought to be perpendicular to the planes of its faces."

The Lippich prism will be mentioned in the section on

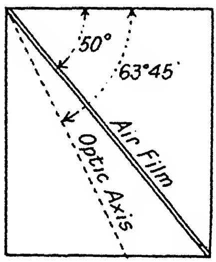

FIG. 121. HOFFMAN'S PRISM

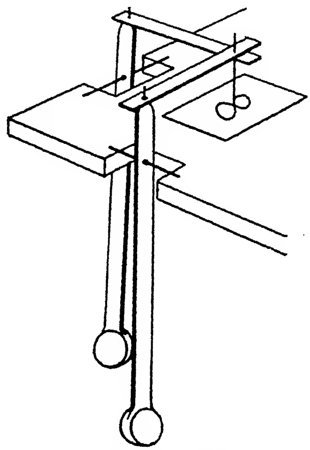

FIG. 122. THE HARMONOGRAPH

"Polarimetry." Papers by S. P. Thompson [2] and W. Grosse [3] may be consulted for comparative details on polarizing prisms.

Circular and Elliptical Polarization. The result of the combination of two simple harmonic vibrations is easily and beautifully illustrated by the harmonograph, Fig. 122, in which two pendulums communicate two mutually perpendicular vibrations to a point which marks out on paper, or on a smoked plate, the figure resulting from the two movements. A short time spent with such a fascinating toy will teach far more than can be gathered from description, but even in imagination some of the results may easily be conceived.

In Fig. 123, BB′ marks the path imparted to the pointer by one pendulum, AA′ the other. If both are acting so that the central point of each path would be simultaneously reached on the journey through O to A and B respectively, the result of the joint movement is a journey to C. Thus, if the periodic time is the same in each movement, CC′ represents the new path.

Again, if the movement in the path AA′ has brought the marker to its right-hand extreme position while the perpendicular movement is passing through its central or zero position towards B, the joint result will be an anti-clockwise circular movement. Change the phase of the BB′ vibration by 180°, so that the movement through O is towards B′, while the A movement is as before, and it will be clear that a clockwise motion results. The conditions under which we can obtain a linear vibration perpendicular to CC′ will also be easily understood.

If the amplitudes are unequal, the vibrations (when the phases

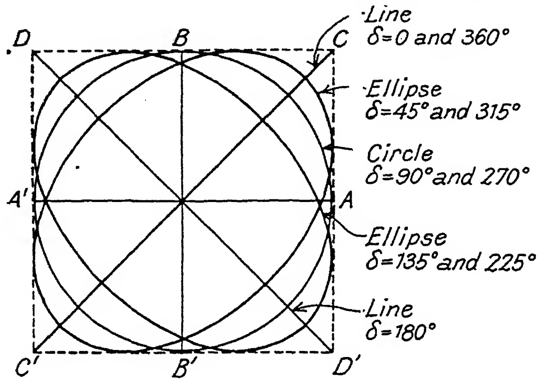

FIG. 123

have the same relations as in the cases above), will either be along straight lines at different angles, or will be elliptical.

With equal amplitudes, the vibration figure will in general be an ellipse. Particular cases of a straight line will, however, occur if the phase difference δ is 0° or 180°; and a circle if δ is 90° or 270°. A relative change of phase of 180° will mean a change of the direction of vibration such as from CC′ to DD′.

If, now, the relative phase of the components is varying, the figure will vary also; with the harmonograph the effect is obtained by making the lengths of the two pendulums differ slightly; the continuous change through linear, elliptical, and circular modes is beautifully represented.

So we may imagine the case with light under certain conditions. Let a ray enter a block of a uniaxial crystal so that the direction of transmission within the block is perpendicular to the axis. Let the incident light be plane polarized, and let the amplitude and vibration direction be represented by the vector OC shown in perspective in Fig. 124. On entering the crystal the vibration may be regarded

as resolved into two components OA and OB, so polarized that OB is parallel and OA perpendicular to the axis. Though there may be no " double refraction " in the sense of a difference of direction, since the components travel along the same line, there will be a difference of velocity and hence a relative change of phase.

Let t be the thickness of the crystal traversed, then the optical path difference p for the ordinary component OA and the extraordinary component OB will be given by

$$p = t(n_o - n_e)$$

and the corresponding difference of phase will be

$$\delta = \frac{2\pi}{\lambda} t(n_o - n_e)$$

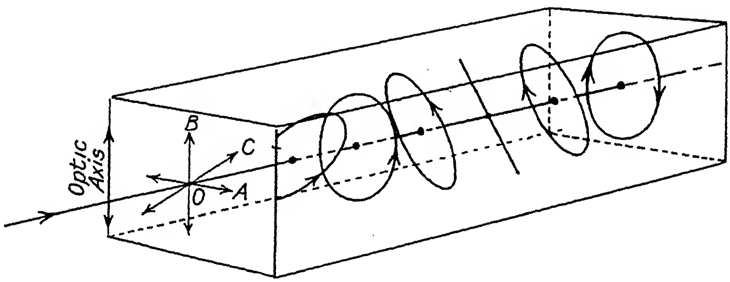

FIG. 124

Fig. 124 will illustrate how, according to the total thickness of the block, the light on emergence may have the distinctive properties of elliptical, circular, or plane polarization.

Fast and Slow Directions. It is usual to distinguish between the " fast " and " slow " vibration directions of a plate. The " fast " direction is naturally the direction of the vibrations which have the greatest velocity and the lowest refractive index; the " slow " direction is that of the vibrations with the lowest velocity and the highest index. Thus, in quartz the extraordinary refractive index is the higher, which means that the slow direction is that for the ray which vibrates " along the grain." The fast direction in quartz is perpendicular to the grain or optic axis.

In calcite the ordinary refractive index is the higher, and the fast direction is for the ray which vibrates " along the grain " or parallel to the axis.

The Simple Polariscope. The simplest form of polariscope is illustrated in Fig. 125. Diffused light from the sheet of opal glass is reflected at 57° (see page 190) from the glass plate. It is usual

to black the underside of the sheet to stop light which might get through the plate from below. Although light reflected from the lower surface should also be plane polarized, any strain or imperfections in the glass might induce elliptical polarization in the part of the light thus traversing the thickness of the plate.

The analyser may be any convenient form of Nicol, Glan-Thompson prism, or the like, held in a suitable mount. Naturally, the field

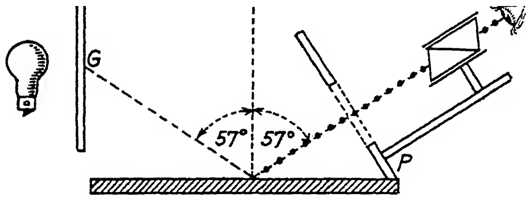

FIG. 125. SIMPLE POLARISCOPE (DIAGRAMMATIC)

becomes quite dark only in one particular portion as the analyser is rotated into the position for the extinction of light; this occurs when the short diagonal of the Nicol (if such is used) is in the plane of incidence. The vibrations of the polarized light are perpendicular to the plane of incidence while the prism transmits only those parallel to the short diagonal (i.e. the extraordinary ray in which the vibrations are in a plane containing the optic axis of the crystal).

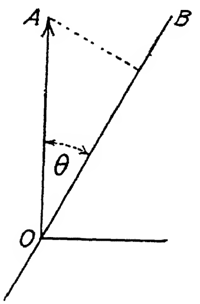

FIG. 126

In the general case let OA (Fig. 126) represent the amplitude and direction of the vibrations in the plane polarized light, and let OB represent the transmission direction of the analyser. The transmitted amplitude is equal to kOA cos θ where $\theta = \widehat{AOB}$, and k is a transmission factor for the prism. (There will be reflection and absorption losses.) The intensity of the transmitted light is proportional to $\cos^2 \theta$.

If two polarizing prisms are arranged to transmit the light in turn, they are said to be " crossed " when extinction is secured. Thus we speak of examination " between crossed Nicols," though this apparatus alone is not really a very practically useful form of polariscope.

Crystal Plates in Polarized Light. Consider a plate of a uniaxial crystal cut with its surface parallel to the axis, and let the thickness be such that the retardation between the components is $\frac{\lambda}{4}$, say. If

this is placed in plane polarized light so that the vibrations are parallel or perpendicular to the axis, they are transmitted without change from the plane polarized condition, but if the vibration direction (amplitude a) makes an angle θ with the crystal axis, the vibration is resolved into two parts of amplitudes—

$a \cos \theta$, parallel to the axis, and

$a \sin \theta$, perpendicular to the axis.

These emerge with a difference of path of $\frac{\lambda}{4}$ or a phase difference of 90°. This results in an elliptical vibration (in general), since the amplitudes in perpendicular directions are unequal except when $\theta = 45°$. A circular vibration then results.

If the plate is held in the polariscope for observation, the extremes of intensity of the light passing through the analyser as it rotates

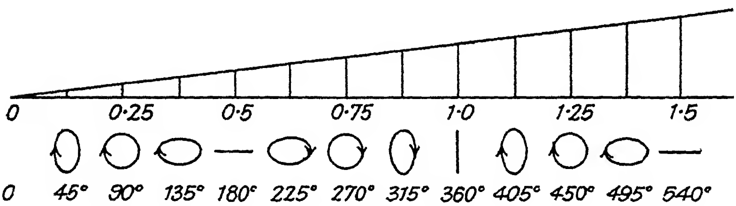

FIG. 127

will be proportional to $a^2 \cos^2 \theta$ and $a^2 \sin^2 \theta$, of which the ratio is $\cot^2 \theta$. The light never totally disappears when elliptical polarization is present, but varies between a maximum and minimum. When the polarization is circular, the intensity remains stationary as the analyser is rotated.

It was shown above that a $\frac{\lambda}{4}$ plate produces circular polarization when held in a plane polarized beam so that $\theta = 45°$ as above.

With a plate of greater thickness still, elliptical or linear polarization is obtained, and a wedge-shaped piece of crystal cut with its thin edge parallel to the axis and held in the polariscope so that the axis direction is at 45° to the vibration direction of the polarized light, will exhibit, along its length, all the varieties of polarization as suggested in Fig. 127.

Interference Colours. Such a wedge as described above, when viewed between crossed Nicols with monochromatic light,* shows a

* The optic axis in the wedge should be at 45° to the vibration direction of the polarized light, as specified in the previous paragraph.

regular variation of illumination, having maxima where the retardation is an odd number of half wavelengths and minima for retardations of integral numbers of whole wavelengths. The interval between successive maxima decreases, however, with decreasing wavelength, thus producing coloured fringes in the bands obtained with white light.

Let the retardation for violet be p_v wavelengths, then if t is the thickness of the plate and λ_v = the wavelength

$$p_v\lambda_v = t(n_o - n_e)_v,$$

while

$$p_r\lambda_r = t(n_o - n_e)_r$$

is the equation for red. Dividing, we obtain

$$\frac{p_v\lambda_v}{p_r\lambda_r} = \frac{(n_o - n_e)_v}{(n_o - n_e} = v \text{ (say)}$$

If the strength of the double refraction $(n_o - n_e)$ is equal for violet and red, the value of v is unity, and the relative retardation will be inversely proportional to the wave-lengths. The order of the interference colours then follows exactly as in Newton's rings or similar phenomena, but the colour succession is modified somewhat in other cases where v is not unity.

Passing from the "minimum" point of darkness in the wedge at zero retardation and zero thickness to places of greater retardation, the energy grows more rapidly in the shorter wavelengths than the longer. Bluish-grey tints are the first to appear; these are followed by yellow, orange, and red, etc., in accordance with the table quoted by Quincke.

It will be understood, therefore, that the *colour* is a valuable indication of the relative retardation.

Imagine now that a separate plate of the same material is held in front of the wedge between "crossed nicols." Let the plate, like the wedge, have its faces parallel to the axis, and let the axis direction in the two be brought into parallelism (" fast " on " fast "). Evidently the retardation of the plate is now added to that of the wedge. If white light is used the colour at any part of the wedge is now of a higher order.

Now let the plate be turned through 90° about the direction of the light. The ordinary ray in the wedge becomes the extraordinary ray in the plate, and vice versa; we have the condition of " fast on slow," relative retardation is reversed, the nett effect being now the difference of the two.

These effects are seen in the field of the polariscope by a shifting of the coloured bands in the field as the plate is introduced or

rotated. If the wedge is furnished with a scale the shift can be measured, and if the angle of the wedge is found, or calculated from a knowledge of the interval between the dark minima for some homogeneous light for which the extraordinary and ordinary refractive indices are known, the thickness of the plate can be measured. Alternatively, if the thickness of a plate of unknown material is measured, and the double refraction produced is estimated by the shift of the minima in the above manner, the result may be a valuable help in the identification of the substance. This is, in the barest outline, one of the most important of petrographic methods.

The chart of Michel-Levy[4] shows the colours characteristic of different thicknesses of crystal plates of varying bi-refringences, and

Colour Scale (adapted from Quincke's Table)

Retardation for "D" Line, $\lambda = 0{\cdot}589\mu$ (in microns)	Order (retardation in wavelengths)	Interference Colours between Crossed Nicols
0·00	0	Black
·04		Iron-grey
·097		Lavender-grey
·158	$\frac{1}{4}$	Greyish-blue
·218		Clearer grey
·234		Greenish-white
·259		White
·267		Yellowish-white
·281		Straw yellow
·306	$\frac{1}{2}$	Light yellow
·332		Bright yellow
·430		Brownish-yellow
·505	$\frac{3}{4}$	Reddish-orange
·536		Red
·551		Deep red
·565		Purple
·575		Violet (the "sensitive violet")
·589	1	Indigo
·728		Greenish-blue
·826		Light green
·850		Yellow-green
·910	$1\frac{1}{2}$	Yellow
·948		Orange
1·101		Violet-red
1·151		Indigo
1·334		Sea-green
1·426	$2\frac{1}{2}$	Greenish-yellow
1·495		Flesh colour
1·534		Carmine
1·652		Violet-grey
1·682		Greyish-blue
1·711		Dull sea-green
1·744	3	Bluish-green

is a useful adjunct in such work. By methods of this kind the minerals present in a rock section may be identified.

Babinet's Compensator. Two quartz wedges of equal angle (Fig. 128) may be cut so that the axis directions in the two may be parallel and perpendicular respectively to the thin end of the wedge. Together they constitute the equivalent of a plane parallel plate which produces no ultimate deviation in the direction of the light which is transmitted perpendicular to the plate. When polarized light is transmitted the ordinary ray in the first becomes the extraordinary in the second, and vice versa, so that if the thicknesses of the two parts traversed by the light are t_1 and t_2, the net relative retardation will be

$$(t_1 - t_2)\ (n_e - n_o)$$

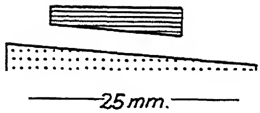

Fig. 128. Babinet Compensator

One wedge can be moved relatively to the other by means of a suitable micrometer screw, the scale and drum of which register the movement very accurately. The position of the central band of zero retardation, found where the wedges have equal thickness, and recognized from the symmetry of the interference colours, can be brought into coincidence with a fixed reference line. With the help of such an instrument the relative retardation produced by various crystal plates can be readily measured with accuracy by compensating the unknown retardation of the crystal with the measured retardation produced by the instrument.

In case the double refraction differs considerably for different wavelengths, separate measurements must be made with monochromatic light, as required.

Finding the Slow and Fast Directions. The two directions, parallel and perpendicular to the axis in a uniaxial crystal plate, in which the vibrations of plane polarized light are propagated without change are easily found by examining the plate in a polariscope. Remember that the " vibrations of the light " extinguished by a Nicol analyser are parallel to the longer diagonal of the rhomb end face. R. W. Wood*[5] describes two ingenious methods of finding which of the two directions corresponds to the greatest retardation in a " quarter-wave plate," i.e. one which produces a relative phase difference of 90° between ordinary and extraordinary vibrations and, consequently, circular polarization when held in the proper azimuth in plane polarized light. Once the fast and slow directions of such a

* It is probable that a number of alternative methods could be devised, such as putting the plate into the path of one of two interfering polarized beams and watching the shift of the fringes as the plate is rotated.

plate are known, i.e. the directions in which the refractive indices are smaller and larger respectively, the fast and slow directions of other plates can be found.

One other method of finding these directions is to use a petrological microscope with polarizer and analyser on a slide which contains some very thin and small quartz crystals, in which the fast direction is perpendicular to the long edges. A thin mica plate placed " fast on fast " over the slide will raise the order of the colour by a maximum amount; the plate is rotated until this occurs, when its fast direction is perpendicular to the long edges of the small crystals. The *exact* angular direction may be checked by examining

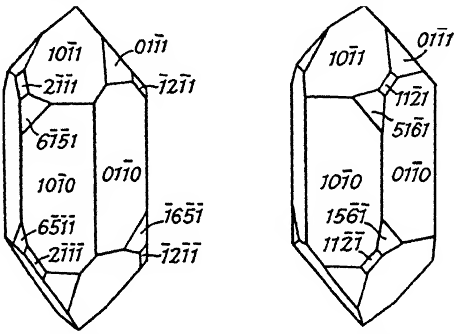

Left-handed Quartz *Right-handed Quartz*

FIG. 129

the same plate in an ordinary polariscope. Another test depending on the examination of the plate in convergent light is explained below.

Quartz. Crystalline quartz belongs to the hexagonal system in which there are three equal " horizontal " axes of symmetry at 120° to each other, and one " vertical " axis. Optically, the crystal may be described as uniaxial in character, but it has certain important characteristics. If polarized light is transmitted along the optical axis the plane of polarization is rotated, the amount being about 21° 67′ per millimetre.

The conventional terminology calls a rotation " right-handed " when it is clockwise to an observer facing the source of light, and vice versa.

Varieties of quartz are known in which the rotation is right-handed and left-handed respectively and the crystals show characteristic differences. Fig. 129 illustrates the appearances of the crystal faces in the two cases.

Fresnel explained the rotation effect by supposing that plane polarized light, when traversing the quartz crystal parallel to the axis, is resolved into two circularly polarized beams which are propagated with slightly different velocities. A linear vibration can be looked upon as the result of two circular motions in which the direction of rotation is opposite. If the relative phase is subject to change due to the unequal velocities, the direction of the vibration will change by 90° for every 180° change of phase.

A 60° quartz prism cut with its axis parallel to the base of an equilateral section will clearly show two images of the slit when mounted in a spectrometer to give minimum deviation when the

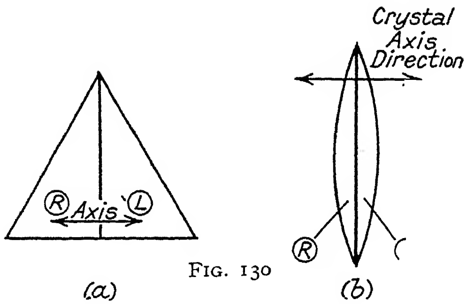

FIG. 130

light traverses the crystal along the axis[6]. If the images are examined with an analyser held behind the eyepiece it will be found that they do not vary much in intensity as the analyser is rotated. They might, therefore, be non-polarized or circularly polarized. If, however, the light is transmitted through a $\frac{\lambda}{4}$ plate it will be understood from the foregoing work that the passage of light perpendicular to the axis by a distance sufficient to cause a relative retardation of $\frac{\lambda}{4}$ or a phase difference of 90°, converts a circular vibration into a linear one. The light becomes plane polarized and can be extinguished by the analyser, thus showing that the two components were circularly polarized, in accordance with Fresnel's theory.

Cornu's device for overcoming this doubling is shown in Fig. 130. The 60° prism is now made in two parts, of right-handed and left-handed quartz respectively. This type of construction may be applied to lenses and lens systems. The two parts of a condenser lens of quartz are right- and left-handed, and even a Ramsden eyepiece in quartz in which the lenses are of equal power is improved by making the field lens and eye lens of the two varieties.

Low-power spectacle lenses are sometimes constructed from blanks cut parallel to the axis of quartz crystal, but it is better for all lenses in quartz to be " cut perpendicular to the axis," so that the optical axis of the lens and the crystallographic optic axis, are parallel. Lenses in quartz are only satisfactory for purposes in which the extreme rays only make small angles with the axis, not more than 5° to 10°; the effects of double refraction become increasingly apparent at larger angles.

Biaxial Crystals. The term " biaxial " has nothing to do with crystallographic axes but simply with " optic axes." If a disturbance starts at a point within a biaxial crystal, the wave-fronts spread

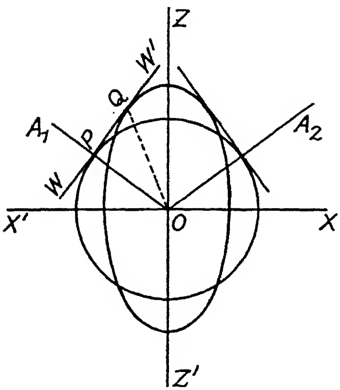

FIG. 131

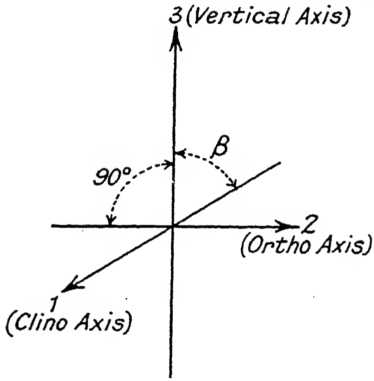

FIG. 132. AXES OF THE MONOCLINIC SYSTEM

out in two sheets; the section of the surfaces by each of the principal Cartesian planes gives a circle and an ellipse. Such a pair of sections (XZ plane) are shown in Fig. 131. Now, imagining the wave-fronts shown in this section to be propagated in a manner similar to that discussed in previous cases, the velocity of a plane wave parallel to the tangent at any point Q of the ellipse will be the velocity of the tangent normal to itself. In the section shown, there is a tangent common to the ellipsoid and the circle. It is further proved in textbooks of physical optics that the crossing point of the circle and ellipse in this section of the two wave-fronts is the lowest point of a kind of dimple in the outer surface formed by the two sheets of the wave-front. An apple resting on a plate may touch the plate at points in a circle round the dimple of the core, and in the same way a tangent surface can be found which touches the outer surface in a

circle. The normal to this surface is a direction of single wave-velocity and forms one axis of the biaxial crystal. A_1 and A_2 represent the two axis directions in the section shown in Fig. 131. Imagining the circle to increase in radius relatively to the ellipse, the two axis directions would evidently approach each other and would finally coincide when vertical; if the circle shrinks, both axes will approach the direction of the x axis.

The Monoclinic System. Selenite or Gypsum and Muscovite Mica. Two minerals of importance from the optical point of view crystallize in the monoclinic system, viz. selenite and muscovite (mica). Both of these, but especially mica, have a very marked and perfect cleavage. Skilled hands produce very large, even, sheets of mica,

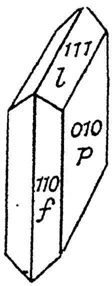

FIG. 133. SELENITE OR GYPSUM

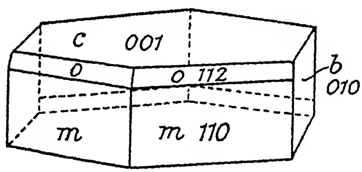

FIG. 134. MUSCOVITE MICA

by inserting a pin between the lamellae, followed by a piece of stiff paper with a curved end, which is used to spread the cleavage. Flakes can be obtained so thin as to show interference colours, and plates of muscovite be obtained of very uniform thickness which can be used for optical purposes. This is not often the case with selenite; it is extremely difficult to obtain good cleavage plates, but the mineral is very soft and can be easily ground and polished so that quarter-wave plates, etc., can be constructed from it.

Mica can only just be scratched by the finger-nail, but selenite is easily marked in this way.

In the monoclinic system (Fig. 132) the vertical axis (3) and the horizontal axis (2) are at right angles, but the other (*clino*) axis is not perpendicular to (3), although it is perpendicular to (2). The angle β shown in the figure may have different values in various crystals.

In gypsum or selinite the parameters are $a : b : c = 0{\cdot}68994 : 1 : 0{\cdot}41241$ and $\beta = 80° \ 42'$. In muscovite $a : b : c = 0{\cdot}57735 : 1 : 3{\cdot}3128$ and $\beta = 89° \ 54'$. Fig. 133 shows a selenite crystal

with "prism" faces f, "hemi-pyramids" l, and "clino-pinacoid" p. The best cleavage is parallel to the clino-pinacoid, which is itself parallel to the plane of symmetry of the crystal containing the clino axis and the vertical axis. This plane of symmetry contains the optic axes of the crystal.

Fig. 134 shows a crystal of muscovite in which b is the "clino-pinacoid," and c is the "basal pinacoid," while the faces m and o are prism faces. The cleavage in muscovite is parallel to the basal pinacoid, and the cleavage surface is within two degrees of perpendicularity to the acute bisectrix of the optical axial angle; the optic axes lie (as in selenite) in the plane of symmetry of the monoclinic crystal. When cleavage plates of muscovite (or selenite) are

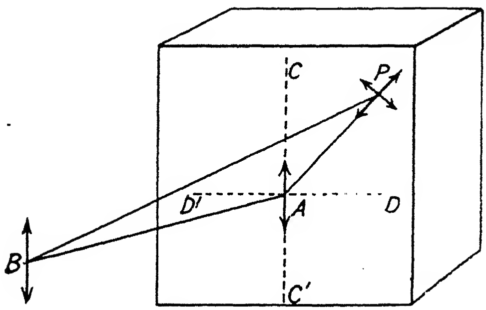

FIG. 135

examined in a polariscope in parallel light they behave very similarly to plates of uniaxial crystal cut parallel to the axis, and the slow direction of vibration for muscovite is at right angles to the line in which the optical axial plane intersects the cleavage surface. Hence, these cleavage plates are very useful for constructing quarter-wave plates, etc. If a sufficiently wide angle transmission can be secured, the directions of the axes can be found by examining the mica plate in convergent light. Then the slow direction is perpendicular to the line through the "eyes" (see below).

The effective values of the refractive indices may vary with the specimen of mica employed. In one case their values were 1·603 and 1·595. To calculate the thickness t for a quarter-wave plate,

$$\frac{\lambda}{4} = t(n_2 - n_1)$$

$$t = \frac{0{\cdot}589 \times 10^{-3}}{4 \times 0{\cdot}008} = 0{\cdot}0184 \text{ mm.}$$

If plates of higher retardation are required they are often made from selenite, which is more colourless than mica. In the clinopinacoid cleavage the maximum difference of refractive indices (measure of bi-refringence) is 0·0095. Hence, for a 1λ retardation plate the thickness required is

$$t = \frac{0{\cdot}589 \times 10^{-3}}{0{\cdot}0095} = 0{\cdot}062 \text{ mm.}$$

In a quartz plate cut parallel to the axis the bi-refringence is 0·009.

Crystal Plates in Convergent Polarized Light. Fig. 135 is intended to represent a block of uniaxial crystal cut with the axis normal to the surface, and thus parallel to the incident normal ray BA which may be imagined as the central ray of a bundle of rays diverging from the point B. These rays are all polarized so that the vibrations are vertical, say, while the line BA is horizontal. It is evident that the vibrations entering the plate along the lines CAC′ or DAD′ will be transmitted unchanged, since they will be respectively *in* and perpendicular to a principal section of the crystal containing the ray and optic axis.

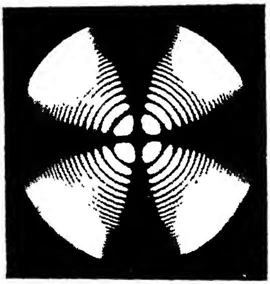

FIG. 136. CALCITE PLATE CUT PERPENDICULAR TO THE AXIS
Examined in convergent light (Nicols crossed)

Consider the oblique ray BP. The vertical vibration will be resolved at P into vibrations parallel and perpendicular to the principal section plane BPA, and these vibrations will be transmitted with differing velocities, emerging therefore with a difference of phase which depends on the angle of obliquity of incidence PBA.

All rays at the same obliquity will have the same retardation; hence, the lines of equal retardation will be circles with centres on the line of symmetry BA. As in other cases the relative retardation increases most rapidly with the shorter wavelength. If the light transmitted by the plate is passed through an analyser "crossed" with respect to the original polarizer, the appearance obtained is shown in Fig. 136 for the case of monochromatic light. The dark circular fringes mark the zones where the retardation amounts to a whole number of wavelengths, so that the vibrations in the transmitted light are parallel to their original directions before transmission.

If the light employed is white the fringes will be coloured in a

similar way to that which arises in Newton's rings or the colours in a wedge.

Reference must be made to textbooks of physical optics for the theory of isochromatic surfaces. It is shown that surfaces may be found in crystals for which the retardation is constant (imagining disturbances to originate within the crystal, being propagated in all directions, and subject to resolution into components as explained above). In a uniaxial crystal the surfaces are hyperboloids of revolution, as suggested in Fig. 137, the line of symmetry is the optic axis, and the central point of the whole system is the origin of the light.

If now we have a crystal plate cut parallel to the axis the dark fringes seen with divergent or convergent light will be hyperbolas.

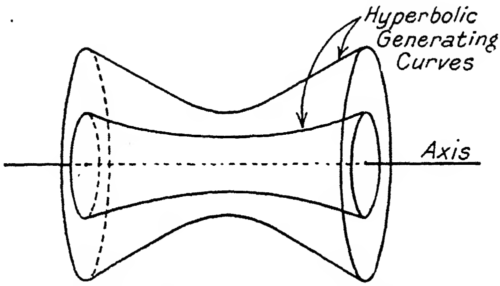

FIG. 137. TWO ISOCHROMATIC SURFACES FOR UNIAXIAL CRYSTAL

If, again, the axis makes a small angle with the normal to the surface, the section of the system of hyperboloids with the surface will be a system of closed curves with their centres to one side of the central ray to an extent varying with the obliquity of the surface.

The form of the isochromatic surface in biaxial crystals resembles a jointed tube (Fig. 138) which may intersect a crystal surface in two closed curves. The systems of closed curves corresponding to isochromatic surfaces of different retardations constitute the "eyes" of the interference figure. Fig. 139 shows a characteristic interference figure for a plate of biaxial crystal; the distance between the "eyes" is a measure of the angle between the axes.

In all crystals there will usually also be found curves along which the vibration directions remain constant; these "curves" take the form of a cross with a uniaxial crystal; the arms of the cross are respectively parallel and perpendicular to the vibration direction. In a biaxial crystal these curves (called *isogyres*) have various forms; they are seen in the figure as curved "brushes" narrowing down to pass through the eyes of the interference figure.

These various phenomena are most simply exhibited by holding the crystal between "crossed" tourmaline crystals. Tourmaline has the property that a plate cut parallel to the optic axis transmits only that one of the polarized beams in which the vibrations are "along the grain." The absorption of the other beam is very strong. As Johannsen[4] put it, "It is as though the crystals were made up of gratings of parallel bars and the polarized light was a sheet of cardboard." Hence, a pair of tourmaline crystals act as polarizer and analyser without other apparatus, and offer a very ready and simple means of distinguishing between uniaxial and biaxial crystals—also of estimating the axis direction. The transmitted light is unfortunately a dull orange, and the colour fringes cannot be well seen.

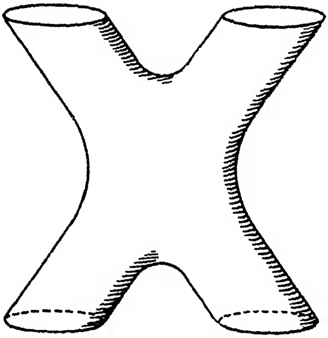

FIG. 138. ISOCHROMATIC SURFACE IN BIAXIAL CRYSTAL

In order to obtain a better rendering of the effects, with a wider angular field also, the crystal plates are mounted in a microscope and the appearances in the upper focal plane of the objective are viewed with the aid of a "Bertrand lens." Reference will be made to this when dealing with applications of the microscope in Part II of the present book.

FIG. 139. BIAXIAL CRYSTAL PLATE IN CONVERGENT LIGHT

Section equally inclined to the two optic axes

If biaxial crystal plates are mounted so that they can be rotated about an axis perpendicular to the direction of view, and are so placed that the two "eyes" are successively brought on to the central crosswire of the microscope, the apparent angle α between the axes (light refracted into air) can be measured with the help of a small divided circle to indicate the rotation. If the mean index of refraction n of the crystal is known, the true angle α_0 between the optic axes may be found from

$$\sin\left(\frac{\alpha_0}{2}\right) = \frac{1}{n}\sin\left(\frac{\alpha}{2}\right)$$

It is sometimes the case that the crystal must be immersed in a

suitable liquid in order to get the light to traverse the plate in the direction of the axes.

The tests in convergent polarized light are very useful for determining the character of a crystal. Textbooks of crystallography describe simple tests with a quarter-wave plate to determine whether a uniaxial crystal is positive or negative. In view of the importance of the whole subject in mineralogy it has undergone a wide development.

Methods involving the use of the polarization microscope are of growing importance in the study of colloids and in biological investigations.

Determination of the Axis Direction. The determination of the axis direction in a crystal of quartz or calcite is comparatively easy if the crystal is undistorted and the various faces can be recognized. Calcite may assume a variety of forms, but its cleavage planes are a definite indication. Quartz or calcite crystals can be mounted on a rotating table so as to rotate about the optic axis; only then can the pyramid faces be brought (by such rotation) into truly parallel directions so that collimated (or parallel) light reflected from them is brought to the same focus in an observing telescope. The crystal is mounted on the turntable with wax.

Good crystals of quartz usually show lines on the alternate faces which are perpendicular to the optic axis.

If the crystal is damaged so that the faces cannot be readily distinguished, it is usually cut into a plate for examination in a polariscope. Examination in convergent light quickly reveals whether the crystal is optically "uniaxial" or "biaxial," and indicates the positions of the axis or axes. The direction of the axis of a uniaxial crystal can in general be found by polishing two pairs of opposite parallel faces on the material, and examining with a simple polariscope. (See ref. 7 at end of chapter.)

Very frequently, "twinning" may occur; there may be a plane of division in the material (to casual observation quite continuous) on each side of which the axis direction and optical qualities are quite different. Such parts must be avoided for optical purposes and they are readily recognized with the polariscope. The writer has met with "pebble" spectacles (of quartz) which gave the greatest discomfort to the wearer through twinning of the crystal in the lens.

Polarimetry. The power of quartz in rotating the plane of polarization of light traversing the crystal in an axial direction is also possessed by other "optically active" substances, and even by certain solutions. Thus, cane sugar solution produces a rotation

which is naturally independent of the direction of transmission through the liquid, but is very closely proportional to the weight of the active material dissolved in unit volume of the solution. The rotation increases the shorter the wavelength of light (rotary dispersion), and varies to some extent with temperature, but the phenomenon provides a ready means of ascertaining the strength of sugar solutions by simple optical observations and is therefore of great importance in industry.

In the polarimeter, observations are usually made with monochromatic light (Mercury green $\lambda = 0{\cdot}546\mu$ is now used in preference to sodium light) but in industrial instruments known as *saccharimeters*, white light may be employed. This is possible because instead of measuring the angle of rotation of the polarized light directly it is *compensated* by a wedge of quartz from which graduated compensatory rotations can be obtained. Since the rotary dispersions of sugar solutions and of quartz are not greatly different the colour phenomena are not troublesome, and the only precaution required is the use of a yellow filter to shorten the spectral range of the light.

The earliest form of polarimeter employed simply a polarizing prism, a tube with flat ends to hold the solution, and an analyser. The analyser could be set into the extinction position before the tube was introduced; the analyser had to be turned through a certain angle to restore the extinction with the tube in place. (The conventional terminology due to Biot calls a clockwise rotation *seen when facing the source of light* a positive or right-handed rotation, and vice versa.)

This simple device fails because the extinction is so far complete for positions of the analyser *near* the real extinction position that the transmitted light cannot be readily recognized, especially as stray light is difficult to eliminate entirely. This led to the invention of instruments in which the "end-point device" gave a field in which the two halves yielded light polarized in slightly different directions. Fig. 140A shows an end view of an ordinary "Nicol" with the transmission vibration directions parallel to the shorter diagonal. This can be cut in two and the parts within the dotted lines removed; the outer parts are then brought together as shown in Fig. 140B, so that the light transmitted by the two parts will be polarized in inclined directions. Let these directions be represented by the vectors OA, OB in Fig. 140C, then, if the lengths represent amplitudes, the amplitudes of the vibrations transmitted by an analyser for which the transmission direction is parallel to the X axis will be represented by the proportion of the projected lengths

OM, ON. These are equal for one position of the analyser not far from the extinction point of both, but far enough to obtain a field of sufficient brightness. It is easily shown that this mode of setting is much more sensitive. The rotary action of the " sugar solution " is, of course, to rotate each vibration by the same extent, so that the rotation can be measured as before.

The above end-point device, known as the Jellet-Cornu prism, is not now often encountered, a device due to Lippich being more commonly employed. In this device the polarizer, a square-ended prism (1), Fig. 141, which may be of the Glan-Thompson type, is followed by a second smaller polarizing prism, which, in the simplest

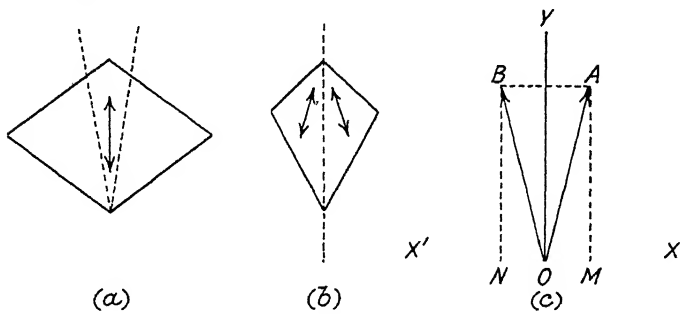

FIG. 140

form, covers one-half the aperture. The polarizing direction of the second is inclined at a small finite angle to that of the first. Hence, of the vibrations from the first prism which enter the second one, it is only the parts resolved in the vibration direction of the second which are transmitted in one-half of the field; the field is thus divided as with the Jellet-Cornu device.

The observer sights upon the edge of the small prism dividing the field in two parts, and it is necessary so to place it that the whole field is illuminated without a gap. In the first place the prism edge at C must be ground perfectly sharp. If the semi-aperture of the cone of light diverging from C and entering the entrance pupil of the observing system is β, it must be possible to displace a convergent cone of the same angular semi-aperture, which enters the face AD of the second prism, and bring its focus to C, as suggested in the figure. A little consideration will show that cones transmitted by AD which try to come to a focus below C will be totally reflected at DC, and that there will be no dark or bright gap in the field.

Referring to the figure, the angle made by DC with the axis of

the instrument is $\beta + \delta$. Let the ray shown by r make an angle of ε with the face DC after refraction, and let the angle $\widehat{ADC} = 90° - \gamma$. Then the angle of incidence of the ray r is $2\beta + \delta + \gamma$ and its angle of refraction will be $(\gamma - \varepsilon)$. If the law of refraction held we should

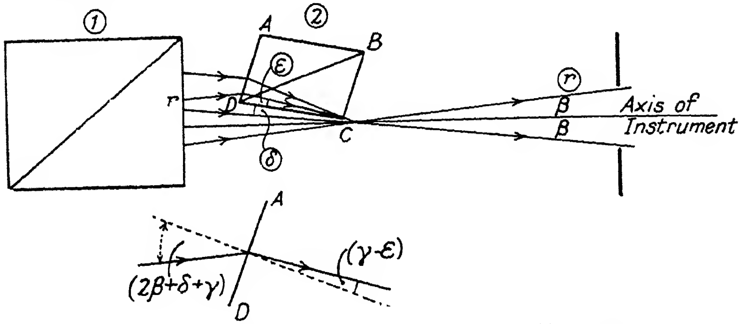

FIG. 141. OPTICAL PRINCIPLES OF LIPPICH END-POINT
Note that the convergence and bending of the rays on entering the auxiliary prism and also the tilt of the prism are exaggerated for the sake of a clear figure

have (since the angles are small), $2\beta + \delta + \gamma = n(\gamma - \varepsilon)$ or, say, $2\beta + \delta + \gamma = 1{\cdot}5\ (\gamma - \varepsilon)$, giving at once

$$\gamma = 4\beta + 3\varepsilon + 2\delta$$

Now ε and δ may be made quite small, say, about 10′, so that if the last two terms add to 1° and β is, say, 0·5°, the angle of the prism would have to be 87° or thereabouts.

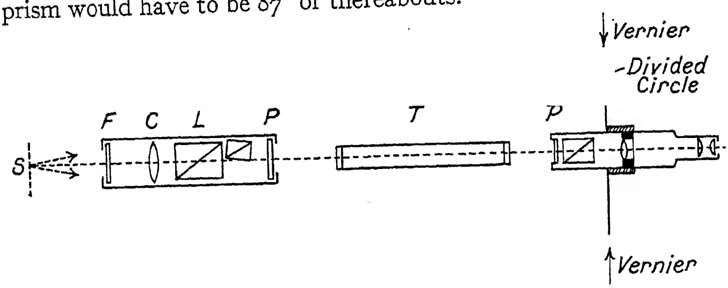

FIG. 142. OPTICAL DIAGRAM OF LIPPICH-TYPE POLARIMETER

Such rhombs in glass are of fairly frequent use in optical instruments. However, in this case the prism is of spar and doubly refracting. If it is one of the Glan-Thompson type (slightly modified), the optic axis will be perpendicular to the plane of the diagram, so that the ordinary law of refraction will be obeyed as the extraordinary wave-front section will be circular. If, however, another form

of prism should be used the extraordinary ray, which is the one transmitted by the prism, may not obey the usual law of refraction, and care must therefore be taken to make sure that the rays can follow the required course.

Fig. 142 shows a diagram of the optical system of the Lippich type polarimeter. In recent forms of the instrument the field has three parts, two auxiliary prisms being used as suggested. An image of the source of light is projected by the lens C into the entrance pupil of the observing telescope. In the figure, S is the source of light, L the Lippich end-point, F a colour filter for use with sodium light, T is the tube for holding the solution, and P and *p* are windows for protection of the prisms.

Saccharimeters usually possess end-point devices similar to those used in polarimeters, but as mentioned above, they employ wedges to compensate the rotation instead of measuring it directly. Further details of such instruments will be found in the present writer's book on *Optical Measuring Instruments*, while details of technical methods will be found in the Bureau of Standards' useful paper on "Polarimetry" (*Circular No.* 44).

References

1. S. P. Thompson: *Proc. Phys. Soc.* 2 (1877).
2. S. P Thompson: *Proc. Opt. Convention*, 1905, p. 216.
3. W. Grosse: *Zeit. f. Inst.* X (1890), 445.
4. Michel Lévy et A. Lacroix: "*Les Mineraux des Roches,*" Paris, 1888. (See also Johannsen: *Petrographic Methods*, New York, 1918.)
5. R. W. Wood: *Physical Optics*, p. 329.
6. Cornu: *Comptes Rendues*, 92 (1881), 13th June; *Journal de Physique* 1, 2e serie (1882), 157.

(Cornu reaches the conclusion that the two refractive indices for the axis direction have the "ordinary" refractive index as their mean.)

7. J. Walker: *Phil. Mag.*, July, 1909, p. 195. Other unpublished methods of getting axis to quartz to high accuracy are in use by technicians.

CHAPTER VII

OPTICAL GLASS, AND THE PRODUCTION AND TESTING OF LENS SYSTEMS

ALTHOUGH the art of glass-making has been known since very early historical times (before 2500 B.C. in Egypt), the varieties of "optical" glass obtainable until the second half of the nineteenth century were practically limited to the old types of "crown" and "flint." Typical compositions of these (as manufactured by Guinand about A.D. 1805 and onwards) were—

Crown: 72 per cent silica, 18 per cent potassium oxide, 10 per cent calcium oxide.

Flint: 45 per cent silica, 12 per cent potassium oxide, 43 per cent lead oxide.

In the manufacture of glass for all purposes, the oxides employed were limited to silica, sodium, potassium, calcium, lead, and aluminium.

The dispersion and refraction of glass was studied by Newton (1643–1727), but in his time he had no means of making very exact measurements owing to the difficulty of isolating sufficiently homogeneous light. He reached the erroneous conclusion that the amount

THE FRAUNHOFER LINES, WITH ADDITIONS

Distinguishing Letter	Wavelength in μ	Line given by	Production in Laboratory	Colour
A′	{0·7699, 0·7665}	K	Flame	Red
A	0·7594	O*		
B	0·6867	O*		
C	0·6563	H	Vacuum tube	,,
D_1	0·5896	*Na*	Flame	Orange-yellow
D_2	0·5890	*Na*		,,
E	0·5270	*Fe*		Green
F	0·4861	H	Vacuum tube	Blue-green
G′	0·4341	H		Violet
G†	0·4308	*Fe, Ca*		
H	0·3969	*Ca*		
K	0·3934	*Ca*		

* Produced by absorption in atmosphere. The wavelength given is really the head of an absorption band which does not make a very good "line" for measurement.

† A double line; the components can be distinguished under high resolving power.

of dispersion in any substance was proportional to the refracting power, a circumstance which would have rendered the making of "achromatic" lenses or prisms impossible, as will be understood from the discussion given below.

Fraunhofer's re-discovery* (A.D. 1814) of the dark lines of the solar spectrum, and the consequent facilitation of the measurement of refractive indices, put the whole subject of achromatism on a more exact basis. The "Fraunhofer lines" were called A, B, C, etc.

The A′ and G′ lines added to the above table are convenient ones for laboratory measurements of refractive index, in which the three hydrogen lines C, F, and G′, together with the A′ lines of potassium and the D lines of sodium are the more usual ones selected for purposes of measurement; they are easily obtained from a small discharge tube and a flame respectively. In what follows, n_C, n_F, etc., will represent the refractive indices for the lines denoted by the suffixes; the wavelengths assumed for A′ and D are the mean values.

Dispersive Power and Constringence. A single lens has refractive indices n_C, n_D, n_F. The corresponding focal lengths are found from

$$\frac{1}{f'_C} = (n_C - 1)\,\mathcal{R},\ \frac{1}{f'_D} = (n_D - 1)\,\mathcal{R},\ \frac{1}{f'_F} = (n_F - 1)$$

Hence
$$\frac{1}{f'_F} - \frac{1}{f'_C} = (n_F - n_C)\,\mathcal{R}$$

or
$$\frac{f'_C - f'_F}{f'_C f'_F} = (n_F - n_C)$$

Since the product $f'_F f'_C$ will not be very different from $(f'_D)^2$, the equation becomes as a close approximation

$$\frac{f'_C - f'_F}{f'_D} = f'_D\,(n_F - n_C)\,\mathcal{R} = \frac{n_F - n_C}{(n_D - 1)} \tag{58}$$

or
$$\frac{f'_D}{f'_C - f'_F} \quad \frac{n_D - 1}{n_F - n_C} = \mathrm{V} \tag{59}$$

The quantity $\dfrac{(n_F - n_C)}{(n_D - 1)}$ is termed the dispersive power of the medium of the lens. It is seen to determine the ratio of the length of the axial spectrum to the whole focal length. Its reciprocal, which we denote by V (often given as ν, following the Jena Works glass lists),

* Wollaston had previously observed the dark lines. Fraunhofer's *earliest* accurate measurements of refractive index were, however, made with an ingenious monochromator.

is convenient in calculations respecting achromatism. The "V value" is sometimes called the "constringence" of the medium.

Achromatism. Denoting the properties of two thin lenses by the additional suffixes a and b, the focal power of the combination of the two when in contact, for the wavelengths of C and F, will be

$$\mathcal{F}_C = (n_{aC} - 1)\,\mathcal{R}_a + (n_{bC} - 1)\,\mathcal{R}_b$$

$$\mathcal{F}_F = (n_{aF} - 1)\,\mathcal{R}_a + (n_{bF} - 1)\,\mathcal{R}_b$$

When the system is achromatized in the usual method the focal powers of the combination for C and F will be equal. Thus, $\mathcal{F}_C = \mathcal{F}_F$, which gives

$$\mathcal{R}_a\,(n_{aF} - n_{aC}) + \mathcal{R}_b(n_{bF} - n_{bC}) = 0$$

Introducing the V values for a and b where

$$V_a = \frac{(n_{aD} - 1)}{(n_{aF} - n_{aC})}, \text{ and } V_b = \frac{(n_{bF} - 1)}{n_{bD} - n_{bC})}$$

we obtain immediately

$$\frac{\mathcal{R}_a\,(n_{aD} - 1)}{V_a} \qquad \frac{\mathcal{R}_b\,(n_{bD} - 1)}{V_b} = 0$$

giving

$$\frac{\mathcal{F}_{aD}}{V_a} + \frac{\mathcal{F}_{bD}}{V_b} = 0$$

Since now

$$\mathcal{F}_D = \mathcal{F}_{aD} + \mathcal{F}_{bD}$$

$$\mathcal{F}_{aD} = \mathcal{F}\left(\frac{V_a}{V_a - V_b}\right) \text{ and } \mathcal{F}_{bD} = \mathcal{F}\left(\frac{V_b}{V_b - V_a}\right)$$

These last equations give for the corresponding focal lengths

$$f'_{aD} = f'_D\left(\frac{V_a - V_b}{V_a}\right) \;\ldots\; \text{and } f'_{bD} = f'_D\left(\frac{V_b - V_a}{V_b}\right) \quad (60)$$

Numerical Example. Let us choose two glasses from Chance's catalogue to make an achromatic doublet by means of this approximate "thin lens" theory.

Melting No.	Type	n_D	V
9322	Hard crown	1·5186	60·3
1034	Dense flint	1·6041	37·8

Let $f_D' = 1$ metre. Then

$$f'_{aD} = 1\left(\frac{22\cdot5}{60\cdot3}\right) \qquad f'_{bD} = 1\left(\frac{-22\cdot5}{37\cdot8}\right)$$

$$= 0\cdot373 \text{ metres} \qquad = -0\cdot595 \text{ metres}$$

To check $\mathcal{F}_{aD} = 2\cdot68 \qquad \mathcal{F}_{bD} = -1\cdot68$

If the lens b is to have a flat back surface—

$$\mathcal{F}_b = (n_b - 1)(\mathcal{R}_1 - 0)$$

$$\therefore \mathcal{R}_1 = \frac{-1\cdot68}{0\cdot6041} = -2\cdot78, \text{ or } r_{1b} = \frac{-0\cdot6041}{1\cdot68} = -0.359 \text{ metres.}$$

If the lens is to be a cemented doublet, $\mathcal{R}_{2a} = \mathcal{R}_{1b}$.

$$\mathcal{F}_a = (n_a - 1)(\mathcal{R}_{1a} - \mathcal{R}_{2a})$$

$$2\cdot68 = (0\cdot5186)(\mathcal{R}_{1a} + 2\cdot78)$$

$$\mathcal{R}_1 = 2\cdot39 \text{ or } r_{1a} = 0\cdot418 \text{ metres.}$$

It is now desired to calculate the difference of the focal lengths of the combination for some other wavelengths, say D and F. We have

$$\frac{1}{f'_D} = (n_{aD} - 1)\,\mathcal{R}_a + (n_{bD} - 1)\,\mathcal{R}_b$$

$$\frac{1}{f'_F} = (n_{aF} - 1)\,\mathcal{R}_a + (n_{bF} - 1)\,\mathcal{R}_b$$

Hence, $\dfrac{1}{f'_F} - \dfrac{1}{f'_D} = \dfrac{f'_D - f'_F}{f'_F f'_D} = (n_{aF} - n_{aD})\,\mathcal{R}_a + (n_{bF} - n_{bD})\,\mathcal{R}_b$

and therefore $\dfrac{f'_D - f'_F}{f'_F} = (n_{aF} - n_{aD})\,\mathcal{R}_a f'_D + (n_{bF} - n_{bD})\,\mathcal{R}_b f'_D$

$$= (n_{aF} - n_{aD})\,\mathcal{R}_a f'_{aD}\,\frac{V_a}{V_a - V_b}$$

$$+ (n_{bF} - n_{bD})\,\mathcal{R}_b f'_{bD}\left(\frac{V_b}{V_b - V_a}\right)$$

$$= \frac{(n_{aF} - n_{aD})}{(n_{aF} - n_{aC})(V_a - V_b)} + \frac{(n_{bF} - n_{bD})}{(n_{bF} - n_{bC})(V_b - V_a)}$$

Now, these partial dispersions such as $(n_F - n_D)$ are entered in the glass lists giving particulars of optical glasses, and sometimes such ratios as $\dfrac{(n_F - n_D)}{(n_F - n_C)}$ are also given. Calling this ratio β, the equation above becomes

$$\frac{f'_D - f'_F}{f'_F} = \frac{\beta_a - \beta_b}{V_a - V_b} \qquad . \quad . \quad . \quad (61)$$

With any two glasses, therefore, the difference of the β values determines the difference of the focal lengths of the combination for the "D" focus and the equalized focus of C and F. The glass lists also give the partial dispersions for other pairs of lines such as C and D, F and G′, where $\alpha = \frac{(n_D - n_A')}{(n_F - n_C)}$ and $\gamma = \frac{(n_G' - n_F)}{(n_F - n_C)}$. Evidently, in order to effect perfect achromatism, the ratio of these differences to the values of $(n_F - n_C)$ should be equal for the glasses chosen, so that

$$\alpha_a = \alpha_b,\ \beta_a = \beta_b,\ \text{and}\ \gamma_a = \gamma_b.$$

If, however, there are outstanding differences, equation (61) above shows that the extent of the differences of focus will be diminished by a large value of the difference $(V_a - V_b)$.

In order to estimate the separation of the foci for D and F in the case of the glasses cited above, we obtain the following additional information from the glass lists—

Melting No.	Type	Mean Dispersion	Partial Dispersions and Relative Partial Dispersions		
		C to F	C to D	D to F	F to G′
9322	Hard crown	·00860	·00254 (·295)	·00606 (·705)	·00489 (·569)
1034	Dense flint	·01599	·00457 (·286)	·01142 (·714)	·00969 (·606)

From these figures

$$\frac{f'_D - f'_F}{f'_F} = \frac{\beta_a - \beta_b}{V_a - V_b} = \frac{0{\cdot}705 - 0{\cdot}714}{22{\cdot}5} = \frac{-1}{2500}$$

Relative Accuracy of Measurement. There are some practical difficulties in obtaining measurements of these partial and relative dispersions which may be illustrated by a numerical example. It is an attainment of a high order to obtain measurements of refractive index correct to one unit in the fifth decimal.

$$\text{If } n_F = 1{\cdot}51794$$
$$n_C = 1{\cdot}50990$$
$$n_F - n_C = {\cdot}00804.$$

Thus, with the above accuracy of absolute measurement, the relative accuracy in the difference is reduced to the order of 1 or 2 parts in 1,000. If the original accuracy of absolute measurement was to

one in the fourth decimal of refractive index, the error in the "mean dispersion" $(n_F - n_C)$ is about 1 or 2 per cent. The error in the partial dispersions of smaller range such as $(n_D - n_C)$ and the *relative* partial dispersions, is naturally more serious still. Therefore the estimation of the differences of focus in a doublet lens requires very accurate refractive index determinations.

Historical. The old types of crown and flint when used as achromatic combinations invariably showed a considerable divergence between the focal points for D and G′ and the common focus for C and F when achromatism was effected in that sense. The variation is illustrated in Fig. 143, in which curve A shows the variation of axial focussing position for the various wavelengths in the spectrum

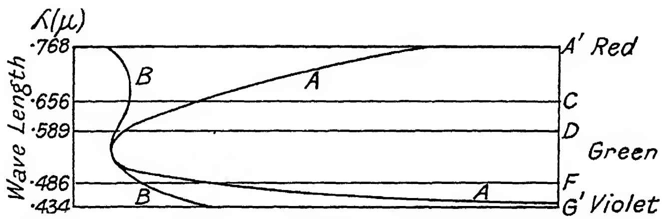

FIG. 143. RELATIVE AXIAL POSITIONS OF FOCI IN AN ACHROMATIC (*A*) AND APOCHROMATIC (*B*) SYSTEM

(the latter are plotted vertically). The length of this "secondary spectrum," (D to F), may be roughly $\frac{1}{2000}$th part of the whole focal length, and the focus for the bright yellow-green region in the spectrum is nearest the lens.

The earliest attempts to produce glasses which allowed of a reduction of the secondary spectrum by avoidance of the irrationality of dispersion (by obtaining $\alpha_a = \alpha_b$, $\beta_a = \beta_b$, etc.) were made by Fraunhofer, working with P. L. Guinand between 1811 and 1813, and alone from 1814 to 1828. Then Harcourt in England carried out experiments between 1834 and 1860, and discovered the important effects of boron and barium on dispersive properties when introduced into the composition of glass, but he produced few specimens of practical utility, although an objective made with a disc of his borate glass had a greatly reduced secondary spectrum.

In 1866, Ernst Abbe began his long connection with the firm of Carl Zeiss. "For years," he said, "we combined with sober optics a species of dream optics, in which combinations made of hypothetical glass, existing only in our imagination, were employed to discuss the progress which might be achieved if the glass makers could only be induced to adapt themselves to the advancing requirements of

practical optics." Failing to induce others to make the necessary trials, he began his work with Schott in 1880. They made tests of introducing boron, phosphorus, barium, fluorine, and other elements, and the result included new and useful series of boro-silicate crowns, barium crowns, barium flints, borate flints, and the phosphate and borate glasses; in these the character of the dispersion varies from type to type. So began the famous Jena Glass Works.

Before the war of 1914–1918, the chief sources of optical glass outside Germany were the Parra-Mantois works in Paris, and Messrs. Chance Bros. & Co., Ltd., in Birmingham. The production of optical glass was of such importance during the war, however, that production in England, France, and America was developed on a very much larger scale, involving a great deal of initial experimental work by Sir Herbert Jackson, C. J. Peddle, and others, in which most of the Jena types were reproduced and a certain number of entirely new glasses manufactured.

To go back to the work of Abbe and Schott, the early work resulted in the production of a number of glasses such as the "phosphate crown" and "borate flint" which, when combined in an achromatic objective, give a double bend in the spectrum as instanced by curve B, Fig. 143. The similar "run of dispersion" has resulted in an extremely small secondary spectrum. Unfortunately, however, some of these glasses were found to be chemically unstable and their use had to be abandoned. Among the really stable glasses, however, the secondary spectrum can be very greatly reduced by using a glass known as "telescope flint" with a hard crown, although it is necessary to use deeper curves than with the usual "dense flint." Some advantage is thereby lost.

Effects of Various Elements on the Optical Properties of Glass. The effect of the high lead content in flint glass is to increase both the total relative dispersion (low V values), and the relative dispersion at the blue end of the spectrum. Thus, the V for crown glass containing no lead is about 60, while for dense flint glass it is about 32. The γ value for silicate crown is 0·568, while for dense flint it may be 0·619.

Some of the lead may be replaced by barium—producing a "barium light flint." The V value may then rise to about 50, while γ falls to about 0·582. Barium may be introduced rather than lead into a crown glass to lower the V value to about 55, while the γ becomes about 0·573. As compared with lead, barium produces a lower refractive index, and a much lower dispersion.

Boron introduced into a glass has the important property of lengthening the red end of the spectrum with regard to the blue;

Types of Optical Glass (Messrs. Chance Bros. & Co., Ltd.)

Type No.	Variety	n_D	$n_F - n_C$	V	$n_D - n_C$	$n_F - n_D$	$n_G' - n_F$	α	β	γ
7423	Fluor crown	1·4785	·00682	70·2	·00202	·00480	·00363	·296	·704	·532
646	Boro-silicate crown . .	1·5087	·00793	64·1	·00237	·00556	·00445	·299	·701	·561
1203	Hard crown	1·5155	·00848	60·8	·00250	·00598	·00482	·295	·705	·568
8065	Dense barium crown . .	1·6130	·01025	59·8	·00302	·00723	·00582	·294	·706	·568
1066	Zinc crown	1·5149	·00890	57·9	·00265	·00625	·00506	·298	·702	·569
7472	Medium barium crown . .	1·5837	·01041	56·1	·00304	·00737	·00596	·292	·708	·573
4469	Light barium flint . . .	1·5661	·01029	55·0	·00301	·00728	·00591	·293	·707	·574
4277	Telescope flint . . .	1·5237	·01003	52·2	·00295	·00708	·00577	·294	·706	·575
7863	Extra light flint . . .	1·5290	·01026	51·6	·00300	·00726	·00593	·292	·708	·578
1018	Light flint	1·5491	·01206	45·5	·00348	·00858	·00714	·289	·711	·592
410	Light flint	1·5760	·01404	41·0	·00402	·01002	·00840	·286	·714	·598
5953	Dense barium flint . . .	1·6059	·01593	38·0	·00453	·01140	·00967	·284	·716	·605
572	Dense flint	1·6182	·01697	36·4	·00484	·01213	·01031	·285	·715	·608
5093	Very dense flint . . .	1·6501	·01936	33·6	·00544	·01392	·01190	·281	·719	·615
7972	Very dense flint . . .	1·7566	·02754	27·5	·00774	·01980	·01736	·281	·719	·630

borate flint glasses are not very stable, although boro-silicate crowns are satisfactory in this respect. This disability also applies to the use of phosphates in glass; as compared with a silicate glass of the same total dispersion, the phosphate glass has about the same

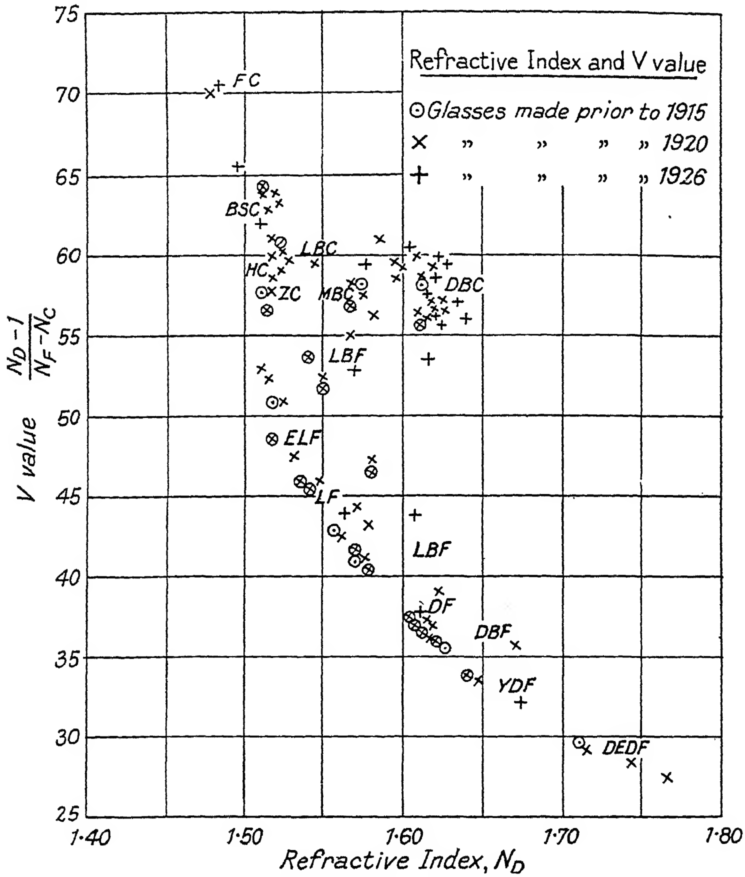

FIG. 144. TYPES OF OPTICAL GLASS (CHANCE)

run of dispersion, while its refractive indices are higher. This is a valuable optical effect, but the use of phosphate glasses has been largely discontinued for the above reason.

The use of extra potassium and sodium in glass decreases the red end of the spectrum relatively to the blue, to some extent, but potassium can only be used in moderate quantities if the glass is to be chemically stable.

The greatest value of some of the elements such as zinc, which are introduced, is in connection with the facility they give in the working of the glass. The optical effects of fluorine are a matter of some discussion.

Advantages of a Variety in Glass Types. The main advantages of the great variety of glass types are not only found in the possibility of reducing the secondary spectrum in doublet lenses; when more perfect achromatism is required it is, in fact, usually best obtained by the employment of three or more lenses. Other aberrations, too, can be controlled by the selection of suitable glasses. Thus, a doublet lens can be secured with only a small degree of coma by choosing a medium barium crown to unite with a dense flint. During the war, an important lens for aerial photography could only be made after a glass "extra light flint" was successfully produced.

Very often in designing a complex system, a computer will assume a trial set of glasses for the components. If large aberrations arise at a deeply-curved surface, it may be possible to reduce the curvature by the choice of another glass for one of the lenses, and so gain control over the aberrations in a manner otherwise impossible. In another case a computer may design his system to abolish spherical aberration, etc., making only rough provision for achromatism. He will have fixed the absolute refractive indices of his glasses, and then when the system is practically complete he may work out the dispersions which the glasses should have in order to give proper achromatism. Fig. 144 represents the glasses available from Messrs. Chance Bros. & Co., Ltd., in which the refractive index is plotted against the V value. If the computer had one glass of refractive index 1·515, he would have a range of possible V values from 64 to 53 amongst different glasses ranging from boro-silicate crowns through hard crowns and zinc crowns. This choice might easily enable the proper glass to be selected, which would produce achromatism.

The Petzval-Coddington equation for the curvature of field of a thin lens system consisting of a number of components is (assume a flat object field)

$$\frac{1}{r} = -\left(\frac{1}{n_a f'_a} + \frac{1}{n_b f'_b} + \text{etc.}\right) \text{ or } -\Sigma\left(\frac{1}{n_a f'_a}\right)$$

It is easily realized that the possible requirement of a flat image field alone calls for a definite relation between the focal lengths and refractive indices of a system; this again illustrates the desirability

of having available several possible values of dispersion for one refractive index.

The modern glass list only gives a selection of types. The glass-maker can usually produce intermediate types if they are required.

The Parsons Optical Glass Company has recently issued a glass list with a much more complete specification of refractive indices. In addition to the usual lines, figures are given for the following—

Symbol	Wavelength (μ)	Element	Produced by
b	0·7065	Helium	Vacuum tube
d	0·5875	,,	,, ,,
e	0·5461	Mercury	Mercury lamp
g	0·4359	,,	,, ,,
h	0·4047	,,	,, ,,

Dispersion Formulae. It is of considerable utility if the relation between refractive index and wavelength for a medium can be

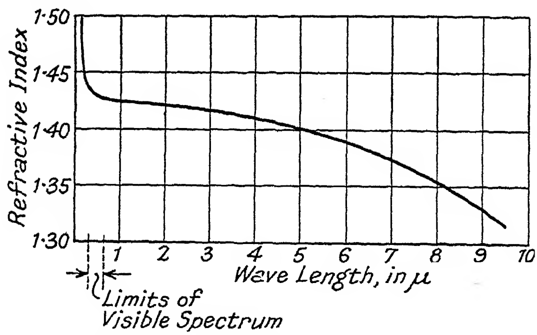

FIG. 145. DISPERSION OF FLUORITE

represented more or less exactly by an algebraic formula. Fig. 145 shows the dispersion of fluorite, refractive index being plotted against wavelength, and this curve is one which shows characteristics very similar to many substances having a good transmission in the visible spectrum. There is generally one absorption band in the ultra-violet and another in the infra-red; the refractive index rises rapidly as the ultra-violet band is approached from the visible regions, and sinks towards the infra-red one. Sellmeier and Helmholtz investigated the velocity of a wave in an elastic solid in which particles capable of vibration in certain frequencies are embedded. The loaded medium thus chiefly absorbs the energy of wave motions having the natural frequencies of the particles, and the velocity of

wave propagation will be diminished most for such frequencies. The "refractive index" of the loaded medium followed from the velocity thus calculated, as compared with that of a wave in the medium without the particles.

Sellmeier's formula (taking account of only one absorption band) was

$$n^2 = 1 + \frac{D\lambda^2}{\lambda^2 - \lambda_m^2} \quad . \quad . \quad . \quad (62)$$

Note that λ represents the wavelength and D is a constant.

It will be noticed that the value of n becomes very great as λ approaches λ_m; this is the wavelength corresponding to the frequency of the embedded particles in the medium. The formula lends itself fairly well to the representation of actual results for refractive indices as of glass, etc., in the shorter wavelength regions. The Helmholtz formula, deduced by somewhat different assumptions was

$$n^2 = 1 - P\lambda^2 + \frac{Q\lambda^4}{\lambda^2 - \lambda_m^2} . \quad . \quad . \quad (63)$$

Practical computation of the constants for a number of substances shows that for the majority of cases P = Q very nearly, and the formula can then with very slight approximation be reduced to the "Cauchy" form: $n = A + B\lambda^{-2} + C\lambda^{-4}$.

The Helmholtz formula, as modified by Ketteler to represent results in the presence of both an ultra-violet and infra-red absorption band becomes

$$n^2 = a^2 + \frac{M_1}{\lambda^2 - \lambda_1^2} - \frac{M_2}{\lambda_2^2 - \lambda^2} \quad . \quad . \quad . \quad (64)$$

For example, the results of Rubens[1] for quartz (ordinary ray) give:

$$a^2 = 3{\cdot}4629, \quad M_1 = 0{\cdot}010654, \quad M_2 = 111{\cdot}47, \quad \lambda_1^2 = 0{\cdot}010627,$$
$$\lambda_2^2 = 100{\cdot}77$$

On the electro-magnetic theory, a dispersion formula of the following type can be derived—

$$n^2 = H\lambda^2 + A + B\lambda^{-2} + C\lambda^{-4} \quad . \quad . \quad (65)$$

A formula proposed by Schmidt,

$$n = n_o + A\lambda^{-1} + B\lambda^{-4}. \quad . \quad . \quad . \quad (66)$$

has been improved by Conrady in the following form

$$n = n_o + A\lambda^{-1} + B\lambda^{-3{\cdot}5} \quad . \quad . \quad . \quad (67)$$

J. W. Gifford[2] found this last form to give more accurate results for interpolation in the visual region than the Cauchy or Ketteler form. While such formulae are fairly safe for interpolation, they cannot well be used for extrapolation.

Having found the "constants" in such a formula by the finding of the actual refractive indices for several known lines, substituting in the dispersion formula, and solving the resulting set of equations for the values of the constants, the results can be employed to determine the wavelength for minimum focus of a doublet if the constants and focal lengths of both glasses are known.

Since
$$\begin{aligned}\frac{1}{f'} &= (n_a - 1)\ \mathcal{R}_a + (n_b - 1)\ \mathcal{R}_b \\ &= (n_{ao} - 1 + A_a\lambda^{-1} + B_a\lambda^{-3\cdot5})\ \mathcal{R}_a \\ &\qquad + (n_{bo} - 1 + A_b\lambda^{-1} + B_b\lambda^{-3\cdot5})\ \mathcal{R}_b\end{aligned}$$

which can be reduced to
$$\frac{1}{f'} = P + Q\lambda^{-1} + R\lambda^{-3\cdot5}$$

Differentiating
$$\frac{d}{d\lambda}\left(\frac{1}{f'}\right) = \left(-\frac{Q}{\lambda^2} - 3\cdot5\,\frac{R}{\lambda^{4\cdot5}}\right)$$

For the minimum value of focal length when $d\left(\frac{1}{f'}\right) = o$, this equation can easily be solved for λ by taking logarithms, obtaining
$$\log\,(\lambda_{min}) = 0\cdot4\,\log\left(-3\cdot5\,\frac{R}{Q}\right)$$

where $Q = A_a\,\mathcal{R}_a + A_b\,\mathcal{R}_b$, and $R = B_a\,\mathcal{R}_a + B_b\,\mathcal{R}_b$.

H. W. Lee has found the Hartmann interpolation formula
$$n = n_o + \frac{C}{(\lambda_o - \lambda)^a} \tag{68}$$

to give good results for interpolation in the range of the visible spectrum. He calculated the constants for a number of representative glasses from the results given in the Parsons catalogue, using the b, F, and h lines. The value of a was taken as 1·2. Except in the cases of glasses of extreme properties the calculated refractive indices for the intermediate lines obtained by the formula did not differ from the measured values by more than 3 units in the fifth

decimal of refractive index. Typical results, for two of the "Parsons" glasses, were

CONSTANTS FOR HARTMANN FORMULA FOR TWO GLASSES
(Value of $a = 1 \cdot 2$)

Glass	n_D	V	n_0	C	λ_0	Errors (in the fifth decimal)			
						c	*d*	*e*	*g*
Dense barium Crown 1 .	1·59644	59·6	1·57699	29·62	138·1	−3	−2	−2	−1
Dense flint 1 .	1·60545	38·0	1·57781	37·77	177·3	+1	0	−1	−2

This formula appears to be useful for interpolation in cases where "fourth place" accuracy (or even a rather higher standard) is required.

Production of Optical Glass. Good descriptions of many details in optical glass manufacture may be found in Wright's "Manufacture of Optical Glass and of Optical Systems."[3] A few notes must suffice here. The ingredients, especially the sand (chosen for its freedom from iron), have to be selected and mixed with care and thoroughness. They are fused in a dome-shaped crucible or pot of Stourbridge clay, with an opening in the top to allow of the stirring necessary to secure homogeneity. Stirring is commenced after the mass has been sufficiently long in the liquid state to get rid of most of the bubbles. The first comparatively quick cooling of the mass of glass results in fractures which split the material into a number of lumps of different sizes, which are re-heated, pressed into flat slabs, and subsequently examined for freedom from cloudiness, stones (fragments of undissolved material), large bubbles, crystallization, etc. The best parts, which often only comprise a quarter of the whole weight, are then re-heated and annealed. This process is carried out in order to avoid the unduly quick cooling and consequent solidification of the outer parts of a mass while the inner portions are still hot. If this condition occurs, the inner parts will still tend, of course, to shrink on cooling, and thus set up a great tension in the material, since the outer parts, having already solidified, cannot shrink correspondingly. Radial stresses appear in the inner parts, and tangential compressional stresses in the outer parts, of a block. The process of annealing consists in cooling the material very slowly through certain ranges of temperature; by this means the development of strain is prevented through the fact that the glass has still a certain fluidity while solidifying, and sufficient flow can take place,

if enough time is allowed, in order to obviate trouble. When the whole is sufficiently solid it can be cooled more quickly without danger.

F. Twyman investigated the annealing question as a viscosity problem, and showed that the mobility of most glasses through the critical range from 400° C. to 800° C., doubles for each 8° rise in temperature. He studied the relief of stress in hot glass by examination in polarized light, and his results agreed with Maxwell's tentative suggestion that the rate of decrease of stress is proportional to the stress itself. Methods of testing for strain are dealt with below. Adams and Williamson in America corrected these ideas in detail, but confirmed the main trend of Twyman's physical results. The practical uses of this work were to determine for various glasses the particular range of temperature over which the cooling after melting should take place very slowly, and this knowledge of the annealing temperature enabled the whole cooling and annealing process for certain kinds of glass, which had sometimes occupied perhaps fourteen days, to be shortened to three and a half days.

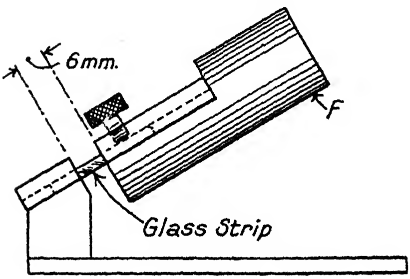

FIG. 146

The question of the annealing temperature of glass is important in the process of moulding " blanks," for lens manufacture, and also in the welding of optical parts. The determination of the critical range is now a well-recognized investigation, and apparatus can be obtained especially designed for the purpose. In Twyman's method for controlling the annealing of glassware, a strip of the glass 6·0 mm. wide, 2·0 mm. thick, and about 15 mm. long is clamped in a small jig (Fig. 146), and bears a weight F in such a way that a length of only 6 mm. is free to bend when heated. The jig is placed in an electric tube furnace and is kept under observation by a telescope as the temperature is raised. The rates of bending at two temperatures near the softening-point being observed, it is possible to obtain from a series of curves given by Messrs. Adam Hilger, Ltd., the makers of the apparatus, the temperature at which the deflection of the lever is 2·2° per hour.* Experience has shown that this is the

* Another criterion which may be useful in observations made of the relief of strain by examination in polarized light is that a strain causing a retardation of 0·1λ per cm. is reduced to 0·05λ per cm. in ten minutes.

best " annealing temperature " for domestic or chemical glassware. Very similar methods can be applied to optical glass.

The process of annealing consists in gently raising the glass to the annealing temperature, and maintaining this for a sufficient period to allow the relief of strain (domestic glassware only requires about 15 minutes), and then allowing the temperature to fall, very slowly at first, and more rapidly afterwards.

Twyman gives the equation

$$\theta_0 - \theta = \frac{\log_{10}\left(\frac{1}{1 - mbt}\right)}{m \log e} \quad . \quad . \quad . \quad . \quad (69)$$

(where $m = 0{\cdot}0865$, b is a factor representing a chosen rate of cooling, θ = temperature, θ_0 = the annealing temperature, t = time for temperature to fall from θ_0 to θ, and e = base of Naperian logarithms) as a suitable one by which to ascertain the best time schedule for cooling.

In connection with the moulding process to which reference will be made below, the work of Twyman and Simeon has shown that the process of moulding, as often carried out with comparatively quick cooling, often introduces heterogeneity of *refractive index.* The relief of this condition requires an annealing at a higher temperature and conducted more slowly than is necessary for the removal of strain.

The annealed lumps may have been moulded into square blocks, prisms, etc., or may be still unshaped. They may be tested by immersion in a liquid of the same refractive index (carbon disulphide and alcohol can be mixed in various proportions to obtain a wide range of refractive indices), or the pieces can be cut into slabs, if necessary, and opposite faces of the slabs can be optically ground and polished for inspection.

Homogeneity. There may be local regions in the melt where the stirring has not yet perfectly mixed the material, but has produced threads or striae similar to those seen when syrup is being mixed in water. Heavy striae may involve differences in refractive index of one or two units in the third decimal place.

The usual method of testing for such defects, as well as bubbles and other small specks of undissolved material, is to place the plate in the path of a convergent beam of light, Fig. 147; AB and CD are the polished faces worked on the specimen. The source of light should not be too bright; a lamp flame serves excellently. The image may be 3 or 4 mm. in diameter. If then the pupil of the eye is placed in this image, the whole aperture of the lens appears filled

with light of uniform brightness unless there are regions where, as suggested at P in the diagram, local variations of refractive index alter the path of some of the light and cause it to fall outside the pupil of the eye. The defect will then show up dark on the lighter ground. A similar test may be applied to a rough or unpolished block if it is immersed in a liquid of the same refractive index contained in a tank with walls of optically-worked glass, but care is necessary to distinguish the effects of the surface in case the liquid is not correctly adjusted to the proper refractive index.

Plates and lenses with polished surfaces are also easily tested by passing a very intense beam of light through them. Scattered light can then be detected against a suitably dark background.

Apart from these extreme irregularities, the measurements of J. W. Gifford have shown that variations of refractive index of

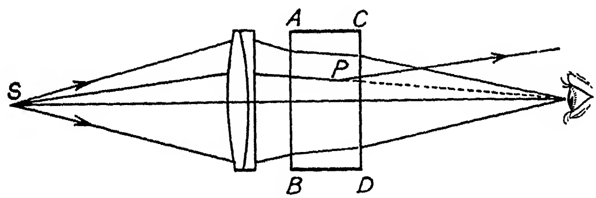

FIG. 147. TESTING FOR STRIAE, ETC.

one or two units in the fifth decimal place must be expected between prisms from different parts of the same melt, and there may be even variations in the fourth decimal in particular cases. In particular, changes of refractive index are most to be expected near the surface of the melt, or near the sides of the pot.

The variations of refractive index which are to be expected between various melts made up to the same batch formula are more considerable, perhaps involving several units in the third decimal place, except in certain cases, such as with boro-silicate crown. The V value may vary by several units in the first decimal place. Wright[3] reproduces diagrams furnished by Schott and Genossen and by Parra Mantois showing variations from melt to melt of various glasses. The most marked variations shown are in the case of a dense flint, Jena type O 102.

Effects of Strain. As early as 1813 it was shown by Brewster that a glass plate under compression behaves like a negative uniaxial crystal, the direction of the load determining the optic axis. When light traverses such a crystal in a direction perpendicular to the axis, the velocity is different for those components of the vibration which are respectively parallel and perpendicular to the axis;

hence, the optical path for these components is different. Taking a specimen of thickness 1 cm. and subject to stresses of the order found in badly annealed material, the above path difference may amount to something of the order of $0{\cdot}05\mu$—i.e. one-tenth of a wavelength for " brightest light " in the spectrum, approximately. This is well below the tolerance of the " Rayleigh limit," i.e. $0{\cdot}25\lambda$,* and the double refraction is therefore found insufficient to account for the marked effects on the image often produced by such strain in the glass from which a lens or prism is made. A further matter for consideration is found in the phenomenon described by Kerr and Pockels, i.e. the absolute increase of refractive index caused by compressional load and the decrease by tensional stress. In his measurements with a refractometer, Kerr found that in the case of compression the wave for which the vibration takes place in the plane normal to the direction of the load is subject to most retardation, being practically double that of the wave vibrating parallel to the load. Even in the absolute variation of refractive index, however, it seems that the effects will usually be too small to affect the image.

It appears probable that the most serious effects of strain lie in the slow movements in the material to which they give rise. Glass is not " solid " in the absolute sense, but must be regarded as a material of extremely high viscosity, even at ordinary temperature. The gradual movement may thus affect the figure of a lens or prism cut from the block, or may result in the fracture of the glass in the grinding or polishing operations; even after a lens is finished it may suddenly crack from the effects of internal strain accentuated by some variation of temperature.

The usual method of inspecting a specimen for the presence of strain is to hold it in the path of the light in a simple polariscope (Fig. 125). In the simplest form of the test the analyser is turned to produce a dark field, and the effects of strain are detected most readily when the direction of the stress in the specimen is at 45° to the plane of polarization.

The effects of increasing amounts of strain are a transmission of light in the formerly dark field, first grey, then yellow, red, blue, and so on, as was described in the chapter on polarization. Owing to the variation of the double refraction with wavelength, the retardation first reaches $\frac{\lambda}{2}$ in the blue end of the spectrum; light is then being restored as a greyish-blue. As the retardation of the

* Page 141.

blue increases to a whole wavelength the remaining light becomes straw-coloured, yellow, red, and so on, as the extinction travels through the spectrum. The table on page 211 shows the *relative* retardation, in microns, for sodium light. The colour produced when white light is employed as the illuminant is also given in the next column.

A piece of glass which shows no "lighting-up" in the dark field of the ordinary polariscope is perfectly suitable for the majority of optical purposes, and even those which show a faint greyness near the borders are usually tolerated. Anything like bright colour, yellow, or red, would be indicative of very bad annealing, and would be rejected.

There are one or two methods of increasing the sensitiveness of the test, which should be mentioned. The first is to place in front of the analyser a thin plate of doubly refracting material of such thickness that the retardation is nearly $1{\cdot}0\lambda$ for sodium light. This produces a violet coloration in the field, and an inspection of the table (page 211) will show that a slight change of retardation produces a considerable alteration in the hue of the field. Thus, slight strain in a glass specimen may show up as an indigo or red.

Another alternative device is to employ a comparatively intense source, such as a small arc. The light is polarized by passage through a Nicol, and an image of the source is projected by a suitable lens or mirror. If a lens is used, it must be perfectly free from strain itself. The eye is (ultimately) placed at the focus (as in Fig. 147; the polarizer and analyser are not shown), when the aperture of the lens or mirror is seen "filled with light." A Nicol analyser is held in front of the eye, rotated into the extinction position, and it will be found that the extinction is only complete in a broad cross of which the arms are respectively parallel and perpendicular to the shorter diagonal of the analyser; the field will, however, be so nearly dark that the cross will not be apparent unless a very intense source is employed. It is due to the slight radial polarization of light passing through the outer zones of the lens. However, very slight degrees of double refraction in a plate held in the path of the light will be apparent through the brightening of the field. It will be clear that the sensitiveness of this test increases with the intensity of the source, and, in fact, it is too sensitive for ordinary purposes. Such arrangements with very intense illumination are, however, of great service in testing the residual structure of fused quartz and certain glasses.

If it is desired to *measure* the amount of the double refraction due to strain, the Babinet compensator is employed.

Transparency. In common with many materials which are practically "transparent" to the visible spectrum, most optical glasses show a rapidly-increasing absorption in the ultra-violet at wavelengths lower than $0{\cdot}35\mu$. The heavy flints tend to show a yellowish hue which points to increasing absorption even in the blue regions. Various glasses* have, however, been introduced in

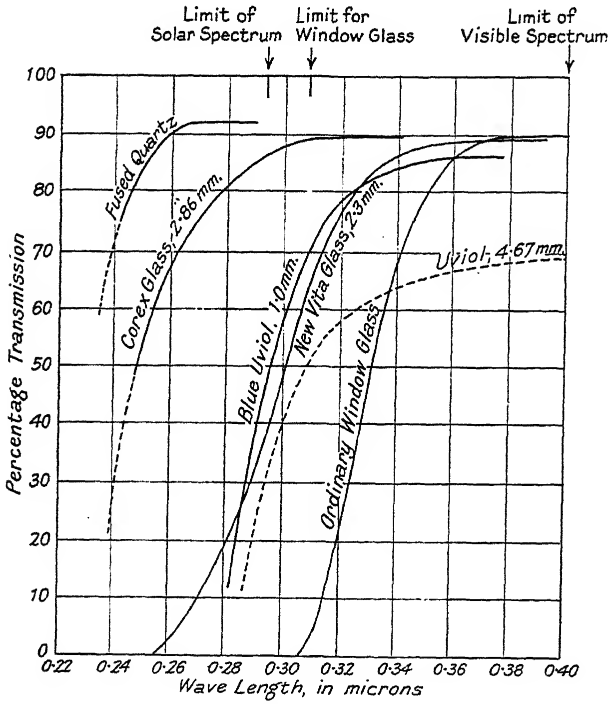

FIG. 148. ULTRA-VIOLET TRANSMISSION OF PLATES OF CERTAIN GLASSES

which the composition confers marked transparency in the ultra-violet. Some comparative results are shown in the curves of Fig. 148. Useful figures are given in Schultz's book, *Das Glas*, p. 134. where there is a table showing the chemical composition of various glasses and the limits of ultra-violet transmission. A glass "Corex" has been produced by the Corning Glass Works, U.S.A., which transmits 80 per cent in two millimetres thickness at $\lambda = 0{\cdot}275\mu$, but the

* The "Uviol glass" of the Jena Glass Works, the "Vita-glass" of Messrs. Chance Bros. & Co., Ltd., and "Holvi-glass," of Messrs. Holophane, Ltd., etc.

material has not yet been produced in an optically homogeneous condition, nor is the surface resistant to weathering.

The following transmission figures represent typical coefficients by which the energy of radiation is reduced (apart from reflection) due to the passage through 1 cm. of the glass-types quoted. (The glasses are from Schott's lists.)

Glass type: Colour:	Borate Crown (White)	Flint (White)	Dense Flint (Yellowish)	Uviol (White)
$\lambda =$				
0·644	0·990	0·992	0·944	0·988
0·578	0·995	0·995	0·957	0·988
0·546	0·995	0·995	0·934	0·991
0·509	0·993	0·994	0·911	0·991
0·480	0·990	0·992	0·860	0·991
0·436	0·987	0·984	0·779	0·982
0·405	0·990	0·987	0·766	0·977
0·366	0·920	0·895	0·754	0·945
0·334	0·710	0·430	0·49	0·895
0·312	0·171	0·00	0·03	0·520
0·302	0·00	—	0·00	0·09
0·281	—	—	—	0·00

In connection with some glasses of high transparency in the ultra-violet, it has been shown that prolonged exposure to sunlight will result in this transparency being markedly reduced.[4] In one sample, when new, the transmission at 0·302μ was about 47 per cent; after prolonged exposure to sunlight the transmission became steady at about 25 per cent.

The "Corex" glass of the Corning Glass Works has not yet been fully tested, but there is evidence that it is not affected by exposure to sunlight. The short wavelength radiations of a mercury arc are said to produce a breakdown much more quickly, but the action may not be closely parallel with that of sunlight.

Slight coloration in glass always indicates appreciable absorption in some region of the visible spectrum. Its most usual cause is iron from the sand, or from the walls of the pot, but other impurities, such as cobalt, copper, chromium, nickel, manganese, or vanadium, may introduce coloration. "Ferrous" iron produces a green coloration which is more marked than the yellowish coloration produced when the iron becomes oxidized to the ferric condition. Success in optical glass production largely depends on the successful removal of such impurities.

The reflection coefficients for a glass surface (refractive index n) was given in the chapter on polarization as $\beta = \frac{(n-1)^2}{(n+1)^2}$. This is

only valid for a perfectly clean surface. H. Dennis Taylor[5] found in 1892 that the loss by reflection can be considerably diminished by tarnishing the surface. Flint glass can be tarnished readily by alkaline sulphides. Kollmorgen[6] has claimed to be able to decrease the amount of light lost in an ordinary flint or barium crown lens from about 10 per cent to 4 per cent. Further work has been carried out by Ferguson and Wright,[3] who cite, amongst other solutions, a 1 per cent aqueous solution of acid sodium phosphate acting for 18 hours at 80° C. as effective for light flint glass. They discuss the cause of this effect, and attribute it to a minute pitting of the polished surface; the pits being small in comparison with the wavelength of light.

Let $k = (1 - \beta)$ be the transmission factor of the surface of a glass block with plane parallel faces, and of thickness t. Imagining parallel light incident normally on the block, the intensity I_0 of the radiation before entering the first surface will be diminished, through reflection, to kI_0 immediately on entering. The amount finally transmitted by the block will be

$$(1 - \beta)^2 I_0 e^{-\alpha t}$$

where α is the absorption coefficient and e is the base of natural logarithms. Some of the light reflected back at the second surface is again sent forward by the first surface. Additional amounts sent forward in this way by internal reflections are

$$(1 - \beta)^2\beta^2 I_0 e^{-3\alpha t}, \quad (1 - \beta)^2\beta^4 I_0 e^{-5\alpha t},$$

the total amount I being

$$\begin{aligned} I &= (1 - \beta)^2 I_0 e^{-\alpha t}(1 + \beta^2 e^{-2\alpha t} + \beta^4 e^{-4\alpha t} + \text{etc.}) \\ &= (1 - \beta)^2 I_0 e^{-\alpha t}(1 - \beta^2 e^{-2\alpha t})^{-1} \end{aligned}$$

For most practical purposes the value of the right-hand bracket may be taken as unity; β is approximately 0·05 for glass, and $e^{-2\alpha t}$ is naturally never greater than unity.

A practical formula for the transmitted light is

$$I = (1 - \beta)^2 I_0 10^{-xt}$$

where x is the "extinction coefficient."

The loss of light by surface reflection in an instrument with many surfaces is extremely serious. Stokes gives figures for the light transmitted and reflected by a number of plates.[7] In the first case (a) there is no absorption in the material of the plate; in the second case (b) each plate absorbs 2 per cent of the energy.

LIGHT TRANSMITTED AND REFLECTED BY GLASS PLATES (NORMAL INCIDENCE)

Number of Plates	Transmitted Light		Reflected Light	
	Case (*a*)	Case (*b*)	Case (*a*)	Case (*b*)
1	0·918	0·900	0·082	0·080
2	0·849	0·815	0·151	0·145
4	0·738	0·679	0·262	0·244
8	0·584	0·490	0·416	0·364
16	0·413	0·276	0·587	0·464
32	0·260	0·097	0·740	0·509

These figures are quoted from a very complete table furnished by Stokes, showing the proportion of polarized and ordinary light reflected at various angles. The results in actual optical instruments are greatly modified from the above by reason of the tendency for the oblique incidence of light on the surfaces, which mainly tends to increase the reflection effects.

It not infrequently happens that the doubly internally reflected light is concentrated, as by reflection at a concave surface or the like, into a small area near the final image plane for the system (the phenomenon is called a "ghost"). In these circumstances it may be extremely objectionable, and it is sometimes difficult to trace its origin.

The above table indicates the extreme desirability of restricting the number of reflecting surfaces to the minimum. As an example of the action, it is well-known that small hand cameras furnished with a single lens yield images of greater contrast than those possessing more complex and expensive lenses, even although the definition of detail is improved and the exposure reduced with the "better" lenses.

In the practical measurement of absorption or extinction coefficients the ratio of I to I_0 can be measured with the aid of a spectrophotometer[8] for two different thicknesses of the same material t_1 and t_2.

The equations are

$$I_1 = (1 - \beta)^2 I_0 10^{-xt_1}$$
$$I_2 = (1 - \beta)^2 I_0 10^{-xt_2}$$

Whence
$$\frac{I_1}{I_2} = 10^{x(t_2 - t_1)}$$

or
$$x = \frac{\log_{10}\left(\frac{I_1}{I_2}\right)}{t_2 - t_1}$$

Coloured Glasses. Light Filters. Glass may be coloured by the use of various metallic compounds, some of which seem to impart their colour directly as solutions in the glass. Others produce the coloration by the "excretion" of colloidal particles in the material. Various metallic oxides, cobalt, nickel, iron, copper, chromium, manganese, and uranium belong to the first group of these direct-colouring materials, while cuprous oxide, gold, and selenium are examples of the second group.

The following table shows some of the materials used in particular cases—

Colour	*Material*
Red	Cuprous oxide, selenium.
Purple	Gold (metallic).
Rose	Selenium and its compounds.
Violet or amethyst	Manganese oxide, nickel oxide.
Yellow	Cadmium sulphide, uranium oxide, ferric oxide, nickel oxide, carbon, metallic silver.
Green	Cupric oxide, chromium oxide, ferrous oxide.
Blue	Cobalt oxide, copper oxide.

Coloured glasses can be obtained commercially from various firms, and their production, which was at one time somewhat uncertain, has become capable of more precise control. Particulars have been published[9] by Zsigmondy and by Grebe for various-coloured glasses produced by the Jena Glass Works, which include glasses designed to transmit special limited regions of the spectrum as for railway signalling, three-colour printing, photography, filters for use with panchromatic plates, and the like.

An important use of coloured glass is for eye-protective spectacles. These are required by furnace workers, welders, and others to protect the eyes from the intense light and heat radiations (infra-red) which are liable to produce cataract. Extensive researches on the production of suitable glasses were carried out by Crookes,[10] who found that green glass containing ferrous iron absorbs the infra-red very strongly. A good absorption of the infra-red is shown by glasses containing cupric oxide, and cobalt with ferric iron, according to measurements by the present writer,[11] who also suggested the use of gold-coated glass for such protective spectacles. Such are now obtainable commercially.

Persons who have to deal with light sources rich in ultra-violet radiation, such as are now used extensively for clinical purposes, require light-filters which will effectively stop all those radiations of wavelength shorter than about $0{\cdot}38\mu$ showing increasing "abiotic" action with decreasing wavelength, which may damage delicate tissues and, in particular, cause marked inflammation of the moist surfaces of the eyeball and eyelids (conjunctivitis). The work of

Crookes, who experimented with glass containing cerium, lead, neodymium, and praseodymium, etc., in addition to the substances mentioned above, showed that cerium conferred marked powers of absorption in the ultra-violet while not greatly affecting the transmission of the visible wavelengths.[12] Various glasses of secret composition are sold commercially under the name of Crookes'

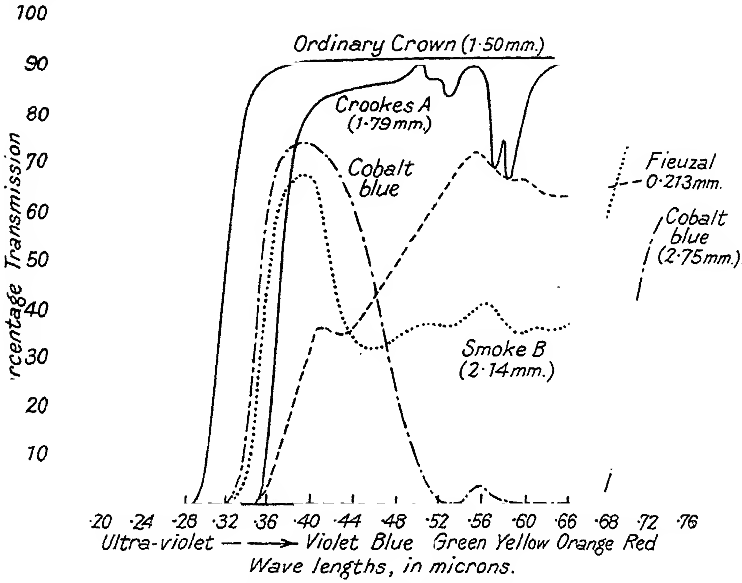

FIG. 149. TRANSMISSION OF VARIOUS GLASSES FOR EYE-PROTECTION

glasses. In many cases, of course, the intensity of the visible radiation has to be reduced for the sake of comfort.

In very bright sunlight, in the tropics, or by the sea, and especially on the mountain snows, the relative intensity of the ultra-violet in sunlight may increase considerably, though ozone absorption is held to account for the absence of the more harmful radiations of wavelengths below 0·295μ. In such conditions spectacles which eliminate the ultra-violet and preferably somewhat reduce the intensity of the visible light are found very useful.

Useful information on the relative transmission of coloured glasses and light filters has been given[13] by Gibson, Tyndall, and McNicholas, whose investigations have covered the visible and ultra-violet regions of the spectrum. Some typical results of interest are given in Fig. 149.

Optical Work—Lens Blanks. Optical glass arrives from the glass

works in the form of small slabs, or, sometimes, moulded blanks, for which the glass has been pressed when plastic into the rough shapes of the lenses. The slabs were reduced, in the method usually employed until recent times, by "a slitting machine," to square pieces of a required diameter and thickness. This machine employs a rotating iron disc, the cutting edge of the disc being charged with diamond dust. The square pieces were then reduced to a fairly circular form by the use of "shanks," a tool slightly resembling a

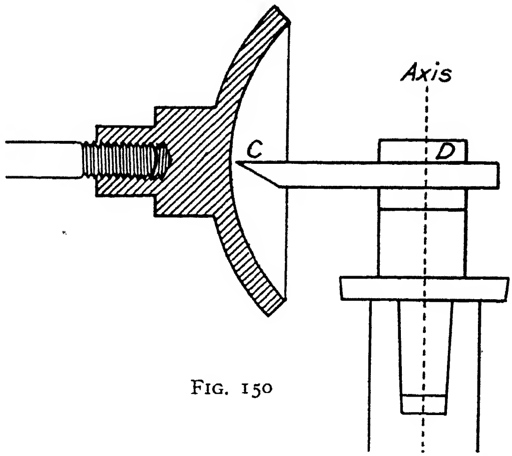

FIG. 150

pair of nut-crackers. The blanks were then cemented together, and the resulting "roll" was made truly cylindrical by grinding, thus producing a number of circular discs. In some modern works, however, the circular pieces are cut directly from the slabs by means of tubular cutters.

Slabs up to $\frac{3}{4}$ in. thickness are sometimes cut up by first making a fairly deep cut with a glazier's diamond, and then pressing along the line of the cut with an iron rod heated almost to redness.

Blanks for spectacles are often made by first rolling the melt into plates; these are inspected for bubbles and other defects, which are avoided when the plate is cut up (with a diamond) into pieces of the right weight. The pieces are then heated, and moulded in suitable dies approximately to the curves required; the moulded blanks are then annealed at a temperature which allows relief of internal strain while the "figure" is retained. If necessary, the blank is roughly ground to its required curvature, either by a coarse abrasive on an iron grinding tool, or by an abrasive wheel.

✓ **Grinding and Polishing.** The process of optical grinding and polishing of spherical surfaces depends on the fact that a pair of

spherical surfaces are the only ones which will fit each other in all relative positions. The grinding tools are of iron and are made to screw to the spindle of the grinding machine. The spherical surface is first prepared on a lathe, as shown in Fig. 150. The grinding "tool" shown, shaded, in section, is rotating about a horizontal axis, while a cutter C is mounted on a "slide rest" which enables it to rotate about the vertical axis. The distance CD in the figure determines the radius of the resulting surface.

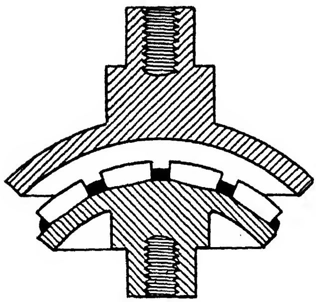

FIG. 151

An optical factory keeps a wide range of these tools, always in pairs, convex and concave. The figures of the surfaces are perfected by grinding them together.

Small glass surfaces of very short radius, and very large surfaces, are ground singly, but for small lenses of medium curvature a number of lenses, from three upwards, may be ground while mounted on the same "block." In the preparation of the block, a suitable mounting or "blocking" tool is selected, and the separate lenses are mounted on the surface with warm pitch, as suggested in Fig. 151. The top surfaces of the blank will have been "roughed" to the correct curvature and an iron tool of the required radius can then be brought down so as to bring the different surfaces into the same spherical locus, while the pitch is still soft; when it has hardened, the grinding operations begin, using the top tool and the block of lenses.

Different methods of blocking are often adopted, especially for prisms, which are usually blocked together in plaster.

The abrasives used in grinding are usually emery or carborundum. These powders are graded by screening for the coarse varieties and by elutriation in water for the finer ones, so that a series of grades having different-sized particles is available. Grinding begins with the coarse abrasive, introduced wet between the tool and the block, which are kept in constant relative motion; the section of a roughly-ground glass surface might be represented, perhaps, if highly magnified, something like the top line in Fig. 152.* After a time the

* Since Fig. 152 was drawn, further observations with the microscope have led the writer to believe that Fig. 152A considerably exaggerates the number of high spots in the average coarse ground surface. It is very difficult to get a real profile edge for observation, and the figures (although based on evidence) are not drawn from any actual specimens, but are to some extent hypothetical.

top of the "peaks," where most wear is experienced through the rolling of the particles of abrasive, become reduced in height, and we might have a section something like the second line, where the same deeper pits and cracks are still to be recognized. If an undue amount of coarse abrasive should be fed on at this stage there may be a production of deeper cracks than the worst of the original

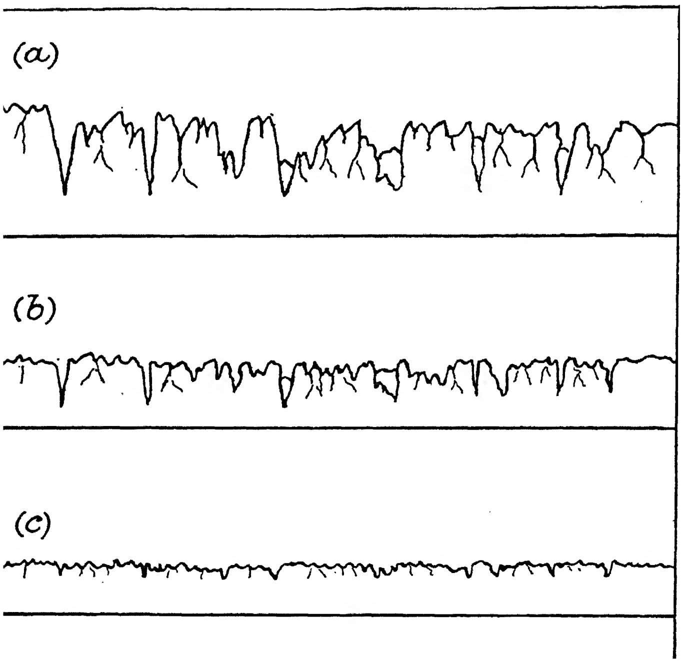

FIG. 152. SKETCHES TO ILLUSTRATE STAGES IN THE GRINDING PROCESS (HYPOTHETICAL)

number. Hence, it is very important that the abrasive shall not contain occasional particles which are much larger than the average size (as is sometimes the case in badly-graded samples). Further application of finer and finer grades should bring the surface down to a state in which there is a uniformly fine grain, no unusually deep cracks or pits being left; if such should accidentally be made, some amount of re-grinding is necessary. The final nature of the grain (before polishing) is supposed to be a flaw-and-fissure complex, in which some of the fissures are wedged open by the displacements of parts of the material, thus throwing the surface regions into a state of strain. Such strain has actually been experimentally observed.

It is not difficult to estimate the fineness to which outstanding irregularities must be reduced before the surface has the characteristic appearance (or *non-appearance*) of perfect polish. In previous work we have seen that vibratory disturbances must arrive in a focus with a difference of path not exceeding $\frac{\lambda}{4}$ if the effect on the image is not to be perceptible.

The thick parabola in Fig. 153 shows an imaginary perfect parabolic reflecting surface, and WW_0 an incident plane wave-front, the ray directions being parallel to the axis; hence, the paths WAF and W_0A_0F are identical. If a bump of thickness d is pushed out from the surface at A, the disturbance now meets the reflector in the point A′, which acts as a secondary centre of disturbances. The relative path difference is found (in a similar manner to the argument for reflection at a thin film) to be $2d \cos i$ where i is the angle of incidence. The greater the angle of incidence, the greater the allowable value of d; hence, a surface which is only partly polished will reflect red light better than blue. This has been used as a method of estimating the relative state of fineness of a surface.

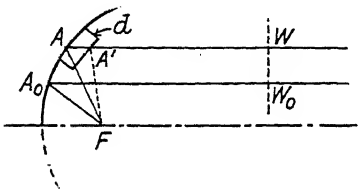

FIG. 153. EFFECT OF SURFACE ELEVATION

In the case of a transmitting surface, the path difference arising through a similar elevation d may be expressed as $\frac{d(n - \cos \overline{i' - i})}{\cos i}$ where i and i' are the angles of incidence in glass and air respectively, and n is the refractive index of the glass.

Hence, we see that for a reflecting surface with normal incidence the condition is

$$2d < \frac{\lambda}{4} \text{ or } d < \frac{\lambda}{8}$$

For a transmitting surface, normal transmission,

$$d(n - 1) < \frac{\lambda}{4} \text{ or } d < \frac{\lambda}{2} \text{ approx. where } n = 1{\cdot}5.$$

The requirements of perfection of the surface are evidently not so strict for transmission as for reflection, but in either case the outstanding irregularities must be small in comparison with the wavelength of light.

In a good fine-ground surface the grain of the structure is about five to six wavelengths deep. Lord Rayleigh has shown that glass is actually removed to about this depth during the polishing operation. It is, therefore, as mentioned above, of the greatest importance that the abrasive shall be uniform so as to prevent the formation of deep pits. With badly-graded carborundum, pits and cracks up

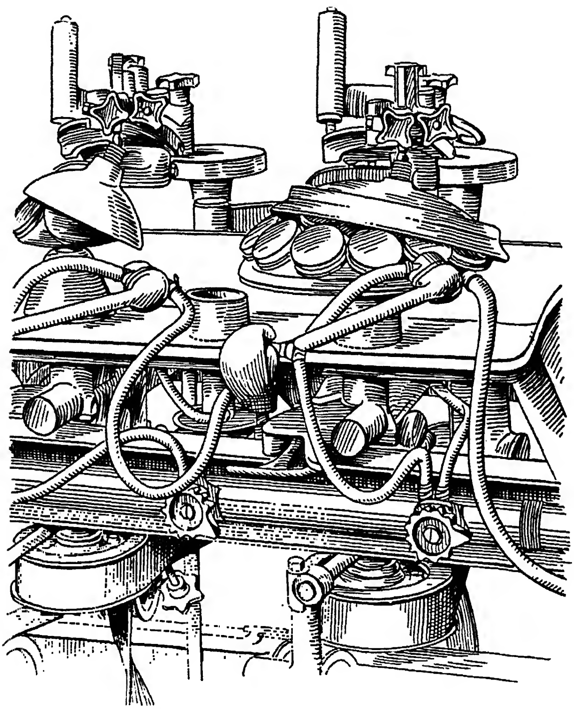

FIG. 154*a*. A MODERN BENCH OF POLISHING SPINDLES

to fifteen wavelengths may be encountered. The "Sira" abrasive developed by the British Scientific Instrument Research Association is especially useful in this respect; the grain is very uniform in size, hence no very deep pits are produced and, owing to the absence of deeper pits, the time of polishing can be very much shortened.

Polishing is performed by rubbing the fine-ground surface on a polisher of pitch carrying wet rouge or putty powder as a polishing medium which is, in reality, a *very* fine grained abrasive.

The pitch polisher is made by covering the surface of a tool having very nearly the required radius with melted pitch (suitably tempered

in hardness by mixture with other ingredients such as resin or turpentine), which is moulded, as it cools, into a curve of the true required radius by pressure against the appropriate iron tool.

A number of V-shaped grooves may be cut into the surface of the polisher, partly for the collection of debris, and also to relieve the wear on certain parts of the surface, as will be explained.

In early days the grinding and polishing operations were carried out by hand. The operator mounted the "work" on a post and moved the grinding and polishing tools by hand. In the modern machine the block of lenses is rotated on a vertical spindle, while the tool may be given a motion by a pin attached to a crank. A bench of spindles is shown in Fig. 154*a*.

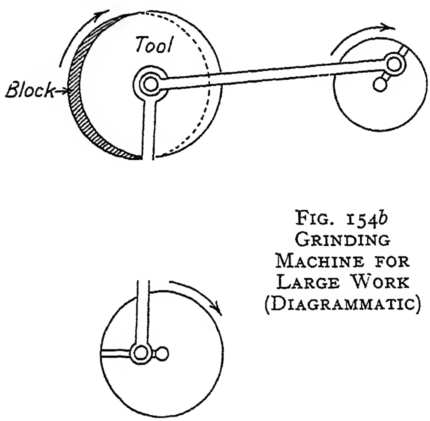

FIG. 154*b*
GRINDING MACHINE FOR LARGE WORK (DIAGRAMMATIC)

During the polishing process the surfaces of the polisher and the glass are periodically supplied with rouge and water; it is the practice to let the surfaces get *almost* dry before putting on a fresh supply. In these machines, made by Messrs. Taylor, Taylor & Hobson, Ltd., of Leicester, the extra torque on the spindle, which occurs when the work gets dry, automatically works a squirt, thus supplying the necessary moisture.

Fig. 154*b* is to illustrate the principle of the type of machine employed for polishing large surfaces—astronomical mirrors and objectives. The block, or surface, is rotated steadily on a vertical axis while the tool is given cross movements by one or two cranks while free to rotate independently. The combination of the cross movements can be arranged in almost any way by varying the eccentricities and relative speeds of the cranks, thus producing circular, elliptical, "figure of eight," and other movements as required.

Control of Figure. As soon as a reasonable degree of polish appears, the form of the surface can be tested by means of a "test plate," a method introduced by Fraunhofer. This is a piece of glass, one side of which has been worked to the radius required and is truly spherical, but opposite in curvature to the surface to be tested. A set of convex lenses on the block would be tested with a concave test plate. Both surfaces being wiped clean, the test plate is slid into

contact so closely that the interference colours can be observed in the thin film between them. Precautions have to be taken regarding the temperature of the blocked lenses. If the latter prove to be (say) too convex, circular coloured rings may be observed. Sometimes the direction of greater thickness in the film can be inferred from the progression of the colours (see Quincke's Table, page 211), but if this fails, another simple test is to move the head so that the light is reflected at a greater angle of incidence and watch the movements of the rings. The retardation in the film is given by $2d \cos i$ where i is the angle of incidence in the air film. If i increases the retardation decreases; to compensate for this, the fringes will move towards a thicker part of the film. Thus, if the blocked lenses are too convex

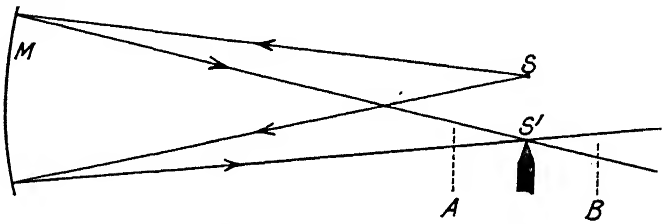

FIG. 155. THE FOUCAULT KNIFE-EDGE TEST

and make contact in the centre of the test plate, the rings will move outwards when the above test is made.

When large surfaces are polished, say 12 in. in diameter and over, for large telescope object-glasses, telescope mirrors, and the like, the testing of the figure is not so conveniently done with a test plate; with concave surfaces of long radius the test is usually made by the Foucault knife-edge method, illustrated in Fig. 155. A small source of light S (a pinhole in metal foil illuminated by a lamp-flame is adequate) is imaged by the concave mirror M at S′. An eye placed close behind this image receives light from all points on the mirror, which thus appears evenly illuminated. If a knife-edge is brought across the exact focus the light from all points is cut off uniformly; if introduced at A the shadow appears to move upwards; if at B the shadow moves downwards. It is thus easy to fix the exact focus of a spherical mirror with considerable precision or even to determine the possible differences of the foci of successive annular zones with the aid of cardboard diaphragms. If the mirror is parabolic the whole gives a characteristic shadow figure, Fig. 156, and the distance between the foci of central and marginal portions is $\frac{y^2}{r}$ where y is the radius of the circular aperture and r the radius

of the curved surface. The whole method of the test will be found well described in Ellison's *Amateur's Telescope*. The ease of making this test makes the optician able to produce concave surfaces of great accuracy with more certainty than the corresponding convex ones.

Having by some means or other tested the curvature of the surfaces undergoing the polishing process and thus knowing the tendency of the "figure" in formation, it is possible by various means to control the final result.

Fig. 157 suggests, by the full circle, a surface being polished; it is mounted to rotate on a central spindle and the polishing tool,

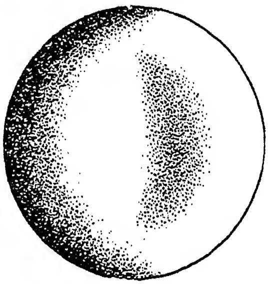

FIG. 156. CHARACTERISTIC SHADOW FIGURE GIVEN BY A PARABOLOIDAL SURFACE IN THE FOUCAULT KNIFE-EDGE TEST

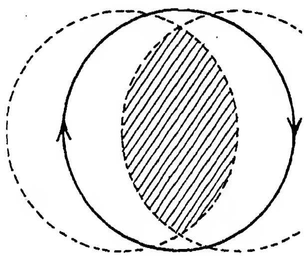

FIG. 157

surfaced with pitch, swings over it backwards and forwards between its extreme positions in which the tool considerably overlaps the surface. It will be seen that while the central parts of the surface are always in contact with some part of the tool, the exterior portions are uncovered for a fraction of the time of each stroke. To some extent the consequent tendency for this to lessen the "wear" on the edges of the surface is counteracted by the higher relative velocity of the outer parts in rotation, but it can be accentuated by increasing the amplitude of the stroke or vice versa. Thus, if the surface being polished is concave and the radius of the outer zones appears to be too short, the wear of the edges must be increased, and this can be done by diminishing the stroke.

The surface of the pitch polisher, too, is always broken to some extent to form cavities in which superfluous water, rouge, and debris can escape, leaving only the thinnest film between pitch and glass. Especially when dealing with small surfaces, more pitch can be removed from near the central or marginal portions of the

polisher when it is desired to lessen the wear towards the centre or edge respectively, or to correct some zonal irregularity.

It is by the aid of methods of this kind, carefully controlled, that a concave mirror can be gradually made to take a parabolic curvature. Elliptic or hyperbolic figures can be produced if required, but except for special purposes spherical curves are of the greatest importance for small surfaces. The exceptions are cylindrical and toroidal forms for spectacle lenses, and non-spherical surfaces of revolution (of which the principal section may be a curve of the fourth degree) for certain high-power spectacle lenses used for eyes from which the lens has been removed for cataract. Similar curves are employed on lenses of greater diameter for use in highly-corrected spectrographs.

✓ **Cylindrical and Toric Surfaces.** The general freedom of movement in grinding and polishing cylindrical surfaces is naturally much more restricted than for spherical surfaces, but the corresponding standard of accuracy need not usually be attained for the modest requirements of spectacle lenses. Motion in grinding or polishing is restricted to a rotary movement of the cylinder (represented by the blocked-up lenses) about the cylindrical axis, combined with a movement of the tool, to and fro, parallel to this axis. The rotation may be only backwards and forwards through a definite angle, or may be continuous, depending on the design of the machine and the methods adopted. A good idea of the action may be obtained if the palm and fingers of the right hand rub the wrist of the left hand parallel with the direction of the forearm, while the left hand twists backwards and forwards.*

The toric surface is one in which the curvature is different in the principal sections, just as in a pneumatic tyre. The radius in one section of a tyre is the radius of the wheel; in the other direction it is the radius of the circular section of the tube. This is, of course, a case in which the difference is extremely accentuated, and in most forms of lenses the radii are more nearly equal. Here the relative movement of block and tool is much more restricted. The block of lenses (often a complete ring) represents the tyre, while the tool could be represented by a "cast" of a portion of the outer surface of the tyre.

In practice, the movement of the tool is limited to comparatively small arcs of rotation about an axis which would be represented (on the tyre analogy) by a short length of the central axis of the tube; this is combined with the circular movement of the block about the axis of symmetry.

* As in turning a screw.

Figuring. Various methods have been employed in producing non-spherical surfaces of rotation, from quite early times. An account of machines for constructing elliptical, parabolic, or hyperbolic surfaces, devised by Fraunhofer before 1814, will be found in a reprint[14] recently issued. In this case, the grinding and polishing tools hang as pendulums, their motion being controlled by a ring bearing on a non-spherical pivot. Annular grinding tools and local rubbing with hand polishing pads have also been employed, but it is not within the writer's knowledge that any success has been achieved in making such work automatic, or free from the necessity of the most careful control by frequent optical tests, by test plate, interferometer, or the like.[15]

The most serious defects in many well-made lens systems like telescope object glasses (and, in fact, in many microscope objectives) are not defects of optical aberration as usually understood, i.e. those calculable from the radii of curvature, refractive indices, and separations of the components. They are the defects arising from the irregularities of construction, lack of homogeneity of the components, lack of true centering, and the like. They are responsible for the lack of adequate concentration of the light in the image, and are revealed at once by the interferometer or the "star test." Either of these methods, but especially the first in this case, may indicate to the experienced optician the possible necessity of *local* figuring (often done by local rubbing with a chamois leather pad charged with rouge) which is the final stage in the making of many of the finest and most perfect lenses. Prisms also are subjected to treatment of this kind.

Centring of Lenses. When the two surfaces of a lens are polished it is usually necessary to give it an edge which is concentric with the optical axis. Unless this is done, the axis would evidently be tilted when placed in a circular mount, and it would be impossible to get the lens coaxial with other lenses of the instrument. A piece of tubing is spun in a lathe and the edge is turned down, rounded and smooth, so that it runs perfectly true. The diameter of the tube is somewhat smaller than the lens. The tube being warmed, the lens can be mounted on it with sealing-wax, or a cement with a basis of pitch, and adjusted by pressure with a wooden peg while rotating, so that the glass surfaces run true also. This is indicated by the steadiness of the reflected images. The edge of the glass may then be ground down true by wet-grinding with carborundum, the "grinding tool" being a piece of sheet brass, usually bent into an angle plate so that contact is made in two places. The abrasive in water should continually drop between the stationary brass and

the edge, while the latter is rotating at a high speed. In this way the diameter of the lens is reduced to the exact value required.

REFERENCES

1. *Ann. d. Phys.*, 54 (1895), 476.
2. *Trans. Opt. Soc.*, 19 (1917–18), 97.
3. Washington, Ordnance Department Document No. 2037. See also Marson's *Glass* (Pitman's "Common Commodities and Industries" Series).
4. Bureau of Standards, U.S.A., Letter Circular No. 235. *Journal of Franklin Institute*, March, 1928.
5. *Adjustment and Testing of Telescope Objectives* (Messrs. Cooke, Troughton & Sims., Ltd.).
6. *Trans. Ill. Eng. Soc. America*, 2 (1916), 220.
7. Stokes: *Phil. Mag.* (4), 24 (1862), 480–485.
8. See Martin: *Optical Measuring Instruments*, Chapter XII.
9. R. Zsigmondy: *Ann. d. Phys.*, 4 (1901), 60; *Zeit. f. Inst.*, 21 (1901), 97. C. Grebe: *Zeit. f. Inst.*, 21 (1901), 101.
10. Crookes: *Phil Trans. A.*, 214 (1914), 1.
11. Martin: *Trans. Opt. Soc.*, XVIII (1917), 31.
12. Taylor (U.S. Patents 1,292,147 and 1,292,148) cites titanium oxide as the essential constituent of certain glasses for absorbing the ultra-violet.
13. Gibson and McNicholas: Bureau of Standards, U.S.A., Technologic Paper No. 118 (on "Eye-Protective Glasses"). Gibson, Tyndall, and McNicholas: Bureau of Standards, U.S.A., Technologic Paper No. 148 (on "Coloured Glasses").
14. *Forschungen zur Geschicte der Optik*, 1 Band., 2 Heft., p. 42 (Julius Springer, Berlin).
15. Machines have been constructed of sufficient accuracy to grind and polish parabolic reflectors for searchlights, motor-car headlights, etc., but not for use in accurate optical instruments.

CHAPTER VIII

SPECTACLES

THE extremely large amplitude of accommodation in youthful eyes is not maintained with advancing years. At 10 years a child can often focus on an object about 7 cm. distance from the eye, but at 40 years no object closer than about 20 cm. can usually be clearly seen by a normal eye which can, however, sharply focus very distant objects. The nearest point for distinct vision is termed the "near point" of accommodation; the point which the eye sees clearly with the accommodation entirely relaxed is the "far point of accommodation."

We shall adopt the usual "left to right" direction of light with the eye "looking" from right to left, so that the distance of the near point for a young normal eye will be negative, and the distance of the far point will be "$-\infty$." At the age of 55, or over, the eye may lose so much refractive power that, when unaccommodated, the incident light must be slightly convergent to arrive in a sharp focus on the retina. The far point is then behind the eye; its distance has the positive sign.

The following table (after Donders) shows the position of the near point and the far point for average normal vision at different ages, the distances being measured in centimetres. If the reciprocals of these distances expressed in metres be computed, and their difference taken, the result gives the difference in power, expressed in diopters, of the optical system of the eye when accommodated for the near and far points respectively.

The following symbols will be used—

Position of the macula	M'
Far point (punctum remotum) . . .	M_R
Near point (punctum proximum) . .	M_P
Distance from 1st principal point of eye to far point	$= k$
,, ,, ,, ,, ,, ,, . ,, near ,,	$= b$

The reciprocal of the distance from the 1st principal point to the far point is termed the "principal point refraction" or "ocular refraction," and is denoted by

$$\mathcal{K} = \frac{1}{k}$$

If k is expressed in metres $\mathcal{K}$ will be expressed in diopters. It is

to be noted that M′ will be a conjugate point to M_R in the unaccommodated eye, and to M_P in the fully accommodated eye. The *Amplitude of Accommodation*, A, is the difference $\left(\frac{1}{k} - \frac{1}{b}\right)$

TABLE

Age in Years	Distance of Near Points in cm. (b)	Distance of Far Point in cm. (k)	Amplitude of Accommodation in diopters $A = \left(\frac{1}{k} - \frac{1}{b}\right)$
10	− 7·1	∞	14
15	− 8·3	∞	12
20	− 10·0	∞	10
25	− 11·8	∞	8·5
30	− 14·3	∞	7·0
35	− 18·2	∞	5·5
40	− 22·2	∞	4·5
45	− 28·6	∞	3·5
50	− 40·0	∞	2·5
55	− 66·6	400	1·75
60	− 200	200	1·0
65	+ 400	133	0·5
70	100	80	0·25
75	57·1	57·1	0·0
80	40	40	0·0

Normal vision with the far point at ∞ is termed the condition of *Emmetropia*. The condition of vision characteristic of age is signified by the term *Presbyopia*. Donders applied this term particularly to cases of vision in which the near point withdraws beyond − 22 cm. approximately, which usually occurs at about 40 years of age.

The condition in which the far point lies behind the eye is known as *Hypermetropia*; then the condition generally developing after age 50 in a normal eye is "acquired hypermetropia."

In the following section the unaccommodated condition of the eye will be assumed. There are various common defects of the eye, the results of which can be alleviated with the aid of spectacles.

Hypermetropia,* in which the far point lies behind the eye, may result from too short an axial length of the eye-ball, or in some cases from a flattening of the cornea, or an abnormal refractive index in one of the media. The eye can only bring to a focus on the retina such rays as are already slightly convergent (i.e. to the far point)

* Sometimes shortened to "Hyperopia."

when they reach the cornea. Parallel incident rays fail to reach a focus as shown by the broken lines in Fig. 158A.

Myopia, in which the far point lies in front of the eye, but at a finite distance, may result from an unduly great anatomical length of the eye-ball, or from too great curvature of the cornea, etc. Thus,

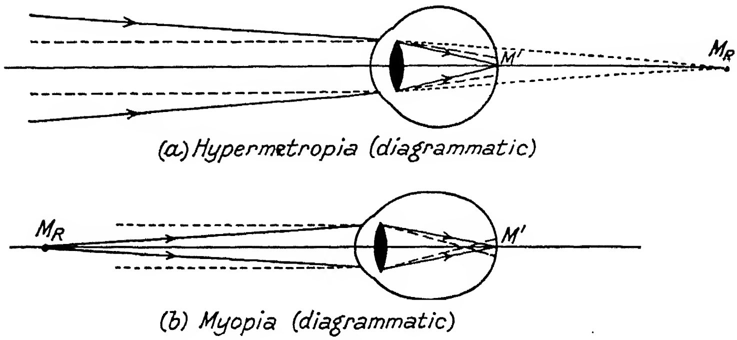

FIG. 158

parallel rays entering the cornea are brought to a focus before reaching the retina, but rays which are still divergent (i.e. from the far point) are focussed at the macula. See Fig. 158B.

Astigmatism arises very frequently from a difference of curvature of the cornea in its various meridians, i.e. sections by planes containing the optical axis. It may also arise from similar defects in the

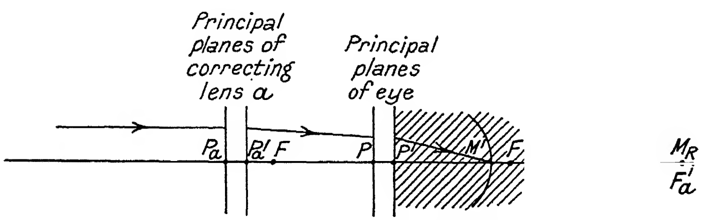

FIG. 159. DIAGRAM TO ILLUSTRATE THE CORRECTION OF A HYPERMETROPIC EYE

(The shading is to indicate that the points M′ and F′, the macular and second principal focus of the eye respectively, are referred to the medium of the image space, i.e. the vitreous humour. The curve passing through M′ is to indicate the retinal surface.)

lens. Thus, the refraction of the eye is different in various sectional planes or meridians, and the position of the far point will vary with the meridian. If the astigmatism is regular there will be two perpendicular meridians in which the maximum and minimum values of the refraction are found. This axial astigmatism must not be

confused with the astigmatism of oblique pencils, which latter only affects images formed away from the optical axis.

Spectacles for Distance Vision. In cases of hypermetropia and myopia *the function of the spectacle lens is to project an image of an infinitely distant (axial) object into the far point, which must therefore coincide with the second principal focus of the spectacle lens.* Thus, in Fig. 159, the points P and P′ are the principal points of a hypermetropic eye of which M′ and F′ (imagined both to lie in the same image space medium) are the macula on the retina, and the second principal focus of the eye respectively. The principal points and second principal focus of the lens a—P_a, P'_a, and F'_a are shown. Incident parallel light falling on lens a is converged towards the

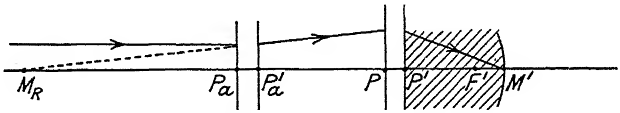

FIG. 160. CORRECTION OF A MYOPIC EYE

second principal focus F'_a; if this coincides with the far point of the eye M_R, the optical system of the eye will bring the light to a focus at M′, since M′ and M_R are conjugate points.

Writing $PM_R = k$, $\mathcal{K} = \frac{1}{k}$, and if $P'_aP = d$, the focal length of lens a is given by

$$f'_a = d + k$$

This may be written

$$f'_a = k\left(1 + \frac{d}{k}\right) = \frac{1 + d\mathcal{K}}{\mathcal{K}}$$

and in accordance with the usual notation, in which $\mathcal{F}_a$ is the power of the correcting lens,

$$\mathcal{F}_a = \frac{\mathcal{K}}{1 + d\mathcal{K}} \quad . \quad . \quad . \quad . \quad (70)$$

The correcting lens necessary in hypermetropia is clearly of the converging type with a positive power.

The correction of a myopic eye is illustrated by Fig. 160. M_R is now to the left of the eye, at a distance which is numerically negative, and the lens required is therefore one of a diverging type, of negative power, with its second principal focus at M_R. The form of the equations remains the same as those given above.

It is *again* to be noted that lengths in such an equation must be expressed in metres if the powers are given in diopters.

Examples of the Practical Use of such Equations. 1. An eye with a principal point refraction of $+ 4{\cdot}25$D is to be corrected by a lens which is to be placed so that its second principal point is at a distance of 14 mm. in front of the first principal point of the eye. Find the power of the lens required.

$$\mathscr{F} = \frac{4{\cdot}25}{1 + (0{\cdot}014)(4{\cdot}25)} = 4{\cdot}01\text{D}$$

2. It is found that an unaccommodated myopic eye is enabled to view distant objects distinctly with a lens of -8D when the distance between the adjacent principal points of lens and eye is 11 mm. Find the principal point refraction of the eye and the position of the far point.

In this case an alternative equation would be more useful. Since

$$f' = d + k$$

$$k = f' - d = f'\left(1 - \frac{d}{f'}\right) = f'(1 - d\mathscr{F})$$

and $$\mathscr{K} = \frac{\mathscr{F}}{1 - d\mathscr{F}}$$

In our numerical case

$$\mathscr{K} = \frac{-8}{1 - ({\cdot}011)(-8)} = \frac{-8}{1{\cdot}088} = -7{\cdot}35\text{D}$$

and $$k = \frac{1}{-7{\cdot}35}\text{ metres} = -13{\cdot}6\text{ cm.}$$

Lenses which produce a true distance correction for the same eye when properly positioned are said to possess the same "effectivity." They have the same effective power at the eye.

Vertex Refractions. The practical aspect of the problem is somewhat simplified if distances are measured from the vertices of the refracting surfaces. Fig. 161 represents the correction of hypermetropia. A_1, A_2 and A_3 are the consecutive surfaces of the lens a and of the eye. M_R coincides with F'_a as before. Then

$$A_2F'_a = A_2A_3 + A_3F'_a$$

or $$f'_v = d_v + k_v$$

where d_v is the distance between adjacent vertices of lens and eye, and k_v is the distance from the vertex of the eye to the far point.

This equation becomes (as above), employing the suffix v to denote the reciprocals of the vertex distances,

$$\mathcal{K}_v = \frac{\quad}{1 - d_n}$$

where $$\mathcal{K}_v = \frac{1}{k_v} \text{ and } \mathcal{F}_v = \frac{1}{f'_v}$$

Hence, if the back vertex focal length (f'_v) or vertex power $\mathcal{F}_v$ of a correcting lens is accurately known, the distance k_v of the far point from the vertex of the cornea can be found directly; this is the "vertex refraction," or "refraction referred to the cornea."

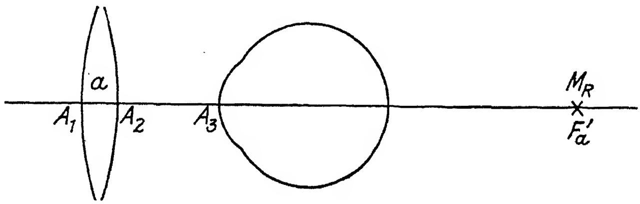

FIG. 161

Two important steps in the determination of the required spectacles for an ametropic eye are—

1. Examination to find the power of a lens which corrects vision when held at a measured distance from the eye;

2. Calculation of the lens required to correct vision when held at a prescribed distance from the eye, which distance may not be identical with that of the lens used in the test in (1).

The test in (1) may be carried out by trials in which a special spectacle frame is used to hold any required lens (or combination of two or three lenses) from a "trial case." Such a case usually contains positive and negative "powers" of 0·25, 0·5, 0·75 diopters, and so on up to 3 or 5, then 3·5, 4·0, 4·5, 5·0, 6·0, and then every integral value up to 20, besides positive and negative lenses for correcting astigmatism, as well as various prisms, etc., the use of which will be referred to below. The "powers" should be the "vertex refractions" of the lenses;* the true powers referred to the principal points are thus slightly weaker than the nominal powers in the case of the positive lenses.

Full details of the various methods of sight testing are outside the scope of this book, although some information on visual acuity

* See below, section on "Neutralization." In the negative lenses the powers may actually represent the value $\frac{1}{f'}$ in the Gaussian sense, i.e. the "equivalent power."

and test-charts will be found in Chapter V. Details may be found in Souter's *The Refractive and Motor Mechanism of the Eye*,[1] or in Laurance's *Visual Optics*.[2]

When the lens or combination of lenses giving the best visual correction has been found with the aid of the trial case and trial frame (illustrated in Fig. 176), it is necessary to mount the new lenses in the actual spectacles for the patient's use so that they have the same effective power at the eye. It is usually sufficient for low powers to position the lens in the trial frame so that it just clears the eye-lashes; then so to design and make the spectacle frame that the actually used spectacle lens falls in the same position. For very high-power lenses, however, the distance between the adjacent vertices of the lens and the eye is *measured*, preferably with the aid of a small instrument* shown in Fig. 162. It

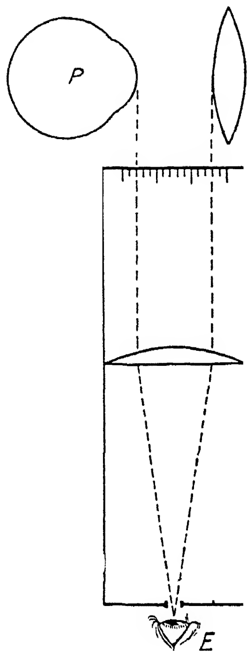

FIG. 162
P. Patient's eye
E. Observer's eye

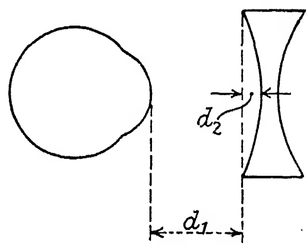

FIG. 163

consists of a scale mounted in front of a lens with a small stop in its principal focus. The only rays which can reach the observer's eye constitute narrow pencils which travel parallel to the axis of the lens before passing through it. Hence, the scale may be used to measure the size of a near object parallel to it, even though not actually in contact, without fear of errors arising through parallax.

The procedure is direct in the case where the lens has a convex surface turned towards the cornea (Fig. 162), but in the case shown where the correcting lens is concave (Fig. 163), the distance d_1

* Called a " keratometer " by some books. This name is, however, usually applied to a more elaborate instrument for measuring the curvature of the cornea.

would be measured by the instrument, and d_2 would be measured by a small depth gauge.

By the methods outlined above it will be clear that we can determine the back vertex focal length or power of a lens which, when placed in a definite coaxial position with regard to an eye of known "vertex refraction," will produce a true distance correction.

Optical Properties of Spectacle Lenses. Spectacle lenses as now worn are commonly given a diameter of about 4 cm., at any rate in the horizontal diameter, in order to allow of an adequate angular field of view unobstructed by the rim. The thickness necessary at the rim will be small but finite, approximately 1 millimetre if the lenses are to be of positive power, and the centre thickness will have to be sufficient to allow of this.

In the negative lenses the thickness at the centre will be least, and this must be sufficient to produce the necessary mechanical strength, say 0·7 mm.

The positions of the principal foci and principal planes with respect to the vertices of a lens are easily calculated by the formulae of Chapter II. The type of results thus found are illustrated in Fig. 164, which shows how the principal planes tend to move as the lens is "bent" so that its power remains constant though the curvatures of the surfaces vary.

The double-convex and plano-convex forms of lens are manufactured for all powers, but there are advantages in giving a more or less meniscus shape to the lens. The "periscopic" form has a second surface of 400 mm. radius, while the "meniscus" form usually has the second radius of 90 mm. These surfaces are those which are turned to the eye in the ordinary use of the lens. In the case of the negative lenses, the surface of greater curvature is again turned to the eye; the periscopic and meniscus types have radii of 400 mm. and 90 mm. respectively on their front faces.

In the commercial manufacture of spectacles a large factory may prepare large numbers of moulded blanks for various powers of periscopic and meniscus lenses; in any lens the one face will be moulded and worked to a standard radius, while the other may be given a variety of radii to cover all the usual requirements.

Then again, the factory prepares large numbers of half-finished lenses. One surface is finished as a cylindrical or toric figure; the other will be left to the "prescription house," which will add the other spherical surface for particular requirements.

In a spectacle lens of + 10D, bi-convex type, with a thickness of (say) 5 mm., the principal points will be found to be about 1·65 mm. within each surface; thus the actual focal length of such a lens will

exceed the "back vertex focal length" by about 1·65 mm. In a lens of the same power, of the meniscus type, the difference may

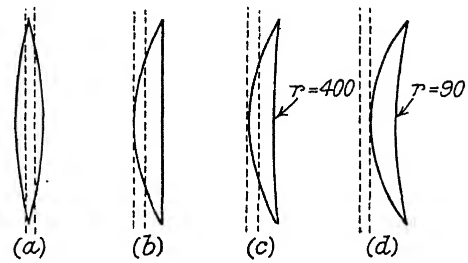

FIG. 164A

Positive lenses { (a) Double convex (b) Plano-convex (c) "Periscopic" form (standard) (d) "Meniscus" form (standard)

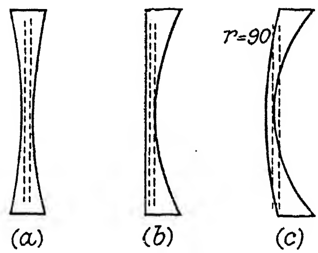

FIG. 164B

Negative lenses { (a) Double concave (b) Plano-concave (c) Meniscus form (standard)

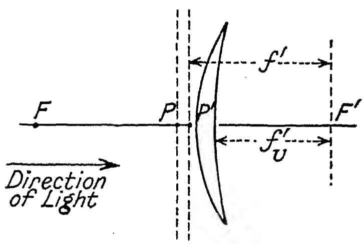

FIG. 164C

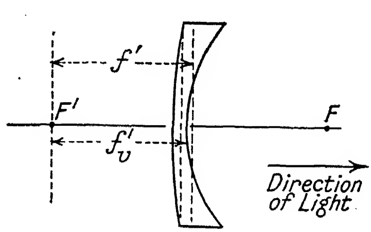

FIG. 164D

increase to 5 mm. when f'_v is measured from the second surface of greater curvature (Fig. 164C).

In the case of diverging lenses, however, these differences are very much smaller. An equi-concave lens of thickness 0·7 mm. has the principal planes 0·2 mm. within the vertices; the numerical

excess of the back vertex focal length over the real focal length* vanishes for the plano-concave form; if the lens is bent into the meniscus form, the differences change sign and only increase to 0·3 mm. for a lens of − 10D (Fig. 164D). The differences may therefore be neglected for most purposes in spectacle work.

The Lateral Test. Let the lens L, Fig. 165, project a virtual image B′ of an axial object point B. The apparent *direction* of the object is obviously not modified by the introduction of the lens provided the observing eye is situated on the axis of the lens also. Now let the lens be moved a short distance in the direction of the arrow A. The optical effect is realized by imagining the lens to keep still while B moves upwards to B_1 and the eye moves upwards

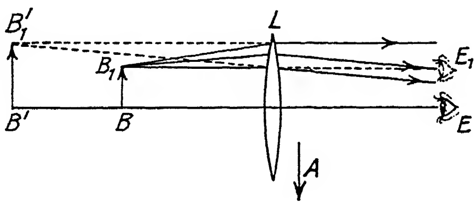

FIG. 165

an equal distance to E_1. The virtual image as seen by the eye has evidently moved in a sense *opposite* to that of the lens.

If the lens were negative or divergent, the image moves in the *same* direction as the lens. The test forms a useful means of distinguishing between weak positive and negative lenses.

We must, however, beware of applying the test in any case where a strong positive lens might form a real image between the lens and the eye. The test is only valid when the image is virtual, or is formed behind the observing eye. As the test is of more use with very weak lenses or combinations, these conditions are usually fulfilled.

Test for Neutralization. In Fig. 166, let B_1 suggest an object at some convenient distance viewed by an eye E, at first without the interposition of any lenses. Let two lenses, *a* and *b*, now be placed in position between object and eye; they are to be such that their vertex powers are equal in the sense that F'_a coincides with F_b, the lenses being held co-axially. Tracing a ray from B_1 parallel to the axis, it will be refracted towards the point F'_a after leaving lens *a*, but will evidently be rendered parallel to the axis again after traversing *b*. It is, however, displaced downwards. If the object B_1 is at a finite distance from the lens its image (which will not generally lie far from

* The vertex focal length measured from the more concave surface.

the object) is shifted a little towards the axis, since the final direction of the ray must intersect the image.

Suppose the lenses reversed so that the negative lens is nearest the object. It will then be seen that the emergent ray is parallel to the axis but displaced upwards; the shift of the image would therefore be reversed.

In making the test for neutralization the two lenses are therefore held together in such a way that they have a common axis. With trial case lenses the mounts or rims are of the same diameter and the two lenses can be held between a thumb and forefinger at about 24 in. from the eye when looking towards some suitable object, such as a vertical window-bar. It is then possible to see the bar above and below the rims and also its image formed by the system, as the lenses are moved slowly from side to side. When the image

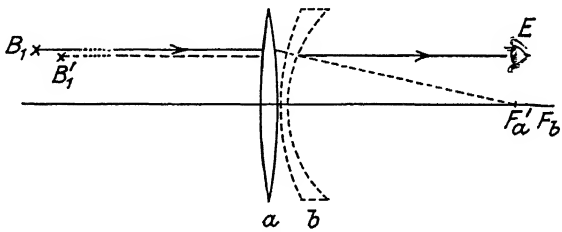

FIG. 166

is seen through the right-hand side of the lenses it will be displaced to the right if the combination is positive, and vice versa.

According to the argument above, we may conclude that the lenses have coincident focal points if the combination appears to be weakly negative with the positive lens held the nearer to the object at a finite distance, but weakly positive with the negative lens the nearer. Such a refinement of the test is, however, hardly of much significance in practice.

Considerable care is necessary in determining the vertex powers of lenses by the neutralization method. Suppose, for example, it is desired to find the vertex power of a meniscus lens, Fig. 167A. The intercept required to be measured is $A_2F'_a$. The trial case lenses enable us to select one for which A_3F_b is known, and the intercept between the vertices, A_2A_3 must be measured with the help of a depth gauge.

If, as sometimes happens, the meniscus lens is reversed so that the lenses come into contact at their vertices (Fig. 167B), the vertex focal length of the meniscus lens so measured will not be the one

which is usually required in the selection of spectacles. It is, however, possible to obtain specially small lenses for the neutralization test, so that the intercept A_2A_3 in the above arrangement becomes very small.

Since the positive and negative lenses of a trial case have, or should have, the same series of vertex refractions, equal powers should neutralize when held in contact. The necessary powers of the surfaces of a lens to give a definite vertex refraction can be calculated from the elementary formulae.

Curvature for a given Vertex Refraction. Consider an equi-convex lens to be given a vertex refraction of + 20D with thickness 9 mm. (say). The general formula for refraction of a paraxial beam is

$$\frac{n'}{l'} - \frac{n}{l} \quad \frac{n' - n}{\ } = \mathcal{F}_1, \text{ where } \mathcal{F}_1 \text{ is the power of the surface.}$$

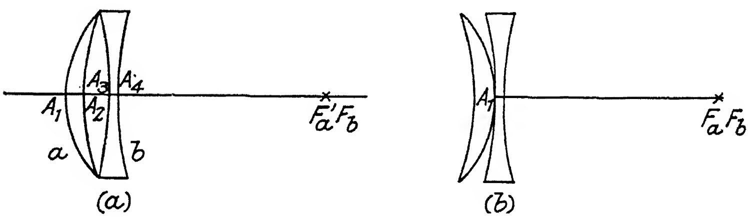

FIG. 167

Taking the case of a lens having refractive index n in air, and assuming parallel incident light

$$\frac{n}{l_1'} = \mathcal{F}_1$$

whence $$l_1' = \frac{n}{\mathcal{F}_1}$$

Since the diopter units are being employed the thickness of the lens, 9 mm., becomes 0·009 (in metres) and

$$l_2 = l_1' - 0{\cdot}009 = \frac{n}{\mathcal{F}_1} - 0{\cdot}009$$

Refraction at the second surface gives

$$\frac{1}{l_2'} - \frac{n}{l_2} = \mathcal{F}_2$$

but $\frac{1}{l_2'}$ is to be 20, and $\mathscr{F}_2 = \mathscr{F}_1$

$$20 - \frac{n}{l_2} = \mathscr{F}_1$$

or, substituting from above,

$$20 - \frac{n}{\dfrac{n}{\mathscr{F}_1} - 0{\cdot}009} = \mathscr{F}_1$$

This simplifies to a quadratic equation in $\mathscr{F}_1$

$$0{\cdot}009\,\mathscr{F}_1^{\,2} - \mathscr{F}_1\,(2n + 0{\cdot}18) + 20n = 0$$

giving two roots, the lower of which is 9·73 when n is taken as 1·5. (The higher root does not concern the problem in hand.)

Hence $\mathscr{F}_1 = \frac{0{\cdot}5}{r_1} = 9{\cdot}73$, and $\mathscr{R}_1 = 19{\cdot}46$D.

Such calculations are readily carried through with the formulæ of Chapter II. Thus for a thick lens (refractive index $= n$ and thickness d) in air.

$$\mathscr{F}_1 = \; n - 1 \qquad \mathscr{F}_2 = \; 1 - n \qquad \bar{d} = \frac{d}{n}$$

$$\mathscr{F} = \mathscr{F}_1 + \mathscr{F}_2 - \mathscr{F}_1\,\mathscr{F}_2\,\bar{d} = (n-1)\;\frac{r_2 - r_1 + (n-1)\bar{d}}{r_1 r_2}\Bigg\}$$

(All distances in metres.)

Also to calculate the vertex powers

$$\frac{1}{\mathrm{FA}_1} \quad \frac{\mathscr{F}}{1 - \mathscr{F}_2\bar{d}} \quad \frac{\mathscr{F}\,r_2}{r_2 + (n-1)d}$$

Thus *front vertex power* $= (n-1)\;\dfrac{r_2 - r_1 + (n-1)\,\bar{d}}{r_1 r_2 + (n-1) r_1 \bar{d}}$

(All distances in metres.)

Similarly $\dfrac{1}{\mathrm{A_2F'}} = \dfrac{\mathscr{F}}{1 - \mathscr{F}_1\bar{d}} = \dfrac{\mathscr{F}\,r_1}{r_1 - (n-1)\bar{d}}$

And *back vertex power* $= (n-1)\left\{\dfrac{r_2 - r_1 + (n-1)\bar{d}}{r_1 r_2 - (n-1) r_2 \bar{d}}\right\}$

(All distances in metres.)

These formulæ lend themselves to the calculation of the radii of lenses, such as trial case lenses, which must be given a definite vertex power.

Size of the Image Obtained by the Use of Spectacles. The size of the image of a very distant object subtending a small angle ω is $f\omega$, where f is the *object-space* focal length of the image-forming system.

Let a lens system of focal length f_a be placed coaxially with another system of focal length f_b, the distance between the adjacent principal focal points being g, then equation (15) gave

$$\frac{1}{f} = -\frac{g}{f_a f_b}$$

If the separation of the adjacent principal points is d, then

$$d = f_a' + g - f_b$$

whence $$g = d - f_a' + f_b = d + f_a + f_b$$

if the system "a" is in air, and

$$\frac{1}{f} = \frac{1}{f_a} + \frac{1}{f_b} + \frac{d}{f_a f_b}$$

Compare this with equation (21).

This equation can be applied directly to ascertain the change in *anterior* focal length of the system forming the retinal image consequent on the use of a spectacle lens. The distance of the anterior focal point of the normal eye from the surface of the cornea is 15·31 mm., according to Gullstrand. Hence, the posterior principal point of the spectacle lens, which usually falls in practice at about 12 mm. from the cornea, will not be far from the anterior focus. Assuming for a moment that these points might be actually coincident, we evidently have $d = -f_b$, whence

$$\frac{1}{f} = \frac{1}{f_a} + \frac{1}{f_b} - \frac{f_b}{f_a f_b} = \frac{1}{f_b}$$

The power of the entire system is the same as that of the unaided eye, but the necessary position of the sharp image has now been attained; i.e. on the retina. In this case, therefore, the size of the *sharp* image in the corrected eye will have the same size as that in the normal eye of the same focal length. (Remember that myopia and hypermetropia usually arise from an abnormal length of the eye-ball and not from a difference in the refracting power of the optical system.)

The user of spectacles is conscious, however, of the magnifying

or minifying power of his glasses. The retina of the uncorrected hypermetropic eye intercepts the rays proceeding towards any image point in the principal focal plane of the refracting system before they reach their focus. It will be understood from Fig. 168 how the centre of the diffuse patch lies closer to the axial point than the sharp image point. The dotted line H is to represent the position of the retina in hypermetropia; M represents the case of myopia, in which the centres of the diffuse image patches are at a greater distance than in the normal eye.

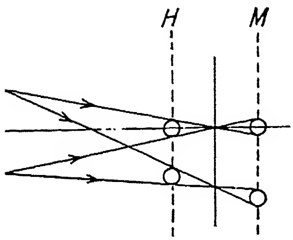

FIG. 168. RELATIVE IMAGE SIZES IN HYPERMETROPIA, EMMETROPIA, AND MYOPIA

The formula

$$\frac{1}{f'} = \frac{1}{f_a'} + \frac{1}{f_b'} - \frac{d}{f_a' f_b'},$$

or

$$\mathscr{F} = \mathscr{F}_a + \mathscr{F}_b - d\,\mathscr{F}_a\,\mathscr{F}_b$$

shows that when two systems are so close together that d vanishes, the power of the system is the sum of the powers of the two components. The effect of a spectacle lens, then, on the power of the whole system of lens and eye is zero when the lens is at the anterior principal focus and increases as it is brought nearer to the cornea. Hence a positive lens increases and a negative lens diminishes the power of the combined system as they approach the eye, the effect of this movement on the image size being a diminution and an increase respectively. A thorough discussion of this subject necessitates the investigation of the path of a principal ray. This will be given in Vol. II, Chapter I.

Spectacle Lenses for Vision of Near Objects. Although such defects as myopia and hypermetropia exist in youthful eyes, it is usually the case that the amplitude of accommodation is practically as great as in normal eyes. Hence, a young person usually requires only one pair of spectacles, which gives clear vision of distant objects when the eyes are at rest. Near objects are then viewed by exerting the accommodation.

As age increases, however, the power of accommodation is lost, and it is no longer possible to see near objects when wearing the distance glasses. Consider a myopic eye with a principal point refraction of (say) -2D, and an amplitude of accommodation of 1D. The far point lies at a distance of 50 cm. in front of the principal point of the eye, and the near point at a distance of $\frac{1}{(-2-1)}$ metres $= -33{\cdot}3$ cm.

The distance correction to be given by a lens with its second principal point at 12 mm. from the first principal point of the eye would be found from the equation

$$\mathcal{F}_a = \frac{\mathcal{F}}{1 + d\mathcal{F}} = \frac{-2}{1 + (\cdot 012 \times -2)} = -2\cdot 05\text{D}$$

If the full amplitude of accommodation is now exerted, any image projected into the plane of the near point is distinctly seen. The near point lies at a distance of $33\cdot3 - 1\cdot20 = 32\cdot1$ cm. in front of the second principal point of the spectacle lens.

To find where an object must be situated in order to project an image into the near point we have

$$\frac{1}{l'} - \frac{1}{l} = \mathcal{F}_a$$

or

$$\frac{1}{-0\cdot321} - \frac{1}{l} = -2\cdot05$$

whence $l = -\left(\frac{1}{1\cdot07}\right.$ metres $= -93\cdot5$ cm. from the 1st principal point of the spectacle lens. Hence, the nearest object which could be seen when wearing the spectacles would be nearly 1 metre distant.

Suppose, now, it is desired to obtain spectacles for reading type situated at a minimum distance of 25 cm. from the first principal point of the eye. Let the separations of the adjacent principal points of lens and eye be 12 mm. as before and let the distance between the principal points of the lens be δ, say. Then the distance of the object from the 1st principal point of the lens will be

$\text{5}) = -(23\cdot8 - \delta)$ cm.

With a dive c ır created by neglecting δ will be
small. c ɔ be projected into the near point,
$l' = -$
Exı ıg metres the equation becomes

$\text{;38)} = \mathcal{F}$

whenc $\mathcal{F} = 1\cdot08$

The le p weak positive power.

Wit y ɛ distance correction is positive and
the " " ırally obtained by increasing the
positi v "reading distance" is taken as
40 cm ı dual needs.

Use of Lenses in Series. When using a trial case it may be desired to find a suitable correction for near objects by using, say, the equi-convex trial lens. It must be pointed out that the condition for equal performance with lenses of other shapes may not be the same. It is not sufficient to substitute a lens with the same vertex power, but a lens must be used such that the distance from the vertex to the image of the (near) object is the same as with the trial lens; i.e. the " vergencies " to the images of the near objects must be the same.

The near object may be real, or may be represented by placing a weak negative lens in front of the spectacle glass to form a virtual image at a finite distance, if using a very distant object.

Let l be the distance of the near object and let $\mathcal{D}_v$ be the vertex power of the lens, then with very thin lenses we have with sufficient accuracy

$$\frac{1}{l'} - \frac{1}{l} = \mathcal{D},$$

or in terms of "vergences," $\mathcal{L}' - \mathcal{L} = \mathcal{D}_v$, from which $\mathcal{L}' = \mathcal{L} + \mathcal{D}_v$, or, if the near object was obtained by using the virtual image of a distant object projected by an auxiliary weak lens of power

$$\mathcal{L}' = \mathcal{L}_a + \mathcal{L}_v$$

This is, however, not quite sufficiently accurate in the case where a strong spectacle lens is concerned.

Take the case of the equi-convex lens of vertex power $+ 20$D, as used with a near object at a distance of 1 metre. The approximate equation for the vergence is

$$\mathcal{L}' = -1 + 20 = 19$$

We must, however, follow the refraction surface by surface. From page 274 above, each surface has a power of 9·73 when the refractive index is 1·5; the thickness is 9 mm.

The general equation

$$\frac{n'}{l'} - \frac{n}{l} = \mathcal{F}_1$$

gives for the first refraction

$$\frac{n'}{l'_1} - \left(\frac{1}{-1}\right) = 9{\cdot}73$$

whence $l'_1 = 0{\cdot}172$ metres (for $n = 1{\cdot}5$).

Since the thickness $t = 0{\cdot}009$ metres

$$l_2 = 0{\cdot}163 \quad ,,$$

For the 2nd refraction

$$\frac{1}{l'_2} - \frac{1{\cdot}5}{0{\cdot}163} = 9{\cdot}73$$

whence $$\frac{1}{l'} = 18{\cdot}94 = 20 - 1 - 0{\cdot}06.$$

The true value for the vergence $\mathscr{L}'$ or $\frac{1}{l'}$ therefore differs from the simple sum of the powers $\mathscr{D}_a + \mathscr{D}_v$ by a correcting term $-0{\cdot}06$.

The same calculation relates to the case where an auxiliary lens is employed, but it is assumed in the above case that the auxiliary lens is in close contact with the main spectacle lens. If this is not the case, the distance between the vertices is an additional factor. Henker[3] gives a useful table showing the effects of various positive powers in conjunction with spectacle lenses. As will be seen below, this table is especially useful in connection with the determination of astigmatism. Students should calculate some typical cases, assuming the usually correct refractive index for spectacle glass (say) 1·523. A systematic scheme of calculation, such as that given on page 49, should be devised and five figure "logs" should be used.

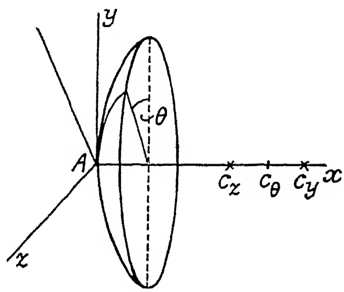

Fig. 169

The effective vertex refraction of a combination of two diverging lenses may usually be taken as the simple sum of the powers owing to the small thicknesses in the lenses. At most, any finite distance might be considered in special cases.

The Axial Astigmatism of the Eye and its Correction. About the years 1825–26, G. B. Airy[4] investigated the axial astigmatism of the eye and the mode of correcting it with lenses having cylindrical surfaces, suitably disposed. It has already been stated that an astigmatic eye usually possesses differences of curvature in the various meridians of the cornea.

We are to imagine the optic axis of the eye, and a series of planes passing through this axis; their intersections with the outer surface of the cornea mark the "meridians."

In order to understand the manner in which the variation of power in the different meridians may be corrected with the help of such lenses as used by Airy, it is necessary first to study some of the properties of cylindrical and "toric" surfaces.

A general theorem due to *Euler* shows that at any point of a curved surface free from discontinuities there may be distinguished two perpendicular sections of maximum and minimum curvature. Then these are the "principal sections" of the surface. As suggested in Fig. 169, let the surface be tangent to the yz plane at the origin, so that the centres of curvature lie in the axis of x. The centres of curvature c_y and c_z for the principal sections have a maximal separation, while the centre for any intermediate section lies between them. Let the intermediate meridianal section making an angle θ with the xy plane have a "curvature" $\mathscr{R}_\theta = \frac{1}{r_\theta}$ where r_θ is the radius of curvature, then according to Euler's theorem

$$\mathscr{R}_\theta = \mathscr{R}_y \cos^2 \theta + \mathscr{R}_z \sin^2 \theta \quad . \quad . \quad . \quad (71)$$

In a section perpendicular to this first one,

$$\mathscr{R}_{\theta + 90^\circ} = \mathscr{R}_y \sin^2 \theta + \mathscr{R}_z \cos^2 \theta$$

Therefore, adding the two equations, we obtain

$$\mathscr{R}_\theta + \mathscr{R}_{\theta + 90^\circ} = \mathscr{R}_y + \mathscr{R}_z$$

Hence, the sum of the curvatures of any two perpendicular sections has a constant value.

The refracting power of such a surface is proportional to the change of refractive index and to the curvature. Since the power of the surface is

$$\mathscr{F} = (n' - n)\,\mathscr{R}$$

then

$$\mathscr{F}_\theta = \mathscr{F}_y \cos^2 \theta + \mathscr{F}_z \sin^2 \theta \quad . \quad . \quad (72)$$

Such an equation would apply to a thin lens having one surface with variable curvature in different meridians and one plane surface. Suppose such a lens held against an eye with a cornea of variable curvature in the different meridians, and let the lens be turned so that the principal sections of the lens and cornea coincide. Let $\mathscr{F}_{b\theta}$ be the power of the cornea in the intermediate section

$$\mathscr{F}_{b\theta} = \mathscr{F}_{by} \cos^2 \theta + \mathscr{F}_{bz} \sin^2 \theta$$

So that the total powers of lens and cornea are

$$\mathscr{F}_\theta + \mathscr{F}_{b\theta} = (\mathscr{F}_y + \mathscr{F}_{by}) \cos^2 \theta + (\mathscr{F}_z + \mathscr{F}_{bz}) \sin^2 \theta$$

Provided that

$$\mathscr{F}_y + \mathscr{F}_{by} = \mathscr{F}_z + \mathscr{F}_{bz}$$

we shall have $(\mathscr{F}_\theta + \mathscr{F}_{b\theta})$ constant, and the power of the combination in all meridians will be the same. An astigmatic refracting surface can therefore be corrected in *all* meridians by another

suitably chosen and disposed surface, provided the principal sections are made to coincide and that the effective powers of the combination are the same in these two sections.

With regard to the above theory it should be noted that Euler's theorem applies generally only to infinitesimally small areas of curved surfaces over which the curvatures may be regarded as reasonably constant in any meridian within the limits of the area. The refracting surfaces of the eye have areas of a definite size, and thus the theorem, while offering a general guide, is often not accurately obeyed in practice; cases of irregular astigmatism may thus be encountered in practice in which the meridians of maximum and minimum power (when found by tests using the whole diameter of the pupil) are not apparently perpendicular. In such cases the defect of vision cannot be completely corrected by the use of cylindrical or toric surfaces.

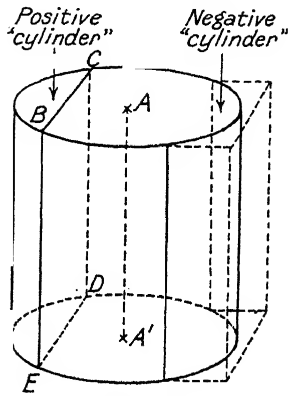

FIG. 170

Forms of Lenses for Correcting Astigmatism. The simplest possible form of surface for correcting astigmatism is that of the cylinder, which is generated by the revolution of one straight line about another one parallel to it, i.e. the *axis* of the cylinder. This is suggested in Fig. 170, where AA′ is the cylinder axis. If we take a slice of the cylinder by cutting it in a plane parallel to the axis, we have the form of a lens with one cylindrical and one plane face. This will be a " positive cylinder." If we place a piece of moulding clay on a plane surface and press the cylinder into it (holding the cylindrical axis parallel to the plane) we shall produce the form of a lens with one surface plane and one concave and cylindrical. Such a lens in glass would constitute a " negative cylinder." Such lenses are held before the eye in such a position that the optical axis of the eye is normally perpendicular to the cylindrical axis.

It is often the case that astigmatism exists in the eye concurrently with other deficiencies such as myopia, hypermetropia, or the usual conditions of presbyopic vision. In such cases it is often necessary to provide a spherical correction for an eye as well as that for astigmatism, and, moreover, to accomplish this by one lens, which may accordingly be given one spherical and one cylindrical surface. Such a lens is technically called a " sphero-cyl."

In the majority of cases the cylindrical correction is not large, and the cylindrical surface may be more or less flat. It will be shown, however, that spectacle lenses are most free from the astigmatism of oblique pencils when they are given forms which are usually of the meniscus type, the centres of curvature of both surfaces lying on the eye side of the lens. When such lenses must correct astigmatism, the use of "toric" or "toroidal" surfaces is called for, which possess a finite curvature in both principal sections.

In Fig. 171A the curve BB′B″ lies in a plane parallel to the line AA′ and has its centre at C_1. When revolved around C_2 on that line it generates a barrel-shaped toric surface in which the radii of the principal sections are $B'C_1$ and $B'C_2$. A segment of such a surface

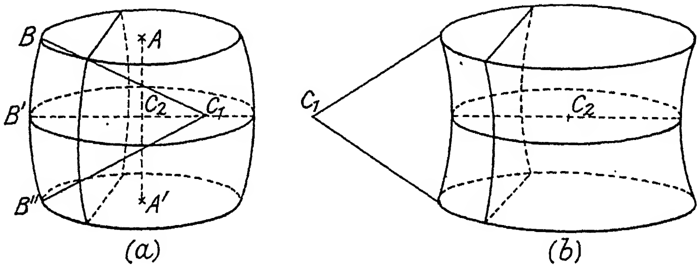

FIG. 171

might represent the form given to one face of a toric lens, the other face being simply spherical.

The various forms of possible toric surfaces can be studied by the revolution of different curves about the cylinder-axis. Fig. 171B shows the generation of a saddle-shaped surface, which is convex in one section and concave in another.

Effects Near the Focus of an Astigmatic Lens. An instructive model may be made to illustrate geometrically the crossing of the ray paths near the focus of an astigmatic beam. Threads are stretched between corresponding points on (1) a circular ring and (2) an elliptical ring, the correspondence being such that the points lie on radii making equal angles with the major and minor axes of the ellipse and the corresponding diameters of the circle as suggested in Fig. 172, the threads crossing between the circle and the ellipse.*

It will be found that there are two perpendicular lines through which the rays all pass. The sections in intermediate and external

* It is convenient in practice to stretch the threads between two plates punched with the necessary holes in the loci of circle and ellipse; the holes may correspond to $\theta = 0°, 30°, 60°, 120°$, etc.

planes have the forms suggested in the figure. Each focal line is perpendicular to the principal ray of the bundle, and is parallel to the major or minor axes of the ellipses which represent the sections of the bundle in various positions.

These effects are characteristic of the simplest form of "astigmatism," and were first investigated by Sturm. In practice the actual section of the bundle beyond or within the focus may not be truly elliptical, and the effects in the actual distribution of light near the focus are not thoroughly investigated by the mere discussion of the ray paths, since they depend on the diffraction of the non-spherical wave-front passing through the (usually circular) aperture of the lens. However, the focal lines are to be actually

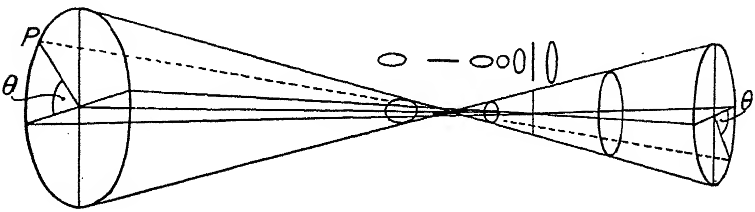

FIG. 172

observed, though they are not strictly *lines* in the ordinary sense, having at least the finite breadth of the usual diffraction disc.

Prevalent Type of Astigmatism in the Human Eye. It is most frequently the case that the curvature in the vertical meridian of the cornea is greater than the horizontal when any difference is found. This is the case of astigmatism "with the rule." The opposite case, where the horizontal curve is the greater, is "astigmatism against the rule."

Visual Characteristics of Astigmatism. Since astigmatism is usually due to a difference of curvature in the meridians of one of the refracting surfaces of the eye, we shall, if the astigmatism is regular, find a maximum difference of power of the refracting system in two mutually perpendicular meridians.

If, then, the principal point refractions of the eye in these meridians be $\mathscr{K}_m$ and $\mathscr{K}_a$, the necessary powers of the correcting lens in the same meridians are (in accordance with equation (70))

$$\mathscr{F}_m = \frac{\mathscr{K}_m}{1 + d\mathscr{K}_m} \qquad \mathscr{F}_a = \frac{\mathscr{K}_a}{1 + d\mathscr{K}_a}$$

The difference between these two principal point refractions of the eye in the principal sections is the TOTAL ASTIGMATISM of the eye.

Consider now an eye which is near-sighted in the vertical principal section, and normal sighted in the horizontal principal section. This case is represented by Fig. 173(*a*) and Fig. 173(*b*), showing in a diagrammatic way a vertical section and a horizontal section of such an eye, together with image-forming rays.

The eye is near-sighted in the vertical section and the principal focus F_1' therefore lies in front of the retina. The principal planes enable us to find the image $B'B_1'$ which corresponds to the object BB_1 situated at the far point M_R. This image lies on the retina,

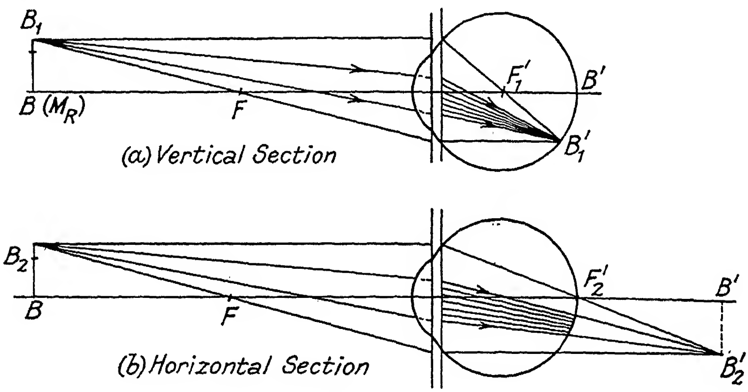

FIG. 173

where it is sharply focussed as far as the rays situated in the plane of the diagram are concerned.

In the horizontal section, however, the eye is normal-sighted and the principal focus F_2' lies at the retina. The far point is at infinity, and the object at B would therefore be imaged behind the retina. The rays consequently fail to reach the focus and these rays (from points such as B or B_2), which lie in the plane of the diagram, meet the retina in a line.

Note that although the principal planes are useful to enable us to find the position of the focus, the rays actually passing into the pupil are the only ones which can have effect. Their limitation is suggested in the diagram in an obvious manner.

Consider the rays from B_1 (Fig. 173(*a*)). Those which lie in the vertical plane meet the retina in one point. Those which lie in a plane perpendicular to the vertical section meet the retina in the horizontal focal line, characteristic of simple astigmatism, through which all the rays pass. Every point in a short horizontal line passing through B_1 is therefore imaged in a horizontal focal line,

and the overlapping of such lines imaging successive points forms a continuous line image apparently sharp, although a vertical line such as BB_1 has a diffuse image. The relations between object and image in such a case are suggested in Fig. 174.

It is characteristic of astigmatism that lines in different directions are not seen equally clearly. Fig. 175 shows types of test objects for astigmatism. If the effect is slight it is detected merely in an apparent difference between the blackness of the various radial lines, those in some one direction appearing darker than those in the direction perpendicular thereto. The " diamond " can be rotated until the radial lines are seen most distinctly; this determines one of the directions of the principal sections. The axis of the correcting cylinder will be perpendicular to the most distinct lines. The actual test objects have to be well printed in considerably larger size.

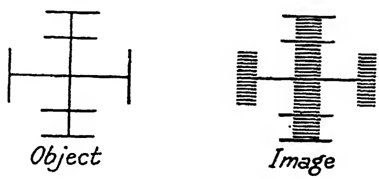

FIG. 174

Direction of the Axis. Fig. 176 illustrates the front of the spectacle frame with the convention adopted in England and America and almost universally elsewhere* for the reckoning of the direction of the cylinder axis. The test of astigmatism is made with the aid of the cylindrical lenses in the trial case, the cylinder being usually placed in front of any necessary spherical correction lens. The axis direction is marked on the cylindrical lens and its position can be read off on the trial frame when the power and direction have been adjusted so as to obtain the best correction.

Suppose that a spherical power Q is required, combined with a cylinder of power P placed with its axis at ϕ degrees, the whole correction is usually conventionally written

$$Q \text{ sph.} \quad P \text{ cyl. Ax. } \phi$$

As, for example,

$$+ 5D \text{ sph.} \supset\!\subset -0{\cdot}75D \text{ cyl. Ax. } 120^\circ$$

Alternatives are to write

$$\frac{Q \text{ sph.}}{P \text{ cyl. Ax. } \phi}, \text{ or } Q \text{ sph.}/P \text{ cyl. Ax. } \phi$$

* Owing to past difficulties with different conventions, many ophthalmologists still think it wise to include a *diagram* of the axis direction in writing a prescription.

Transposition. Consider the case of an eye which is near-sighted in both principal sections, but to different amounts. Suppose that it requires a correction of $-5D$ in the vertical section to bring images of distant horizontal lines to a sharp focus, and a power of $-3D$ in the horizontal section to bring images of vertical lines to a

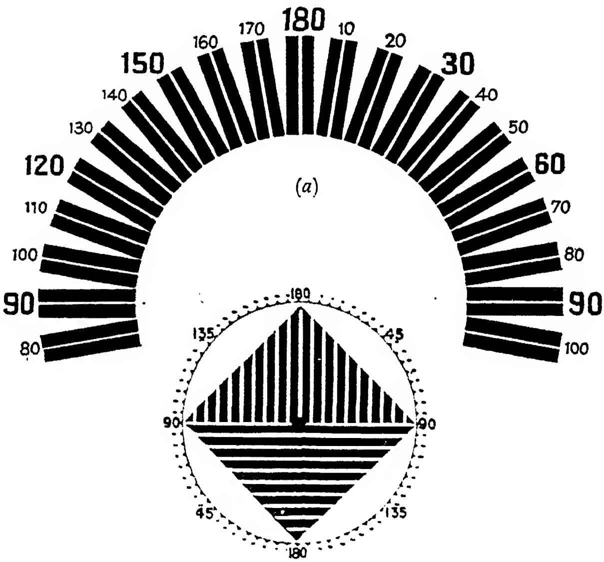

(b)

FIG. 175. OBJECTS FOR TESTING ASTIGMATISM (LAURANCE)

sharp focus. (Assume that this distance correction is all that is required.)

The necessary lens can theoretically be made up in several different ways—

1. 1st face. Cylinder $-$ 5D axis horizontal.
   2nd ,, Cylinder $-$ 3D ,, vertical.

The corrections are given separately in each face.

2. 1st face. Spherical $-$ 5D.
   2nd ,, Cylinder + 2D axis vertical.

The cylinder has no power in a vertical direction, the resultant powers thus being $-5D$ vertical, $-3D$ horizontal.

3. 1st face. Spherical $-$ 3D.
   2nd ,, Cylinder $-$ 2D, axis horizontal.

The cylinder has no power in the horizontal direction.

4. 1st face. Toric. Powers $\begin{cases}(P-5), \text{ vertical section.}\\(P-3), \text{ horizontal section.}\end{cases}$
   2nd ,, Spherical Power $-$ P.

The powers of P on the first face and $-$ P on the second neutralize.

5. 1st face. Spherical $+$ P
   2nd ,, Toric $-$ (P $+$ 5), vertical section.
   $-$ (P $+$ 3), horizontal section.

All these forms could be reversed in front of the eye, rotating the lens through 180° about either of the principal directions (horizontal

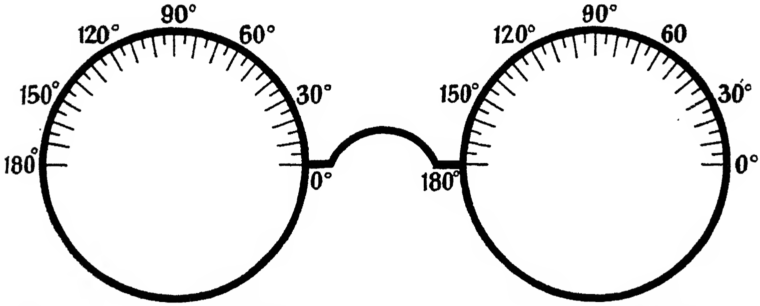

FIG. 176. FRONT OF FRAME SEEN BY A PERSON FACING THE WEARER—TO SHOW CONVENTION FOR AXIS DIRECTION

or vertical), while still retaining the prescribed correction. Not all of these arrangements are, however, equally advantageous.

Cylindrical surfaces cost more than spherical; toric are more expensive than either. As mentioned above, the conditions for maximum freedom from oblique astigmatism usually call for a bent form, which, if axial astigmatism is to be corrected, must have one of its surfaces toric. Hence the choice of the lens actually used as a spectacle glass depends upon several considerations. The most inexpensive form in ordinary cases is the "sphero-cyl" when astigmatic correction is needed. The meniscus forms which give better oblique vision will be selected when their cost is not an obstacle.

General Case of Transposition. In general, when the axis of the correcting cylinder lies in any direction ϕ, the following transpositions are possible, excluding toric lenses—

	Power Parallel to the Direction ϕ	Power Perpendicular to the Direction ϕ
Sphero-cyl. Q sph. $\supset$ P cyl. Ax. ϕ . .	Q	P + Q
,, (P + Q) sph. $\supset$ $-$ P cyl. Ax. ($\phi \pm 90°$)	Q	P + Q
Cross cyl. (P + Q) cyl. Ax. $\phi \supset$ Q cyl. Ax. ($\phi \pm 90°$)	Q	P + Q

In any combination it is easy to check the result by considering the power parallel to one cylindrical axis and the power perpendicular thereto. In addition to the above there are, of course, all the possibilities of meniscus lenses with toric surfaces.

EXAMPLES OF TRANSPOSITION

a	− 1·25 sph.	$\supset$ + 1·75 cyl.	Ax. 160°
	+ 0·5 sph.	− 1·75 cyl.	Ax. 70°
	− 1·25 cyl. Ax. 70°	$\supset$ + 0·5 cyl.	Ax. 160°
b	+ 3·50 cyl. Ax. 120°	$\supset$ − 0·75 cyl.	Ax. 30°
	+ 3·50 sph.	$\supset$ − 4·25 cyl.	Ax. 30°
	− 0·75 sph.	$\supset$ + 4·25 cyl.	Ax. 120°

"Bending a Lens." The total power of a thin lens is often expressed as the sum of the powers of the two surfaces.

$$\mathscr{F} = \mathscr{F}_1 + \mathscr{F}_2 = (n - 1)\,(\mathscr{R}_1 - \mathscr{R}_2) = (n - 1)\,\mathscr{R}_1 + (1 - n)\,\mathscr{R}_2$$

The optician speaks of "bending a lens" when he changes (on paper) the curvatures of the two surfaces by an equal numerical amount, k, say

$$\mathscr{F} = (\mathscr{F}_1 + \delta) + (\mathscr{F}_2 - \delta) = (n - 1)\,(\mathscr{R}_1 + k) + (1 - n)\,(\mathscr{R}_2 + k)$$

This operation thus adds to the power of one surface the same amount that it removes from the other.

In this way we may look upon the meniscus lenses as simply the result of "bending" the simple forms such as the sphero-cyls.

The "base curve of a toric surface" is *usually* the one having the lower power. If, for example, a specification

$$+ 1 \text{ sph.} \supset 1{\cdot}5 \text{ cyl.}$$

is required in toric form with a + 6D base, it would be obtained by using a front surface having powers in the two principal sections of + 6D and + 7·5D respectively. Since the total power of the lens are to be + 1D and + 2·5D in the principal sections, the second surface of this meniscus is given a power of − 5D.

Obliquely-crossed Cylinders. When two cylindrical lenses are used in series, as is sometimes the case in sight testing, their combined effect is in general that of a sphere with one cylinder.

Let OA and OB, Fig. 177, be the principal sections of maximum power of cylindrical lenses a and b; these sections are perpendicular to the axes of the cylinders; they make angles ϕ_a and ϕ_b with the axis of X. The lenses have no power in the direction parallel to the cylinder axis.

The power in some other direction θ is calculable from equation

(72). Let $\mathscr{F}_a$ and $\mathscr{F}_b$ be the powers of the cylinders, then the effective power $\mathscr{F}_\theta$ in direction θ is

$$\mathscr{F}_\theta = \mathscr{F}_a \cos^2 (\theta - \phi_a) + \mathscr{F}_b \cos^2 (\theta - \phi_b)$$

which may be written more concisely

$$\mathscr{F}_\theta = \mathscr{F}_a \cos^2 \alpha_a + \mathscr{F}_b \cos^2 \alpha_b$$

where $\alpha_a = \theta - \phi_a$, and $\alpha_b = \theta - \phi_b$.

The power in a direction perpendicular to that given by θ will be

$$\mathscr{F}_{\theta + 90} = \mathscr{F}_a \sin^2 \alpha_a + \mathscr{F}_b \sin^2 \alpha_b$$

Now, assuming that the powers of the equivalent sphere and cylinder are Q and P respectively, the maximum power of the equivalent lens will be P + Q and the minimum will be Q.

If the power in the direction θ is the maximum

$$\mathscr{F}_\theta = P + Q = \mathscr{F}_a \cos^2 \alpha_a + \mathscr{F}_b \cos^2 \alpha_b$$

and $$\mathscr{F}_{\theta + 90} = Q = \mathscr{F}_a \sin^2 \alpha_a + \mathscr{F}_b \sin^2 \alpha_b$$

by adding $P + 2Q = \mathscr{F}_a + \mathscr{F}_b$

and by subtracting

$$P = \mathscr{F}_a(\cos^2 \alpha_a - \sin^2 \alpha_a) + \mathscr{F}_b(\cos^2 \alpha_b - \sin^2 \alpha_b)$$

$$= \mathscr{F}_a \cos 2\alpha_a + \mathscr{F}_b \cos 2\alpha_b$$

The maximum power must also conform to the condition that the differential coefficient of the power with respect to the variable θ must be zero.

Hence $$\frac{d(\mathscr{F}_\theta)}{d\theta} = -\mathscr{F}_a(2 \cos \alpha_a) \sin \alpha_a - \mathscr{F}_b(2 \cos \alpha_b) \sin \alpha_b = 0$$

whence $$0 = \mathscr{F}_a \sin 2 \alpha_a + \mathscr{F}_b \sin 2 \alpha_b$$

From above $$P = \mathscr{F}_a \cos 2\alpha_a + \mathscr{F}_b \cos 2\alpha_b$$

Squaring and adding these last equations

$$P^2 = \mathscr{F}_a^2 + \mathscr{F}_b^2 + 2\mathscr{F}_a \mathscr{F}_b \cos 2(\alpha_a - \alpha_b)$$

$$= \mathscr{F}_a^2 + \mathscr{F}_b^2 + 2\mathscr{F}_a \mathscr{F}_b \cos 2(\phi_b - \phi_a)$$

$$P = \pm\sqrt{\mathscr{F}_a^2 + \mathscr{F}_b^2 + 2\mathscr{F}_a \mathscr{F}_b \cos 2(\phi_b - \phi_a)}$$

Of course $(\phi_b - \phi_a)$ is the angle between the principal sections of maximum power. In order to obtain Q we can substitute the positive value of P found above in the equation

$$Q = \frac{\mathscr{F}_a + \mathscr{F}_b - P}{2}$$

From the equation above

$$\mathscr{F}_a \sin 2\alpha_a + \mathscr{F}_b \sin 2\alpha_b = 0$$

$$\mathscr{F}_a(\sin 2\theta \cos 2\phi_a - \cos 2\theta \sin 2\phi_a)$$
$$+ \mathscr{F}_b(\sin 2\theta \cos 2\phi_b - \cos 2\theta \sin 2\phi_b) = 0$$

whence $$\tan 2\theta = \frac{\mathscr{F}_a \sin 2\phi_a + \mathscr{F}_b \sin 2\phi_b}{\mathscr{F}_a \cos 2\phi_a + \mathscr{F}_b \cos 2\phi_b}$$

This enables us to find the direction of maximum power.

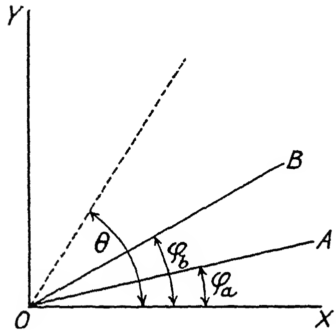

FIG. 177

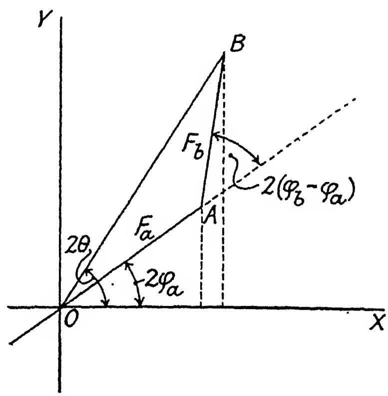

FIG. 178

The negative solution for P corresponds to the case where we have instead of

$$Q \text{ sph.} \supset P \text{ cyl. Ax. } \phi$$

the alternative $(P + Q)$ sph. $\supset -$ P cyl. Ax. $(\phi + 90°)$

which can be obtained from the first by simply transposing. The cylinder in the second case is of the opposite sign but equal power.

Graphical Method. A simple graphical method of obtaining these relations is shown in Fig. 178. OA $= \mathscr{F}_a$ is set off on some convenient scale at an angle $2\phi_a$, and AB $= \mathscr{F}_b$ at an angle $2\phi_b$, with the direction of OX.

Since $OB^2 = \mathscr{F}_a^2 + \mathscr{F}_b^2 + 2\mathscr{F}_a.\mathscr{F}_b \cos 2(\phi_b - \phi_a)$, from the triangle BOA, OB must represent P by its length.

Further, since $\tan \widehat{BOX} = \dfrac{\mathscr{F}_a \sin 2\phi_a + \mathscr{F}_b \sin 2\phi_b}{\mathscr{F}_a \cos 2\phi_a + \mathscr{F}_b \cos 2\phi_b}$ we see that $\widehat{BOX} = 2\theta$.

Thus we can at once find θ the direction of maximum power.

Since the axis directions are always at right angles to the direction

of maximum power, the calculation and construction may be performed by treating ϕ_a and ϕ_b as the axis directions, and obtaining θ as the axis direction of the resultant. In case the work is to be reduced to a minimum we can obtain $\tan 2(\theta - \phi_a) = \tan \widehat{BOA}$.

$$\tan 2(\theta - \phi_a) = \frac{\mathcal{F}_b \sin 2\,(\phi_b - \phi_a)}{\mathcal{F}_a + \mathcal{F}_b \cos 2(\phi_b - \phi_a)}$$

$$\text{and } P = \frac{\mathcal{F}_a + \mathcal{F}_b \cos 2\,(\phi_b - \phi_a)}{\cos 2\,(\theta - \phi_a)}$$

H. H. Emsley has devised a useful calculator or protractor by means of which the combination of obliquely-crossed cylinders can be obtained without the necessity of drawing, although its fundamental principles rest upon the above construction. It may be obtained from the Elliott Optical Co.

It will be noticed that with two cylindrical lenses of equal power we can produce by relative rotation the effect of sphero-cylindrical lenses with cylindrical components of any magnitude from zero up to double the power of either.

In case the visual test for astigmatism is made with a fairly strong cylinder and a strong positive lens in the trial frame, some care must be exercised in finding the effective powers in the principal meridians, as discussed above in the section on " Lenses in Series." Corrections for those effects and also for the distance (if any) between the vertices of the lenses may be required. Tables may be consulted for such corrections, which are, however, mainly negligible with weak position lenses and most negative lenses.

The Image Field and Its Curvature. It was shown in the case of a single spherical refracting surface that an object surface concentric with the refracting surface would possess a correspondingly concentric image surface. If the curvature of the object surface is modified, the image surface has a new curvature, of which the radius is calculable; in such a way the curvature of the final image surface can be calculated surface by surface through a system, as in equations (52) and (53).

Coddington and Petzval independently investigated this theory. The curvature of the field corresponding to a plane object is the " Petzval curvature " and the curved image surface itself, calculated in this way, is called the " Petzval surface." In the presence of aberration no sharp image may be found in such a surface, but when, for example, the oblique astigmatism is removed from a thin lens used in conjunction with a suitable stop, the best image is duly found in or very close to the Petzval surface.

Oblique Astigmatism in Spectacles. In the chapter on aberrations it was also shown that the rays derived from the extremities of two perpendicular diameters Y and Z in the circular exit pupil of a system subject to astigmatism of oblique pencils, and passing towards an image point away from the axis of the system in the Y direction, intersect each other so that the intersection of the Y pair is at three times the distance away from the Petzval surface of the intersection of the Z pair. This condition results, as was illustrated in Fig. 80, in the formation of two focal lines T, and S, the first, T (the " tangential " focal line), being perpendicular to the radial line (in the focal surface) from the optic axis to the image, the other, S (the " sagittal " focal line), being itself radial. In cases

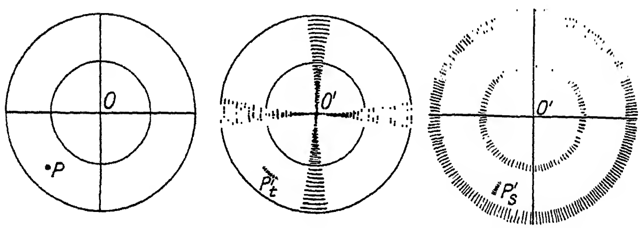

FIG. 179. EFFECTS OF ASTIGMATISM
(The dimensions of the figures have no significance)

where the coma and spherical aberration are negligible, the sagittal focal line may be thought of as perpendicular to the principal ray. See the note on page 137. We thus have a condition of the *oblique* rays very similar to that suggested in the diagram, Fig. 172, showing astigmatism of the type caused by refraction by a cylinder.

As was pointed out in the previous discussion, each object point is imaged as a line in two focal surfaces, the line being tangential in the tangential focal surface, radial in the sagittal surface. Thus, in Fig. 179, the point P is imaged in such lines at P'_t and P'_s. The diagram of the object is to be imagined as placed with the point O on the optical axis. The two " images " are to suggest the results found, in the tangential and sagittal image surfaces respectively. Each point in a line or circle is imaged as described, so that we have a series of short overlapping lines in the apparently sharp circles or in the radial lines in the image surfaces. Thus, in the tangential focal surface we have clear circles and diffuse radial lines; in the sagittal surface the radial lines are clear. If the object contains lines which are neither radial nor tangential they will not be sharply imaged in any surface.

The Petzval surface of a simple thin lens has a radius of curvature

$$r = -nf'$$

where n is the refractive index and f' is the focal length. When the stop which limits the aperture is close against the lens, or when the boundary of the lens itself limits the rays, the astigmatism of

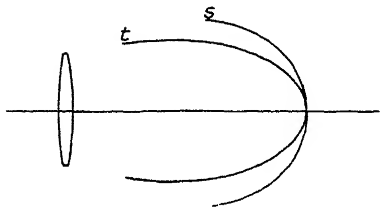

FIG. 180

oblique pencils cannot be eliminated, and the tangential and sagittal focal surfaces can be distinguished (Fig. 180). They depart greatly from the spherical form as the angles of the rays with the axis increase. (See also Fig. 81.)

Consider the case of a spectacle lens mounted in front of a moving eye, as suggested by Fig. 181. As the eye rotates, the pupil, of

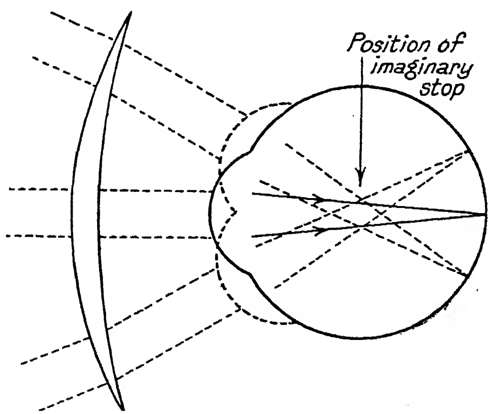

FIG. 181

course, moves with it, and the rays focussed on the fovea in various positions of the eye are those transmitted by different parts of the spectacle lens. The rays are evidently limited in the same way as

would be the case if a diaphragm of suitable diameter were placed at the centre of rotation of the eye-ball.

The point of rotation may be taken as 13 to 15 mm. behind the vertex of the cornea in the average eye. The vertex of the spectacle lens is usually placed 12 or 13 mm. from the cornea in order to allow adequate room for the eyelashes. Hence the "effective stop" may be taken as 25 to 28 mm. behind the vertex of the lens.

It can be shown that when a lens is used in conjunction with such a stop at a finite distance, it is possible within certain limits of lens power to remove the astigmatism of oblique pencils by "bending" the lens to the appropriate form. This calls for meniscus forms with the concavity towards the stop.

Action of Lenses Free from Astigmatism. The large aperture of spectacle lenses (35–40 mm., perhaps) in proportion to the diameter of the pupil itself, which scarcely ever rises as high as 8 mm., and is usually only 3 to 4 mm., is only required to give a sufficiently large angular field of vision as the eyes rotate.

It is possible to calculate the spherical aberration and coma produced by a lens under such conditions; these aberrations prove negligible, at least with ordinary spectacle lenses. The astigmatism of oblique pencils of, say, a 5D lens (equi-convex) is, however, considerable, and the variation of accommodation required to focus tangential and radial images at an angle of 25° with the axis of the spectacle lens is rather more than 1 diopter.

Should the oblique astigmatism be removed by the selection of a suitable figure for the lens, the sharp images of distant objects are then formed in the Petzval surface. The lens will, of course, have the required vertex power, and its principal focus in the centre of the Petzval surface will coincide with the far-point of the eye.

As the eye rotates, the locus of the far point is the far point sphere, with its centre in the point of rotation of the eye, i.e. the position of the effective imaginary stop. This is illustrated by Fig. 182. Consider a + 10D lens (back vertex refraction). The distance of the principal focus from the vertex of an eye 12 mm. behind the lens will be 8·8 cm. The vertex refraction of the corrected eye is thus 11·36D.

The distance of the far point from the centre of rotation will be 7·3 cm., and this gives the numerical value of the radius of the far point sphere. The radius of the Petzval surface is, however, $-nf' = -1{\cdot}5 \times 10 = -15$ cm. sufficiently near; both surfaces have their centres to the left in the diagram. Since the Petzval surface is flatter than the far point sphere, the distance of the focus from the vertex of the eye when the latter is inclined at 20° to the axis

of the spectacle lens is found to be approximately 9·08 cm.—calling for a vertex refraction of 11·01D—a difference of about one-third of a diopter, which would have to be allowed for by changing the accommodation of the eye.

The corresponding case of the negative lens used with the myopic eye will easily be worked out. In such a case both far point sphere and Petzval surfaces will have their centres to the right of the

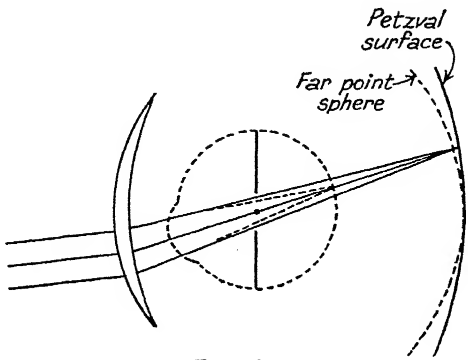

FIG. 182

surfaces as in the case illustrated in Fig. 183. It will be noticed that the centre of the Petzval surface must (from the equation for the radius) be situated about half the focal length to the right of the spectacle lens, while the centre of the far point sphere is not far from

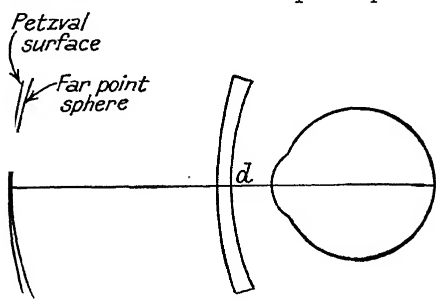

FIG. 183

2·5 cm. to the right of the lens. Hence the difference in the curvatures of the surfaces, which is generally less than with positive lenses, would vanish for a lens of -5 cm. focal length of -20 diopters. Such strong lenses are, however, not often used, and when called for it would probably be for cases of such bad vision that the above coincidence would not be of much significance to the patient.

Astigmatism Arising from Oblique Refraction at a Spherical Surface. We will first investigate the refraction of a narrow tangential fan of rays, such as would lie in the plane of the diagram, Fig. 184, represented by LAB_t and MPB_t directed towards the "object point" B_t. They are refracted at the spherical surface AP separating media of refractive indices n and n'; the centre of curvature is at C. Let the angles of incidence of the two rays be i_1 and i_2. The lines PB_t and AC cross one another at E.

The law of refraction is

$$n \sin i = n' \sin i'$$

Differentiating, we obtain

$$n\, di \cos i = n'\, di' \cos i' \qquad . \quad . \quad . \quad (73)$$

The two rays considered may be supposed to have angles of incidence which are very nearly equal; if so, we may put in the equation above

$$di = i_1 - i_2 = CAB_t - CPB_t$$

and since from the triangles PEC and AEB_t

$$CPB_t + \widehat{PCA} = \widehat{CAB_t} + \widehat{AB_tP}$$

$$di = \widehat{CAB_t} - \widehat{CPB_t} = \widehat{PCA} - \widehat{AB_tP}$$

The values of the angles on the right of this equation can be represented by their angular measure, expressed sufficiently nearly by

$$\widehat{PCA} = \frac{AP}{r},\quad \widehat{AB_tP} = \frac{AP \cos i}{t},\ \text{where } t = AB_t\text{*}$$

Thus $$di = AP\left(\frac{1}{r} - \frac{\cos i}{t}\right)$$

Similarly,† $$di = AP\left(\frac{1}{r} - \frac{\cos i}{t'}\right),\ \text{where } t' = AB'_t$$

Substituting these values in equation (73) and dividing both sides by AP

$$n \cos i \left(\frac{1}{r} - \frac{\cos i}{t}\right) = n' \cos i' \left(\frac{1}{r} - \frac{\cos i'}{t'}\right)$$

On re-arranging

$$\frac{n' \cos^2 i}{t'} \quad \frac{n \cos^2 i}{t} \quad n' \cos i' - n \cos i \qquad (74)$$

* Imagine a perpendicular dropped from A to the line PB_t.
† A similar argument could have been carried out for this case.

This equation, then, gives the relation between the distances of the convergence points of a very narrow fan of rays, lying in a plane passing through the centre of curvature of the refracting surface, before and after refraction, the distances being measured from the surface. The rays have the same limitations with respect

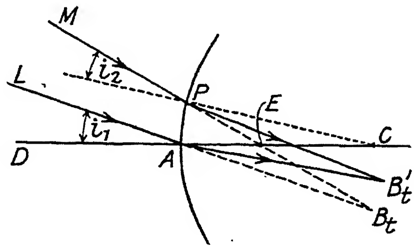

FIG. 184

to each other as the paraxial ray has to the axis in the Gaussian theory.

Sagittal Fan. Referring to Fig. 185, imagine a spherical refracting surface represented by the section AP, with its centre of curvature at C. A ray LA in the plane of the diagram is refracted at A into

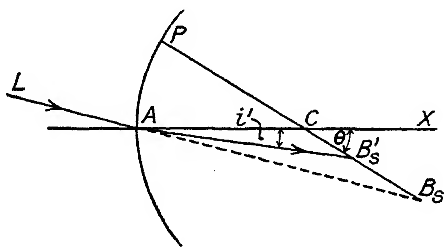

FIG. 185

the direction AB'_s. Take some convenient point such as B'_s on the refracted ray and draw the line PCB'_sB_s cutting the original direction of the ray, before refraction, in the point B_s.

If the diagram were slightly rotated about the axis $PCB_s'B_s$, the points B_s' and B_s would remain in the plane of the paper, and the section of the surface in the diagram would have the same position, but the sections LA and AB'_s of the ray would have new positions slightly above or below the present plane of the diagram, although still directed towards B_s and B_s' respectively. In this manner we have obtained two ray paths of a sagittal fan; the convergence points before and after refraction are B_s and B'_s.

Let $AB_s = s$, and $AB'_s = s'$. Then, from the triangle ACB_s'

$$\frac{CB'_s}{\sin i'} = \frac{s'}{\sin \widehat{ACB}_s}$$

whence $\sin ACB_s = \dfrac{s' \sin i'}{CB'_s}$

Similarly, $$\frac{CB_s}{\sin i} = \frac{s}{\sin ACB_s}$$

whence $$\sin \widehat{ACB}_s = \frac{s \sin i}{CB_s}$$

Then $$\frac{s' \sin i'}{CB'_s} = \frac{s \sin i}{CB_s}$$

but $$n' \sin i' = n \sin i$$

Dividing, we obtain $\dfrac{CB'_s \,.\, n'}{s'} = \dfrac{CB_s \,.\, n}{s}$

In order to obtain the ratio of CB'_s to CB_s, project these lengths on the line ACX by multiplying by $\cos \widehat{XCB}_s = \cos\theta$. Then $CB'_s \cos\theta = (s' \cos i' - r)$, and similarly. Then

$$n'(s' \cos i' - r) \qquad n(s \cos i - r)$$

and on re-arranging

$$\frac{n'}{s'} - \frac{n}{s} \qquad n' \cos i' - n \cos i \tag{75}$$

It will be noticed in this expression that the quantity appearing on the right of the equation is the same as that which occurs in the rather more complicated " tangential " equation.

Astigmatism of a Thin Lens Passed centrally by an Oblique Pencil. Formulae 74 and 75 may be applied to find the tangential and sagittal powers of a thin lens traversed obliquely through its centre by a bundle of rays which is parallel on entry. The principal ray, which passes through the centre of the lens, will be refracted symmetrically, so that the angle θ of emergence from the second face will be equal to the angle of incidence on the first face. Let the

internal angle of refraction be ϕ and the refractive index n. Successive applications of the tangential formula give

$$\frac{n\cos^2\phi}{t_1'} = \frac{n\cos\phi - \cos\theta}{r_1}$$

$$\frac{\cos^2\theta}{t_2'} - \frac{n\cos^2\phi}{t_1'} = \frac{\cos\theta - n\cos\phi}{r_2}$$

Writing t_2' as f_t' (the tangential focal distance) we obtain

$$\frac{1}{f'_t} = \left(\frac{n\cos\phi - \cos\theta}{\cos^2\theta}\right)\left(\frac{1}{r_1} - \frac{1}{r_2}\right) = \left(\frac{n\cos\phi - \cos\theta}{(n-1)\cos^2\theta}\right)\frac{1}{f'}.$$

Similarly, two successive applications of the sagittal formula give

$$\frac{}{f'_s} = (n\cos\phi - \cos\theta)\left(\frac{1}{r_1} - \frac{1}{r_2}\right) = \left(\frac{n\cos\phi - \cos\theta}{n-1}\right)\frac{1}{f'}.$$

In order to evaluate these expressions, we remember $n\sin\phi = \sin\theta$ and write

$$\frac{n\cos\phi - \cos\theta}{n-1} \qquad \frac{\left(1 - \frac{\sin^2\theta}{n^2}\right)^{\frac{1}{2}} - (1 - \sin^2\theta)^{\frac{1}{2}}}{n-1}$$

When θ is so small that powers of $\sin\theta$ above the second may be neglected, we may expand the brackets and finally obtain—

$$\frac{n\cos\phi - \cos\theta}{n-1} = 1 + \frac{\sin^2\theta}{2n}$$

Thus $\frac{1}{f'_s} = \frac{1}{f'}\left(1 + \frac{\sin^2\theta}{2n}\right) = \frac{1}{f'}\left(1 + \frac{\sin^2\theta}{3}\right)$, approximately, if $= 1{\cdot}5$.

And $\frac{1}{f'_t} = \frac{1}{f'} \frac{1 + \frac{\sin^2 t}{2n}}{\cos^2\theta}$, so that under the same conditions,

$$\frac{1}{f'_t} = \frac{1}{f'}\left(1 + \frac{2n+1}{2n}\qquad\right) = \frac{1}{f'}\left(1 + \frac{4\sin^2\theta}{3}\right),$$

approximately, if $n = 1{\cdot}5$.

The "powers" are thus approximately

$$\mathscr{F}_s = \mathscr{F}\left(1 + \frac{\sin^2\theta}{3}\right)$$

$$\mathscr{F}_t = \mathscr{F}\left(1 + \frac{4\sin^2\theta}{3}\right)$$

and the difference $\mathscr{F}_t - \mathscr{F}_s = \mathscr{F}\sin^2\theta$. As at the foot of page 147, we can also show that $\mathscr{F}_t - \mathscr{F}_s = \mathscr{F}_s\tan^2\theta$.

The lens action in the direction θ is that of a sphero-cyl having a spherical power $= \mathscr{F}_s$ as given above combined with a cylinder of $\mathscr{F} \sin^2 \theta$. This formula is, however, only accurate over small ranges of obliquity, and the cylindrical power increases more rapidly than the $\sin^2$ term allows. The empirical expression, $\mathscr{F} \tan^2 \theta$, for the cylindrical power, holds fairly accurately up to about 30°.

Removal of Astigmatism from a Lens with the Aid of a Narrow Axial Stop. In Fig. 186, AP is a refracting surface. A narrow axial stop is situated at R′. Let the ray LP be the principal ray directed towards the centre of the entrance pupil R, which pupil may be regarded as the image of R′, formed by the refraction of imaginary light passing from right to left through the surface. Let AR $= l$, and AR′ $= l'$. Let the "object point" be astigmatic,* O_t and O_s being the tangential and sagittal foci respectively; then I_t and I_s are the corresponding image points.

Now $$\frac{n' \cos^2 i'}{t'} - \frac{n \cos^2 i}{t} = \frac{n' \cos i' - n \cos i}{r} = \frac{n'}{s'} - \frac{n}{s}$$

or $$\frac{n' \cos^2 i'}{PI_t} - \frac{n \cos^2 i}{PO_t} = \frac{n'}{PI_s} - \frac{n}{PO_s}$$

The principal ray must only be allowed a small angle of obliquity. (The diagram exaggerates this obliquity only for the sake of clearness of the lines and points.) Then the following approximation may be introduced—

$$\cos^2 i = 1 - i^2 \quad (\text{approximation for } \overline{1 - \sin^2 i})$$

$$\cos^2 i' = 1 - i'^2$$

Then $$\frac{n'}{PI_t} - \frac{n'i'^2}{PI_t} - PO_t + \frac{ni^2}{PO_t} = \frac{n'}{(PI_t + I_tI_s)} - \frac{n}{(PO_t + O_tO_s)}$$

$$= (\text{sufficiently nearly})\dagger \; \frac{n'}{PI_t} - \frac{n' \,.\, I_tI_s}{PI_t^2} - \frac{n}{PO_t} + \frac{n \,.\, O_tO_s}{PO_t^2}$$

or $$\frac{n' \,.\, I_tI_s}{PI_t^2} - \frac{n \,.\, O_tO_s}{PO_t^2} \quad \frac{n'i'^2}{PI_t} - \frac{ni^2}{PO_t}$$

$$\frac{n' \,.\, I_tI_s}{t'^2} \quad n \,.\, O_tO_s \quad \frac{n'i'^2}{t'} - \frac{ni^2}{t}$$

* The "object" may be an astigmatic image formed by another part of the optical system.

† $(PI_t - I_tI_s)^{-1} = \dfrac{\left(1 - \dfrac{I_t I_s}{PI_t}\right)^{-1}}{PI_t}$ Expand by Binonial theorem and neglect terms of high orders.

If y denotes the distance of P from the axis, we may write

$$i = y\left(\frac{1}{l} - \frac{1}{r}\right), \text{ and } i' = y\left(\frac{1}{l'} - \frac{1}{r}\right)$$

sufficiently nearly, and also for small angles of obliquity the law of refraction gives as a first approximation $n'i' = ni$.

Then $$\frac{n' \,.\, I_tI_s}{t'^2} - \frac{n \,.\, O_tO_s}{t^2} = n'^2 i'^2 \left(\frac{1}{n't'} - \frac{1}{nt}\right)$$

$$= n'^2 y^2 \left(\frac{1}{l'} - \frac{1}{r}\right)^2 \left(\frac{1}{n't'} - \frac{1}{nt}\right)$$

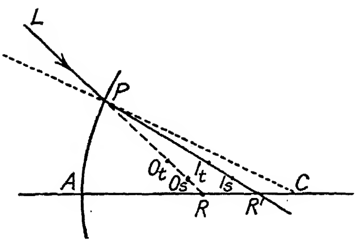

FIG. 186

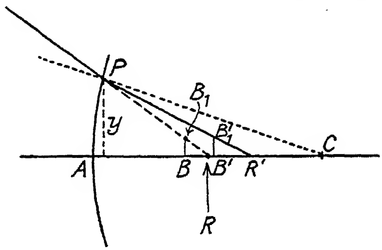

FIG. 187

In order to simplify the expression, we may introduce

$$Q_t = n\left(\frac{1}{r} - \frac{1}{t}\right) = n'\left(\frac{1}{r} - \frac{1}{t'}\right)$$ (an alternative form of equation (7), Chapter I.)

$$Q_l = n\left(\frac{1}{r} - \frac{1}{l}\right) = n'\left(\frac{1}{r} - \frac{1}{l'}\right)$$

Now, Fig. 187 represents the same case of refraction as Fig. 186, except that the separation of the astigmatic foci* is now not shown, and the conjugate positions are B_1 and B_1' respectively. The points B and B′ are conjugate positions on the axis, so that $BB_1 = h$ and $B'B_1' = h'$ are a small "object" and "image" respectively, both perpendicular to the axis.

We have $\frac{y}{l} = \frac{h}{BR} = \frac{h}{l - t}$ (very nearly); remember that the investigation is limited to small values of y, so that $\frac{l - t}{l} = \frac{h}{y}$; and

$$Q_l - Q_t = n\left(\frac{1}{t} - \frac{1}{l}\right) = n\left(\frac{l - t}{lt}\right) = \frac{nh}{yt}$$

* The separation suggested in Fig. 186 was greatly exaggerated for the sake of clearness in the diagram.

Hence,
$$y = \frac{nh}{t\,(Q_l - Q_t)}$$

Also the Lagrange relation

$$nha = n'h'a' \qquad \text{(Equation (9), Chapter I)}$$

can be put into the form (by imagining a ray PB refracted through PB′)

$$\frac{nhy}{\mathrm{AB}} = \frac{n'h'y}{\mathrm{AB'}}$$

which under the limitations of angle and incidence height adopted in the present investigation can be written sufficiently nearly

$$\frac{nh}{t} = \frac{n'h'}{t'}$$

The main equation thus becomes

$$\frac{\mathrm{I}_t\mathrm{I}_s}{n'h'^2} - \frac{\mathrm{O}_t\mathrm{O}_s}{nh^2} = \frac{Q_l^2}{(Q_l - Q_t)^2}\left(\frac{1}{n't'} - \frac{1}{nt}\right)$$

If this equation be applied to a series of refracting surfaces, and the resulting equations are added, there will be a cancellation of terms on the left-hand side of the equation, finally leaving

$$(\text{final})\ \frac{\mathrm{I}_t\mathrm{I}_s}{n'h'^2} - (\text{initial})\ \frac{\mathrm{O}_t\mathrm{O}_s}{nh^2} = \Sigma\ \frac{Q_l^2}{(Q_l - Q_t)^2}\left(\frac{1}{n't'} - \frac{1}{nt}\right)$$

The condition for the absence of astigmatism for an instrument must therefore be that the sum on the right-hand side of the equation is zero. This is known as the Zinken-Sommer condition.

Application to the Case of a Thin Lens. As in Chapter I, the formula for the focal length of a thin lens

$$\frac{1}{f'} = (n_a - 1)\left(\frac{1}{r_1} - \frac{1}{r_2}\right)$$

may be written

$$\mathscr{F} = (n_a - 1)\,(\mathscr{R}_1 - \mathscr{R}_2) = (n_a - 1)\,\mathscr{R}$$

where $\mathscr{R} = \mathscr{R}_1 - \mathscr{R}_2$ is the difference of the curvatures of the two faces. In order to evaluate the Q values it is convenient to assume t, the object distance, as infinite. The distance of the pupil or stop from the lens will be l', and the distance of the corresponding entrance pupil will be l. Both are finite; (in practice l' will be about 28 mm., in the case of a spectacle lens).

Since, if $\mathscr{F}$ is the power of the lens

$$\frac{1}{l'} - \frac{1}{l} = \mathscr{F}, \text{ or } \mathscr{L}' - \mathscr{L} = \mathscr{F}$$

$$-\mathscr{L} = \mathscr{F} - \mathscr{L}'$$

where $\mathscr{L}$ and $\mathscr{L}'$ are the vergencies to the object and final image respectively.

Hence we have for the first surface

$$Q_l = \mathscr{R}_1 + \mathscr{F} - \mathscr{L}'$$

Also $$Q_t = n\left(\frac{1}{r_1} - \frac{1}{t}\right)$$

If $n = 1$ and $t = \infty$, $Q_t = \mathscr{R}_1$.

Whence $$Q_l - Q_t = \mathscr{F} - \mathscr{L}'$$

Since $t = \infty$ the refraction at the first surface gives

$$\frac{n_a}{t'} = \mathscr{F}_1$$

where $\mathscr{F}_1$ is the power of the first surface.

Hence A_1 = Astigmatism for 1st surface

$$= \frac{Q_l^2}{(Q_l - Q_t)^2}\left(\frac{1}{n't'} - \frac{1}{nt}\right) = \frac{(\mathscr{R}_1 + \mathscr{F} - \mathscr{L}')^2}{(\mathscr{F} - \mathscr{L}')^2} \cdot \frac{\mathscr{F}_1}{n_a^2}$$

2nd Surface. The refraction at this surface is represented by

$$\mathscr{L}_2' - n_a \mathscr{L}_2 = (1 - n_a)\, \mathscr{R}_2 = \mathscr{F}_2$$

whence $Q_l = n'\left(\frac{1}{r} - \frac{1}{l'}\right)$ in the general expression,

$$= \mathscr{R}_2 - \mathscr{L}_2' = \mathscr{R}_1 - \mathscr{R} - \mathscr{L}'$$

and $$Q_t = n'\left(\frac{1}{r} - \frac{1}{t'}\right)$$ in the general expression,

$$= \mathscr{R}_2 - \frac{1}{f'}$$

since the final image will be situated in the focal plane, as the object point is at infinity. Thus,

$$Q_t = \mathscr{R}_2 - \mathscr{F} = \mathscr{R}_1 - \mathscr{R} - \mathscr{F}$$

To evaluate the bracket: $\left(\frac{1}{n't'} - \frac{1}{nt}\right)$, for the second surface, note that $t' = f'$. The standard equation gives

$$\frac{1}{t'} - \frac{n_a}{t} = \mathscr{F}_2$$

or

$$\mathscr{F} - \frac{n_a}{t} = \mathscr{F}_2$$

whence

$$\frac{n_a}{t} = \mathscr{F}_1$$

Hence the bracket is evaluated as

$$\mathscr{F} - \frac{\mathscr{F}_1}{n_a^2}$$

and the astigmatism of the second surface, A_2, is given by

$$A_2 = \frac{(\mathscr{R}_1 - \mathscr{R} - \mathscr{L}')^2\,(n_a^2\mathscr{F} - \mathscr{F}_1)}{(\mathscr{F} - \mathscr{L}')^2 n_a^2}$$

The total astigmatism therefore becomes

$$A = \frac{(\mathscr{R}_1 + \mathscr{F} - \mathscr{L}')^2 \mathscr{F}_1 + (\mathscr{R}_1 - \mathscr{R} - \mathscr{L}')^2\,(n_a^2\mathscr{F} - \mathscr{F}_1)}{(\mathscr{F} - \mathscr{L}')^2 n_a^2}$$

The condition for the elimination of astigmatism of oblique pencils is obtained by equating the above expression to zero.

It may be simplified by writing

$$\mathscr{R}_1 = \frac{\mathscr{F}_1}{(n_a - 1)}$$

$$\mathscr{R} = \frac{\mathscr{F}}{(n_a - 1)}$$

and the final condition reduces, after some algebraical transformations, to

$$n\mathscr{F}^2 - (n + 2)\mathscr{F}\mathscr{F}_1 + (n + 2)\mathscr{F}_1^2 - 2(n^2 - 1)\mathscr{L}'\mathscr{F}_1 + n(n - 1)^2\mathscr{L}'^2 + 2n(n - 1)\mathscr{L}'\mathscr{F} = 0$$

in which n is written for n_a, the refractive index of the lens.

If $\mathscr{L}'$ and n are taken as constant, this is an equation of the second degree in $\mathscr{F}$ and $\mathscr{F}_1$. It plots as an ellipse.

Fig. 188 shows the ellipses *a*, *b*, and *c* resulting from the assumption of different values for the distance of the effective pupil, viz. 20, 25, and 28 mm. Note that the value of $\frac{1}{l'}$ as it appears in the equation

must be expressed in the same units as the other "powers," viz., in diopters. The refractive index assumed is 1·52.

It will be seen that the powers $\mathcal{F}$ of the lenses are plotted horizontally, the powers of the front surfaces vertically. With a value of $l' = 25$ mm. it is possible to select forms giving freedom from spherical aberration for all powers *between* about $-24{\cdot}75$D and $+7{\cdot}5$D. With $l' = 20$ mm., the range is greater.

In order to illustrate the significance of the figure it will be noticed that when $l' = 28$ mm. a lens of -10D can be corrected by using a front surface of either $+2{\cdot}5$D or $+14{\cdot}5$D approximately (requiring

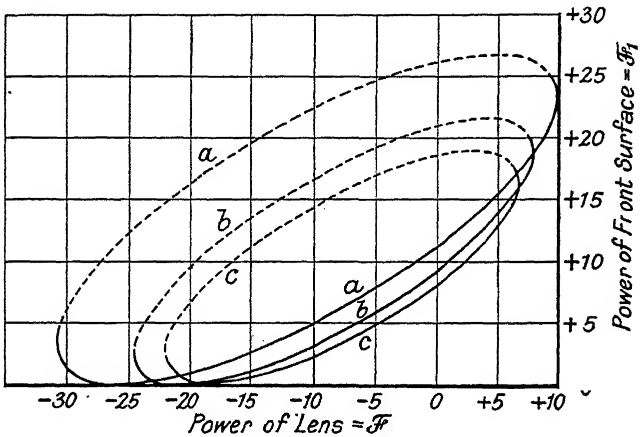

FIG. 188. FORMS OF LENSES FOR THE REMOVAL OF OBLIQUE ASTIGMATISM WHEN USED WITH A ROLLING EYE

Distance of centre of rotation: (*a*) 20 mm.; (*b*) 25 mm.; (*c*) 28 mm.

radii of about 21 and 3·6 cm.). The powers of the back surfaces would therefore be (approximately) $-12{\cdot}5$D and $-24{\cdot}5$D (radii about 4·2 and 2·1 cm.). Both are thus meniscus lenses; the one with shallower curves being obviously the more practical type, and cheaper to make. The profiles of the two lenses are illustrated in Fig. 189.

It will be seen that the range of negative or diverging lenses possible to correct thus is adequate to cover all ordinary requirements. When $l' = 28$ mm., the positive lenses of higher powers than about 7·5D cannot be corrected by "bending." Recourse must thus be had to the use of non-spherical surfaces, and lenses of this kind for use by patients who have had the lens of the eye removed for "cataract" were suggested by Gullstrand and actually computed in 1908 by M. von Rohr. Such lenses, under the name "Katral

lenses " are produced by the firm of Zeiss, an optical performance of some difficulty.

It is of interest to note that the use of meniscus lenses was suggested on more or less empirical principles by Wollaston, and also on theoretical grounds by Ostwalt.*

The thin lens theory outlined above is a useful guide, but in the actual designing of " best-form " lenses, trigonometrical trials are necessary. It is not difficult to calculate the tangential and sagittal foci, for a ray passing through the centre of a given stop, by the aid of formulae 74 and 75.

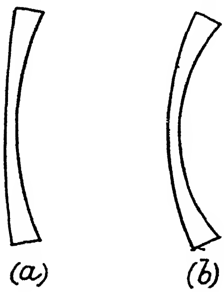

FIG. 189
(a) Ostwalt type
(b) Wollaston type

Prisms. Ophthalmic prisms are employed in the correction of strabismus or " squint." Their " power " is reckoned in terms of the apparent lateral displacement (in centimetres) produced in the image of an object at a distance of 1 metre. Thus, in Fig. 190, the displacement of the image from B to B′, a distance of h cm., indicates a power of $\frac{h}{l}$ " prism diopters " where l is the distance of the object in metres. The notation usually employed is exemplified by $6^{\triangle}$ signifying a prism of six " prism diopters."

Let a prism of power $\triangle$ be placed in front of an eye at a distance δ from the point of rotation. The eye rotates so as to receive the image, on the fovea, Fig. 191.

The displacement h is given by

$$h = \triangle l$$

where l is the distance in metres. The deviation of the eye is the same as would be produced by a prism of power

$$\frac{h}{l+\delta} = \frac{\triangle l}{l+\delta}$$

placed in the position of the centre of the eye. The effective power of a prism is therefore somewhat less for nearer than for distant objects.

Decentration of Lenses. Prismatic effects are produced by mounting a lens in front of an eye so that the optical centre of the lens is displaced from the normal intersection point of the visual axis.

* The two forms of meniscus lens possible in correcting oblique astigmatism have been named after Ostwalt and Wollaston, as shown in Fig. 189.

In Fig. 192 consider the action of a lens decentred through a distance y and focal length f'. The axis of the lens is GAF′. A ray parallel to the axis incident at a height y is deviated towards the

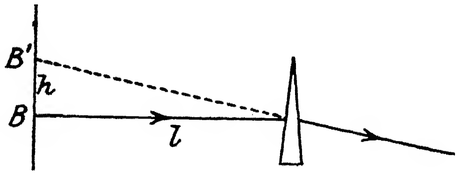

FIG. 190

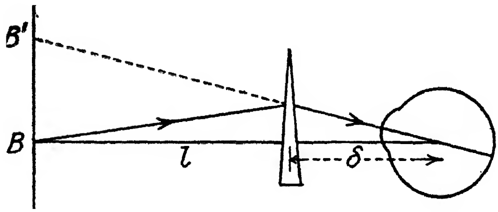

FIG. 191

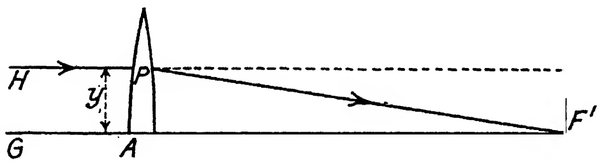

FIG. 192

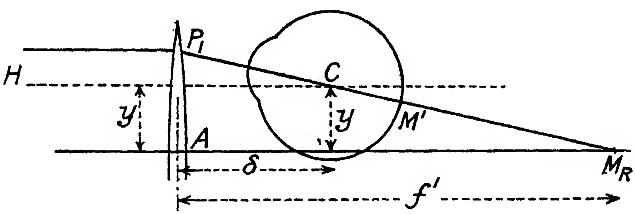

FIG. 193

principal focus F′, i.e. through an angle equivalent to the deviation produced by a prism of power $\frac{y}{f'}$ prism diopters if y is measured in centimetres and f' in metres.

Prismatic power $= y\mathscr{F} =$ (decentration in centimetres) times (power of lens).

The effect is modified when the lens is held before a rotating eye. In Fig. 193, let C be the centre of rotation of the eye, and let HC be the original direction of the visual axis, along which the distant object is seen with the aid of a centred lens of requisite power.

Let the lens be decentred by a distance of y (cm.), keeping the axis parallel to the original direction. The eye has then to be rotated so that its far point M_R coincides with the new position of the principal focus, the object being seen apparently in the direction CP_1.

The actual deviation of the eye is therefore expressed as

$$\frac{f'}{AP_1} = \frac{y}{f' - \delta} = \frac{y\mathscr{F}}{1 - \delta\mathscr{F}}$$

Decentration for Required Prismatic Effect. In optical prescriptions it is usual, when a correction for strabismus is to be given, to specify the prismatic power required for an eye in the horizontal and vertical directions, the direction of the base being also indicated. Thus a prescription might read—

" Right eye 4·5 D Sph with 1△ base out and 2△ base up."

When a spherical surfaced lens is in use, the prismatic effects are easily obtained by the necessary decentrations calculated from the formula above. Thus

$$\text{Decentration} = \frac{\text{Prism power}}{\text{Power of lens}}$$

In the case given the decentration necessary will be $\frac{1}{4{\cdot}5} = 0{\cdot}22$ cm. outwards, plus $\frac{2}{4{\cdot}5} = 0{\cdot}44$ cm. upwards.

When cylindrical or toric surfaces are prescribed for an eye, it is possible to obtain a pure prismatic effect by decentration of the lens along one of the principal sections. If the axial direction of the effective cylinder should be oblique, it is not possible to obtain a simple horizontal or vertical effect alone by decentering the lens in the corresponding directions.

It is possible, however, to calculate the necessary components of the horizontal and vertical decentrations.

Let $\mathscr{F}_s$ = power of spherical component of the lens.

$\mathscr{F}_c$ = power of cylindrical component of the lens.

θ = axis direction of the cylinder.

Let the centre of the lens be situated at the centre of co-ordinates, then the components of the prismatic deviation at any point x, y, such as G, Fig. 194, may be determined.

The prismatic effect of the spherical component in the direction GO is $\mathscr{F}_s \times$ GO, and this may be resolved into

$$\text{Vertical component} \;\; = \mathscr{F}_s y \text{ (base down)}$$

and $$\text{Horizontal component} = \mathscr{F}_s x \text{ (base left)}$$

The prismatic effect due to the cylinder is understood if we draw the principal directions OA (the axis) and OP. Draw also GR

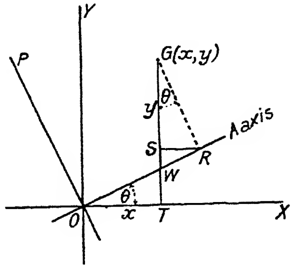

FIG. 194

perpendicular to OA, and RS, the perpendicular to GT as shown in the diagram.

The prismatic effect at G due to the cylinder is $\mathscr{F}_c \times$ GR in the direction GR, and this may be resolved into

$$\text{Vertical component} \;\; = \mathscr{F}_c \times \text{GS (base down).}$$

$$\text{Horizontal component} = \mathscr{F}_c \times \text{SR (base to right).}$$

It is not difficult to see that

$$\text{GR} = (y - x \tan \theta) \cos \theta = (y \cos \theta - x \sin \theta)$$

and $$\text{GS} = (y \cos \theta - x \sin \theta) \cos \theta$$

and $$\text{SR} = (y \cos \theta - x \sin \theta) \sin \theta$$

Adding the total Vertical and Horizontal components, denoting the vertical (base down) by V, and the horizontal base left by H, we thus obtain

$$\text{V} = \mathscr{F}_s y + \mathscr{F}_c \cos \theta \, (y \cos \theta - x \sin \theta), \text{ base down.}$$

$$\text{H} = \mathscr{F}_s x - \mathscr{F}_c \sin \theta \, (y \cos \theta - x \sin \theta), \text{ base left.}$$

These equations give, by straightforward algebra

$$x = \frac{\text{H}\mathscr{F}_s \times \text{H}\mathscr{F}_c \cos^2 \theta + \text{V}\mathscr{F}_c \sin \theta \cos \theta}{\mathscr{F}_s \, (\mathscr{F}_s + \mathscr{F}_c)}$$

$$y = \frac{\text{V}\mathscr{F}_s + \text{V}\mathscr{F}_c \sin^2 \theta + \text{H}\mathscr{F}_c \sin \theta \cos \theta}{\mathscr{F}_s \, (\mathscr{F}_s + \mathscr{F}_c)}$$

If, therefore, the required vertical and horizontal components V and H for the prismatic effect are given in prism diopters, the lens has to be decentred so that the line of vision cuts it in the point G with co-ordinates x and y given by the above equations.

Spectacles of Special Types. Owing to limitations of space it has not been possible to include discussions of spectacles of special types, such as the bi-focal lenses, telescope spectacles, and the like.

Reference may be made to Emsley and Swaine's *Ophthalmic Lenses* for a discussion of special lenses, while a description of telescopic spectacles, which usually comprise a compact Galilean telescope, will be found in Henker's *Introduction to the Theory of Spectacles* (English edition, published by Messrs Carl Zeiss).

References

1. Souter: *The Refractive and Motor Mechanism of the Eye* (Keystone Publishing Co., Philadelphia, 1910).
2. Laurance: *Visual Optics* (The School of Optics, Ltd.).
3. Henker: *Introduction to the Theory of Spectacles*, p. 253.
4. G. B. Airy: *Camb. Phil. Trans.*, 2 (1827), 267.

APPENDIX I

Note on Sign Conventions. In the computing classes at the Imperial College, the formulae developed in Chapter I are used for ray-tracing with either direction of the light, i.e. from left to right or right to left. The " dash " added to a length then means a quantity measured to the right of a point or surface, the absence of a dash indicates a quantity measured to the left. Thus, the paraxial equation for refraction at a curved surface,

$$\frac{n'}{l'} \quad l \quad {}^{n'-n} \quad = \mathscr{P}$$

gives an identity which must remain unaffected by the reversal of the direction of a ray because the path of a ray is unaltered by such reversal.

The standard computing equations retain the same forms, whether we proceed from " plain " to " dash " quantities, or vice versa. Thus, the equations

$$i' = \frac{l'-r}{r} u'$$

$$i = {}^{i' \,.\, n'}$$

$$u = u' + i' - i$$

$$l - r = {}^{r \,.\, i}$$

$$l = (l-r) + r$$

are in the same form as those of page 18. Very similar use can be made of the various other formulae, and this is the general method advised in Prof. Conrady's *Applied Optics and Optical Design.*

For the purposes of the general Gaussian theory, however, it may be required to deal with cases of reflection, in which the direction of light is actually physically reversed in proceeding from object to image. In order to be able to deal with such cases, we shall here assume that a " dash " signifies a quantity in the image space, while its absence denotes a quantity in the object space. Consider then the equation

$$\frac{n'}{l'} - \frac{n}{l} \quad {}^{n'-n} \quad = \mathscr{F}$$

Let the quantities on the left of the curved surface be n_1, l_1, while on the right they are n_2, l_2. Then "left to right" the general equation becomes

$$\frac{n_2}{l_2} - \frac{n_1}{l_1} = \frac{n_2 - n_1}{r} = \mathscr{F}$$

but "right to left" it becomes

$$\frac{}{l_1} - \frac{}{l_2} \qquad \frac{n_1 - n_2}{} = - \mathscr{F}$$

The necessity of altering the sign of the power of a surface or system would not be acceptable to ophthalmic opticians, who always assign the same positive sign to the "converging" type of spectacle lens. In order to remove this difficulty, note that the signs of angles made by rays with the axis are independent of the direction of the light. Thus, if a ray intersects the axis at a distance l from a surface, and intersects the latter in the height y, the tangent of the angle made between the ray and the axis will be given, to the usual approximation, as

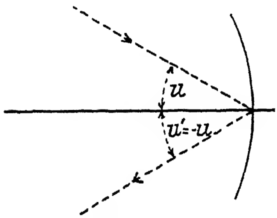

FIG. 195

$$\tan \alpha = \frac{y}{l}$$

Also, if a ray crosses the axis in a point X, and meets a plane perpendicular to the axis at a height h, the axial distance from X to this plane being k, the angle ω between the ray and the axis will be given by

$$\tan \omega = -\frac{h}{k}$$

The condition of reflection of a ray at the axial point of a reflecting surface would, therefore, evidently be expressed by $u' = -u$. (See Fig. 195.)

The ordinary law of refraction at an axial point of a surface,

$$n' \sin u' = n \sin u$$

takes this form if we put $n' = -n$, whence $u' = -u$. This device now enables us to deal with the general formula

$$\frac{n'}{l'} \cdot \cdot \frac{n}{l} \qquad \frac{n' - n}{r} = \mathscr{F}$$

and apply it to the case of reflection at a spherical surface. It becomes, on simplification,

$$\frac{1}{l'} + \frac{1}{l} = \frac{2}{r}$$

Note, however, that the power $\mathscr{F}$ of the surface in the general formula is $-\frac{2n}{r}$.

We see then that the case of light passing from right to left is dealt with by assigning negative signs to the refractive indices. The general equation applied to the case right to left is now

$$\frac{(-n_1)}{l_1} - \frac{(-n_2)}{l_2} = \frac{(-n_1) - (-n_2)}{r} = \text{Power}$$

Thus, if the negative refractive indices are used to indicate reversal of the light, the power of a surface will be unchanged; this conclusion is also valid for a more complex system. This is practically equivalent to applying the same formula for both cases, as above, page 311.

In applying this method it must be carefully remembered that the formula for a system in air—

$$\frac{1}{l'} - \frac{1}{l} = \mathscr{F}$$

is only a simplified form of the general formula

$$\frac{n'}{l'} - \frac{n}{l} = \frac{n'}{f'} = -\frac{n}{f} = \mathscr{F}$$

(See page 50.) If l_1 and l_2 are the conjugate quantities measured on the left and right of a system in a medium of refractive index n, the left to right equation is

$$\frac{n}{l_2} - \frac{n}{l_1} = \mathscr{F}$$

while the right to left version is (interpreting the dash in the general formula to refer to the image space)

$$\frac{(-n)}{l_1} - \frac{(-n)}{l_2} = \mathscr{F};$$

again this is equivalent to applying the "left to right" formula to the "right to left" case.

We now see, however, that the general equations can be applied to any combination of refracting and reflecting surfaces. The separation $P_a'P_b$ of systems will be measured, as before, *from* P_a' to P_b, the order of meeting the systems by the light being *ab*.

Take the case of Fig. 196, in which a system *a* is mounted in front of a spherical mirror *b*. The light traverses *a*, is reflected by

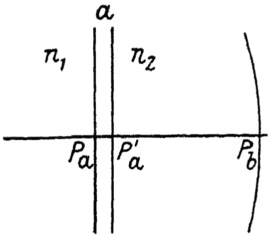

FIG. 196

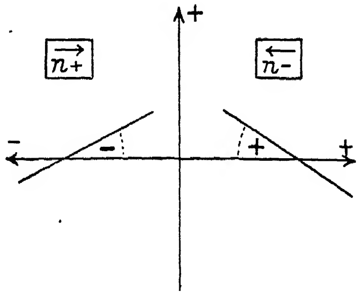

FIG. 197

b, and re-traverses *a*. The " separations " appearing in the Gaussian formulae are the *reduced* separations. Hence

$$d_1 = \frac{P_a'P_b}{\cdot} \qquad d_2 = \frac{P_bP_a}{-n_2}$$

Since the light is reversed after reflection the negative refractive idea is used. Hence, $d'' = d'$ in this case, and $\mathscr{F}_3 = \mathscr{F}_1$ while

$$\mathscr{F}_2 = -\frac{2n_2}{r}$$

The form of the resulting expression appears on page 63.

Fig. 197 is a diagram intended to express the conventions explained above.

It may be noted that the reversal of the sign of the refractive index to denote reversal of the light gives consistent results with the Lagrange formula, and the optical sine relation, also with equations for optical path, i.e. (refractive index) $\times$ (distance). In optical equations, both will change sign on reversal of the direction of the light.

APPENDIX II

The "Wave Curvature" Method. The following introductory outline may be useful to teachers who wish to use the method as supplementary to the usual geometrical treatments. It has the advantage of making conventions more simple in the elementary stages, as they depend more on the physical aspects of the problem, but it should not be used till Huygens' principle can be understood.

Curvature. The mathematical definition of curvature is the ratio of the angular turn of a curve to the length of the arc *when both are indefinitely small.* It can be theoretically shown that this is measured by the reciprocal of the radius r. The unit of curvature is the curve of radius 1 metre (Diopter). Curvature $\mathscr{R} = \frac{1}{r}$.

Curvatures of surfaces, including toric surfaces, are discussed on page 279. Drysdale recommends that examples of various curvatures of arcs should be cut in wood for demonstration.

Relation to Sag. In Fig. 1, AO is the axis of a circle of radius r, and PQ is a chord perpendicular thereto. The length $PQ = 2y$. The intercept AS is the "sagitta" or "sag" s of the arc at the centre of the chord. Then

$$y^2 = s(2r - s) = 2rs - s^2.$$

If y is small, s may become small enough for its square to be neglected; (check numerically) so that,

$$\mathscr{R} = \frac{1}{r} = \frac{2s}{y^2} \quad . \quad . \quad . \quad . \quad . \quad (a)$$

If we take a standard length for the chord, the curvature will be proportional to the sag.

The *vergence* of light is the curvature of the wave-front. When light is diverging from an object or focus the vergence or curvature is negative. When converging towards a focus it is positive. See below for relations with geometrical conventions.

Refraction at Single Curved Surface. In Fig. 2, the section of the curved surface is QAP. It separates media of refractive indices n and n', and its curvature is $\mathscr{R}$ (Positive if the convexity is turned towards the incident light and vice versa). The incident wave has a curvature $\mathscr{L}$, and is shown in section by the full line exterior to the

points P and Q. If no refraction had occurred, it would have had the dotted form QTP, but the actual wave-front after refraction passes through R, where

Optical path AT in medium n = optical path AR in medium n'.

If it is assumed that the refracted wave-front is circular, this gives

$$n\frac{y^2}{2}(\mathscr{R}-\mathscr{L}) = n'\frac{y^2}{2}(\mathscr{R}-\mathscr{L}'),$$

or $$n'\mathscr{L}'-n\mathscr{L} = (n'-n)\mathscr{R}. \quad . \quad . \quad . \quad . \qquad (b)$$

or (page 34) $\overline{\mathscr{L}}' - \overline{\mathscr{L}} = \mathscr{F}$ (the power of the surface) . (c)

Plane Surface. If the surface is *plane* $\mathscr{R} = o$ and

$$\overline{\mathscr{L}}' = \overline{\mathscr{L}}, \text{ or } n'\mathscr{L}' = n\mathscr{L} \quad . \quad . \quad . \quad . \quad . \qquad (d)$$

Magnification. The refraction of an oblique wave-front at the axial point of the surface, imagined limited to a very small aperture,

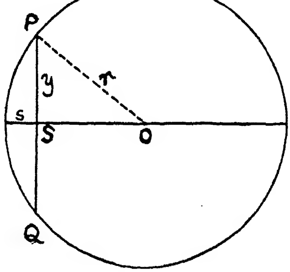

FIG. 1

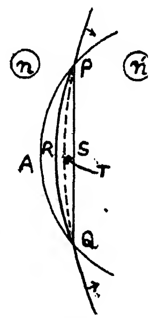

FIG. 2

is dealt with by Huygens' construction, and the ray is introduced as the normal to the wave-front. A discussion on the same lines as given on page 27 shows that

$$\overline{\mathscr{L}}h = \overline{\mathscr{L}}'h',$$

or $$\text{Magnification} = \frac{h'}{h} = \frac{\overline{\mathscr{L}}'}{\overline{\mathscr{L}}} \quad . \qquad (e)$$

and, as before, the same form holds for the action of a number of surfaces.

Change of Vergence. The change of reduced vergence of a wave travelling a distance d, from a position (1) to position (2), is given by (page 35)

$$\overline{\mathscr{L}}_2 = \frac{\overline{\mathscr{L}}'_1}{1-\bar{d}\ \ {}_1'} \quad . \quad . \quad . \quad . \quad . \quad . \quad . \qquad (f)$$

Refraction at two Successive Surfaces. The surfaces are (1) and (2).

$$(1) \quad . \; . \; . \; . \quad \overline{\mathscr{L}_1}' - \overline{\mathscr{L}_1} = \mathscr{F}_1 = (n_1' - n_1)\mathscr{R}_1$$

The separation is d. The change of vergence is given by (f) above.

$$(2) \quad . \; . \; . \quad \overline{\mathscr{L}_1}' - \overline{\mathscr{L}_2} = \mathscr{F}_2 = (n_2' - n_1')\mathscr{R}_2.$$

Special case when $d = o$ (thin lens). Then $\overline{\mathscr{L}_2} = \overline{\mathscr{L}_1}'$ and the addition of above equations gives—

$$\overline{\mathscr{L}_2}' - \overline{\mathscr{L}_1} = \mathscr{F}_1 + \mathscr{F}_2$$

Thin Lens in Air. If also $n_1 = n_2' = 1$, (and internal refractive index is n)

$$\mathscr{L}_2' - \mathscr{L}_1 = (n - 1)\,(\mathscr{R}_1 - \mathscr{R}_2) = \mathscr{F}.$$

This equation can be memorized in the form—
Final curvature $\mathscr{L}'$ = Initial curvature $\mathscr{L}$ + Impressed curvature $\mathscr{F}$.

The power of a system appears as "impressed curvature"; the unit being the "Diopter." Fig. 3 shows a simple *ad hoc* treatment

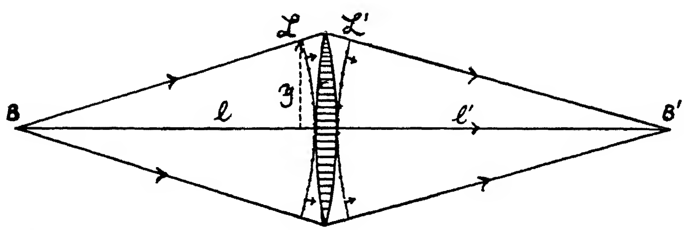

FIG. 3

of the thin lens. The *marginal* optical path between the two positions of the wave-front is equal to the axial optical path, i.e.

$$\tfrac{1}{2}y^2(-\mathscr{L} + \mathscr{R}_1 - \mathscr{R}_2 + \mathscr{L}') = n.\tfrac{1}{2}y^2\,(\mathscr{R}_1 - \mathscr{R}_2).$$

Hence $\quad \mathscr{L}' - \mathscr{L} = (n - 1)\,(\mathscr{R}_1 - \mathscr{R}_2).$

The student should work out a number of cases including meniscus and concave lenses to see the application of the formulae.

Thick Lens in Air. The internal refractive index is n. Assume a distant object subtending an angle α; the size of the image formed

by the first surface is $\frac{a}{\mathscr{F}_1}$. From the above equations if $\overline{\mathscr{L}}_1 = o$ $\overline{\mathscr{L}}_1' = \mathscr{F}_1$. The magnification $\frac{h'}{h}$ produced by the second surface is $\frac{\mathscr{F}_1}{(\mathscr{F}_1 + \mathscr{F}_2 - \bar{d}\ \mathscr{F}_1\mathscr{F}_2)}$. Hence the size of the final image is $\frac{a}{(\mathscr{F}_1 + \mathscr{F}_2 - \bar{d}\ \mathscr{F}_1\mathscr{F}_2)}$. A thin lens of power $\mathscr{F}$ would give an image of size $\frac{a}{\mathscr{F}}$. Hence the equivalent power of the thick lens is $\mathscr{F}_1 + \mathscr{F}_2 - \bar{d}\ \mathscr{F}_1\mathscr{F}_2$.

Two Coaxial Lenses. A similar argument holds for two coaxial lenses of powers $\mathscr{F}_1$ and $\mathscr{F}_2$, and the formula is the same except that the separation d appears directly instead of a " reduced " distance $\bar{d}$.

Principal and Nodal Points, etc. For methods in this connection see Drysdale, *Proc. Phys. Soc.* 19 (1905.) Drysdale's sign conventions are different in some details. An extension of the method to the discussion of aberrations is given by the same writer (*Phot. Jour*, March, April, and May, 1928).

Connection between " Wave Curvature " Equations and " Geometrical " equations. The above equations and conventions constitute a simple scheme independent of geometrical frameworks of reference. The paraxial equations of Chapters I and II have simple reciprocal relations with the wave curvature equations, provided that light travels from left to right. Thus compare

$$\frac{n'}{l'} - \frac{n}{l} = \frac{n' - n}{} \qquad \text{and} \qquad n'\mathscr{L}' - n\mathscr{L} = (n' - n)\mathscr{R},$$

and so on. The negative sign of the curvature of a divergent wave meeting a lens will correspond to a negative distance l, Fig. 3.

If, however, the light goes from right to left the reciprocal relation can only be maintained if distances are reckoned in the usual way (page 17), curvatures are reckoned positive only when the centre lies to the right of the surface, and vice versa, and refractive indices are positive only for a " left to right " and negative for a " right to left " direction of the light. In short, all the conventions explained in the Appendix on Sign Conventions are observed.

The conventions for divergence and convergence are then modified thus—

The *reduced curvature* or *reduced vergence* will be negative if the light is divergent, and positive if it is convergent. The " powers " of surfaces and systems will again be independent of the direction

of the light, so that the establishment of a complete reciprocity hardly adds any great complication. Take the following numerical example—

$$n'\mathscr{L}' \quad - n\mathscr{L} = (n' - n)\mathscr{R}$$

Left to right	$(1{\cdot}5)(4{\cdot}0) - (1{\cdot}0)(2{\cdot}0) = (1{\cdot}5 - 1{\cdot}0)8$
	$+ 6$ (Convergent) $- (+ 2)$ Convergent $= + 4$
Right to left; image acts as object	$(- 1{\cdot}0)(2{\cdot}0) - (- 1{\cdot}5)(4{\cdot}0) = \{- 1{\cdot}0 - (- 1{\cdot}5)\}8$
	$- 2$ (Divergent) $- (- 6)$ (Div.) $= + 4$.

It should be remembered again that the thin lens equation is only a reduction form of the more general equation $\overline{\mathscr{L}}' - \overline{\mathscr{L}} = \mathscr{F}$.

INDEX TO VOLUME I

PRINTED IN GREAT BRITAIN AT THE PITMAN PRESS, BATH
C—(5494)

AN ABRIDGED LIST OF

TECHNICAL BOOKS

PUBLISHED BY

Sir Isaac Pitman & Sons, Ltd.

Parker Street, Kingsway, London, W.C.2

The prices given apply only to Great Britain

A complete Catalogue giving full details of the following books will be sent post free on application

---

CONTENTS

C—4

TEXTILE MANUFACTURE, ETC.

	s.	d.
ARTIFICIAL SILK AND ITS MANUFACTURE. By Joseph Foltzer. Translated into English by T. Woodhouse. Fourth Edition	21	0
ARTIFICIAL SILK. By Dr. V. Hottenroth. Translated from the German by Dr. E. Fyleman, B.Sc.	30	0
ARTIFICIAL SILK. By Dr. O. Faust	10	6
ARTIFICIAL SILK OR RAYON, ITS MANUFACTURE AND USES. By T. Woodhouse, F.T.I. Second Edition	7	6
ARTIFICIAL SILK OR RAYON, THE PREPARATION AND WEAVING OF. By T. Woodhouse, F.T.I.	10	6
BLEACHING, DYEING, PRINTING, AND FINISHING FOR THE MANCHESTER TRADE. By J. W. McMyn, F.C.S., and J. W. Bardsley	6	0
COLOUR IN WOVEN DESIGN. By Roberts Beaumont, M.Sc., M.I.Mech.E. Second Edition, Revised and Enlarged.	21	0
COTTON SPINNER'S POCKET BOOK, THE. By James F. Innes	3	6
COTTON SPINNING COURSE, A FIRST YEAR. By H. A. J. Duncan, A.T.I.	5	0
COTTON WORLD, THE. Compiled and Edited by J. A. Todd, M.A., B.L.	5	0
DRESS, BLOUSE, AND COSTUME CLOTHS. DESIGN AND FABRIC MANUFACTURE. By Roberts Beaumont, M.Sc., M.I.Mech.E., and Walter G. Hill	42	0
FLAX AND JUTE, SPINNING, WEAVING, AND FINISHING OF. By T. Woodhouse, F.T.I.	10	6
FLAX CULTURE AND PREPARATION. By F. Bradbury. Second Edition	10	6
FUR. By MAX BACHRACH, B.C.S.	21	0
FURS AND FURRIERY. By Cyril J. Rosenberg	30	0
HOSIERY MANUFACTURE. By W. Davis, M.A.	7	6
MEN'S CLOTHING, ORGANIZATION, MANAGEMENT, AND TECHNOLOGY IN THE MANUFACTURE OF. By M. E. Popkin.	25	0
PATTERN CONSTRUCTION, THE SCIENCE OF. For Garment Makers. By B. W. Poole	45	0
TEXTILE CALCULATIONS. By J. H. Whitwam, B.Sc. (Lond.)	25	0
TEXTILE EDUCATOR, PITMAN'S. Edited by L. J. Mills, *Fellow of the Textile Institute*. In three volumes	63	0
TEXTILES, INTRODUCTION TO. By A. E. Lewis, A.M.C.T.	3	6
TOWELS AND TOWELLING, THE DESIGN AND MANUFACTURE OF. By T. Woodhouse, F.T.I., and A. Brand, A.T.I.	12	6
UNION TEXTILE FABRICATION. By Roberts Beaumont, M.Sc., M.I.Mech.E.	21	0
WEAVING AND MANUFACTURING, HANDBOOK OF. By H. Greenwood, A.T.I.	5	0
WOOLLEN YARN PRODUCTION. By T. Lawson	3	6
WOOL SUBSTITUTES. By Roberts Beaumont	10	6
YARNS AND FABRICS, THE TESTING OF. By H. P. Curtis.	5	0

TEXTILE MANUFACTURE, ETC.

	s.	d.
ARTIFICIAL SILK AND ITS MANUFACTURE. By Joseph Foltzer. Translated into English by T. Woodhouse. Fourth Edition	21	0
ARTIFICIAL SILK. By Dr. V. Hottenroth. Translated from the German by Dr. E. Fyleman, B.Sc.	30	0
ARTIFICIAL SILK. By Dr. O. Faust	10	6
ARTIFICIAL SILK OR RAYON, ITS MANUFACTURE AND USES. By T. Woodhouse, F.T.I. Second Edition	7	6
ARTIFICIAL SILK OR RAYON, THE PREPARATION AND WEAVING OF. By T. Woodhouse, F.T.I.	10	6
BLEACHING, DYEING, PRINTING, AND FINISHING FOR THE MANCHESTER TRADE. By J. W. McMyn, F.C.S., and J. W. Bardsley	6	0
COLOUR IN WOVEN DESIGN. By Roberts Beaumont, M.Sc., M.I.Mech.E. Second Edition, Revised and Enlarged.	21	0
COTTON SPINNER'S POCKET BOOK, THE. By James F. Innes	3	6
COTTON SPINNING COURSE, A FIRST YEAR. By H. A. J. Duncan, A.T.I.	5	0
COTTON WORLD, THE. Compiled and Edited by J. A. Todd, M.A., B.L.	5	0
DRESS, BLOUSE, AND COSTUME CLOTHS. DESIGN AND FABRIC MANUFACTURE. By Roberts Beaumont, M.Sc., M.I.Mech.E., and Walter G. Hill	42	0
FLAX AND JUTE, SPINNING, WEAVING, AND FINISHING OF. By T. Woodhouse, F.T.I.	10	6
FLAX CULTURE AND PREPARATION. By F. Bradbury. Second Edition	10	6
FUR. By MAX BACHRACH, B.C.S.	21	0
FURS AND FURRIERY. By Cyril J. Rosenberg	30	0
HOSIERY MANUFACTURE. By W. Davis, M.A.	7	6
MEN'S CLOTHING, ORGANIZATION, MANAGEMENT, AND TECHNOLOGY IN THE MANUFACTURE OF. By M. E. Popkin.	25	0
PATTERN CONSTRUCTION, THE SCIENCE OF. For Garment Makers. By B. W. Poole	45	0
TEXTILE CALCULATIONS. By J. H. Whitwam, B.Sc. (Lond.)	25	0
TEXTILE EDUCATOR, PITMAN'S. Edited by L. J. Mills, *Fellow of the Textile Institute*. In three volumes	63	0
TEXTILES, INTRODUCTION TO. By A. E. Lewis, A.M.C.T.	3	6
TOWELS AND TOWELLING, THE DESIGN AND MANUFACTURE OF. By T. Woodhouse, F.T.I., and A. Brand, A.T.I.	12	6
UNION TEXTILE FABRICATION. By Roberts Beaumont, M.Sc., M.I.Mech.E.	21	0
WEAVING AND MANUFACTURING, HANDBOOK OF. By H. Greenwood, A.T.I.	5	0
WOOLLEN YARN PRODUCTION. By T. Lawson	3	6
WOOL SUBSTITUTES. By Roberts Beaumont	10	6
YARNS AND FABRICS, THE TESTING OF. By H. P. Curtis.	5	0

DRAUGHTSMANSHIP

	s.	d.
Blue Printing and Modern Plan Copying. By B. J. Hall, M.I.Mech.E.	6	0
Blue Print Reading. By J. Brahdy, B.Sc., C.E.	10	6
Drawing and Designing. By Charles G. Leland, M.A. Fourth Edition	3	6
Drawing Office Practice. By H. Pilkington Ward, M.Sc., A.M.Inst.C.E.	7	6
Engineer Draughtsmen's Work. By A Practical Draughtsman	2	6
Engineering Hand Sketching and Scale Drawing. By Thos. Jackson, M.I.Mech.E., and Percy Bentley, A.M.I.Mech.E.	3	0
Engineering Workshop Drawing. By A. C. Parkinson, B.Sc.	4	0
Machine Design, Examples in. By G. W. Bird, B.Sc.	6	0
Machine Drawing, A Preparatory Course to. By P. W. Scott	2	0
Plan Copying in Black Lines. By B. J. Hall, M.I.Mech.E.	2	6

PHYSICS, CHEMISTRY, ETC.

	s.	d.
Biology, Introduction to Practical. By N. Walker.	5	0
Botany, Test Papers in. By E. Drabble, D.Sc.	2	0
Chemical Engineering, An Introduction to. By A. F. Allen, B.Sc. (Hons.), F.C.S., LL.B.	10	6
Chemistry, A First Book of. By A. Coulthard, B.Sc. (Hons.), Ph.D., F.I.C.	3	0
Chemistry, Definitions and Formulae for Students. By W. G. Carey, F.I.C.	–	6
Chemistry, Test Papers in. By E. J. Holmyard, M.A.	2	0
With Points Essential to Answers	3	0
Chemistry, Higher Test Papers in. By the same Author. 1. Inorganic. 2. Organic. . . . Each	3	0
Dispensing for Pharmaceutical Students. By J. W. Cooper and F. J. Dyer. Second Edition	7	6
Electricity and Magnetism, First Book of. By W. Perren Maycock, M.I.E.E. Fourth Edition	6	0
Magnetism and Electricity, Higher Test Papers in. By P. J. Lancelot Smith, M.A.	3	0
Magnetism and Electricity, Questions and Solutions in. Solutions by W. J. White, M.I.E.E.	5	0
Engineering Principles, Elementary. By G. E. Hall, B.Sc.	2	6
Engineering Science, A Primer of. By Ewart S. Andrews, B.Sc. (Eng.). Complete Edition	3	6
Part I. First Steps in Applied Mechanics	2	6
Pharmacy, A Course of Practical. By J. W. Cooper, Ph.D., and F. N. Appleyard, B.Sc., F.I.C., Ph.C.	7	6
Physical Science, Primary. By W. R. Bower, B.Sc.	5	0
Physics, Experimental. By A. Cowling. With Arithmetical Answers to the Problems	1	9
Physics, Test Papers in. By P. J. Lancelot-Smith, M.A.	2	0
Points Essential to Answers, 4s. In one book	5	6

Physics, Chemistry, etc.—contd.

	s.	d.
Volumetric Analysis. By J. B. Coppock, B.Sc. (Lond.), F.I.C., F.C.S. Second Edition	3	6
Volumetric Work, A Course of. By E. Clark, B.Sc.	4	6

METALLURGY AND METAL WORK

Ball and Roller Bearings, Handbook of. By A. W. Macaulay, A.M.I.Mech.E.	7	6
Electroplating with Chromium, Copper, and Nickel. By Benjamin Freeman, Ph.D., and Frederick G. Hoppe	21	0
Engineering Materials. Vol. I. Ferrous. By A. W. Judge, Wh.Sc., A.R.C.S.	30	0
Engineering Materials, Vol. II. Aircraft and Automobile Materials—Non-Ferrous and Organic. By A. W. Judge, Wh.Sc., A.R.C.S.	25	0
Engineering Materials. Vol. III. Theory and Testing. By A. W. Judge, Wh.Sc., A.R.C.S.	21	0
Engineering Workshop Exercises. By Ernest Pull, A.M.I.Mech.E., M.I.Mar.E. Second Edition, Revised.	3	6
Files and Filing. By Ch. Fremont. Translated into English under the supervision of George Taylor	21	0
Fitting, The Principles of. By J. Horner, A.M.I.M.E. Fifth Edition, Revised and Enlarged	7	6
Ironfounding, Practical. By J. Horner, A.M.I.M.E. Fourth Edition	10	0
Iron Rolls, The Manufacture of Chilled. By A. Allison	8	6
Metal Turning. By J. Horner, A.M.I.M.E. Fourth Edition, Revised and Enlarged	6	0
Metal Work, Practical Sheet and Plate. By E. A. Atkins, A.M.I.M.E. Third Edition, Revised and Enlarged	7	6
Metallurgy of Cast Iron. By J. E. Hurst	15	0
Pattern Making, The Principles of. By J. Horner, A.M.I.M.E. Fifth Edition	4	0
Pipe and Tube Bending and Jointing. By S. P. Marks, M.S.I.A.	6	0
Pyrometers. By E. Griffiths, D.Sc.	7	6
Steel Works Analysis. By J. O. Arnold, F.R.S., and F. Ibbotson. Fourth Edition, thoroughly revised	12	6
Turret Lathe Tools, How to Lay Out. Second Edition	6	0
Welding, Electric. By L. B. Wilson.	5	0
Welding, Electric Arc and Oxy-Acetylene. By E. A. Atkins, A.M.I.M.E.	7	6
Workshop Gauges and Measuring Appliances. By L. Burn, A.M.I.Mech.E., A.M.I.E.E.	5	0

MINERALOGY AND MINING

Blasting With High Explosives. By W. Gerard Boulton	5	0
Coal Carbonization. By John Roberts, D.I.C., M.I.Min.E., F.G.S.	25	0
Coal Mining, Definitions and Formulae for Students. By M. D. Williams, F.G.S.	–	6

Mineralogy and Mining—contd.

	s.	d.
COLLIERY ELECTRICAL ENGINEERING. By G. M. Harvey. Second Edition	15	0
COMPRESSED AIR POWER. By A. W. Daw and Z. W. Daw	21	0
ELECTRICAL ENGINEERING FOR MINING STUDENTS. By G. M. Harvey, M.Sc., B.Eng., A.M.I.E.E.	5	0
GOLD PLACERS, THE DREDGING OF. By J. E. Hodgson, F.R.G.S.	5	0
ELECTRICITY APPLIED TO MINING. By H. Cotton, M.B.E., M.Sc., A.M.I.E.E.	35	0
ELECTRIC MINING MACHINERY. By Sydney F. Walker, M.I.E.E., M.I.M.E., A.M.I.C.E., A.Amer.I.E.E.	15	0
LOW TEMPERATURE DISTILLATION. By S. North and J. B. Garbe	15	0
MINERALOGY. By F. H. Hatch, Ph.D., F.G.S., M.I.C.E., M.I.M.M. Fifth Edition, Revised	6	0
MINING CERTIFICATE SERIES, PITMAN'S. Edited by John Roberts, D.I.C., M.I.Min.E., F.G.S., Editor of *The Mining Educator*—		
MINING LAW AND MINE MANAGEMENT. By Alexander Watson, A.R.S.M.	8	6
MINE VENTILATION AND LIGHTING. By C. D. Mottram, B.Sc.	8	6
COLLIERY EXPLOSIONS AND RECOVERY WORK. By J. W. Whitaker, Ph.D. (Eng.), B.Sc., F.I.C., M.I.Min.E.	8	6
ARITHMETIC AND SURVEYING. By R. M. Evans, B.Sc., F.G.S., M.I.Min.E.	8	6
MINING MACHINERY. By T. Bryson, A.R.T.C., M.I.Min.E.	12	6
WINNING AND WORKING. By Prof. Ira C. F. Statham, B.Eng., F.G.S., M.I.Min.E.	21	0
MINING EDUCATOR, THE. Edited by J. Roberts, D.I.C., M.I.Min.E., F.G.S. In two vols.	63	0
MINING SCIENCE, A JUNIOR COURSE IN. By Henry G. Bishop.	2	6
MODERN PRACTICE OF COAL MINING SERIES. Edited by D. Burns, M.I.M.E., and G. L. Kerr, M.I.M.E.		
II. EXPLOSIVES AND BLASTING—TRANSMISSION OF POWER	6	0
IV. DRILLS AND DRILLING—COAL CUTTING AND COAL-CUTTING MACHINERY	6	0
TIN MINING. By C. G. Moor, M.A.	8	6

CONSTRUCTIONAL ENGINEERING

	s.	d.
REINFORCED CONCRETE, DETAIL DESIGN IN. By Ewart S. Andrews, B.Sc. (Eng.)	6	0
REINFORCED CONCRETE. By W. Noble Twelvetrees, M.I.M.E., A.M.I.E.E.	21	0
REINFORCED CONCRETE MEMBERS, SIMPLIFIED METHODS OF CALCULATING. By W. Noble Twelvetrees. Second Edition, Revised and Enlarged	5	0
SPECIFICATIONS FOR BUILDING WORKS. By W. L. Evershed, F.S.I.	5	0
STRUCTURES, THE THEORY OF. By H. W. Coultas, M.Sc., A.M.I.Struct.E., A.I.Mech.E.	15	0

CIVIL ENGINEERING, BUILDING, ETC.

	s.	d.
AUDEL'S MASONS' AND BUILDERS' GUIDES. In four volumes Each	7	6
1. BRICKWORK, BRICK-LAYING, BONDING, DESIGNS		
2. BRICK FOUNDATIONS, ARCHES, TILE SETTING, ESTIMATING		
3. CONCRETE MIXING, PLACING FORMS, REINFORCED STUCCO		
4. PLASTERING, STONE MASONRY, STEEL CONSTRUCTION, BLUE PRINTS		
AUDEL'S PLUMBERS' AND STEAM FITTERS' GUIDES. Practical Handbooks in four volumes . . . . . Each	7	6
1. MATHEMATICS, PHYSICS, MATERIALS, TOOLS, LEADWORK		
2. WATER SUPPLY, DRAINAGE, ROUGH WORK, TESTS		
3. PIPE FITTING, HEATING, VENTILATION, GAS, STEAM		
4. SHEET METAL WORK, SMITHING, BRAZING, MOTORS		
"THE BUILDER" SERIES—		
ARCHITECTURAL HYGIENE; OR, SANITARY SCIENCE AS APPLIED TO BUILDINGS. By Banister F. Fletcher, F.R.I.B.A., F.S.I., and H. Phillips Fletcher, F.R.I.B.A., F.S.I. Fifth Edition, Revised	10	6
CARPENTRY AND JOINERY. By Banister F. Fletcher, F.R.I.B.A., F.S.I., etc., and H. Phillips Fletcher, F.R.I.B.A., F.S.I., etc. Fifth Edition, Revised . .	10	6
QUANTITIES AND QUANTITY TAKING. By W. E. Davis. Sixth Edition	6	0
BUILDING, DEFINITIONS AND FORMULAE FOR STUDENTS. By T. Corkhill, F.B.I.C.C., M.I.Struct.E.	–	6
BUILDING EDUCATOR, PITMAN'S. Edited by R. Greenhalgh, A.I.Struct.E. In three volumes	63	0
FIELD MANUAL OF SURVEY METHODS AND OPERATIONS. By A. Lovat Higgins, B.Sc., A.R.C.S., A.M.I.C.E.	21	0
FIELD WORK FOR SCHOOLS. By E. H. Harrison, B.Sc., L.C.P., and C. A. Hunter	2	0
HYDRAULICS. By E. H. Lewitt, B.Sc. (Lond.), M.I.Ae.E., A.M.I.M.E. Third Edition	10	6
JOINERY & CARPENTRY. Edited by R. Greenhalgh, A.I.Struct.E. In six volumes . . . . Each	6	0
PAINTING AND DECORATING. Edited by C. H. Eaton, F.I.B.D. In six volumes . . . . Each	7	6
PLUMBING AND GASFITTING. Edited by Percy Manser, R.P., A.R.San.I. In seven volumes . . . . . Each	6	0
SURVEYING, TUTORIAL LAND AND MINE. By Thomas Bryson	10	6
WATER MAINS, LAY-OUT OF SMALL. By H. H. Hellins, M.Inst.C.E.	7	6
WATERWORKS FOR URBAN AND RURAL DISTRICTS. By H. C. Adams, M.Inst.C.E., M.I.C.E., F.S.I.	15	0

MECHANICAL ENGINEERING

	s.	d.
AUDEL'S ENGINEERS' AND MECHANICS' GUIDES. In eight volumes. Vols. 1–7 . . . . Each	7	6
Vol. 8	15	0
CONDENSING PLANT. By R. J. Kaula, M.I.E.E., and I. V. Robinson, M.I.E.E.	30	0
DEFINITIONS AND FORMULAE FOR STUDENTS—APPLIED MECHANICS. By E. H. Lewitt, B.Sc., A.M.I.Mech.E.. . .	–	6
DEFINITIONS AND FORMULAE FOR STUDENTS—HEAT ENGINES. By A. Rimmer, B.Eng.	–	6
DIESEL ENGINES: MARINE, LOCOMOTIVE, AND STATIONARY. By David Louis Jones, *Instructor, Diesel Engine Department, U.S. Navy Submarine Department*	21	0
ENGINEERING EDUCATOR, PITMAN'S. Edited by W. J. Kearton, M.Eng., A.M.I.Mech.E., A.M.Inst.N.A. In three volumes	63	0
FRICTION CLUTCHES. By R. Waring-Brown, A.M.I.A.E., F.R.S.A., M.I.P.E.	5	0
FUEL ECONOMY IN STEAM PLANTS. By A. Grounds, B.Sc., A.I.C., A.M.I.Min.E.	5	0
FUEL OILS AND THEIR APPLICATIONS. By H. V. Mitchell, F.C.S.	5	0
MECHANICAL ENGINEERING DETAIL TABLES. By John P. Ross	7	6
MECHANICAL ENGINEER'S POCKET BOOK, WHITTAKER'S. Third Edition, entirely rewritten and edited by W. E. Dommett, A.F.Ae.S., A.M.I.A.E.	12	6
MECHANICS' AND DRAUGHTSMEN'S POCKET BOOK. By W. E. Dommett, Wh.Ex., A.M.I.A.E.	2	6
MECHANICS FOR ENGINEERING STUDENTS. By G. W. Bird, B.Sc., A.M.I.Mech.E.	5	0
MOLLIER STEAM TABLES AND DIAGRAMS, THE. Extended to the Critical Pressure. English Edition adapted and amplified from the Third German Edition by H. Moss, D.Sc., A.R.C.S., D.I.C.	7	6
MOLLIER STEAM DIAGRAMS. Separately in envelope . . .	2	0
MOTIVE POWER ENGINEERING. For Students of Mining and Mechanical Engineering. By Henry C. Harris, B.Sc. . .	10	6
STEAM CONDENSING PLANT. By John Evans, M.Eng., A.M.I.Mech.E.	7	6
STEAM PLANT, THE CARE AND MAINTENANCE OF. A Practical Manual for Steam Plant Engineers. By J. E. Braham, B.Sc., A.C.G.I.	5	0
STEAM TURBINE THEORY AND PRACTICE. By W. J. Kearton, A.M.I.M.E. Second Edition	15	0
STRENGTH OF MATERIALS. By F. V. Warnock, Ph.D., B.Sc. (Lond.), F.R.C.Sc.I., A.M.I.Mech.E.	12	6
THEORY OF MACHINES. By Louis Toft, M.Sc.Tech., and A. T. J. Kersey, B.Sc.	12	6

Mechanical Engineering—contd. *s. d.*

THERMODYNAMICS, APPLIED. By Prof. W. Robinson, M.E., M.Inst.C.E. 18 0
TURBO-BLOWERS AND COMPRESSORS. By W. J. Kearton, A.M.I.M.E. 21 0
WORKSHOP PRACTICE. Edited by E. A. Atkins, M.I.Mech.E., M.I.W.E. In eight volumes . . . . . . Each 6 0

AERONAUTICS, ETC.

AEROBATICS. By Major O. Stewart, M.C., A.F.C. 5 0
AERONAUTICS, DEFINITIONS AND FORMULAE FOR STUDENTS. By J. D. Frier, A.R.C.Sc., D.I.C. . . . . . . – 6
AERONAUTICS, ELEMENTARY; OR, THE SCIENCE AND PRACTICE OF AERIAL MACHINES. By A. P. Thurston, D.Sc. Second Edition 8 6
AEROPLANE DESIGN AND CONSTRUCTION, ELEMENTARY PRINCIPLES OF. By A. W. Judge, A.R.C.S., Wh.Ex., A.M.I.A.E. 7 6
AEROPLANE STRUCTURAL DESIGN. By T. H. Jones, B.Sc A.M.I.M.E., and J. D. Frier, A.R.C.Sc., D.I.C. . . 21 0
AIRCRAFT, MODERN. By Major V. W. Pagé, Air Corps Reserve, U.S.A. 21 0
"AIRMEN OR NOAHS": FAIR PLAY FOR OUR AIRMEN. By Rear Admiral Murray F. Sueter, C.B., R.N., M.P. . . 25 0
AIRSHIP, THE RIGID. By E. H. Lewitt, B.Sc., M.I.Ae.E.. 30 0
LEARNING TO FLY. By F. A. Swoffer, M.B.E. With a Foreword by Air Vice-Marshal Sir Sefton Brancker, K.C.B., A.F.C. . 7 6
PARACHUTES FOR AIRMEN. By Charles Dixon 7 6
PILOT'S "A" LICENCE Compiled by John F. Leeming, *Royal Aero Club Observer for Pilot's Certificates*. Third Edition . 3 6

MARINE ENGINEERING

MARINE ENGINEERING, DEFINITIONS AND FORMULAE FOR STUDENTS. By E. Wood, B.Sc. . . . . . . – 6
MARINE SCREW PROPELLERS, DETAIL DESIGN OF. By Douglas H. Jackson, M.I.Mar.E., A.M.I.N.A. 6 0

OPTICS AND PHOTOGRAPHY

AMATEUR CINEMATOGRAPHY. By Capt. O. Wheeler, F.R.P.S. . 6 0
APPLIED OPTICS. Volume I. By L. C. Martin, D.I.C., A.R.C.S. (*In the Press*)
CAMERA LENSES. By A. W. Lockett 2 6
COLOUR PHOTOGRAPHY. By Capt. O. Wheeler, F.R.P.S.. . 12 6
COMMERCIAL PHOTOGRAPHY. By D. Charles 5 0
COMPLETE PRESS PHOTOGRAPHER, THE. By Bell R. Bell. . 6 0
LENS WORK FOR AMATEURS. By H. Orford. Fourth Edition . 3 6
PHOTOGRAPHIC CHEMICALS AND CHEMISTRY. By T. L. J. Bentley and J. Southworth 3 6
PHOTOGRAPHIC PRINTING. By R. R. Rawkins 3 6

Optics and Photography—contd.

	s.	d.
PHOTOGRAPHY AS A BUSINESS. By A. G. Willis	5	0
PHOTOGRAPHY THEORY AND PRACTICE. Edited by G. E. Brown (*In the Press*)		
RETOUCHING AND FINISHING FOR PHOTOGRAPHERS. By J. S. Adamson	4	0
STUDIO PORTRAIT LIGHTING. By H. Lambert, F.R.P.S. . .	15	0

ASTRONOMY

	s.	d.
ASTRONOMY, PICTORIAL. By G. F. Chambers, F.R.A.S.. .	2	6
ASTRONOMY FOR EVERYBODY. By Professor Simon Newcomb, LL.D. With an Introduction by Sir Robert Ball . . .	5	0
GREAT ASTRONOMERS. By Sir Robert Ball, D.Sc., LL.D., F.R.S.	5	0
HIGH HEAVENS, IN THE. By Sir Robert Ball	5	0
STARRY REALMS, IN. By Sir Robert Ball, D.Sc., LL.D., F.R.S.	5	0

ILLUMINATING ENGINEERING

	s.	d.
MODERN ILLUMINANTS AND ILLUMINATING ENGINEERING. By Leon Gaster and J. S. Dow. Second Edition, Revised and Enlarged	25	0
ELECTRIC LIGHTING IN FACTORIES AND WORKSHOPS. By Leon Gaster and J. S. Dow	–	6
ELECTRIC LIGHTING IN THE HOME. By Leon Gaster . .	–	6

MOTOR ENGINEERING

	s.	d.
AUTOMOBILE AND AIRCRAFT ENGINES. By A. W. Judge, A.R.C.S., A.M.I.A.E.	30	0
CARBURETTOR HANDBOOK, THE. By E. W. Knott, A.M.I.A.E.	10	6
COIL IGNITION FOR MOTOR-CARS. By C. Sylvester, A.M.I.E.E A.M.I.Mech.E.	10	6
GAS AND OIL ENGINE OPERATION. By J. Okill, M.I.A.E..	5	0
GAS ENGINE TROUBLES AND INSTALLATION, WITH TROUBLE CHART. By John B. Rathbun, M.E..	2	6
GAS, OIL, AND PETROL ENGINES. By A. Garrard, Wh.Ex. .	6	0
MAGNETO AND ELECTRIC IGNITION. By W. Hibbert, A.M.I.E.E.	3	6
MOTOR TRUCK AND AUTOMOBILE MOTORS AND MECHANISM. By T. H. Russell, A.M., M.E., with numerous Revisions and Extensions by John Rathbun	2	6
THORNYCROFT, THE BOOK OF THE. By "Auriga" . . .	2	6
MOTOR-CYCLIST'S LIBRARY, THE. Each volume in this series deals with a particular type of motor-cycle from the point of view of the owner-driver . . . . Each	2	0
A.J.S., THE BOOK OF THE. By W. C. Haycraft. Second Edition		
ARIEL, THE BOOK OF THE. By G. S. Davison. Second Edition		
B.S.A., THE BOOK OF THE. By "Waysider." Third Edition		

Motor Engineering—contd.

	s.	d.
Douglas, The Book of the. By E. W. Knott. Second Edition		
Imperial, Book of the New. By F. J. Camm		
Motor-cycling for Women. By Betty and Nancy Debenham. With a Foreword by Major H. R. Watling		
P. and M., The Book of the. By W. C. Haycraft.		
Raleigh Handbook, The. By "Mentor." Second Edition		
Royal Enfield, The Book of the. By R. E. Ryder		
Rudge, The Book of the. By L. H. Cade		
Triumph, The Book of the. By E. T. Brown		
Villiers Engine, Book of the. By C. Grange.		
Motorists' Library, The. Each volume in this series deals with a particular make of motor-car from the point of view of the owner-driver. The functions of the various parts of the car are described in non-technical language, and driving repairs, legal aspects, insurance, touring, equipment, etc., all receive attention		
Austin Twelve, The Book of the. By B. Garbutt and R. Twelvetrees. Illustrated by H. M. Bateman. Second Edition	5	0
Singer Junior, Book of the. By G. S. Davison.	2	6
Standard Car, The Book of the. By "Pioneer"	6	0
Clyno Car, The Book of the. By E. T. Brown	3	6
Motorist's Electrical Guide, The. By A. H. Avery, A.M.I.E.E.	3	6

ELECTRICAL ENGINEERING, ETC.

Accumulator Charging, Maintenance, and Repair. By W. S. Ibbetson	3	6
Accumulators, Management of. By Sir D. Salomons, Bart. Tenth Edition, Revised	7	6
Alternating Current Bridge Methods of Electrical Measurement. By B. Hague, D.Sc. Second Edition	15	0
Alternating Current Circuit. By Philip Kemp, M.I.E.E..	2	6
Alternating Current Machinery, Papers on the Design of. By C. C. Hawkins, M.A., M.I.E.E., S. P. Smith, D.Sc., M.I.E.E., and S. Neville, B.Sc.	21	0
Alternating Current Power Measurement. By G. F. Tagg	3	6
Alternating Current Work. By W. Perren Maycock, M.I.E.E. Second Edition	10	6
Alternating Currents, The Theory and Practice of. By A. T. Dover, M.I.E.E. Second Edition	18	0
Armature Winding, Practical Direct Current. By L. Wollison	7	6
Cables, High Voltage. By P. Dunsheath, O.B.E., M.A., B.Sc., M.I.E.E.	10	6

	s.	d.
Continuous Current Dynamo Design, Elementary Principles of. By H. M. Hobart, M.I.C.E., M.I.M.E., M.A.I.E.E.	10	6
Continuous Current Motors and Control Apparatus. By W. Perren Maycock, M.I.E.E..	7	6
Definitions and Formulae for Students—Electrical. By P. Kemp, M.Sc., M.I.E.E.	–	6
Direct Current Electrical Engineering, Elements of. By H. F. Trewman, M.A., and C. E. Condliffe, B.Sc..	5	0
Direct Current Electrical Engineering, Principles of. By James R. Barr, A.M.I.E.E.	15	0
Direct Current Dynamo and Motor Faults. By R.M. Archer	7	6
Direct Current Machines, Performance and Design of. By A. E. Clayton, D.Sc., M.I.E.E.	16	0
Dynamo, The: Its Theory, Design, and Manufacture. By C. C. Hawkins, M.A., M.I.E.E. In three volumes. Sixth Edition—		
Volume I	21	0
,, II	15	0
,, III	30	0
Dynamo, How to Manage the. By A. E. Bottone. Sixth Edition, Revised and Enlarged	2	0
Electric and Magnetic Circuits, The Alternating and Direct Current. By E. N. Pink, B.Sc., A.M.I.E.E.	3	6
Electric Bells and All About Them. By S. R. Bottone. Eighth Edition, thoroughly revised by C. Sylvester, A.M.I.E.E.	3	6
Electric Circuit Theory and Calculations. By W. Perren Maycock, M.I.E.E. Third Edition, Revised by Philip Kemp, M.Sc., M.I.E.E., A.A.I.E.E.	10	6
Electric Light Fitting, Practical. By F. C. Allsop. Tenth Edition, Revised and Enlarged	7	6
Electric Lighting and Power Distribution. By W. Perren Maycock, M.I.E.E. Ninth Edition, thoroughly Revised and Enlarged		
Vol. I.	10	6
Vol. II	10	6
Electric Machines, Theory and Design of. By F. Creedy, M.I.E.E., A.C.G.I.	30	0
Electric Motors and Control Systems. By A. T. Dover, M.I.E.E., A.Amer.I.E.E.	15	0
Electric Motors (Direct Current): Their Theory and Construction. By H. M. Hobart, M.I.E.E., M.Inst.C.E., M.Amer.I.E.E. Third Edition, thoroughly Revised	15	0
Electric Motors (Polyphase): Their Theory and Construction. By H. M. Hobart, M.Inst.C.E., M.I.E.E., M.Amer.I.E.E. Third Edition, thoroughly Revised	15	0
Electric Motors for Continuous and Alternating Currents, A Small Book on. By W. Perren Maycock, M.I.E.E.	6	0
Electric Traction. By A. T. Dover, M.I.E.E., Assoc.Amer. I.E.E. Second Edition	25	0

	s.	d.
ELECTRIC TRACTION AND POWER DISTRIBUTION, EXAMPLES IN. By A. T. Dover, M.I.E.E. *(In the Press)*		
ELECTRIC WIRING DIAGRAMS. By W. Perren Maycock, M.I.E.E.	5	0
ELECTRIC WIRING, FITTINGS, SWITCHES, AND LAMPS. By W. Perren Maycock, M.I.E.E. Sixth Edition. Revised by Philip Kemp, M.Sc., M.I.E.E.	10	6
ELECTRIC WIRING OF BUILDINGS. By F. C. Raphael, M.I.E.E.	10	6
ELECTRIC WIRING TABLES. By W. Perren Maycock, M.I.E.E., and F. C. Raphael, M.I.E.E. Fifth Edition	3	6
ELECTRICAL CONDENSERS. By Philip R. Coursey, B.Sc., F.Inst.P., A.M.I.E.E.	37	6
ELECTRICAL EDUCATOR. By Sir Ambrose Fleming, M.A. D.Sc., F.R.S. In two volumes	63	0
ELECTRICAL ENGINEERING, CLASSIFIED EXAMPLES IN. By S. Gordon Monk, B.Sc. (Eng.), A.M.I.E.E. In two parts—		
Vol. I. DIRECT CURRENT	2	6
Vol. II. ALTERNATING CURRENT	3	6
ELECTRICAL ENGINEERING, ELEMENTARY. By O. R. Randall, Ph.D., B.Sc., Wh.Ex.	5	0
ELECTRICAL ENGINEER'S POCKET BOOK, WHITTAKER'S. Originated by Kenelm Edgcumbe, M.I.E.E., A.M.I.C.E. Sixth Edition. Edited by R. E. Neale, B.Sc. (Hons.).	10	6
ELECTRICAL INSTRUMENT MAKING FOR AMATEURS. By S. R. Bottone. Ninth Edition.	6	0
ELECTRICAL INSULATING MATERIALS. By A. Monkhouse, Junr., M.I.E.E., A.M.I.Mech.E.	21	0
ELECTRICAL GUIDES, HAWKINS'. Each book in pocket size	5	0
1. ELECTRICITY, MAGNETISM, INDUCTION, EXPERIMENTS, DYNAMOS, ARMATURES, WINDINGS		
2. MANAGEMENT OF DYNAMOS, MOTORS, INSTRUMENTS, TESTING		
3. WIRING AND DISTRIBUTION SYSTEMS, STORAGE BATTERIES		
4. ALTERNATING CURRENTS AND ALTERNATORS		
5. A.C. MOTORS, TRANSFORMERS, CONVERTERS, RECTIFIERS		
6. A.C. SYSTEMS, CIRCUIT BREAKERS, MEASURING INSTRUMENTS		
7. A.C. WIRING, POWER STATIONS, TELEPHONE WORK		
8. TELEGRAPH, WIRELESS, BELLS, LIGHTING		
9. RAILWAYS, MOTION PICTURES, AUTOMOBILES, IGNITION		
10. MODERN APPLICATIONS OF ELECTRICITY. REFERENCE INDEX		
ELECTRICAL MACHINES, PRACTICAL TESTING OF. By L. Oulton, A.M.I.E.E., and N. J. Wilson, M.I.E.E. Second Edition	6	0
ELECTRICAL TECHNOLOGY. By H. Cotton, M.B.E., M.Sc., A.M.I.E.E.	12	6
ELECTRICAL TERMS, A DICTIONARY OF. By S. R. Roget, M.A., A.M.Inst.C.E., A.M.I.E.E.	7	6

Electrical Engineering—contd.

	s.	d.
Electrical Transmission and Distribution. Edited by R. O. Kapp, B.Sc. In eight volumes. Vols. I to VII, each	6	0
Vol. VIII	3	0
Electrical Wiring and Contracting. Edited by H. Marryat, M.I.E.E., M.I.Mech.E. In eight volumes . Each	6	0
Electro-Motors: How Made and How Used. By S. R. Bottone. Seventh Edition. Revised by C. Sylvester, A.M.I.E.E.	4	6
Electro-Technics, Elements of. By A. P. Young, O.B.E., M.I.E.E.	5	0
Engineering Educator, Pitman's. Edited by W. J. Kearton, M.Eng., A.M.I.Mech.E., A.M.Inst.N.A. In three volumes.	63	0
Induction Coils. By G. E. Bonney. Fifth Edition, thoroughly Revised	6	0
Induction Coil, Theory of the. By E. Taylor-Jones, D.Sc., F.Inst.P.	12	6
Induction Motor, The. By H. Vickers, Ph.D., M.Eng.	21	0
Kinematography Projection: A Guide to. By Colin H. Bennett, F.C.S., F.R.P.S.	10	6
Mercury-Arc Rectifiers and Mercury-Vapour Lamps. By Sir Ambrose Fleming, M.A., D.Sc., F.R.S.	6	0
Oscillographs. By J. T. Irwin, M.I.E.E.	7	6
Power Station Efficiency Control. By John Bruce, A.M.I.E.E.	12	6
Power Wiring Diagrams. By A. T. Dover, M.I.E.E., A.Amer. I.E.E. Second Edition, Revised	6	0
Practical Primary Cells. By A. Mortimer Codd, F.Ph.S.	5	0
Railway Electrification. By H. F. Trewman, A.M.I.E.E.	21	0
Steam Turbo-Alternator, The. By L. C. Grant, A.M.I.E.E.	15	0
Storage Batteries: Theory, Manufacture, Care, and Application. By M. Arendt, E.E.	18	0
Storage Battery Practice. By R. Rankin, B.Sc., M.I.E.E.	7	6
Transformers for Single and Multiphase Currents. By Dr. Gisbert Kapp, M.Inst.C.E., M.I.E.E. Third Edition, Revised by R. O. Kapp, B.Sc.	15	0

TELEGRAPHY, TELEPHONY, AND WIRELESS

	s.	d.
Automatic Branch Exchanges, Private. By R. T. A. Dennison	12	6
Baudôt Printing Telegraph System. By H. W. Pendry. Second Edition	6	0
Cable and Wireless Communications of the World, The. By F. J. Brown, C.B., C.B.E., M.A., B.Sc. (Lond.)	7	6
Crystal and One-Valve Circuits, Successful. By J. H. Watkins	3	6
Loud Speakers. By C. M. R. Balbi, with a Foreword by Professor G. W. O. Howe, D.Sc., M.I.E.E., A.M.I.E.E., A.C.G.I.	3	6
Radio Communication, Modern. By J. H. Reyner. Second Edition	5	0

Telegraphy, Telephony, and Wireless—contd.

	s.	d.
TELEGRAPHY. By T. E. Herbert, M.I.E.E. Fifth Edition .	20	0
TELEGRAPHY, ELEMENTARY. By H. W. Pendry. Second Edition, Revised	7	6
TELEPHONE HANDBOOK AND GUIDE TO THE TELEPHONIC EXCHANGE, PRACTICAL. By Joseph Poole, A.M.I.E.E. (Wh.Sc.). Seventh Edition	18	0
TELEPHONY. By T. E. Herbert, M.I.E.E.	18	0
TELEPHONY SIMPLIFIED, AUTOMATIC. By C. W. Brown, A.M.I.E.E., *Engineer-in-Chief's Department, G.P.O., London*	6	0
TELEPHONY, THE CALL INDICATOR SYSTEM IN AUTOMATIC. By A. G. Freestone, *of the Automatic Training School, G.P.O., London*	6	0
TELEPHONY, THE DIRECTOR SYSTEM OF AUTOMATIC. By W. E. Hudson, B.Sc. Hons. (London), Whit.Sch., A.C.G.I. . .	15	0
TELEVISION : TO-DAY AND TO-MORROW. By Sydney A. Moseley and H. J. Barton Chapple, Wh.Sc., B.Sc. (Hons.), A.C.G.I., D.I.C., A.M.I.E.E.	7	6
PHOTOELECTRIC CELLS. By Dr. N. I. Campbell and Dorothy Ritchie	15	0
WIRELESS MANUAL, THE. By Capt. J. Frost. Second Edition	5	0
WIRELESS TELEGRAPHY AND TELEPHONY, INTRODUCTION TO. By Sir Ambrose Fleming	3	6

MATHEMATICS AND CALCULATIONS FOR ENGINEERS

	s.	d.
ALGEBRA, COMMON-SENSE, FOR JUNIORS. By F. F. Potter, M.A., B.Sc., and J. W. Rogers, M.Sc. . . .	3	0
With Answers	3	6
ALGEBRA, TEST PAPERS IN. By A. E. Donkin, M.A.	2	0
With Answers	2	6
With Answers and Points Essential to Answers	3	6
ALTERNATING CURRENTS, ARITHMETIC OF. By E. H. Crapper, M.I.E.E.	4	6
CALCULUS FOR ENGINEERING STUDENTS. By John Stoney, B.Sc., A.M.I.Min.E. . .	3	6
DEFINITIONS AND FORMULAE FOR STUDENTS—PRACTICAL MATHEMATICS. By L. Toft, M.Sc.	–	6
ELECTRICAL ENGINEERING, WHITTAKER'S ARITHMETIC OF. Third Edition, Revised and Enlarged	3	6
ELECTRICAL MEASURING INSTRUMENTS, COMMERCIAL. By R. M. Archer, B.Sc. (Lond.), A.R.C.Sc., M.I.E.E.	10	6
GEOMETRY, ELEMENTS OF PRACTICAL PLANE. By P. W. Scott	2	6
Also in Two Parts . . . . Each	1	0
GEOMETRY, TEST PAPERS IN. By W. E. Paterson, M.A., B.Sc.	2	0
Points Essential to Answers, 1s. In one book. . .	3	0
GRAPHIC STATICS, ELEMENTARY. By J. T. Wight, A.M.I.Mech.E.	5	0
KILOGRAMS INTO AVOIRDUPOIS, TABLE FOR THE CONVERSION OF. Compiled by Redvers Elder. On paper	1	0
LOGARITHMS FOR BEGINNERS. By C. N. Pickworth, Wh.Sc. Fourth Edition	1	6

	s.	d.
LOGARITHMS, FIVE FIGURE, AND TRIGONOMETRICAL FUNCTIONS. By W. E. Dommett, A.M.I.A.E., and H. C. Hird, A.F.Ae.S. (Reprinted from *Mathematical Tables*)	1	0
LOGARITHMS SIMPLIFIED. By Ernest Card, B.Sc., and A. C. PARKINSON, A.C.P.	2	6
MATHEMATICAL TABLES. By W. E. Dommett, A.M.I.A.E., and H. C. Hird, A.F.Ae.S.	4	6
MATHEMATICS AND DRAWING, PRACTICAL. By Dalton Grange.	2	6
With Answers	3	0
MATHEMATICS, ENGINEERING, APPLICATION OF. By W. C. Bickley, M.Sc.	5	0
MATHEMATICS, EXPERIMENTAL. By G. R. Vine, B.Sc.		
Book I, with Answers	1	4
Book II, with Answers	1	4
MATHEMATICS FOR ENGINEERS, PRELIMINARY. By W. S. Ibbetson, B.Sc., A.M.I.E.E.	3	6
MATHEMATICS FOR TECHNICAL STUDENTS. By G. E. Hall	5	0
MATHEMATICS, INDUSTRIAL (PRELIMINARY), By G. W. Stringfellow	2	0
With Answers	2	6
MATHEMATICS, INTRODUCTORY. By J. E. Rowe, Ph.D.	10	6
MEASURING AND MANURING LAND, AND THATCHERS' WORK, TABLES FOR. By J. Cullyer. Twentieth Impression	3	0
MECHANICAL TABLES. By J. Foden	2	0
MECHANICAL ENGINEERING DETAIL TABLES. By John P. Ross	7	6
METALWORKER'S PRACTICAL CALCULATOR, THE. By J. Matheson	2	0
METRIC CONVERSION TABLES. By W. E. Dommett, A.M.I.A.E.	1	0
METRIC LENGTHS TO FEET AND INCHES, TABLE FOR THE CONVERSION OF. Compiled by Redvers Elder		
On paper	1	0
On cloth, varnished	2	0
MINING MATHEMATICS (PRELIMINARY). By George W. Stringfellow	1	6
With Answers	2	0
QUANTITIES AND QUANTITY TAKING. By W. E. Davis. Sixth Edition	6	0
REINFORCED CONCRETE MEMBERS, SIMPLIFIED METHODS OF CALCULATING. By W. N. Twelvetrees, M.I.M.E., A.M.I.E.E. Second Edition, Revised and Enlarged	5	0
RUSSIAN WEIGHTS AND MEASURES, WITH THEIR BRITISH AND METRIC EQUIVALENTS, TABLES OF. By Redvers Elder	2	6
SLIDE RULE, THE. By C. N. Pickworth, Wh.Sc. Seventeenth Edition, Revised	3	6
SLIDE RULE: ITS OPERATIONS; AND DIGIT RULES, THE. By A. Lovat Higgins, A.M.Inst.C.E.	–	6
STEEL'S TABLES. Compiled by Joseph Steel	3	6
TELEGRAPHY AND TELEPHONY, ARITHMETIC OF. By T. E. Herbert, M.I.E.E., and R. G. de Wardt	5	0
TEXTILE CALCULATIONS. By J. H. Whitwam, B.Sc.	25	0

Mathematics for Engineers—contd.

	s.	d.
TRIGONOMETRY FOR ENGINEERS, A PRIMER OF. By W. G. Dunkley, B.Sc. (Hons.)	5	0
TRIGONOMETRY FOR NAVIGATING OFFICERS. By W. Percy Winter, B.Sc. (Hons.), Lond.	10	6
TRIGONOMETRY, PRACTICAL. By Henry Adams, M.I.C.E., M.I.M.E., F.S.I. Third Edition, Revised and Enlarged	5	0
VENTILATION, PUMPING, AND HAULAGE, MATHEMATICS OF. By F. Birks	5	0
WORKSHOP ARITHMETIC, FIRST STEPS IN. By H. P. Green	1	0

MISCELLANEOUS TECHNICAL BOOKS

	s.	d.
BREWING AND MALTING. By J. Ross Mackenzie, F.C.S., F.R.M.S. Second Edition	8	6
CERAMIC INDUSTRIES POCKET BOOK. By A. B. Searle	8	6
ENGINEERING ECONOMICS. By T. H. Burnham, B.Sc. (Hons.), B.Com., A.M.I.Mech.E.	10	6
ENGINEERING INQUIRIES, DATA FOR. By J. C. Connan, B.Sc., A.M.I.E.E., O.B.E.	12	6
ESTIMATING. By T. H. Hargrave	7	6
FURNITURE STYLES. By. H. E. Binstead. Second Edition	10	6
GLUE AND GELATINE. By P. I. Smith	8	6
LIGHTNING CONDUCTORS AND LIGHTNING GUARDS. By Sir Oliver J. Lodge, F.R.S., LL.D., D.Sc., M.I.E.E.	15	0
MUSIC ENGRAVING AND PRINTING. By Wm. Gamble	21	0
PETROLEUM. By Albert Lidgett, *Editor of the "Petroleum Times."* Third Edition	5	0
PRINTING. By H. A. Maddox	5	0
REFRACTORIES FOR FURNACES, CRUCIBLES, ETC. By A. B. Searle	5	0
REFRIGERATION, MECHANICAL. By Hal Williams, M.I.Mech.E., M.I.E.E., M.I.Struct.E.	20	0
SEED TESTING. By J. Stewart Remington	10	6
STONES, PRECIOUS AND SEMI-PRECIOUS. By Michael Weinstein. Second Edition	7	6
STORES ACCOUNTS AND STORES CONTROL. By J. H. Burton	5	0
TECHNICAL DICTIONARY OF ENGINEERING AND INDUSTRIAL SCIENCE IN SEVEN LANGUAGES: ENGLISH, FRENCH, SPANISH, ITALIAN, PORTUGUESE, RUSSIAN, AND GERMAN. Compiled by Ernest Slater, M.I.E.E., M.I.Mech.E., in collaboration with leading authorities. Complete in four volumes. £8	8	0

PITMAN'S TECHNICAL PRIMERS

	s.	d.
Each in foolscap 8vo, cloth, about 120 pp., illustrated	2	6

In each book of the series the fundamental principles of some subdivision of technology are treated in a practical manner, providing the student with a handy survey of the particular branch of technology with which he is concerned. They should prove invaluable to the busy practical man who has not the time for more elaborate treatises.

ABRASIVE MATERIALS. By A. B. Searle.

s. d.

PITMAN'S TECHNICAL PRIMERS—*contd.* Each 2 6

A.C. PROTECTIVE SYSTEMS AND GEARS. By J. Henderson, B.Sc., M.C., and C. W. Marshall, B.Sc., A.M.I.E.E.

BELTS FOR POWER TRANSMISSION. By W. G. Dunkley, B.Sc. (Hons.).

BOILER INSPECTION AND MAINTENANCE. By R. Clayton.

CAPSTAN AND AUTOMATIC LATHES. By Philip Gates.

CENTRAL STATIONS, MODERN. By C. W. Marshall, B.Sc., A.M.I.E.E.

COAL CUTTING MACHINERY, LONGWALL. By G. F. F. Eagar, M.I.Min.E.

CONTINUOUS CURRENT ARMATURE WINDING. By F. M. Denton, A.C.G.I., A.Amer.I.E.E.

CONTINUOUS CURRENT MACHINES, THE TESTING OF. By Charles F. Smith, D.Sc., M.I.E.E., A.M.I.C.E.

COTTON SPINNING MACHINERY AND ITS USES. By Wm. Scott Taggart, M.I.Mech.E.

DIESEL ENGINE, THE. By A. Orton.

DROP FORGING AND DROP STAMPING. By H. Hayes.

ELECTRIC CABLES. By F. W. Main, A.M.I.E.E.

ELECTRIC CRANES AND HAULING MACHINES. By F. E. Chilton, A.M.I.E.E.

ELECTRIC FURNACE, THE. By Frank J. Moffett, B.A., M.I.E.E., M.Cons.E.

ELECTRIC MOTORS, SMALL. By E. T. Painton, B.Sc., A.M.I.E.E.

ELECTRIC POWER SYSTEMS. By Capt. W. T. Taylor, M.Inst.C.E. M.I.Mech.E.

ELECTRICAL INSULATION. By W. S. Flight, A.M.I.E.E.

ELECTRICAL TRANSMISSION OF ENERGY. By W. M. Thornton, O.B.E., D.Sc., M.I.E.E.

ELECTRICITY IN AGRICULTURE. By A. H. Allen, M.I.E.E.

ELECTRICITY IN STEEL WORKS. By Wm. McFarlane, B.Sc.

ELECTRIFICATION OF RAILWAYS, THE. By H. F. Trewman, M.A.

ELECTRO-DEPOSITION OF COPPER, THE. And its Industrial Applications. By Claude W. Denny, A.M.I.E.E.

EXPLOSIVES, MANUFACTURE AND USES OF. By R. C. Farmer, O.B.E., D.Sc., Ph.D.

FILTRATION. By T. R. Wollaston, M.I.Mech.E.

FOUNDRYWORK. By Ben Shaw and James Edgar.

GRINDING MACHINES AND THEIR USES. By Thos. R. Shaw, M.I.Mech.E.

HOUSE DECORATIONS AND REPAIRS. By Wm. Prebble.

HYDRO-ELECTRIC DEVELOPMENT. By J. W. Meares, F.R.A.S., M.Inst.C.E., M.I.E.E., M.Am.I.E.E.

ILLUMINATING ENGINEERING, THE ELEMENTS OF. By A. P. Trotter, M.I.E.E.

INDUSTRIAL AND POWER ALCOHOL. By R. C. Farmer, O.B.E., D.Sc., Ph.D., F.I.C.

INDUSTRIAL ELECTRIC HEATING. By J. W. Beauchamp, M.I.E.E.

INDUSTRIAL MOTOR CONTROL. By A. T. Dover, M.I.E.E.

d.

PITMAN'S TECHNICAL PRIMERS—*contd.* Each 6

INDUSTRIAL NITROGEN. By P. H. S. Kempton, B.Sc. (Hons.), A.R.C.Sc.

KINEMATOGRAPH STUDIO TECHNIQUE. By L. C. Macbean.

LUBRICANTS AND LUBRICATION. By J. H. Hyde.

MECHANICAL HANDLING OF GOODS, THE. By C. H. Woodfield, M.I.Mech.E.

MECHANICAL STOKING. By D. Brownlie, B.Sc., A.M.I.M.E. (Double volume, price 5s. net.)

METALLURGY OF IRON AND STEEL. Based on Notes by Sir Robert Hadfield.

MUNICIPAL ENGINEERING. By H. Percy Boulnois, M.Inst.C.E., F.R.San.Inst., F.Inst.S.E.

OILS, PIGMENTS, PAINTS, AND VARNISHES. By R. H. Truelove.

PATTERNMAKING. By Ben Shaw and James Edgar.

PETROL CARS AND LORRIES. By F. Heap.

PHOTOGRAPHIC TECHNIQUE. By L. J. Hibbert, F.R.P.S.

PNEUMATIC CONVEYING. By E. G. Phillips, M.I.E.E., A.M.I.Mech.E.

POWER FACTOR CORRECTION. By A. E. Clayton, B.Sc. (Eng.) Lond., A.K.C., A.M.I.E.E.

RADIOACTIVITY AND RADIOACTIVE SUBSTANCES. By J. Chadwick, M.Sc.

RAILWAY SIGNALLING: AUTOMATIC. By F. Raynar Wilson.

RAILWAY SIGNALLING: MECHANICAL. By F. Raynar Wilson.

SEWERS AND SEWERAGE. By H. Gilbert Whyatt, M.I.C.E.

SPARKING PLUGS. By A. P. Young and H. Warren.

STEAM ENGINE VALVES AND VALVE GEARS. By E. L. Ahrons, M.I.Mech.E., M.I.Loco.E.

STEAM LOCOMOTIVE, THE. By E. L. Ahrons, M.I.Mech.E., M.I.Loco.E.

STEAM LOCOMOTIVE CONSTRUCTION AND MAINTENANCE. By E. L. Ahrons, M.I.Mech.E., M.I.Loco.E.

STEELS, SPECIAL. Based on Notes by Sir Robert Hadfield, Bart.; compiled by T. H. Burnham, B.Sc. (Double volume, price 5s.)

STEELWORK, STRUCTURAL. By Wm. H. Black.

STREETS, ROADS, AND PAVEMENTS. By H. Gilbert Whyatt, M.Inst.C.E., M.R.San.I.

SWITCHBOARDS, HIGH TENSION. By Henry E. Poole, B.Sc. (Hons.), Lond., A.C.G.I., A.M.I.E.E.

SWITCHGEAR, HIGH TENSION. By Henry E. Poole, B.Sc. (Hons.), A.C.G.I., A.M.I.E.E.

SWITCHING AND SWITCHGEAR. By Henry E. Poole B.Sc. (Hons.), A.C.G.I., A.M.I.E.E.

TELEPHONES, AUTOMATIC. By F. A. Ellson, B.Sc., A.M.I.E.E. (Double volume, price 5s.)

TIDAL POWER. By A. M. A. Struben, O.B.E., A.M.Inst.C.E.

TOOL AND MACHINE SETTING. For Milling, Drilling, Tapping, Boring, Grinding, and Press Work. By Philip Gates.

s. d.

PITMAN'S TECHNICAL PRIMERS—*contd.* Each 2 6

TOWN GAS MANUFACTURE. By Ralph Staley, M.C.

TRACTION MOTOR CONTROL. By A. T. Dover, M.I.E.E.

TRANSFORMERS AND ALTERNATING CURRENT MACHINES, THE TESTING OF. By Charles F. Smith, D.Sc., A.M.Inst.C.E., Wh.Sc.

TRANSFORMERS, HIGH VOLTAGE POWER. By Wm. T. Taylor, M.Inst.C.E., M.I.E.E.

TRANSFORMERS, SMALL SINGLE-PHASE. By Edgar T. Painton, B.Sc. Eng. (Hons.) Lond., A.M.I.E.E.

WATER POWER ENGINEERING. By F. F. Fergusson, A.M.Inst.C.E.

WIRELESS TELEGRAPHY, CONTINUOUS WAVE. By B. E. G. Mittell, A.M.I.E.E.

WIRELESS TELEGRAPHY, DIRECTIVE. Direction and Position Finding, etc. By L. H. Walter, M.A. (Cantab.), A.M.I.E.E.

X-RAYS, INDUSTRIAL APPLICATION OF. By P. H. S. Kempton, B.Sc. (Hons.).

COMMON COMMODITIES AND INDUSTRIES SERIES

Each book is crown 8vo, cloth, with many illustrations, etc. . 3 0

In each of the handbooks in this series a particular product or industry is treated by an expert writer and practical man of business.

ACIDS, ALKALIS, AND SALTS. By G. H. J. Adlam, M.A., B.Sc., F.C.S.

ALCOHOL IN COMMERCE AND INDUSTRY. By C. Simmonds, O.B.E., B.Sc., F.I.C., F.C.S.

ALUMINIUM. Its Manufacture, Manipulation, and Marketing. By George Mortimer, M.Inst.Met.

ANTHRACITE. By A. Leonard Summers.

ASBESTOS. By A. Leonard Summers.

BOOKBINDING CRAFT AND INDUSTRY, THE. By T. Harrison.

BOOKS: FROM THE MS. TO THE BOOKSELLER. By J. L. Young.

BOOT AND SHOE INDUSTRY, THE. By J. S. Harding.

BREAD AND BREAD BAKING. By John Stewart.

BRUSHMAKER, THE. By Wm. Kiddier.

BUTTER AND CHEESE. By C. W. Walker Tisdale, F.C.S., and Jean Jones, B.D.F.D., N.D.D.

BUTTON INDUSTRY, THE. By W. Unite Jones.

CARPETS. By Reginald S. Brinton.

CLAYS AND CLAY PRODUCTS. By Alfred B. Searle.

CLOCKS AND WATCHES. By G. L. Overton.

CLOTHS AND THE CLOTH TRADE. By J. A. Hunter.

CLOTHING INDUSTRY, THE. By B. W. Poole.

COAL. Its Origin, Method of Working, and Preparation for the Market. By Francis H. Wilson, M.Inst.M.E.

COAL TAR. By A. R. Warnes, F.C.S., A.I.Mech.E.

s. d.

Common Commodities and Industries Series—*contd.* Each 3 0

Coffee. From Grower to Consumer. By B. B. Keable.

Cold Storage and Ice Making. By B. H. Springett.

Concrete and Reinforced Concrete. By W. Noble Twelvetrees, M.I.M.E., A.M.I.E.E.

Copper. From the Ore to the Metal. By H. K. Picard, M.Inst. of Min. and Met.

Cordage and Cordage Hemp and Fibres. By T. Woodhouse and P. Kilgour.

Corn Trade, The British. By A. Barker.

Cotton. From the Raw Material to the Finished Product. By R. J. Peake.

Cotton Spinning. By A. S. Wade.

Cycle Industry, The. By W. Grew.

Drugs in Commerce. By J. Humphrey, Ph.C., F.J.I.

Dyes and Their Application to Textile Fabrics. By A. J. Hall, B.Sc., F.I.C., F.C.S.

Electric Lamp Industry, The. By G. Arncliffe Percival.

Electricity. By R. E. Neale, B.Sc. (Hons.).

Engraving. By T. W. Lascelles.

Explosives, Modern. By S. I. Levy, B.A., B.Sc., F.I.C.

Fertilizers. By H. Cave.

Film Industry, The. By Davidson Boughey.

Fishing Industry, The. By W. E. Gibbs, D.Sc.

Furniture. By H. E. Binstead. Second Edition.

Furs and the Fur Trade. By J. C. Sachs.

Gas and Gas Making. By W. H. Y. Webber, C.E.

Glass and Glass Manufacture. By P. Mason, *Honours and Medallist in Glass Manufacture.*

Gloves and the Glove Trade. By B. E. Ellis.

Gold. By Benjamin White.

Gums and Resins. Their Occurrence, Properties, and Uses. By Ernest J. Parry, B.Sc., F.I.C., F.C.S.

Incandescent Lighting. By S. I. Levy, B.A., B.Sc., F.I.C.

Ink. By C. Ainsworth Mitchell, M.A., F.I.C.

Iron and Steel. Their Production and Manufacture. By C. Hood.

Ironfounding. By B. Whiteley.

Jute Industry, The. By T. Woodhouse and P. Kilgour.

Knitted Fabrics. By John Chamberlain and James H. Quilter.

Lead. Including Lead Pigments. By J. A. Smythe, Ph.D.,D.Sc.

Leather. From the Raw Material to the Finished Product. By K. J. Adcock.

Linen. From the Field to the Finished Product. By Alfred S. Moore.

Locks and Lock Making. By F. J. Butter.

Match Industry, The. By W. H. Dixon.

Meat Industry, The. By Walter Wood.

Motor Industry, The. By Horace Wyatt, B.A.

COMMON COMMODITIES AND INDUSTRIES SERIES *contd.*

NICKEL. By F. B. Howard White, B.A.

OIL POWER. By Sidney H. North, A.Inst.P.T.

OILS. Animal, Vegetable, Essential, and Mineral. By C. Ainsworth Mitchell, M.A., F.I.C.

PAINTS AND VARNISHES. By A. S. Jennings, F.I.B.D.

PAPER. Its History, Sources, and Production. By Harry A. Maddox, *Silver Medallist Papermaking*. Second Edition.

PATENT FUELS. By J. A. Greene and F. Mollwo Perkin, C.B.E., Ph.D., F.I.C.

PERFUMERY, RAW MATERIALS OF. By E. J. Parry, B.Sc., F.I.C., F.C.S.

PHOTOGRAPHY. By William Gamble, F.R.P.S.

PLATINUM METALS. By E. A. Smith, A.R.S.M., M.I.M.M.

PLAYER PIANO, THE. By D. Miller Wilson.

POTTERY. By C. J. Noke and H. J. Plant.

RICE. By C. E. Douglas, M.I.Mech.E.

RUBBER. Production and Utilization of the Raw Product. By H. P. Stevens, M.A., Ph.D., F.I.C., and W. H. Stevens, A.R.C.Sc., A.I.C.

SALT. By A. F. Calvert, F.C.S.

SHIPBUILDING AND THE SHIPBUILDING INDUSTRY. By J. Mitchell, M.I.N.A.

SILK. Its Production and Manufacture. By Luther Hooper.

SILVER. By Benjamin White.

SOAP. Its Composition, Manufacture, and Properties. By William H. Simmons, B.Sc. (Lond.), F.C.S.

SPONGES. By E. J. J. Cresswell.

STARCH and STARCH PRODUCTS. By H. A. Auden, D.Sc., F.C.S.

STONES AND QUARRIES. By J. Allen Howe, O.B.E., B.Sc., M.Inst. Min. and Met.

STRAW HATS. By H. Inwards.

SUGAR. Cane and Beet. By the late Geo. Martineau, C.B., and Revised by F. C. Eastick, M.A. Fifth Edition.

SULPHUR AND THE SULPHUR INDUSTRY. By Harold A. Auden, M.Sc., D.Sc., F.C.S.

TALKING MACHINES. By Ogilvie Mitchell.

TEA. From Grower to Consumer. By A. Ibbetson.

TELEGRAPHY, TELEPHONY, AND WIRELESS. By Joseph Poole, A.M.I.E.E.

TEXTILE BLEACHING. By Alex. B. Steven, B.Sc. (Lond.), F.I.C.

TIMBER. From the Forest to Its Use in Commerce. By W. Bullock. Second Edition.

TIN AND THE TIN INDUSTRY. By A. H. Mundey.

TOBACCO. From Grower to Smoker. By A. E. Tanner.

VELVET AND THE CORDUROY INDUSTRY. By J. Herbert Cooke.

WALLPAPER. By G. WHITELEY Ward.

WEAVING. By W. P. Crankshaw.

WHEAT AND ITS PRODUCTS. By Andrew Millar.